An Analysis of Optimal Agricultural Fertilizer Application Decisions in the Presence of Market and Weather Uncertainties and Nutrient Pollution

by

Xinyuan Yang

A thesis
presented to the University of Waterloo
in fulfillment of the
thesis requirement for the degree of
Doctor of Philosophy
in
Applied Economics

Waterloo, Ontario, Canada, 2023

© Xinyuan Yang 2023

Examining Committee Membership

The following served on the Examining Committee for this thesis. The decision of the Examining Committee is by majority vote.

External Examiner:	Alfons Weersink Professor, Dept. of Food, Agricultural and Resource Economics University of Guelph Awards Committee, American Applied Economics Association
Supervisor:	Margaret Insley Associate Professor, Dept. of Economics University of Waterloo Fellow, Canadian Resource and Environmental Economics Association Co-Investigator, Lake Futures, The Water Institute
Internal Members:	Roy Brouwer Professor, Dept. of Economics, University of Waterloo Executive Director, Water Institute, University of Waterloo ISAC, Chinese Research Academy of Environmental Sciences
	Horatiu A. Rus Associate Professor, Dept. of Economics, University of Waterloo Associate Professor, Dept. of Political Science, University of Waterloo
Internal-External Member:	Andrea Brookfield Assistant Professor, Integrated Hydrologic Systems Dept. of Earth and Environmental Sciences, University of Waterloo

Author's Declaration

This thesis consists of materials, all of which I authored or co-authored: see Statement of Contributions included in the thesis. This is a true copy of the thesis, including any required final revisions, as accepted by my examiners.

I understand that my thesis may be made electronically available to the public.

Statement of Contributions

The second, third, and fourth chapters are co-authored with my supervisor, Dr. Margaret Insley. In all chapters, I have contributed to all aspects of the research, including the development of research objectives, literature reviews, modeling and calibration, mathematical derivation, customizing the numerical approach, and analyzing the results.

Abstract

This thesis addresses the questions of how uncertain corn market and weather factors affect optimal fertilizer application decisions of the farmer and the social planner, and what factors drive the divergence between the two. Nutrient runoff from agricultural activities has become a primary source of surface water quality deterioration worldwide. Over-application of fertilizer in agricultural production represents a non-point source pollution which is causing extensive nutrient loading in water bodies and has a severe impact on the global environment. There is evidence that farmers apply more fertilizer than is socially optimal and more than is recommended by government agencies. This thesis first investigates the farmer's optimal fertilizer application under crop price uncertainty by constructing an inter-temporal farmer's decision model under two alternative stochastic price processes. Closed form results are derived, which indicate that an increase in price uncertainty implies a reduction in the quantity of fertilizer applied in the farmer's optimal decision problem. Numerous factors that could impact the optimal fertilization decision are examined as well. The farmer's decision model is then enhanced by allowing for two possible fertilizer application times in the growing season and the inclusion of additional stochastic state variables such as rainfall and temperature, in the corn yield model. The model is parameterized for average conditions in Iowa corn growing regions. Employing a Monte Carlo approach, numerical results conclude that for a wide range of parameter assumptions the farmer's optimal strategy is to apply fertilizer at planting rather than later as a side dressing. This thesis analyzes the impacts of price uncertainty, fertilizer cost and other economic parameters on the farmer's optimal fertilizer application strategy. The thesis also analyzes the optimal decisions of a social planner whose objective function includes an estimate of the damages caused by nitrogen leakage and denitrification. Numerical results show that including the damages from pollution affect both the quantity and timing

of fertilizer application. Assumptions about the frequency and quantity of rainfall have an important impact on the optimal decision. This is an important consideration for public policy as climate change affects weather patterns over the next decade and beyond.

Acknowledgements

I would like to thank all the people who made this thesis possible.

Foremost, my sincere gratitude is devoted to my supervisor, Margaret Insley, for her knowledgeable, rigorous, careful, and thoughtful supervision and instruction. It is her devoted help and forgiving care that keep my research on track and build a solid theoretical background for future research. I am more than certain that all of my life will benefit from her phenomenal expertise and her teaching, both in words and by example. There is absolutely no way I can accomplish this thesis without her help. I can't remember exactly how many times we discussed or worked on research problems in her office, but I do remember each of the one-on-one reading classes she gave, and every meeting starts with full preparation and ends with passionate encouragement. Her knowledgeable suggestions for both life and study are so beneficial that I can quickly get out of binds and focus on research objectives.

I am also very grateful for all my supervision committee members, Dr. Alfons Weersink, Dr. Roy Brouwer, Dr. Horatiu A. Rus, and Dr. Andrea Brookfield, who dedicated their precious and unconditional help and profound suggestions for improving my thesis. I want to say thanks to the Lake Futures team, the Water Institute at the University of Waterloo, and the Global Water Futures research program, which was funded in part by the Canada First Research Excellence Fund, for providing opportunities for my research extension, practice enhancement, and collaboration across different teams. I am deeply grateful to all the extraordinary faculty members in the Economics Department, especially to Dr. Philip Curry, Dr. Lutz-Alexander Busch, Dr. Francisco M. Gonzalez, Dr. Matthew Doyle, Dr. Margaret Insley, Dr. Roy Brouwer, Dr. Horatiu A. Rus, Dr. Thomas Parker, and Dr. Ana Ferrer, from whom I took courses. Their informative and thought-provoking courses are the bedrock on which my current and future research is based.

Above all, I could not have completed this thesis without taking the fabulous financial modeling courses from Dr. Yuying Li and Dr. Peter A. Forsyth at the David R. Cheriton School of Computer Science at the University of Waterloo. Informative courses have strengthened my modeling skills, and their classes are so passionate and attractive that they piqued my interest in computational finance. Those experiences with questioning, discussion, and team learning can always motivate me to pursuing a higher academic standard. I am deeply grateful to all of these extraordinary people.

Moreover, I want to thank the administrative graduate coordinator in the Economics Department, Maureen Stafford and Pat Shaw (retired). Their remarkable work makes my life with complicated paperwork way easier than I thought. I am so grateful to Pat Shaw, who was the first person I met on campus and helped me avoid getting lost in Hagey Hall, for her selfless encouragement and considerate mental support all through my years in Waterloo. I'll never forget those moments when we laughed together.

Dedication

This is dedicated to my parents, Jiayong Yang and Shuyun Liu, and all those who have ever helped and touched me in these years.

"You see things; and you say 'Why?' But I dream things that never were; and I say 'Why not?'"—George Bernard Shaw

"Dreams and ambition are the best fuel for a person who struggles to make a difference in his life inexorably."—Yang, Xinyuan

"Nothing can help us find the dawn better than the spirit of independence, the thought of freedom, and the love of life."—Yang, Xinyuan

Gratitude is dedicated to life. In spite of financial stresses caused by Chinese state-owned enterprise layoffs in the 1990s and the 1997 Asian financial crisis, my parents shed light on my childhood using their unconditional love. Playing below par in the 2008 Chinese GaoKao totally shattered my hope of getting into my dream university. My confidence could never be rebuilt without my parents' love. I am much more aware than most of my peers of how hard a person can work to realize his or her dreams. I asked myself more than once, "If someone else can accomplish it, why not me?" From then on, my journey to becoming an extraordinary independent scholar starts. Fortunately, my cumulative hard work pays off. I got the highest GPA in the M.A. Class of 2015, was granted Excellent Graduate Award by the Department of Economics at the University of Windsor, and was admitted to the University of Waterloo. Yes, I did it.

Research is a road, starting from confusion, suspicion, and perturbation, paved with patience, perseverance, and persistence, leading to medals, flowers, and applause. Tough issues often arise in this process, and nothing can help us persist rather than retreat better than our faith: "If someone else can do it, why not me?" On this road, my parents dedicated their devoted love and super-normal patience to strengthening my courage and affirming my determination. It is passion and ambition by myself, profession and amelioration from all Waterloo professors, and love for my parents that move me forward.

Arguments may fade, but spirits endure. This thesis is not only a milestone in my life but also a microcosm of my inexorable struggle for a better me. I hope this thesis will bring dawn to all those ordinary people, like me, who are fighting for an extraordinary life by surmounting our disheartened stereotypes of "No, I can't" with motivated convictions of "If others can, why not me?".

Table of Contents

List of Figures

List of Tables

Chapter 1

Introduction and Motivation

Over the past century, humans have successfully adopted advanced fertilization techniques and applied high-efficiency fertilizers for boosting agricultural productivity. However, the runoff of nutrients from agricultural uses of fertilizer has become a primary source of water quality deterioration in surface water (USEPA[1] and Chen (2007)). Intensive fertilizer application in agricultural production is causing extensive nitrogen and phosphorus discharge, a non-point source pollution which is a challenge to control. In high concentrations, these nutrients lead to nuisance algal blooms, which yield unpleasant odor and appearance resulting in declines in fishing and swimming and hurting local tourism. As algae die and decompose, dissolved oxygen levels decline, resulting in high fish mortality. Harmful algal blooms can produce toxins which are dangerous to humans and animals, raising treatment costs for drinking water (USEPA[2]). Based on a recent U.S. Geological Survey[3], in their 20 Study Units, it is estimated that about 90 percent of nitrogen and 75

[1]United States Environmental Protection Agency, source:https://www.epa.gov/nutrientpollution [Accessed on 7th December, 2017]

[2]United States Environmental Protection Agency, source:www.epa.gov/nutrientpollution/harmful-algal-blooms

[3]Sources of nutrients and pesticides. Available from:https://pubs.usgs.gov/circ/circ1225/pdf/sources.pdf [Accessed on 7th December, 2017]

percent of phosphorus originates from non-point sources, while the remaining percentages are from point sources.

In North America, the Great Lakes contain one fifth of the world's fresh surface water supply, provide healthy drinking water to tens of millions of Canadians and Americans and are important to the economies of both countries, supporting manufacturing, transportation, farming, tourism, recreation, and other forms of economic activity. The Great Lakes Basin is a major world supplier of crops such as corn and soybeans which are highly dependent on nitrogen and other fertilizers. However, excess nutrient loading in Lake Erie and near-shore areas of Lakes Huron, Michigan and Ontario are causing severe impacts on the local environment due to the formation of toxic and nuisance algae. During the 1960s, water quality issues in the Great Lakes became a public concern. In particular, Lake Erie was perceived to be "dying" because of extensive algal growth that occurred throughout the lake as a result of excessive emission of phosphorus. By the late 1960s, Canada and the United States were in agreement that limiting phosphorus inputs to the Great Lakes, particularly Lake Erie, was the key to controlling excessive algal growth. In 1972, the signing of the Great Lakes Water Quality Agreement (GLWQA) by the governments of Canada and the United States commits both countries to working cooperatively to restore and protect the water quality and aquatic ecosystem health of the Great Lakes. In the 1980s, efforts were successful at reducing nutrient-related runoff and conditions in the Great Lakes improved. These efforts included the regulation of phosphorus concentrations in detergents and investments in water treatment plants. However, in the mid-1990s, excessive algal growth began to re-emerge as a problem in the Great Lakes. Nowadays, nitrogen and phosphorus remain primary factors in influencing excessive algal growth. In 2017, the Report of the State of the Great Lakes[4] evaluated the environmental status of

[4]The report was published by Canada-US Collaboration for Great Lakes Water Quality. Available from: https://binational.net/wp-content/uploads/2017/06/SOGL17−EN.pdf

the Great Lakes using a set of 9 indicators of ecosystem health. That report showed the Great Lakes still have a nutrient imbalance problem, which has resulted in a deterioration in the overall trend of water quality indicators. Algal blooms are still causing harm to both ecosystem and human health. The western basin of Lake Erie and some parts of Lake Ontario have experienced a resurgence of algal blooms since 2008, strongly and negatively impacting ecosystem health as well as commercial fishing, drinking water systems and recreational activities. Algal blooms are particularly harmful when it comes to their impact on drinking water safety.

Most of the nutrients that are applied to agricultural lands serve their intended purpose of increasing crop yields, but also cause significant pollution of ground and surface water. Iowa is the largest corn producer in the U.S., and the second largest producer of nitrate pollution in the Mississippi River Basin[5]. Despite of hundreds of millions of dollars spent to stem nutrients entering the waterways, nitrogen pollution flowing out of Iowa to the Gulf of Mexico has grown by close to 50% over nearly two decades[6]. Nitrogen and phosphorus losses from farm fields have been driven by a variety of factors. Since the mid-twentieth century, statewide corn and soybean acres have increased as extended rotations, hay, and pasture declined. Compared to perennial crops and small grain rotations, according to Iowa State University[7], corn-soybean and continuous corn rotations are leaky systems. They require increased fertilizer rates creating vulnerability to nutrient loss, have a lower capacity for capturing and holding nitrogen during wet conditions. In addition, Iowa has made very limited progress in solving the fertilizer over-application problem. According to the Sierra

[5]See details in https://www.nationalgeographic.com/science/article/iowa-agriculture-runoff-water-pollution-environment

[6]See details in https://www.desmoinesregister.com/story/money/agriculture/2018/06/22/iowa-water-pollution-gulf-mexico-dead-zone-nitrogren-missouri-mississippi-river-quality-nirtate/697370002/

[7]See details in "Measuring Conservation and Nutrient Reduction in Iowa Agriculture", source: https://crops.extension.iastate.edu/cropnews/2020/07/measuring-conservation-and-nutrient-reduction-iowa-agriculture

Club[8], the Iowa Nutrient Research and Education Council surveyed farmers in 2017, 2018 and 2019, and found that they did not follow ISU's fertilizer recommendations and were applying fertilizer at rates more than 30 pounds greater than guidelines recommended by the Iowa State University maximum return to nitrogen (MRTN) calculator[9]. As a result, substantial nutrient flows from fields into waterways, where they degrade water quality in Iowa's streams, lakes, and groundwater, create challenges for local communities in maintaining safe nitrate levels in drinking water. It is interesting to note how US corn acreage and yields have increased since 1970, with much of the growth caused by expanded ethanol production which accounts for nearly 40% of total production in 2021[10]. A wide range of management practices have been developed and a growing body of agricultural practitioners have engaged in to reduce the non-point nutrient pollution associated with fertilizer application[11].

Similar problems have been reported in China where intensive agricultural practices have contributed substantially to the emission of the pollutants (excessive nitrogen and phosphorus) into water bodies and soils (Smil 1997). China is the world's second largest producer of corn. Water bodies in China have become seriously polluted since the 1990s and there has been no marked improvements in recent years. According to an evaluation of eutrophication in 131 major lakes in 2000 in China, about 50% of them were eutrophic (Yuan 2000), and for 75% of these lakes the eutrophication is getting worse. Over half

[8]See details in "Over-application of Fertilizer on Iowa's Farm Fields-Although Fertilizer is Expensive, Farmers are Indeed Wasting It". https://www.sierraclub.org/sites/www.sierraclub.org/files/sce/iowa-chapter/Ag-CAFOs/FertilizerRates.pdf

[9]Iowa, Illinois, Minnesota, Wisconsin, Indiana, Michigan, and Ohio corn N fertilizer application recommendations are based on extensive N response trials conducted over several years in each state. These trials have determined the N rate at which the last pound of added nitrogen fertilizer returns a yield increase large enough to pay for the cost of the additional fertilizer, which is called the maximum return to nitrogen (MRTN). The widely adopted calculator in finding the MRTN, initiated by the Iowa State University, can be accessed by http://cnrc.agron.iastate.edu

[10]USDA Economic Research Service, Feedgrains Sector at a Glance, https://www.ers.usda.gov/topics/crops/corn-and-other-feedgrains/feedgrains-sector-at-a-glance

[11]More details regarding current nutrient management practices in Iowa and Ontario are discussed in Appendix A.

of the rivers and about two-thirds of the lakes in the seven river systems and 28 major lakes were assessed to be of poor quality during 2000−2008 (SEPA 2000−2008)[12]. Nitrogen concentrations in large rivers, especially the Yangtze and Yellow river, have been increasing in recent years (Tao et al. 2010).

The socially efficient fertilizer application rate balances the tradeoff between crop nutritional needs and damages to the environment and human health caused by nutrient pollution. Quantification of societal damages is a difficult challenge and the subject of much current research, as is reviewed in Chapter 4. However, even ignoring damages from nutrient pollution there is evidence that in many locations farmers apply more than the recommended amount of fertilizer and more than the amount that maximizes farming profits. Data on nitrogen use efficiency (the ratio of nitrogen input to nitrogen uptake by the crop) is instructive as an indicator of the potential over-use of fertilizer. Data from Food and Agriculture Organization of the United Nations[13] shows a huge variation in fertilizer use efficiency per hectare across the world, likely implying some regions would benefit by more fertilizer use and others by reductions. There is also a large variation in nitrogen use efficiency worldwide. In Canada and the US nitrogen use efficiency from 2000-2014 was in the range of 60 to 70 percent (Lassaletta et al. (2014), Ritchie (2021)).

From the farmer's viewpoint, the efficient fertilizer application rate will depend on a host of factors including weather, soil and market conditions all of which are uncertain. In addition to these factors, the efficient application rate from society's viewpoint will depend on environmental conditions that affect fate and transport of applied nitrogen in a farmer's field and the associated damages. The extent to which the farmer's optimal choices differ from the social planner's dictate the degree of market failure from agricultural fertilizer use. This thesis undertakes an in depth analysis through economic modelling and

[12]State Environment Protection Agency (SEPA), 2000−2008. Report are found on the State Environment website in Chinese. http://www.sepa.gov.cn/

[13]Nitrogen fertilizer use per hectare of cropland, 1961-2019, https://ourworldindata.org/fertilizers

numerical computation of the factors affecting the socially efficient fertilizer application rate in contrast with the efficient rate from the farmer's point of view.

Farmers' decisions on fertilizer use are based on profitability considerations and are influenced by regulations and, recommendations from government agencies and fertilizer manufacturers. Nitrogen fertilizer recommendations have typically reflected the amount of fertilizer required to meet a crop yield goal (Vanotti & Bundy (1994)). For example, some general fertilizer recommendations in Ontario such as those found in OMAFRA[14] publications are formed based on expected grain yield levels[15]. A general fertilizer recommendation by an Ontario grain agribusiness firm[16] is reported as 1 pound (lb) nitrogen for every bushel (bu) of yield goal. The total (fall and spring) nitrogen recommendations for soft winter wheat in Indiana, Michigan and Ohio were based on wheat yield targets (Culman et al. (2020)). However, a uniform recommendation will not be optimal for all farms or in all years (Vanotti & Bundy (1994)). Nitrogen and phosphorus not fully utilized by growing plants can be washed away by significant rain events or as snow melts. More specific recommendations in U.S. and Ontario are based on soil testing and provide a wide range of recommendations, depending on the test results or spring nitrate nitrogen content[17]. Evidence from Babcock (1992) suggested that typical U.S. farmers apply more nitrogen inputs than the economically optimum rate, defined as the point where the last unit increment of fertilizer returns a grain yield increase large enough to pay for that unit of fertilizer. Newer empirical evidence from Shi et al. (2016) indicates the extent to which fertilizer was over-applied relative to the nutrient needs for normal crop growth was 50.74% on average in China based on provincial level cost-benefit survey data of agricultural products

[14]OMAFRA refers to the Ontario Ministry of Agriculture, Food and Rural Affairs.

[15]Greg Stewart, OMAFRA Corn Specialist, 2001, "Table: General recommended nitrogen rates for corn". www.gocorn.net/v2006/Nitrogen/articles/Setting%20Nitrogen%20Rate%20Targets.html

[16]Source: The Andersons, source: https://www.thompsonslimited.com/2017/06/22/

[17]The information on soil test-based fertilizer suggestions can be found in Culman et al. (2020) and Table 1-18 in OMAFRA (2017*a*)

from 2004 to 2013.

The reasons for over-application of fertilizer are not well understood. Moreover, the term over-application as used in the scientific literature or the popular press can have several different meanings. Over-application can be relative to expert recommendations, relative to the economically optimal amount from the farmer's point of view, or relative to the economically optimal amount from society's viewpoint. Over-application may also be considered in an ex-ante context at the start of the growing season or in an ex-post context once the crop has matured. Considering first the ex-ante context, farmers may follow expert recommendations based on target yield goals[18] or simply follow the maximum yield principle[19], but may be overly optimistic about their yield goal. Further, expert recommendations may be based on average rules of thumb that are not appropriate for a given farmer's circumstances. Expert recommendations, based on yield goals, may not represent the economically optimal application rate for the farmer. Estimates of the economically optimal amount for the farmer may be incorrect due to a failure to take into account key factors such as weather and price uncertainty. Ex-post, given the growing conditions that prevailed, it may be evident that too much fertilizer was applied. Finally, the optimal (ex-ante) fertilizer application should be considered in terms of environmental impacts. The evidence of significant damages from excess nutrients in groundwater and surface water is an indication the fertilizer application levels are not optimal and represent an over-application from a societal point of view.

The extent to which a farmer's economically optimal fertilizer decision differs from

[18] According to a report by Montana State University, the sufficiency approach of N application recommends applying the minimum amount of fertilizer necessary to maximize yield in the current year. Source: https://landresources.montana.edu/soilfertility/documents/PDF/pub/FertRecAgMT200703AG.pdf

[19] For example, farmers in two Iowa watersheds (Floyd and Rock) were applying nitrogen fertilizer at more than double the ISU recommendation rate, which may be attributed to their willingness to maximize crop yields. See Erin Jordan, "Iowa State University's fertilizer recommendations "flawed", Farm Bureau says". https://www.thegazette.com/agriculture/iowa-state-university-fertilizer-recommendations-flawed-farm-bureau-says/

standard recommendations has been a subject of study in the literature. One possibility suggested in the literature is that standard recommendations do not account for uncertainty (Babcock (1992), Sheriff (2005) and Rajsic et al. (2009)). The focus in the literature has been on weather uncertainty, rather than crop price uncertainty, and most analysis has used a static model framework. A few papers undertake dynamic analysis but there is rarely much discussion of the detailed specification of weather or crop price models. Farmers' optimal decisions regarding fertilizer application will depend on how uncertainty in key variables affects the return on fertilizer application. Empirical studies have revealed that agricultural crop yields are highly affected by weather conditions, especially by growing season weather (Qian et al. (2002)). Farmers can update their decisions over time in response to both weather and price, which implies that a dynamic decision framework is most appropriate.

To the best of our knowledge, optimal fertilizer application under both price and weather uncertainties from a farmer's and a social planner's perspective have rarely been examined in the literature in a dynamic framework. Detailed literature reviews are included in Chapters two through four. Briefly, some previous studies have analyzed the impact of weather or climate variables on crop yield (including Dixon et al. (1994), Aggarwal (1995), Mavromatis & Hansen (2001), Turvey (2001), Derby et al. (2005), Schlenker & Roberts (2006), Lobell et al. (2007), Cabas et al. (2010), Ortiz-Bobea (2013), Shi et al. (2013) and Kablan et al. (2017)). These studies have examined relations between weather and crop yield given various land conditions and climate assumptions, but the agricultural nutrient input and crop price factors are omitted. Some other studies investigated optimal agricultural nutrient use but include very simplified models for crop price and crop yield without incorporating weather uncertainties as inputs (including SriRamaratnam et al. (1987), Babcock (1992), Ramaswami (1992), Isik (2002), Rajsic et al. (2009)). Thus, to the best of our knowledge, there are no studies which examine the optimal nitrogen appli-

cation by a farmer in a dynamic model, incorporating realistic models of crop price and climate variability. Further, incorporating these factors into a social planner's problem has also not been undertaken.

The main research question of this thesis is a follows: "How do uncertain corn market and weather factors affect optimal fertilizer application decisions of the farmer and the social planner, and what factors drive the divergence between the two?". In Chapter 2, the impact of price uncertainty, on the optimal fertilization decision from the farmer's perspective is explored, in an environment in which the evolution of crop price is described by two alternative stochastic processes. A real options approach is used in that the crop price model is specified in the $\mathbb{Q}$-measure (risk neutral equivalent measure). The farmer's optimal control problem is expressed as a Hamilton-Jacobi-Bellman equation (HJB). Under various simplifying assumptions about the farmer's decision problem, we derive closed form solutions for the optimal fertilizer choice under crop price uncertainty.

In Chapter 3, the farmer's economic model is enhanced to include both price and weather uncertainties as well as the option to apply fertilizer at two times over the growing season. A crop yield function is specified which gives crop output as a function of average soil nutrient content and weather conditions over the crop growing season. Stochastic state variables in the model include corn price, cumulative Corn Heat Units over growing season and cumulative precipitation over growing season. Due to the complexity caused by the number of stochastic variables and path dependent state variables, there is no closed form solution to the associated HJB equation. Implementation of a numerical solution based on the finite difference approach is also problematic since more than 3 state variables and path-dependent variables included. As an alternative, we parameterize the model and undertake Monte Carlo simulations to describe the expected outcomes for a range of possible optimal controls. By limiting the number of possible controls the optimal solution can be found by exhaustive search. In the numerical example, corn and nitrogen are the

crop and the fertilizer choice studied, as Iowa is the largest corn producer in the U.S. and corn plants need high quantities of nitrogen to grow (N:P:K=1:0.3:0.5). In addition, corn is also a major crop around the Great Lakes in Ontario and in the US Heartland region. The models and subsequent analysis in this chapter enhance our understanding of how key economic and environmental factors affect optimal fertilizer decisions from a private perspective, which will be informative for farmers and policy makers seeking to implement or design effective regulations and best management practices.

The social planner's problem regarding fertilizer application is discussed in Chapter 4, combining the farmer's decision model in Chapter 3 and the social damage model from nitrogen fertilizer application. Social damages from agricultural nitrogen leaching and denitrification are constructed in two ways: a linear damage model and a threshold damage model. An extensive literature survey on the measurement of externalities and social costs of agricultural nitrogen pollution is included. Socially optimal fertilizer application decisions from both social damage models are derived and compared with the private optimal results in Chapter 3. A wide range of sensitivity analysis regarding parameter assumptions is performed. The findings concluded in this chapter broaden our understanding of the degree of market failure from agricultural fertilizer use which is dictated by the extent to which the farmer's optimal choice differs from the social planner's decision. In addition, analysis on how parameter assumptions affect the socially optimal fertilizer applications from a social planner's perspective is informative for helping policy makers knowing the sophistication of considering farmer's behaviour and social cost of N as a whole.

This thesis is organized as follows: Chapter 2 presents a theoretical model examining the optimal fertilizer application under price uncertainty, and derives closed-forms for the farmer's optimal strategies for fertilizer application. Chapter 3 develops a more realistic model of the farmer's fertilizer application decision with both price and weather uncertainties taken into account. This model is analyzed using Monte Carlo analysis. Chapter 4

elaborates the social planner perspective. Chapter 5 summarizes and presents conclusions.

Chapter 2

Optimal Fertilizer Application Under Crop Price Uncertainty

Current expert recommendations for fertilizer application rates typically do not consider crop price or production uncertainty. However corn price uncertainty is a key consideration for farmer decisions as is evidenced by attention paid to the outlook for corn prices in agricultural trade magazines[1]. Some farmers may reduce the impact of price uncertainty by purchasing futures contracts on the Chicago Mercantile Exchange (CME). A recent study found that in 2016 over 10 percent of corn and soybean farmers traded in futures contracts while 20–25 percent used marketing contracts. In the U.S., some farmers also draw on commodity support programs and Federal crop and livestock insurance, as well as private insurance (Prager et al. (2020)). Similarly in Canada, crop production insurance is available through the AgriInsurance program[2] and revenue insurance is available through

[1]See for example, Successful Farming, an agronomy news agency, "Continued uncertainty is seen for 2021, agricultural experts say", Dec 4, 2020, by Mike McGinnis. Source: https://www.agriculture.com/markets/analysis/continued-uncertainty-is-seen-for-2021-agricultural-experts-say

[2]AgriInsurance is a federal-provincial-producer cost-shared program, delivered provincially, that stabilizes your income by minimizing the economic effects of primarily production losses caused by severe but

the AgriStability program[3]. Farmer's risk management strategies vary by the specifics of a farming operation including size of farm and by farmer characteristics, and the cost and availability of insurance.

This chapter takes a first step at modelling optimal fertilizer application under crop price uncertainty, which is presented as a stochastic optimal control problem using a real option approach in the spirit of Insley & Lei (2007) and Insley & Wirjanto (2010), assuming fertilizer application is a one-off decision made at the beginning of planting. Historical corn prices in U.S. dollars from 2010 to 2019 are plotted in the following Figure 2.1, which shows significant volatility for past two decades.

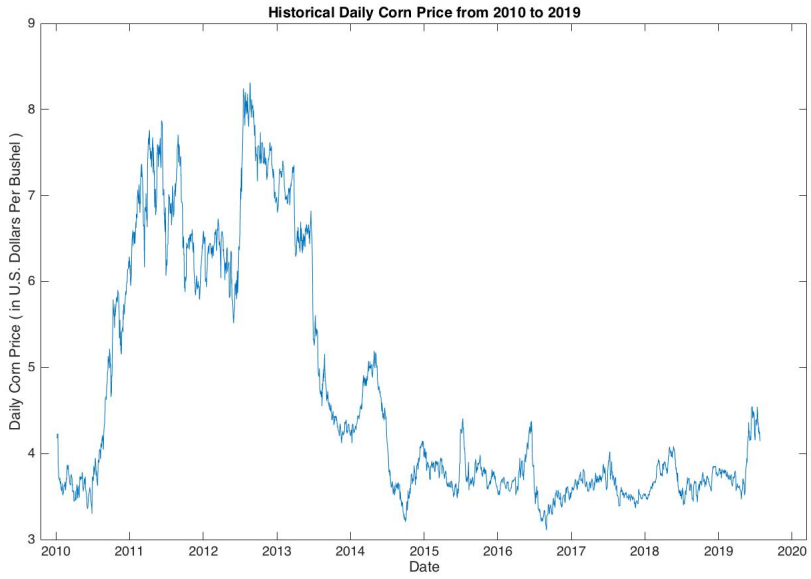

Figure 2.1: Corn Price from 2010 to 2019

Crop prices are modelled as a simple Ito process in this chapter, either geometric Brownian motion (GBM) or mean reverting (MR). Closed form solutions are derived and

uncontrollable natural hazards. The AgriInsurance Program is described on the Government of Canada website: https://agriculture.canada.ca/en/agricultural-programs-and-services/agriinsurance-program.

[3]AgriStability protects Canadian producers against large declines in farming income for reasons such as production loss, increased costs and market conditions. Source: https://agriculture.canada.ca/en/agricultural-programs-and-services/agristability

comparative statics undertaken to examine optimal farmer responses to changes in key parameters such as crop price volatility and fertilizer cost.

2.1 Optimal fertilization and uncertainty: An overview of selected literature

A substantial volume of literature has been devoted to optimal fertilizer application under uncertainty. One early empirical paper by SriRamaratnam et al. (1987) evaluated the farmer's optimal fertilizer decisions using subjective beliefs about future crop yields and prices. His study found the relationship between farmers' subjective beliefs and experimental data on the yield response of crops to different nitrogen levels. In particular, to model the fertilization decision, SriRamaratnam et al. (1987) used a single-decision-variable response process: $Y = f(N|X_2, .., X_k|X_{k+1}, ..., X_m)$, where Y is grain yield, N is a single input, $X_2...X_k$ are predetermined state variables, soil type ,etc, and $X_{k+1}...X_m$ are uncertain random variables. The farmer's objective function is to maximize expected utility over a single growing season with choice input variable N. To assess subjective yield probabilities, SriRamaratnam et al. (1987) conducted a field survey with Texas farmers, and obtained a distribution of beliefs about future crop yield. Subjective grain price probabilities were obtained by a mail survey from participating producers. SriRamaratnam et al. (1987) solved for optimal fertilization rates and concluded that expected utility maximization could explain actual fertilizer use better than expected profit maximization.

An early theoretical paper by Ramaswami (1992) examined how production uncertainty affects optimal input use. The static profit function Ramaswami (1992) used is $\pi(q, x) = q - wx$, x is input, w is normalized input price and output q is a random variable with a cumulative density function $F(q, x)$ which specifies output q as a normal distribution. By

Ramaswami (1992), an input is defined to be risk-increasing if it increases the variability of the deviations from output mean. He reached a conclusion that whether farmers use more or fewer inputs under production uncertainty depends on whether the sign of marginal risk premium is negative or positive, which is determined by risk preference and technology.

One early paper that studies the nitrogen over-application problem was Vanotti & Bundy (1994), who compared the yield goal-based nitrogen recommendation rate in Wisconsin and recommendations based on soil- and year-specific data. They found that, in most areas of the U.S., corn nitrogen recommendations are based on yield goals with some adjustments for soil characteristics, which could lead to an overestimate of actual nitrogen needs. As a result, nitrogen was over-applied and there were nitrate losses to the environment. In an attempt to remedy this problem, Vanotti & Bundy (1994) separated Wisconsin experimental data into groups based on high-yielding years and low-yielding years, on which the high-yielding and low-yielding recommended nitrogen rates were built respectively. They investigated the feasibility of basing corn N recommendations on soil and year-specific data rather than on yield goals. Vanotti & Bundy (1994) were the first to calculate recommended nitrogen rates based on historical low and high yield productivity scenarios. The crop yield response functions they used were quadratic and quadratic-plateau forms with nitrogen rate as the independent variable. However, they found their results to be immune to the choice between these two yield response functional forms. Vanotti & Bundy (1994) computed for the optimum nitrogen rate based on field productivity in terms of low and high yield levels, but did not consider weather uncertainty.

Also focusing on the fertilizer over-application problem, Rajsic & Weersink (2008) examined empirically whether the differences in the economically optimal application rate of fertilizer across functional forms for yield response could provide a rationale for over-application. After statistically comparing four yield response functions, they calculated the cost of fertilizer over-application as: $Cost(N_{st}^{A}) = P_c[f_{st}(N_{st}^{MERN}) - f_{st}(N_{st}^{A})] - P_N[N_{st}^{MERN} -$

$N_{st}^{A}]$, P_c and P_N are price of corn and nitrogen, f_{st} is the estimated production function for site s and year t, N_{st}^{A} is the *ex ante* recommendation rate for site s in year t, N_{st}^{MERN} is the calculated *ex post* profit maximizing nitrogen rate for site s in year t. Rajsic & Weersink (2008) concluded that the major reason why farmers would apply more fertilizer than the level recommended by Ontario's Agricultural Extension Services was that the form of yield response function underlying the recommendations may be incorrect or differs from farmer perceptions, which means general recommendations are not appropriate for their individual situations.

Uncertainties associated with optimal input use have been suggested as the possible reason for fertilizer over-application relative to recommended rates in crop planting (including Babcock (1992), Sheriff (2005) and Rajsic et al. (2009)). Both Babcock (1992) and Rajsic et al. (2009) investigated possible reasons for fertilizer over-application. Specifically, Babcock (1992) employed a linear crop production function where weather factors W is included without specifying the functional form of $f(W)$:

$$F(Nitrogen, Weather) = min(\alpha + \beta N, f(W))$$

where N is the applied nitrogen and W is the random weather variable that refers to rainfall in their paper, α, β are constant parameters. Using this linear plateau function, Babcock (1992) analyses the impact of weather uncertainty and soil nitrate uncertainty on the optimal nitrogen application which is derived from solving a static expected profit maximization problem. Babcock (1992) found that three sort of uncertainties could result in fertilizer over-application. The first is estimation uncertainty which could arise from production functional form specification error. Recommended rates are generally based on the estimated production function which is treated as the "true" underlying function. However, this usually ignores the uncertainty inherent in this estimated production rela-

tionship. The second is weather uncertainty could be taken as another reason for excess fertilizer application. Because farmers do not know for sure what the growing conditions will be in the future, it is optimal for them to plan for good growing years (plentiful rainfall and sunshine), apply larger amounts of nitrogen fertilizer, so that fertilizer will not limit their potential profits. Third, nitrogen availability uncertainty, which is uncertainty about the amount of nitrogen or concentration present in the soil, was considered as a reason why farmers would apply excessive fertilizer to reduce yield risk. Nitrogen losses are mainly from leaching and denitrification, which are uncertain and depend on weather or the type of crop. As a conclusion, they found that the conventional perception that farmers should reduce fertilizer use for the reason that nitrogen is risk-increasing is contradicted by their empirical results, which indicated that risk-neutral farmers would reduce the possibility of a nitrogen shortfall by applying more fertilizer than recommended amounts.

Rajsic et al. (2009) examined the effect of production risk on a farmer's fertilizer application by using time series corn yield data from field trials in Ontario over 1993 to 2001. By Rajsic et al. (2009), an input is defined to be risk-increasing if higher input increases the variance of profit. Yield functions employed by Rajsic et al. (2009) are in quadratic and quadratic plateau forms, which are respectively

$$Y = \alpha + \beta_1 N + \beta_2 N^2$$

and

$$Y = \begin{cases} \alpha + \beta_1 N + \beta_2 N^2 & \text{when } N \leq -\frac{\beta_1}{2\beta_2} \\ Y^{max} & \text{otherwise} \end{cases} \tag{2.1}$$

where Y is the corn yield, Y^{max} is the constant yield level and N is the amount of applied fertilizer. The effect of unforeseeable growing conditions on yield, representing the production risk, is assumed to have a normal distribution. The effect of production risk

on optimal nitrogen application for risk-averse farmers is examined in an expected utility maximization model, while that for risk-neutral farmers is examined through the expected profit maximization model. In conclusion, results by Rajsic et al. (2009) suggested that the optimal fertilization rate varies significantly across time (8 years). For risk-neutral farmers, production risk could increase fertilizer application if the expected return from over-applying fertilizer is higher than that from the recommended rate. For risk-averse farmers, production risk may lower the fertilization rate if the variance of return associated with the recommended rate is smaller. Both Babcock (1992) and Rajsic et al. (2009) found nitrogen fertilizer to be risk-increasing, but over-application can still be justified because of a higher expected return. However, by Rajsic et al. (2009), uncertainty cannot justify fertilizer over-application for those risk-averse farmers.

Isik (2002) examines the impacts of environmental and agricultural policies on a risk-averse farmer's input use, especially for changed taxes on profits, inputs, and outputs under output price and production uncertainty. As part of a policy implementation analysis, he examines the impacts of production and output price uncertainty on input use. A yield specification from Just and Pope (1979) is used: $y = f(x) + h(x)\epsilon$ to represent the production uncertainty, where y is output, x is an input, ϵ is a random variable. Output price $P = \bar{P} + \theta$, where $\bar{P}$ is the expected price value, captures price uncertainty. After solving a static expected utility maximization problem, Isik (2002) concluded that a risk-averse farmer applies less input under both uncertainties (production and output price uncertainty) if input is risk-increasing, which is equivalent to the conclusion Ramaswami (1992) reached. If the input is risk decreasing, the impact of uncertainties depend on the degrees of both uncertainties. Interestingly, considering another sort of uncertainty in his later research, Isik (2004) analyzed how uncertainty about cost-share subsidy policies (aimed at reducing pollution) would impact adoption decisions of new farming systems. As part of his option value method, adoption return and adoption cost uncertainties were

all described as GBM processes. Then the adoption decision problem was to maximize net returns by choosing the optimal time to adopt a new farming system. Numerical simulation results indicated that policy uncertainty has the potential to impact a farmer's investment decision. If the policy maker wants to accelerate the adoption of new environmentally friendly farming technologies through providing cost-share subsidies, the best strategy would be to enact a subsidy program right away, threaten to remove it soon, and promise never to restore it again.

To examine the uncertainty in yield model parameter estimation on fertilizer recommendations, Henke et al. (2007) quantified the impact of using different yield response functional forms. They used several yield response models to estimate optimum nitrogen fertilization rates: quadratic, linear plateau and a quadratic plateau function. The objective function was specified as: $max \sum_{i=1}^{I}(p_w Y_i(N) - p_n N)$. $Y_i(N)$ is the yield in year i, I is the total number of years, p_w is the crop price, p_n is price of fertilizer. Experimental data from a field experiment were used to compute optimal fertilizer recommendations. After carrying out Monte-Carlo simulations of yield functions of years 1996, 1997, 1998, 1999 and 2002, Henke et al. (2007) reached a conclusion that uncertainty tends to increase the optimal fertilization rate. Since each parameter of the yield model is uncertain and has its own distribution, the only sort of uncertainty they investigated was happened in estimation process instead of price or production uncertainty.

Another focus of the literature is the specification of the crop yield function. A wide variety of yield models have been discussed in different research papers (e.g., Gandorfer & Rajsic (2008), Rajsic & Weersink (2008), Rajsic et al. (2009), Meyer-Aurich et al. (2010), Hyytiäinen et al. (2011), Boyer et al. (2013), Leslie et al. (2017) and Kablan et al. (2017)). Most of these studies adopted a quadratic form corn yield response function, $Y(N) = aN^2 + bN + c$, where a, b, c, are constant parameters, omitting any weather variables (e.g., Rajsic & Weersink (2008), Rajsic et al. (2009) and Leslie et al. (2017)). Rajsic

et al. (2009) contributed to the estimation of a quadratic yield response using Ontario site-specific experimental data. Leslie et al. (2017) compared the environmentally recommended fertilizer application rate with the actual application rate by adopting the estimated yield response function from Rajsic et al. (2009), namely $Y = 1431 + 48.33N - 0.1364N^2$. Gandorfer & Rajsic (2008) and Meyer-Aurich et al. (2010) studied winter wheat yield response to nitrogen input. They both estimated a quadratic yield response function using experimental data for winter wheat on different sites and under given experimental field climate states (precipitation and temperature). Furthermore, Schlegel & Havlin (2017) estimated the corn quadratic-form yield response function to nitrogen based on various climate factors, soil PH and soil NH_4^+ properties, using a 50-year field study data-set.

In conclusion, these selected papers address the optimal fertilization under uncertainty problem from different perspectives. A common conclusion is that risk-averse farmers tend to apply less fertilizer than recommended rates because fertilizer is risk-increasing, Rajsic et al. (2009) studied only temporal production risk while Isik (2002) studied both production and price uncertainty with specified stochastic processes. In analyzing the fertilizer over-application problem empirically, Babcock (1992) attributed it to three uncertainties while Rajsic & Weersink (2008) found improper yield function choice should be responsible for over-application. Besides, Henke et al. (2007) argued that uncertainties in the production function and optimal nitrogen application rate estimation could result in excess fertilizer application. Using a different approach from Ramaswami (1992) to measure production uncertainty, Rajsic et al. (2009) found a result that was consistent with the conclusion made by Babcock (1992) that fertilizer could be over-applied by risk-neutral farmers. Despite achieving the economically efficient principle from farmer's perspective, the nitrogen still is over-applied relative to the recommended rate. Different from his earlier paper (Isik 2002), Isik (2004) measured policy uncertainty using an option value approach.

However, these selected papers that involve uncertainties in optimal fertilizer applica-

tion research have rarely much discussion of the specification of weather or price uncertainty models. For example, SriRamaratnam et al. (1987), Ramaswami (1992), Babcock (1992), Vanotti & Bundy (1994), Isik (2002), Sheriff (2005), Rajsic & Weersink (2008) and Rajsic et al. (2009) derived their conclusions with price or yield uncertainty represented by a normally distributed stationary random variable. As well, in the associated yield function estimation, little attention has been devoted to the dynamics of the crop production progress. For example, the timing of the input decision and output benefit occur have rarely been considered. The objective function is typically static expected utility maximization or profit maximization and these studies do not consider crop growth in a realistic inter-temporal way (e.g. profit can only be realized after one growth cycle), which makes the derivation of site-specific agri-environmental policy less reliable.

2.2 Farmer's decision model

2.2.1 Yield response function

To choose a reasonable model that can describe the relationship between fertilizer application and crop output, this paper surveyed previous empirical research on the crop yield-nitrogen relationship. A wide variety of crop yield models have been studied in the literature including linear and quadratic functional forms (e.g., Cerrato & Blackmer (1990), Dahnke et al. (1990), Willcutts et al. (1998), Bélanger et al. (2000), Gandorfer & Rajsic (2008), Rajsic & Weersink (2008), Rajsic et al. (2009), Meyer-Aurich et al. (2010), Hyytiäinen et al. (2011), Boyer et al. (2013), Leslie et al. (2017) and Kablan et al. (2017)). The concave quadratic model has been very popular for describing the crop yield response to nitrogen, $Y(N) = aN^2 + bN + c$, where a, b, c, are constant parameters, omitting any weather variables (e.g., Rajsic & Weersink (2008), Rajsic et al. (2009) and Leslie et al.

(2017)).

From an ecological point of view, excessive application of nitrogen fertilizer will interrupt the soil salinity balance and weaken disease resistance and lodging resistance of crops, which accordingly may result in a decline in fertilizer efficiency and yield (Hilbert et al. (2015) and Kong et al. (2017)). The quadratic model is able to capture this adverse effect. Thus, we employ the following quadratic model in this chapter as the representative deterministic relation between crop yield and fertilizer input.

$$Q_T = a_1 N_t^2 + a_2 N_t + a_3, \qquad 0 \leq t \leq T \tag{2.2}$$

where Q_T is crop output level at crop maturity time T, N_t is the total amount of fertilizer used at time t, $a_1 < 0$, a_2, $a_3 > 0$ are parameters which need to be estimated by crop yield data. Ecologically, $a_3 > 0$ denotes the natural productivity of soil without fertilizer.

2.2.2 Modelling corn price uncertainty

Like other commodities, corn prices tend to be highly volatile, which needs to be taken into account by farmers in making the optimal fertilizer application decisions. Geometric Brownian motion (GBM) and mean reversion (MR) are two stochastic processes that are extensively used for describing commodity prices (Schwartz (1997) and Chen & Insley (2012)), and are also adopted in our analysis. Schwartz (1997) argues that some commodities prices, especially for most natural resources, follow mean-reverting processes (MR) with a long-run mean price level determined by market factors such as the cost of substitutes. We contrast results derived from the GBM and mean reverting (MR) models.

We first present these price processes in the $\mathbb{P}$-measure, meaning that the drift terms

are not risk adjusted. The common GBM process is given as

$$dP_t = \alpha P_t dt + \sigma_1 P_t dZ_t \tag{2.3}$$

where P_t is the crop price at time t. α is the drift rate[4]. The first term on the RHS denotes the drift term and the remaining term represents the random disturbance in the level of crop price with σ_1 representing the price volatility. This disturbance may be the result of crop market fluctuations, temporary changes in government market policy, and other factors those are not captured by the drift term. The term dZ_t is an increment in a stochastic process Z that follows the standard Brownian motion.

The choice of mean reverting model is a common variation of the Ornstein-Uhlenbeck process ($\mathbb{P}$-measure):

$$dP_t = \theta\left(\bar{P} - P_t\right) dt + \sigma P_t dZ_t \tag{2.4}$$

where $\bar{P}$ is the constant long-run mean or equilibrium of the crop price and θ is constant as the speed of mean reversion. As the OU process is used to model price mean reverting behaviour we have $\theta > 0$. σ represents the price volatility.

2.2.3 Farmer's value function

Consider a representative profit-maximizing farmer who chooses the quantity of fertilizer application N at the fixed application time $t = 0$ (spring seeding date), over one typical crop production cycle. The crop market price will evolve continuously as specified by the assumed Ito process, however, the spot transaction price will not be realized until the crop reaches maturity, denoted time T, which is assumed to be the fixed fall

[4]Another associated concept is the risk-adjusted drift rate μ under $\mathbb{Q}$-measure. The relation between α and μ is $\mu = \alpha - \lambda_P \sigma_1$, where λ_P represents the market price of risk for crop prices. The contrast between $\mathbb{P}$-measure and $\mathbb{Q}$-measure valuation is elaborated on Appendix C. Under the $\mathbb{Q}$-measure, the risk adjusted price process would substitute μ for the drift rate, rather than α.

harvesting date. Considering only one typical crop production cycle, the payoff at $t = T$ is $\pi_T = P_T(a_1N^2 + a_2N + a_3)$. Our objective function for the representative farmer is the maximization of the following expected net profit flow:

$$V(P, N, t = 0) = \max_N E_{\mathbb{Q}}\left\{e^{-rT}P_T(a_1N^2 + a_2N + a_3) - cN\right\}, \; P(0) = p_0 \tag{2.5}$$

where $V(P, N, t)$ denotes the value of the corn at time t when N is chosen optimally. For the GBM scenario, we use $r > 0$ as the constant risk free discount rate assuming that the expected crop price is found under the risk-neutral or $\mathbb{Q}$-measure. Using the standard contingent claims approach, the $\mathbb{P}$-measure price processes given in section 2.2.2 can be transformed to the $\mathbb{Q}$-measure by deducting a risk premium. This is elaborated on in Appendix C as well as in Dixit et al. (1994). The initial crop price p_0 is observed by the farmer. c is the constant price of per unit of fertilizer. N is the fertilizer application decision made at the seeding date. It is assumed that the farmer not only has rational expectations on the future price but also realizes the future price is a stochastic process. $\left\{e^{-rT}P_T(a_1N^2 + a_2N + a_3)\right\}$ is the present value of total crop revenue received at T. The yield level at maturity is predetermined when the fertilization decision is made. cN is the current cost of fertilizer.

2.3 Closed form solutions

Crop price follows GBM

In this simple setting, we are able to derive closed form expressions for the optimal fertilization decision. We are looking for the fertilizer choice at time zero that maximizes the expected value of discounted net benefits from planting the crop. This is easy to do under the GBM assumption as we can find the expectation directly. First determine the

expected value under the $\mathbb{Q}$-measure. Let μ denoted the risk adjusted drift rate. Then, the expected value of price at maturity is given as $E(P_T) = p_0 e^{\mu T}$ where μ is defined as $\mu = \alpha - \lambda_P \sigma_1$ and λ_P is the market price of risk[5]. Substituting this expected value back into Equation (2.5), we can rewrite the objective function as:

$$V(P, N, t = 0) = \max_N \left\{ e^{-rT} p_0 e^{\mu T} \left(a_1 N^2 + a_2 N + a_3 \right) - cN \right\} \tag{2.6}$$

Then, we can find the optimal solution through the first order condition:

$$\frac{\partial V}{\partial N} = e^{-rT} p_0 e^{\mu T} \left(2a_1 N + a_2 \right) - c = 0$$

Therefore, after necessary substitution, we can write the closed form expression for the optimal amount of fertilization under the assumption that price follows a GBM process as

$$N^{\star gbm} = \frac{1}{2a_1} \left[\frac{c}{p_0} e^{(r-\mu)T} - a_2 \right], \quad where \quad \mu = \alpha - \lambda_p \sigma_1 \tag{2.7}$$

or equivalently,

$$N^{\star gbm} = \frac{1}{2a_1} \left[\frac{c}{p_0} e^{(r-\alpha+\lambda_p \sigma_1)T} - a_2 \right] \tag{2.8}$$

With the restriction of $N^{\star gbm} > 0$, and given $a_1 < 0$ and $a_2 > 0$, it follows that $a_2 > \frac{c}{p_0} e^{(r-\alpha+\lambda_p \sigma_1)T}$ is a necessary constraint.

Crop price follows MR process

We now consider the optimal decision under the mean-reverting price uncertainty assumption. With a generalized mean-reverting process assumption, we can no longer directly find an expression for the expected price at time T in the $\mathbb{Q}$-measure. Instead we use the

[5]The derivations of $E(P_T)$ and λ_P can be found in Appendix B and C.

contingent claims approach to derive a partial differential equation describing the value of the farmer's asset. This PDE can be solved analytically (Insley & Lei (2007) and Insley & Wirjanto (2010)).

Applying Ito's lemma to Equation (2.5) and using standard contingent claim arguments, we can derive the following Hamilton-Jacobi-Bellman (HJB) equation that describes the value function V:

$$\left[\theta(\bar{P} - P) - \lambda_P \sigma P\right] V_P + \frac{1}{2}\sigma^2 P^2 V_{PP} - rV + V_t = 0, \quad t > 0, \; P(0) = p_0 \tag{2.9}$$

We omit the time subscript on P when there is no ambiguity. At the initial time $t = 0$, $P = p_0$. V_P and V_{PP} are first order and second order partial derivatives respectively. V_t is the partial derivative with respect to time variable $V_t = \frac{\partial V}{\partial t}$. Also, we have a value matching condition for the maturity payoff:

$$V(N, P, t = T) = P_T \left(a_1 N^2 + a_2 N + a_3\right) \tag{2.10}$$

To solve for the value function V in the PDE Equation (2.9), we first rewrite Equation (2.9) to the following form:

$$V_\tau = \left[\theta\bar{P} - (\theta + \lambda_P \sigma)P\right] V_P + \frac{1}{2}\sigma^2 P^2 V_{PP} - rV \tag{2.11}$$

where τ defined as $\tau = T - t$ denotes the remaining time to crop maturity. V_τ is the partial derivative with respect to time variable $V_\tau = \frac{\partial V}{\partial \tau}$.

The partial differential equation (2.11) can be analytically solved by first guessing the solution for V as $V = A(\tau)P + B(\tau)$. Substituting $V_\tau = A_\tau P + B_\tau$ where $A_\tau = \frac{\partial A(\tau)}{\partial \tau}$, $B_\tau = \frac{\partial B(\tau)}{\partial \tau}$, $V_P = A(\tau)$ and $V_{PP} = 0$ back into Equation (2.11) gives us the following

identity:

$$A_\tau P + B_\tau = \theta\bar{P}A(\tau) - rB(\tau) - PA(\tau)(\theta + r + \lambda_P\sigma) \tag{2.12}$$

Equating corresponding parts gives us $A_\tau = -A(\tau)(\theta+r+\lambda_P\sigma)$ and $B_\tau = \theta\bar{P}A(\tau)-rB(\tau)$ which implies

$$A(\tau) = A_0 e^{-(\theta+r+\lambda_P\sigma)\tau} \tag{2.13}$$

$$B_\tau + rB(\tau) = \bar{P}\theta A_0 e^{-(\theta+r+\lambda_P\sigma)\tau} \tag{2.14}$$

Solving Equation (2.14) by employing the integrating factor technique, we use the fact $\frac{\partial}{\partial\tau}[e^{r\tau}B(\tau)] = e^{r\tau}[B_\tau + rB(\tau)]$. Then Equation (2.14) will evolve to

$$e^{-r\tau}\frac{\partial}{\partial\tau}\left[e^{r\tau}B(\tau)\right] = B_\tau + rB(\tau) = \bar{P}\theta A_0 e^{-(\theta+r+\lambda_P\sigma)\tau} \tag{2.15}$$

Rearranging and integrating (2.15) between the interval $[0,\tau]$ for both sides at the same time,

$$\int_0^\tau \frac{\partial}{\partial\tau'}\left[e^{r\tau'}B(\tau')\right]d\tau' = \int_0^\tau \bar{P}\theta A_0 e^{-(\theta+\lambda_P\sigma)\tau'}d\tau' \tag{2.16}$$

$$e^{r\tau'}B(\tau')\Big|_0^\tau = -\frac{\bar{P}\theta A_0}{\theta+\lambda_P\sigma}e^{-(\theta+\lambda_P\sigma)\tau'}\Big|_0^\tau \tag{2.17}$$

which finally gives the expression for $B(\tau)$,

$$B(\tau) = B_0 e^{-r\tau} + \frac{\bar{P}\theta A_0}{\theta+\lambda_P\sigma}\left(e^{-r\tau} - e^{-(\theta+r+\lambda_P\sigma)\tau}\right) \tag{2.18}$$

Substituting (2.13) and (2.18) back into $V = A(\tau)P + B(\tau)$ results in:

$$V(N,P,\tau) = A_0 P e^{-(\theta+r+\lambda_P\sigma)\tau} + B_0 e^{-r\tau} + \frac{\bar{P}\theta A_0}{\theta+\lambda_P\sigma}\left(e^{-r\tau} - e^{-(\theta+r+\lambda_P\sigma)\tau}\right) \tag{2.19}$$

Using value matching condition for the maturity payoff $V(N,P,\tau=0) = P_T\left(a_1N^2 + a_2N + a_3\right)$

to solve for $A_0 = (a_1 N^2 + a_2 N + a_3)$, $B_0 = 0$. Then combining A_0, B_0 and rearranging Equation (2.19) gives the closed form expression for the value function, with the current one-off fertilizer cost cN at initial seeding date $t = 0$ ($\tau = T$):

$$V(N, P, t = 0) = (a_1 N^2 + a_2 N + a_3) \left[P e^{-(\theta + r + \lambda_P \sigma)T} + \frac{\bar{P}\theta}{\theta + \lambda_P \sigma} \left(e^{-rT} - e^{-(\theta + r + \lambda_P \sigma)T} \right) \right] - cN \tag{2.20}$$

To determine the optimal fertilizer application amount N, we simply take the first order derivative for $V(N, P, t = 0)$ with respect to N and set it to 0, which eventually gives the optimal fertilizer application amount N under the $\mathbb{Q}$-measure:

$$N_{\mathbb{Q}}^{\star mr} = \frac{1}{2a_1} \left[\frac{c}{e^{-(\theta + r + \lambda_P \sigma)T} \left(p_0 - \frac{\bar{P}\theta}{\theta + \lambda_P \sigma} \right) + \frac{\bar{P}\theta}{\theta + \lambda_P \sigma} e^{-rT}} - a_2 \right] \tag{2.21}$$

With the restriction of $N_{\mathbb{Q}}^{\star mr} > 0$, and given $a_1 < 0$, it follows that

$$a_2 > \frac{c}{e^{-(\theta + r + \lambda_P \sigma)T} \left(p_0 - \frac{\bar{P}\theta}{\theta + \lambda_P \sigma} \right) + \frac{\bar{P}\theta}{\theta + \lambda_P \sigma} e^{-rT}}$$

as a constraint.

2.4 Results analysis

This section analyzes the results that are derived from both closed form expressions of the farmer's optimal fertilization decision under GBM and MR assumptions.

2.4.1 The GBM case

From Equation (2.7), under the GBM scenario, it may be observed that crop price uncertainty (σ_1) shows up explicitly as a component of the risk premium $\lambda_P\sigma$, which means price uncertainty has a direct impact on the initial one-off fertilization decision. λ_P, called the market price of risk of P, represents the excess return over the risk free rate per unit of variability. $\lambda_P\sigma$ reflects the total excess return over the risk free return demanded by investors in order to be willing to hold assets that depend on P. In particular, assuming $\lambda_P > 0$, a higher σ or σ_1 implies a higher risk premium, $\lambda_P\sigma$ or $\lambda_P\sigma_1$.

Using the fact that $a_1 < 0$, we have $\frac{\partial N^{\star gbm}}{\partial \sigma_1} < 0$ implying that a higher level of uncertainty as reflected in a higher σ_1 will reduce the optimal fertilizer quantity, assuming that $\lambda_P > 0$. The fertilizer application is irreversible and the decision is made (at t_0) before the corn price realized at maturity (T). Higher price volatility implies that the corn price has both higher upside and lower downside potentials (relative to the lower price volatility scenario). If prices at maturity are very low, farmers will have lost money on the fertilizer application. If corn prices are very high at maturity, farmers will benefit from a boost in total corn revenue, but there is still a decreasing marginal benefit from fertilizer as a result of $a_1 < 0$ - a concave yield function property.

From Equation (2.7), we observe that a larger value of current price p_0 or a lower value of fertilizer cost, c, will increase the optimal quantity of fertilizer. For example, an input tax policy will give a larger unit cost $c' = c(1 + tax)$ which will correspondingly reduce the farmer's optimal fertilizer application amount.

Next, we consider how maturity date T, will affect fertilizer application. Since $a_1 < 0$ in Equations (2.7 and 2.8), the impact of T depends on the sign of $(r - \alpha + \lambda_P\sigma)$. If $r > \alpha - \lambda_P\sigma$, the risk free discount rate exceeds the risk adjusted expected crop price return, implying that farming the type of crop with a longer growth cycle will reduce

the optimal fertilizer quantity. Intuitively, a longer time before crop maturity reduces the present value of applying fertilizer at the margin. Instead, if $\alpha - \lambda_P \sigma > r$, a longer time to crop maturity increases the marginal benefit of applying fertilizer. Finally we observe from Equation (2.8) that $\frac{\partial N^{\star gbm}}{\partial \alpha} > 0$. An increase in the P-measure price drift rate, increases the optimal quantity of fertilizer. This implies that the farmer's excessive application of fertilizer might be explained by the case where the farmer overestimates the actual crop price return α. A summary of the comparative statics for the GBM process is provided in Table (2.1).

In many agricultural papers such as Baethgen et al. (1995) and Cui et al. (2010), the key dilemma facing farmers is specified as how to maximize yield based on the yield response curve. Cui et al. (2010) provide evidence that pursuing high grain yield has been the top priority in many regional recommendation policies and site-level farming practices. Let $N^{\star maxyield}$ refers to the optimal fertilizer application when the goal is yield maximization. As $a_1 < 0$ and $c > 0$, it is easy to show the relation $N^{\star GBM} < N^{\star maxyield} = -\frac{a_2}{2a_1}$, which means using the yield maximization principle, instead of crop value maximization principle, will lead to an over-application of nutrients. Therefore, our results from the GBM scenario suggest that current over-application of nutrient relative to the economically optimal amount could be attributed to the fact that the current fertilizer recommendation is mistakenly built on the yield-maximizing principle, as well as the farmer's potential overestimation of crop price return. Even though an increase in price uncertainty will increase the optimal amount of fertilizer applied, which is not an over-application from the farmer's viewpoint, this ignores the negative environmental consequences of increased fertilizer use.

2.4.2 The MR case

From Equation (2.21), it may be observed that when prices follow a mean reverting stochastic process, crop price uncertainty (σ) has an impact on the initial one-off fertilization decision. We show in Appendix D that $\frac{\partial N^{*mr}_{\mathbb{Q}}}{\partial \sigma} < 0$, which is consistent with what was shown for the GBM case, $\frac{\partial N^{*gbm}}{\partial \sigma_1} < 0$. An increasing level of price uncertainty as represented by a higher σ will reduce the optimal fertilizer application. Since $a_1 < 0$, from Equation (2.21), a higher observed initial price p_0 will also cause the farmer apply more fertilizer.

Measuring the effect of the mean reverting speed θ is less straightforward, as shown in Appendix D. Intuitively, even though the current crop price is below the mean level or certain critical value, an observed higher reversion speed could describe a "promising future" to the farmer, which will increase the amount of fertilizer use as a result. Similarly, even if a high price above the mean level presents for now, a higher reversion speed may indirectly lower the amount of fertilizer the farmer will apply by describing a "dismal prospect".

Interestingly, if we relax the assumption that true mean reversion speed θ is observed as part of the information set at initial time, then our results could partially explain the fertilizer over-application problem. Regarding θ (the true mean-reverting speed) as an unobserved information, farmers with full knowledge of P_0 and $\bar{P}$ would use all information they have to form an estimate (could be denoted as $\hat{\theta}$). However, this estimation $\hat{\theta}$ could be larger or smaller than the true value θ as a result of estimation errors. If the overestimation $\hat{\theta} > \theta$ (or underestimation $\hat{\theta} < \theta$) happens with the low observed initial price $P_0 < \bar{P}$ (or high observed initial price $P_0 > \bar{P}$), the over-application of fertilizer will be present relative to the economically optimal amount. Therefore, fertilizer over-application problem could be partially attributed to the misspecification or estimation error regarding price process

caused by asymmetric information on crop market.

Similar to the GBM scenario, our results under the mean-reverting process could provide an explanation for the fertilizer over-application resulting from mistakenly adopting the yield-maximizing principle, as showed in Appendix D. A summary of the comparative statics is provided in the following Table 2.1:

Table 2.1: A summary of parameter sensitivity results

Parameter Sensitivity	Under GBM assumption	Under MR assumption
$\frac{\partial N}{\partial c}$	< 0	< 0
$\frac{\partial N}{\partial P_0}$	> 0	> 0
$\frac{\partial N}{\partial \alpha}$ or $\frac{\partial N}{\partial \theta}$	> 0	> 0 iff $\bar{P}(1+F) > P_0$
$\frac{\partial N}{\partial \sigma}$	< 0	< 0
$\frac{\partial N}{\partial T}$	> 0 iff $r < \alpha - \lambda\sigma$	> 0 iff $\frac{P_0}{\bar{P}} < \psi_{\mathbb{Q}}$

Note that λ_P is assumed to be positive.
where $\psi_{\mathbb{Q}} = \left[1 - \frac{re^{(\theta+\lambda_P\sigma)T}}{\theta+\lambda_P\sigma+r}\right] \frac{\theta}{\theta+\lambda_P\sigma}$ and $F = \frac{2\theta}{\theta+\lambda\sigma} + \frac{2\theta+\lambda\sigma}{T(\theta+\lambda\sigma)^2}\left[e^{(\theta+\lambda\sigma)T} - 1 - (\theta+\lambda\sigma)T\right]$.

These findings, of course, depend on the particular modelling assumptions. For example, to derive the closed-form solution for optimal fertilizer application, a simplified crop price process (GBM or MR) is assumed. Thus, the effect of price uncertainty on optimal fertilization may vary with the change of price process choice. Parameter sensitivity may also differ from these results when we depart from our particular decision model setting to a more complex scenario. In this price uncertainty discussion, our decision model assumes the farmer makes a one-off unchangeable decision regarding fertilizer application that affects total profit only at the payoff at maturity. This implies that the farmer does not have any options to adjust the fertilizer decision.

In later Section 3.5.2, an exponential corn yield function is proposed in Equation 3.16.

Correspondingly, using the exponential corn yield function and assuming the farmer makes a one-off unchangeable decision, we re-derive the closed form optimal fertilizer applications under GBM and MR assumptions (Equation (2.8) and (2.21)) as Equation (E.2) and (E.4). Details are presented in Appendix E. Results based on the exponential corn yield model give us the same sensitivity conclusions as Table 2.1.

2.5 Limitations and conclusion

In this chapter we explored the impact of crop price uncertainty on a farmer's optimal fertilizer application decision using two different models of prices. Given the simplifying assumptions in the decision model, closed form solutions are derived. A simplified crop yield function popular in the literature is adopted for the analysis. Crop prices are specified following as geometric Brownian motion or a generalized mean-reverting process. Both closed form solutions indicate that price uncertainty has a negative effect on farmer's one-off fertilizer application decision in our model setting. Many other factors or parameters that could affect the optimal decision are found and examined in this paper. In addition, two possible reasons of fertilizer over-application are also discussed. Assuredly, we should treat this model as a simplified unique growth cycle problem which provides a benchmark for comparison with more detailed models.

Much research remains to be done in the field of optimal fertilization under uncertainty. First, instead of using a deterministic crop production function, a stochastic crop yield function with both fertilizer input and weather uncertainty need to be examined in the next chapter. Second, as part of the optimal fertilization problem for farmers, the assumption of an one-off application needs to be relaxed. Optimal fertilizer choices with more than one application date, weather variation and price uncertainty are analyzed in the next chapter.

Chapter 3

Optimal Fertilizer Application Under Price and Weather Uncertainties

3.1 Introduction

Agricultural crop yields are highly affected by weather conditions. In addition to the impact on overall crop health, weather conditions may also affect farmers' fertilizer application decisions. For example, N (Nitrogen) can be lost from the soil in a rain intensive season and as a result, crops may have a low N uptake efficiency. Qian et al. (2002) note that precipitation regimes are perceived as playing an essential role in agricultural water management, which in return affects crop productivity. As a result, farmers' fertilizer application decisions are expected to be adjusted in a response to current or anticipated weather states. Thus, to fully understand farmers' fertilizer application decisions, both weather and crop price uncertainties need to be examined.

The key question this chapter tries to answer is how farmers will change their optimal fertilizer application in the presence of growing season weather and crop price uncertain-

ties. Several papers have attempted to address these impacts, as discussed in the literature review section in Chapter 2. To summarize, uncertainty associated with optimal input use has been suggested as a possible reason for the fertilizer over-application of fertilizer (Babcock (1992) and Sheriff (2005)). In investigating this issue, both Babcock (1992) and Rajsic et al. (2009) found nitrogen fertilizer to be risk-increasing, meaning that a higher fertilizer rate increases the variance of crop profit. For a risk neutral farmer, Rajsic et al. (2009) found that increased production risk could increase the expected return from applying more than recommended amounts. However, risk averse farmers may lower fertilizer application rates in response to the increased production risk. It should be noted that these papers use static objective functions and there is limited analysis of the specification of weather and price uncertainty.

In this chapter, we extend the farmer's decision model of Chapter 2 to include crop price uncertainty, weather factors and two fertilizer decisions. In practice, more than two fertilizer decisions may be made during the growing season, but we restrict our model to only two decisions for simplicity. We specify the farmer's fertilizer application decision problem as an optimal control problem. The farmer maximizes net benefit through the optimal choice of fertilizer amounts at both split application dates. A crop yield function for corn is specified and estimated which gives crop output as a function of average soil nutrient content and weather conditions over the crop growing season. We focus on the optimal application of nitrogen fertilizer. Soil nutrient content is determined by fertilizer application as well as nutrient loss due to daily precipitation.

Weather conditions over the growing season are uncertain and are summarized by an index which reflects cumulative heat effects as indicated by corn heat units ($\bar{H}$) and cumulative precipitation ($\bar{R}$). $\bar{H}$ is calculated from daily temperature variables, which are modelled as mean-reverting stochastic processes. Precipitation is characterized by two models: the first capturing whether or not rain occurs in a given time period, and the

second capturing the rainfall rate per unit of time. The crop price is modelled as a mean reverting stochastic process as is done in Chapter 2. Harvesting is assumed to happen at a fixed time at the end of the growing season. The fertilizer application decision is made at two points during the corn growing cycle, which reflects a typical one rotation period farm operation whereby fertilizer may be applied at the beginning of the growing cycle and then a second application may be done several weeks later, if deemed desirable.

Given the number of stochastic and path dependent state variables, closed form solutions are not available. Numerical solution using a dynamic programming algorithm is also impractical. Instead, our approach is to specify the HJB partial differential equation (PDE) that fully describes the decision problem. We then undertake Monte Carlo analysis to determine the expected value of a range of possible farmer decisions regarding fertilizer application. By limiting the number of admissible controls, we are able to determine the optimal solution through exhaustive search. The decision model is parameterized using data on weather, corn growth and fertilizer application from Iowa, which is a main corn growing area and is the source of serious nitrogen pollution in local water bodies and in the Mississippi River watershed. Our results provide considerable intuition about the optimal fertilizer application principle from a rational farmer's perspective. Our numerical example applies to corn planting, so we will refer to the crop as corn, although the model is applicable to a number of different crops.

3.2 Literature on weather modelling

The uncertainty analysis in this thesis requires a crop output model as a function of weather (temperature effect as measured by Crop Heat Units, H, and cumulative precipitation, $\bar{R}$) as well as soil nutrient content, S. Soil nutrient content depends on fertilizer application, N, as well as daily nutrient losses due to rainfall. There is a large volume

of current literature that models temperature and precipitation as inputs to agricultural production. However, there is a lack of literature addressing weather and fertilizer impacts as joint crop production inputs. In this section, we integrate and compare the existing diverse research linking weather factors to crop yields as background for our crop production model which relates crop output to both temperature, precipitation and fertilizer input.

3.2.1 Stochastic weather generators

Stochastic weather generators, including Weather GENerator (WGEN) (Richardson (1981) and Richardson & Wright (1984)), the CLIMate GENerator (CLIMGEN) (Nicks & Gander (1994), Nicks et al. (1995) and Stöckle et al. (1999)), Weather Generators (WeaGETS) (Chen et al. (2012*a*) and Chen et al. (2012*b*)) and the Long Ashton Research Station-Weather Generator (LARSWG) (Semenov & Barrow (2002)), have been used in climate and agronomic research for many years to create synthetic time series of weather data for describing the distribution of future weather patterns at particular locations (Chen & Brissette (2014)). These weather generator models have focused on modelling of the precipitation process and temperature on a long time series basis. Chen & Brissette (2014) compare these popular stochastic weather generator models in terms of their ability to simulate precipitation and temperature for a particular region in China. Depending on the particular application, other weather variables such as humidity and wind speed are also included in some of weather generator models.

Wilks & Wilby (1999) and Ailliot et al. (2015) have provided good overviews of weather generator models which include daily maximum, minimum temperature model and daily precipitation models. Maximum and minimum daily temperature models are discussed in Wilks (1999*b*), Mavromatis & Hansen (2001), Qian et al. (2002) and Mraoua (2007). For example, in classic weather generator WGEN and WTGROWS models (Wilks (1999*b*) and

Qian et al. (2002)), meteorological variables like minimum and maximum daily temperature have been generally modeled by autoregressive processes. This also applies to the Matlab-based daily weather generator WeaGETS (Chen et al. (2012*a*) and Chen et al. (2012*b*)).

In most weather generator models, the occurrence of daily precipitation and the amount of daily precipitation are modelled separately. The occurrence of daily precipitation is typically modelled as a Markov chain of first order (including Qian et al. (2002), Yusuf et al. (2014), Kannan & Farook (2015) and Hersvik & Endrerud (2017)). For example, Wilks & Wilby (1999) and Qian et al. (2002) model daily precipitation occurrence, daily precipitation amounts, maximum or minimum temperature as a first-order two-state Markov model, a double exponential distribution and a first-order autoregression model respectively. Yusuf et al. (2014) study the possibility of daily low rainfall, moderate rainfall and high rainfall based on a Markov chain model for daily precipitation occurrence. Kannan & Farook (2015) use the classic first-order Markov chain for simulating daily precipitation occurrence and a double exponential distribution for generating daily rainfall intensity, which are most commonly used in weather generators WGEN and LARS-WG. In WeaGETS (Chen et al. (2012*a*) and Chen et al. (2012*b*)), exponential distribution is used to produce wet day precipitation quantity.

An alternative to using Markov chain models to generate the occurrence of wet and dry days, are spell-length models (Wilks (1999*a*), Schoof & Pryor (2008) and Li et al. (2014)). For example, Wilks (1999*a*) examined different formulations for the occurrence- and amounts-components of stochastic daily precipitation models with respect to the overall goodness of fit. For the first-order Markov model, the frequencies of the lengths of dry or wet spells (x consecutive days) follow the simple geometric distribution. That is, a geometric spell lengths model is equivalent to the first-order Markov model, and the

probability distribution function for the spell length is

$$Pr(X = x) = p(1-p)^{x-1}, p = p_{ij}, i = 0, 1; j = 0, 1; x = 1, 2, 3...$$

where X is the number of consecutive days being wet, $p = p_{01}$ is the transition probability from dry to wet for dry spells and $p = p_{11}$ is for remaining in wet spells. Using this simple version of a spell-length model, precipitation occurrence is not simulated day by day, but rather the length x of the next spell (alternating between wet and dry spells) is simulated. In addition, Schoof & Pryor (2008) compare the distributions of wet and dry spells length from simulated first order Markov chains and those from spell-length models with the observed monthly rainfall occurrence process at 831 stations in the contiguous United States. They find that results from spell-length models are consistent with those from Markov chain models for the majority (68.4%) of all the stations and months examined.

Precipitation amounts are strongly skewed to the right with frequent small amounts of daily precipitation along with rarer large precipitation occurrences. Common models of daily precipitation amount include the exponential distribution, the gamma distribution, and mixed exponential distribution (Todorovic & Woolhiser (1975), Woolhiser & Roldan (1982), Wilks (1999*a*), Wilks (1999*b*), Qian et al. (2002), Martin-Vide (2004), Brissette et al. (2007), Chen et al. (2012*a*), Chen & Brissette (2014) and Li et al. (2014)). Wilks & Wilby (1999) compare the fitted values from these three probability distributions with historical data for precipitation at Ithaca, New York, from 1900 to 1998, and indicate that the mixed exponential distribution provides the best fit. Besides, Wilks (1999*a*) and Qian et al. (2002) find that using gamma distributions to represent precipitation amounts appears to be clearly inferior to the mixed exponential distributions. One-parameter exponential distribution is first employed by Todorovic & Woolhiser (1975) and Woolhiser & Roldan (1982) to model daily precipitation distribution. Afterwards, both Martin-Vide

(2004) and Brissette et al. (2007) have attempted to model daily rainfall amounts distribution as the simple exponential distribution. Martin-Vide (2004) contends that the distribution of rainfall amount frequencies can be represented by exponential distribution for the reason that in a given period many small daily amounts of precipitation will occur, whereas few large daily amounts will do. These authors also note that most stochastic weather generators assume precipitation amounts conditional on precipitation occurrence are independent. In Chen et al. (2012*a*), the gamma and exponential distributions are both examined as models of the daily rainfall amount distribution at the Ottawa and Churchill weather stations. Their results demonstrate that the most widely used model, the first-order Markov chain, is adequate at producing precipitation occurrence and the gamma distribution seems better than the exponential distribution in generating precipitation quantity. However, both the exponential and gamma distributions reproduce the uncertainty of daily precipitation very well. Thus, in our thesis, we will compare the simulated daily precipitation using a one-parameter exponential distribution and a gamma distribution.

3.2.2 Weather models for valuing financial derivatives

The stochasticity of weather in agriculture is creating an emerging market for weather derivatives which serve as a new agricultural risk management tool to hedge weather risks. For example, there are weather options and a futures market for contracts on weather indices such as heating and cooling degree-days (Turvey (2001), Sun & van Kooten (2015), Wang et al. (2015), Wang et al. (2015), Sun & van Kooten (2015), Ivana et al. (2016) and Gyamerah et al. (2019)). The finance literature has sought parsimonious models of temperature that could adequately capture temperature uncertainty for pricing weather derivatives. Ivana et al. (2016) have given a good summary of insights from the literature

on the hedging effectiveness of weather derivatives in agriculture. The underlying index in most weather derivatives is built on temperature or precipitation.

Starting from the farmers' profit maximization problem, Turvey (2005) includes the weather variable W (represented by cumulative degree-days) into a crop production function $Q(W)$ as the unique input. In Turvey (2005), W is described as following a continuous time stochastic differential equation (geometric Brownian motion process) and is used in the pricing of degree-day derivatives. Besides, daily averaged temperature has been modelled as a mean reverting Ornstein-Uhlenbeck processes in most literature (Alaton et al. (2002), Benth & Benth (2007), Mraoua (2007), Wang et al. (2015), Sun & van Kooten (2015) and Gyamerah et al. (2019)). The main differences among these studies is the seasonality factor and the volatility form in their temperature processes. For example, Gyamerah et al. (2019) presented a seasonal fluctuation component ($sin(\cdot)$) in the long run mean of averaged daily temperature, while Benth & Benth (2007) modeled the volatility of daily average temperature to be a seasonal function where seasonality was captured by a combination of $sin(\cdot)$ and $cos(\cdot)$ functions.

However, most of these finance papers focus only on weather derivatives pricing with daily average temperature as the underlying weather index and employ long run time series weather index data for empirical studies. Rare attention has been paid to incorporating the weather model into the crop yield process as well as modelling precipitation in the stochastic manner.

3.3 Literature on crop growth modelling

It is common in the agricultural economics literature to use stylized models whereby crop growth is a function of either nitrogen application or weather, depending on the focus

of the study. In this thesis we seek to include both weather (temperature and precipitation) and nitrogen application as determinants of crop growth. To support our modelling choices we first present a review of the relevant literature.

3.3.1 Literature on yield and fertilizer application

Several papers have attempted to examine the relation between corn yield and fertilizer inputs (Babcock (1992), Sheriff (2005) and Rajsic et al. (2009)). Specifically, Babcock (1992) employed a Leontief crop production function that involves nitrogen input in a linear form:

$$F(Nitrogen, Weather) = min(\alpha + \beta N, f(W))$$

where N is the applied nitrogen and W is the random weather variable that refers to rainfall in there paper, α, β are constant parameters. Using this linear plateau function, Babcock (1992) analyses the impact of weather uncertainty and soil nitrate uncertainty on the optimal nitrogen application which is derived from solving a static expected profit maximization problem. Rajsic et al. (2009) employed quadratic and quadratic plateau yield functions to represent the relation between corn yield Y and nitrogen input N, which are

$$Y = \alpha + \beta_1 N + \beta_2 N^2$$

and

$$Y = \begin{cases} \alpha + \beta_1 N + \beta_2 N^2 & \text{when } N \leq -\frac{\beta_1}{2\beta_2} \\ Y^{max} & \text{otherwise} \end{cases} \tag{3.1}$$

respectively, where α and $\beta_1 > 0$, $\beta_2 < 0$. Using the above functions, Rajsic et al. (2009) examines the effect of production risk on farmers' optimal nitrogen rate and contrasts objective functions featuring expected profit maximization with expected utility maximization.

Equation (3.1) shows yield rising at a decreasing rate with the quantity of nitrogen applied up to a maximum yield level, after which any applied nitrogen has no impact. An alternative is a concave exponential yield function such as $Y = \alpha(1 - e^{-\beta N})$ for α, $\beta > 0$. A concave exponential curve can describe the natural corn growth process where corn yield will rise at a decreasing speed with respect to the soil nutrient level and will peak at the end of growing season when maturity conditions are met. This type of corn production function is also reasonable for describing the impact of other inputs into corn production, such as corn heat units. Concave exponential type crop growth curves have been used in several empirical studies (including Budantsev et al. (2010), Tadesse & Kim (2014), Pires et al. (2015), Dasgupta (2018), Abid et al. (2018) and Addy et al. (2020)).

Tadesse & Kim (2014), Pires et al. (2015) and Addy et al. (2020) used experimental data to estimate the exponential grain yield-nitrogen relationship. For instance, a concave exponential yield-input form was adopted by Pires et al. (2015) to describe the yield-nitrogen effect. Calculating nitrogen-use efficiency (NUE) over a period of 1970-2011 in Brazil, Pires et al. (2015) estimated the effect of applied nitrogen fertilizer on cereal yield as a statistic form: $Yield = 4.8096(1 - e^{-0.0009N})$, where $Yield$ is in ton/ha and N is nitrogen fertilizer in 1000 tons unit. Tadesse & Kim (2014) also estimated two concave exponential grain yield-nitrogen relations for maize by conducting experiments in two locations of Ethiopia. A recent study focuses on the inter-annual weather effect on cereal yield function; Addy et al. (2020) used a long-term winter wheat and barley yield experiment from 1968 to 2016 to estimate the linear-plus-exponential (LEXP) yield-nitrogen response curve, which is generally modelled as $y = a + br^N + cN$, where y is grain yield in ton/ha, N is nitrogen in kg/ha, a is the asymptotic yield, b, c, r are parameters that need to be estimated while r relates to the curvature of the response. Estimated parameters a, c, and r were positive, while b was negative. The fitted yield-nitrogen relations across different years are plotted in the Figure 3.1:

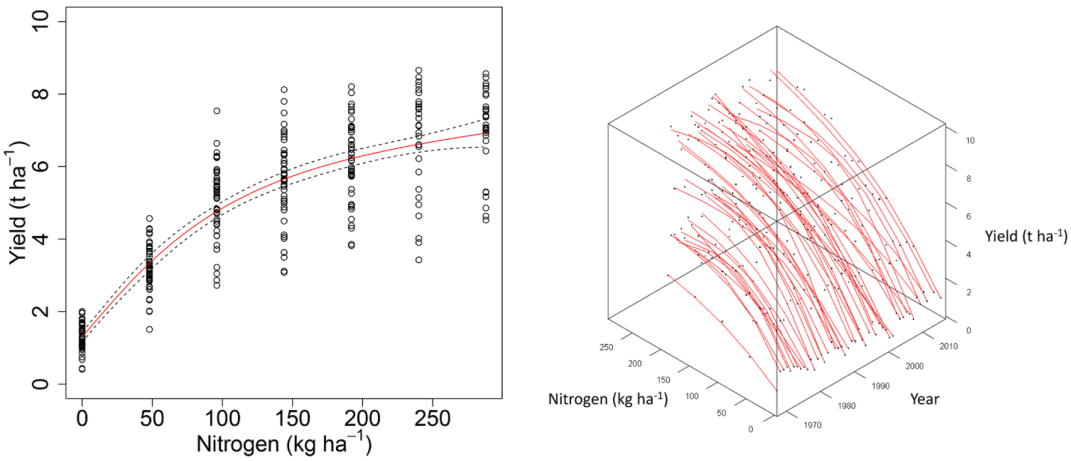

Figure 3.1: Relationship between winter wheat grain yield and applied nitrogen by Addy et al. (2020)

Weather conditions at key stages of crop development period were found to have a significant effect on the difference of estimated nitrogen-yield response curves across years, and thus will significantly change the nitrogen-yield parameter estimates (in Figure 3.1). Yield function in Addy et al. (2020) implies concave-shape yield-nitrogen response curves that indicate yield increases with respect to nitrogen at a decreasing rate, peaking at a certain level and remaining stable thereafter, which is consistent with findings from all the other studies.

3.3.2 Literature on yield and weather variables

This literature review section lists and discusses the existing studies on representing the relationship between crop yields and weather variability. There are a large number of papers on this topic across the agronomic and agricultural economics literature encompassing a wide variety of approaches. Literature is classified into four groups: statistical regression models; process-based models; statistical models with a Just-Pope stochastic production function; and models describing yield or return uncertainty as an Ito process. This section

makes a contribution to the literature by integrating and comparing how a range of different studies describe the link between weather factors and crop production.

One key distinction in the literature is between process bases and statistical models. Roberts et al. (2017) provides a good review of this issue. Process-based approaches use data and assumptions about key factors known to affect crop growth (such as soil characteristics, solar radiation, rainfall, temperatures, management practices) as inputs into mathematical models of plant growth and seed formation to arrive at yield predictions. The impact of changes in the levels and variability of any of the key factor inputs can thereby be examined. The statistical model approach uses statistical regression models to examine the historical relation between key determinants of crop growth (the independent variables) and yields. The estimated statistical relationship is used to make predictions about future yields under alternative scenarios for the independent variables. Roberts et al. (2017) notes that the two approaches are similar to what economists call structural and reduced form methods.

Statistical regression models Among those studies that examined the statistical relation between crop yield and weather indices, Vanotti & Bundy (1994) is an early paper to consider nitrogen recommendations and variations in corn yield, possibly caused by weather. In most areas of U.S., corn nitrogen recommendations are based on yield goals, sometimes with adjustments for soil characteristics. The paper reports a lack of consensus with how yield goals should be determined and notes that recommended nitrogen levels may be inconsistent with the yield potential of a particular area. Overestimating actual nitrogen needs results nitrate losses to the environment. Vanotti & Bundy (1994) separated Wisconsin experimental data into high-yielding years and low-yielding years and determined the associated optimal nitrogen application rates. They find that the optimal nitrogen rate for a specific soil is not closely related with the corn yield obtained. High

corn yields resulted in more crop nitrogen uptake than lower yields, but did not necessarily require higher nitrogen application rates. The authors explored the feasibility of basing environment-friendly corn nitrogen recommendations on soil and year-specific data rather than on yield goals. Vanotti & Bundy (1994) was one of the first to link nitrogen application rates with corn yield regimes. The corn yield response functions assumed to be quadratic and quadratic-plateau forms, which produced similar results.

Turvey (2001) empirically examined the impact of cumulative rainfall and a heat index (degree-days) on corn and soybean yields in Oxford County, Ontario. Yield data was obtained from OMAFRA[1] reports and weather data was selected from corresponding weather stations. Correlations between rainfall, heat and yields indicate that the most significant factor for corn and soybean yields is heat. Rainfall did not appear to contribute significantly to corn or soybean yield variability. Using a Cobb-Douglas form yield function, he obtained the following estimated equations

$$log(Y_{corn}) = 3.33 + 0.03Rain + 0.18GDD$$

$$log(Y_{soybean}) = 1.62 + 0.03Rain + 0.26GDD$$

where Y_{corn} and $Y_{soybean}$ are corn yield and soybean yield in bushels per acre (BU/A) unit, $Rain$ and GDD refer to the cumulative rainfall in mm unit and cumulative degree-day heat units from June 1 to August 31 each year. Their results indicated a low statistical significance of $Rain$ in both above regressions and higher corn or soybean yield always comes with a higher temperature-rainfall combination. A sensitivity analysis of yield to weather variability was performed. Rain and heat effects were classified to 3 regimes: High, Mean, Low. As a result, Turvey (2001) found that higher corn or soybean yield always comes with a higher temperature-higher rainfall regime.

[1]Ontario Ministry of Agriculture, Food and Rural Affairs . http://www.omafra.gov.on.ca/english/

Building a fixed-effect model in which temperature is perfectly substitutable over time and using a unique data set of corn yields and daily weather records for 1950-2004 from more than 2000 eastern US counties, Schlenker & Roberts (2006) found a nonlinear relationship between the effect of a 1-day period at a given temperature relative to 8^oC and the percentage change of annual corn yield. For example, a day of 36^oC will reduce annual corn yield by 3.1 percent and the threshold when temperature becomes harmful is 30^oC. In other words, corn yields were found to increase with moderate temperature raises, but decrease once above 30^oC.

Another paper that covered the effects of both temperature and precipitation on crop yields is Lobell et al. (2007), who collected data on six Californian crops (e.g. vegetables and fruits, excluding grain crops) and Californian climate data (daily maximum and minimum temperature, monthly precipitation) in their research. To assess the effect of climate on yields, they modeled yield as a function of time and two climate variables:

$$Y = a_0 t + a_1 X_1 + a_2 X_2 + a_{11} X_1^2 + a_{22} X_2^2$$

where X_1 and X_2 are monthly mean temperature and monthly total precipitation. As a primary conclusion, Lobell et al. (2007) listed, for each individual type of all six crops respectively, the most significant weather factor for yield or flowering (one of maximum or minimum temperature, precipitation) and the crucial growth periods that affecting yields.

All studies that examine impacts of climate change on crop yields are distinct from each other in their location of interest, crop type, weather variable choice and statistical crop-weather model. Lobell et al. (2006) used 1980–2003 records of state-wide yield, monthly average temperatures (minimum and maximum) and rainfall variations to estimate statistical yield responses to weather for six perennial crops in California. Lobell et al. (2006) argued that the advantage of using a statistical yield function is it intrinsi-

cally accounts for a wide range of mechanisms that can affect yields, while uncertainties in process-based models are often difficult to measure. Perennial crop yield response models are then used with monthly simulations of minimum, maximum temperatures and precipitation for 1980–2099 to evaluate yield uncertainty. The effect of climate uncertainty was represented by the yield distribution resulting from applying statistical yield models to each individual climate model scenarios. For example, the statistical response function of wine grapes yields to temperature and precipitation changes used in his study was

$$Y = 2.65T_{n,4} - 0.17T_{n,4}^2 + 4.78P_6 - 4.93P_6^2 - 2.24P_9 + 1.54P_9^2 - 10.50$$

where Y is the yield level (ton/acre), $T_{n,a}$ is the monthly average minimum temperature (n) of a^{th} month, P_a is the monthly rainfall of a^{th} month. One unique contribution made by Lobell et al. (2006) is that they specify the weather variable effects in terms of the month of the year. However, the statistical crop models his study used did not allow explicit consideration of nutrient inputs.

Even though Chen et al. (2016) note that agronomic literature has long suggested precipitation, temperature and radiation as the three most important factors for plant growth, radiation has been emphasised as an important input only for rice and wheat growth. Like the previous articles, Mearns et al. (1984), Wheeler et al. (2000) and Lobell et al. (2011) also examined the role that temperature plays in the crop growth and yield. These three articles are distinct in emphasizing temperature effects using data sets from different countries. Wheeler et al. (2000) reviewed the significance of temperature variability for annual crop yields, say, wheat or corn, but without giving any explicit statistical form for the relation between crop yield and weather variables. It is found that doubling the standard deviation of daily temperature with an unchanged seasonal mean would reduce grain yield to the same extent as a 2^oC increase in mean seasonal temperature.

Similar to Schlenker & Roberts (2006) in methodology, Lobell et al. (2011) found evidence for a nonlinear relationship between heat and maize yield in tropical regions using historical maize trials data from Africa. The effect of temperature on maize yield was modeled using a linear fixed-effect model, with an assumption that yield growth is a nonlinear function of heat, which included $GDD_{8,30}$ (Growing degree days between 8^oC and 30^oC) and GDD_{30+} as temperature variables. $GDD_{8,30}$ indicated a normal maize growing condition and GDD_{30+} indicated harmful heat. The estimations showed a decreasing concave nonlinear relationship between the yield change from 1^oC warming at different average growing-season temperature. A negative effect of GDD_{30+} was also found, which indicated that daytime heating is more harmful to maize than night-time warming. Mearns et al. (1984) studied the impact of extreme high temperature events on crop yields in U.S. without including an average temperature index or other weather variables. Both Mearns et al. (1984) and Lobell et al. (2011) selected 35^oC as the basic threshold for defining extreme weather events as well as examined how significant a change in the probability of extreme high temperature would affect crop yields. However, a statistical relation between crop yield and specified weather indices is not presented in their studies.

The most frequent statistical yield-weather model employed by the weather impact studies is a quadratic weather-yield relation. For example, Dixon et al. (1994), Cabas et al. (2010) and Shi et al. (2013) modelled precipitation and temperature as having a quadratic effect on yield, whereas Roberts et al. (2012) modelled the quadratic effect of growing Degree-day (GDD). Derby et al. (2005) is unique in analyzing the effects of four different inputs: nitrogen, soil characteristics, weather and irrigation variation on corn yield. The weather-yield models in the above papers are diverse, but all results indicate that corn yield has a nonlinear relationship with weather variation, which is consistent with Schlenker & Roberts (2006) and Lobell et al. (2011). Instead of using growing-season average temperature and cumulative precipitation, Hansen (1991) and Kaufmann & Snell

(1997) did statistical regressions of corn yield on July variables (average temperature, rainfall, irrigation and daily maximum temperature).

Chen et al. (2016) developed an empirical framework to estimate the relation between corn and soybean yields and weather factors in China. The study used estimated coefficients for weather variables to quantify the economic impact of changing climate conditions on China's corn and soybean crops. A non-linear and inverted U-shape relationship between crop yields and weather variables (temperature, precipitation and radiation) was found. It is worth noting that crop yield y_i is assumed as an endogenous function $y_i = y_i(x_{i,k}, weather, technology)$, which can be expressed as function

$$y_i = y_i(P_{crop}, P_{input}, x_{i,k}, H, precp, precp^2, rad, rad^2)$$

where $x_{i,k}$ is the quantity of input k of crop i, $precp$ is the precipitation, rad is the radiation length, P_{crop} is expected crop price, P_{input} is input price, H is heat accumulated over crop growing season. Empirically assuming that the climate effects on yields are cumulative and substitutable over crop growing seasons, Chen et al. (2016) estimated the fixed effect model:

$$logY_{r,t} = H_{r,t}\beta_0 + Z_{r,t}\beta_1 + S_{r,t}\beta_2 + c_r + \lambda_t + \epsilon$$

where $Y_{r,t}$ is yield in county r and year t, $H_{r,t}$ is the seasonal heat accumulation, $Z_{r,t}$ is the sum of precipitation and radiation variables, $S_{r,t}$ includes socioeconomic variables, c_r is the time-invariant county fixed effect and λ_t is year fixed effect. Yields for corn and soybeans were obtained from the National Bureau of Statistics of China. Weather data are obtained from the China Meteorological Data Sharing Service System, which records daily minimum, maximum, and average temperatures, precipitation, and solar radiation for 820 weather stations in China. Compared with Mearns et al. (1984) and Lobell et al. (2011) selecting 35^oC as the threshold for defining extreme weather events, their study found that yields

increase with temperature up to 29^oC for corn and 28^oC for soybeans, temperatures above these thresholds are very harmful for crop growth. Results also indicated the existence of nonlinear and inverted U-shaped relationships between weather variables and corn or soybean yields.

The other recent study relevant to the weather-yield impact is Tao et al. (2017), who highlighted the different impacts of maximum (T_{max}) and minimum temperature (T_{min}) during different growth stages for winter wheat in China. Using 1981-2009 experimental time series data of average maximum temperature, minimum temperature, solar radiation (SRD) and accumulated precipitation (P) during each of five growth stages, the study constructed a multiple linear regression to estimate yield responses to climate variables:

$$Yd_t = \beta_0 + \beta_1 t + \beta_{i2} T_{\max t_i} + \beta_{i3} T_{\min t_i} + \beta_{i4} P_{t_i} + \beta_{i5} SRD_{t_i} + \epsilon_t$$

This regression was used to estimate the sensitivity of yield to changes in weather variables for each growth stage of wheat at each experimental station during 1981-2009. Yd_t represents annually observed yields in year t, t is time trend, T_{max} and T_{min} are daily maximum and minimum temperature, t_i means the averaged value during the $i-th$ growth stage (5 growth stages in total) in year t. The yield response function did not take fertilizer input into account.

Distinguished from all former statistical studies on estimating the weather impact on crop yields, Paltasingh et al. (2012) use the composite aridity index variable in the yield-weather regression model. The aridity index was designed to distinguish dry climates from moist climates of different regions. The original application of the aridity index was a consideration of the evapotranspiration process of crops. Rainfall and temperature were recognized as two important weather factors that affect crop yields and the evaporation process in his studies. In econometric modelling of the impact of weather on crop yields,

Paltasingh et al. (2012) proposed similar models that take evapotranspiration into consideration, for example, the following equations show different versions of crop-weather models:

$$Y = \beta_0 + \beta_1(\frac{P}{T}) + \beta_2 T + \beta_3 t + \beta_4 t^2 + \beta_5 t^3 + \epsilon$$

$$Y = \mu_0 + \mu_1(\frac{P}{T+10}) + \mu_2 T + \mu_3 t + \mu_4 t^2 + \mu_5 t^3 + \epsilon$$

$$Y = \theta_0 + \theta_1(\frac{P}{1.07^T}) + \theta_2 T + \theta_3 t + \theta_4 t^2 + \theta_5 t^3 + \epsilon$$

where Y is the yield of crop per acre, P is the average precipitation during the growing period in mm. June, July and August were taken as growing period in the study by Paltasingh et al. (2012), T is average daily maximum temperature of same period and t is time variable. The inclusion of aridity index (the fraction in bracket) in the model underlined the standing point that the yield response of precipitation $\frac{dY}{dP}$ is a function of temperature instead of a constant that is typically assumed by other literature.

Process-based models Process-based models, which are based on a series of ecological processes, provide a useful framework to incorporate specific crop growth responses to altered environmental conditions. Process-based models are usually designed to predict crop yields from the simulation of plant functioning, and can offer significant advantages in predicting the effects of global climate change on crop yield as compared to purely statistical models based on historical data. Among studies that estimate weather effects by employing process-based models, an early paper by Aggarwal (1995) quantified the effect of soil and weather inputs uncertainties on crop nitrogen uptake, evapotranspiration and yield. The crop growth simulation model $WTGROWS$ was used to simulate the effects of climate and management factors on the productivity of spring wheat. From the study, grain yield depends on the accumulation of dry matter as well as temperature and applied nitrogen. The grain growth process will be terminated when the crop reaches

physiological maturity. The results showed that yield uncertainties will increase as the production environment changed from a sufficient inputs scheme to a scheme where water and nitrogen inputs were constrained. Modelling crop yield and inputs in a linear way:

$$y = b_0 + \sum_{j=1}^{n} b_j x_j$$

where y and x_j are the total uncertainty captured by the percent deviation in output and input relative to the deterministic level respectively, n is the number of inputs, Aggarwal (1995) estimated the importance of each input uncertainty to the overall yield uncertainty.

Mavromatis & Hansen (2001) compared four stochastic weather generators in their ability to simulate inter-annual variability of monthly climate. Rather than giving a formal statistical crop yield model, they used the process-based crop simulation model $CERES$ to simulate harvest maturity and final maize yields in response to generated weather for given soil parameters. A key strength of such a process-based crop model is that it provides a clear physiological mechanism for linking weather to crop yield outcome, with many of the essential parameters in this model having been established through laboratory experiments. For example, $CERES$ can simulate the process of daily plant growth based on many weather variables variability. Weather variables discussed in the study involve precipitation, temperature, solar radiation.

In the field of agronomy research, there have also been numerous empirical studies exploring the impact of climate change on crop production since 1990s (Racsko et al. (1991), Lobell et al. (2006), Janjua et al. (2014), Chen et al. (2016), Tao et al. (2017) and Challinor et al. (2018)). For example, as an early paper that used weather generators in modelling weather impacts, Racsko et al. (1991) discussed processes for three weather variables, by using a weather generator that includes 3-dimensional stochastic weather processes. The weather generator is able to provide as long a time series as their study needed.

Using Hungary as an example, Racsko et al. (1991) stated that daily average temperature, precipitation and solar hours are the main three factors that need to be considered into crop production risk analysis. Sharing a similar objective, Challinor et al. (2018) conducted a comprehensive ecological literature review on crop modelling for integrated assessment of risks from climate change.

Predicting crop yield changes due to climate change but different from others' research that studied similar climate effects, Lobell & Burke (2010) used three types of data (time series, panel, and cross-sectional) to estimate the effect of changed growing-season average temperature and total precipitation on yield. For example, The log-linear weather impact panel model for 198 sites, with 39 years simulated data was:

$$log(Y_{i,t}) = \beta_{i,0} + \beta_1 T_{i,t} + \beta_2 P_{i,t} + \beta_3 T_{i,t}^2 + \beta_4 P_{i,t}^2 + \epsilon_{i,t}$$

where $Y_{i,t}$, $P_{i,t}$, $T_{i,t}$ are simulated maize yield, growing-season total precipitation and growing-season average temperature for site i and year t. Maize yields were simulated using CERES-Maize (version 4.0.2.0), a commonly used process-based model in agronomic research, and simulated weather data are obtained from the MarkSIM model. Estimates for linear term were all positive and all negative for the quadratic terms, which was consistent with Chen et al. (2016) in finding the inverted U-shape nonlinear relationship.

A most recent paper by Kabir et al. (2021) adopted a process-based model of nitrogen fluxes from agricultural soils (DeNitrification and DeComposition model) for simulating corn yields and environmental N losses based on various combinations of weather and split N application strategies. The data used to parameterize the DNDC model were collected from a field trial at Elora, Ontario. For each combination of split N application plan and weather scenario, simulated corn yields from the DNDC model are combined with prices and costs to estimate the profit of corn. Weather uncertainty in Kabir et al.

(2021) is restricted to nine simulated weather scenarios (five rainfall scenarios and five temperature scenarios) under which the effects of eleven split N application strategies (varying in split timing and amount) on corn yield, profit, and environmental N losses were evaluated. Results showed that grain yield in wetter weather was generally greater than that achieved in average weather. The greatest yield was achieved when the growing season was warmer and wetter than average. Pre-plant fertilizer application maximizes profit only under average weather conditions. Split N application is beneficial to corn yield only in wet scenarios and is more profitable in certain non-average weather scenarios where yield is greater and loss is lower. Split N application reduces leaching, volatilization, and denitrification under most of the weather conditions compared to pre-plant application. As an important conclusion for policy making, Kabir et al. (2021) found that the lowest V13 split application in dry weather scenarios will achieve a "win-win" scheme where both profit and environmental benefit are maximized. However, no "win-win" strategy is found in all non-dry weather scenarios. It is worthwhile noting that the corn price is assumed to be constant, and the environmental loss is measured in kg/ha.

Statistical models with a Just-Pope stochastic production function In contrast to the previous papers that have examined explicit relationships between crop yields, fertilizer input or weather variables, the Just-Pope stochastic production function (Just & Pope (1979)) was used in weather impact studies Chen et al. (2004), Chen & Chang (2005), Kim & Pang (2009) and Cabas et al. (2010). Among these papers, the Just-Pope production function is usually constructed without specifying the statistical relation between each weather input and production. The production function is represented by

$$Y = f(X) + h(X)\epsilon$$

Y is the yield level, X is a set of independent variables such as climate variables, ϵ is the stochastic term and follows a standard normal distribution. $E(\epsilon) = 0$ and $var(\epsilon) = 1$. $f(X)$ represents the average effect of weather variables on yield, $h(X)$ represents the variance effect on yield. Kim & Pang (2009) used this approach to find that the average rice yield in Korea is positively related to temperature and adversely related to precipitation, and weather variables (both temperature and precipitation) will enlarge the rice yield variability as risk-increasing inputs. The finding from Kim & Pang (2009) is partly consistent with previous literature conclusions that there exists a positive relationship between yield and temperature. Kim & Pang (2009) used two functional forms for estimation, which were

(Cobb-Douglas)

$$f(X|\beta) = \beta_0 + \beta_t T + \prod_j X_j^{\beta_j}$$

and

(Linear-Quadratic)

$$f(X|\beta) = \beta_0 + \beta_t T + \sum_j \beta_{1j} X_j + \sum_j \beta_{2j} X_j^2 + \sum_j \sum_k \beta_{jk} X_j X_k$$

with $h(X) = \alpha_0 + \alpha_t T + \prod_j X_j$, T is a time trend variable, X_j and X_k are inputs including weather variables. Chen & Chang (2005) adopted a log-linear form, focused on weather impacts on crop yield and implications for crop insurance, using pooled time-series cross-sectional data for seven major crops for Taiwan. Monthly mean temperature and precipitation are regarded as the major climate input variables in X. Chen & Chang (2005) concluded that increased variation in temperature and precipitation increases corn yields. Besides, Chen & Chang (2005) compared uncertain yields with and without a crop insurance policy. However, fertilizer input was neither explicitly nor separately examined in assumed yield functions in both Chen & Chang (2005) and Kim & Pang (2009).

The Just-Pope stochastic production function was also used in Chen et al. (2004) and Cabas et al. (2010). Rather than addressing climate change effects on mean yields, Chen et al. (2004) studied how weather has an impact on yield variance using panel data for corn, soybean, cotton and other major US crops. Similar to Kim & Pang (2009), Chen et al. (2004) adopted linear and Cobb-Douglass form of $f(X|\beta)$, and temperature and precipitation are included as inputs in X. In contrast to the Kim & Pang (2009) rice yield study, rainfall and temperature are separately found to have opposite effects on yield levels and variability for corn and cotton. For example, corn yields increase with more rainfall and decrease with higher temperatures. On the other hand, higher temperature was found to have a positive effect on soybean yields and a negative effect on wheat yields.

Using a different data[2] from southwestern Ontario over the period 1981-2006 and the Just-Pope yield function, Cabas et al. (2010) find that climate variables (average temperature and precipitation, such as monthly average or seasonal average temperature and rainfall) have a major impact on mean yield and the length of the growing season (measured as $GrowDays$) had a positive effect on mean yield for the main crops around Great Lakes: corn, soybean and winter wheat. Nevertheless, the marginal effect decreases with the increasing number of growing degree days. Average crop yields were examined increased at a decreasing rate with the quantity of inputs used. Both temperature and precipitation were found to be statistically significant for corn and wheat yields. Cabas et al. (2010) found that increases in the variability of temperature and precipitation decrease mean yield and increase its variance. This result is consistent with Chen et al. (2004) that the variability effect was found to be negative on corn yields for average temperature over the season. For example, according to Cabas et al. (2010), for a given length of growing season, corn

[2]Yield data were collected from 1981 to 2006 for the counties of Essex, Kent, Elgin, Huron, Perth, Haldimand-Norfolk, Middlesex and Lambton, which are sub-units within the province of Ontario. The basis for their selection of these counties is data availability and the importance of the field crops in this region of Ontario over the period of study. Climate data in their research were obtained from Environment Canada based on a representative weather station that located centrally within the county.

and wheat yields are higher for a lower and more evenly dispersed heat pattern. However, precipitation is found to be the only factor that affects soybean yield, which has an inverse effect on yields. Total precipitation over growing season was found to decrease soybean yield but increases corn and wheat yields.

Furthermore, according to Cabas et al. (2010), even though the length of growing season and its mean temperature are major determinants of average yield, the timing of the heat or precipitation matters. Warmth in the spring allows the crop to be planted sufficiently early to allow for the possibility of full maturity, and warmth in the fall allows the crop to be harvested with less field loss. In a moderate range, an increase in temperature for the summer months will contribute to a higher yield growth rate. However, excess heat in summer can leave crops under heat stress and lower yields. Similarly, increases in precipitation at the beginning of growing season will increase yield at a decreasing rate while the inverse impact on yield will present for the time around planting and harvesting.

Models describing yield or return uncertainty as Ito processes Several papers have studied the effects of uncertainties on farm investment decisions, but have not explicitly modelled the effects of weather, fertilizer input on crop yield (Price & Wetzstein (1999), Khanna et al. (2000) and Furtan et al. (2003)). Price & Wetzstein (1999) examined optimal entry and exit thresholds for Georgia commercial peach production by using an option value framework. Price & Wetzstein (1999) used Geometric Brownian motion to represent peach yield (q) uncertainty,

$$dq = \alpha_q q dt + \sigma_q q dZ_q$$

with peach price process

$$dp = \alpha_p p dt + \sigma_p p dZ_p$$

$$E(dZ_p, dZ_q) = \rho dt$$

where ρ is the correlation between two standard Brownian motion. Khanna et al. (2000) examined the effect of uncertainty on optimal timing of crop management system investment while Furtan et al. (2003) investigated the optimal time to license the genetically modified wheat technology. Khanna et al. (2000) assumed the value (V) represents the present value of rent of farmland, which could be approximated by the SDE $dV/V = \alpha_V dt + \sigma_V dz$. The same GBM model was employed by Furtan et al. (2003) where V represents the returns to Canadian wheat industry from licensing a policy. Another paper on the farmer's investment decision problem is Song et al. (2011), who studied a farmer's optimal decision to make a conversion between traditional cropland and energy crop farmland. Instead of including weather or fertilizer input in farmland value, Song et al. (2011) assumed that the overall farmland uncertainty, which is the return to planting corn-soybean rotation or switch-grass, denoted by $\pi(t)$, could be characterized by an Ito's process, which is similar to the processes used by Price & Wetzstein (1999), Khanna et al. (2000) and Furtan et al. (2003):

$$d\pi(t) = \alpha(\pi, t)dt + \sigma(\pi, t)dz$$

Though these papers provide us alternative ways to assess weather's contribution to corn yield, a deficiency is that nutrient input was omitted in yield modeling.

3.4 Literature on estimating the loss of nitrogen applied as fertilizer

Our objective is to summarize the complex relationship between rainfall and soil nitrogen loss in terms of the average nitrogen loss per millimeter of rainfall. This section

reviews empirical estimates of nitrogen loss. The main sources of fertilizer loss are leaching, erosion, surface runoff, ammonia volatilization, and denitrification. Figure 3.2 depicts the fate and transport processes of nitrogen added to the soil.

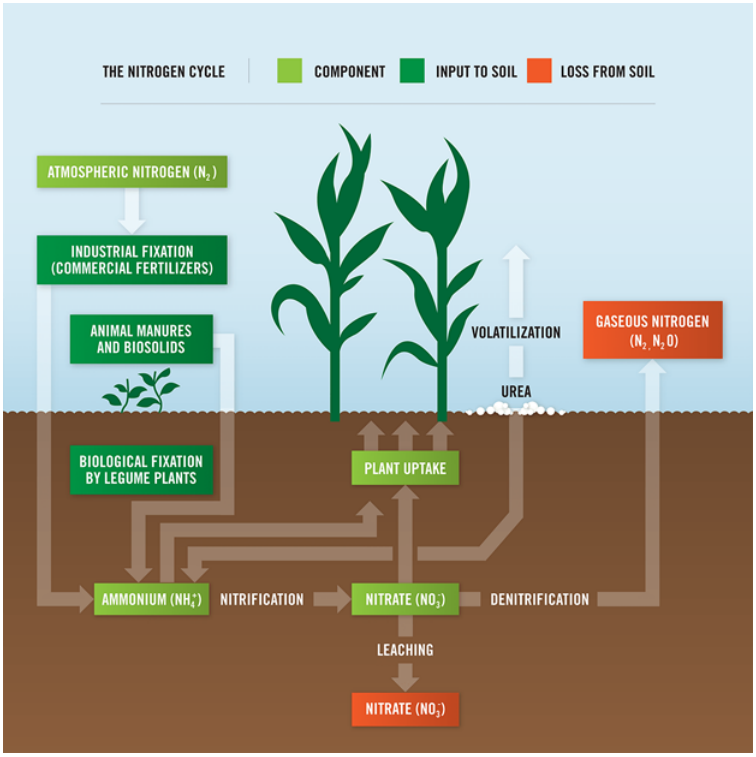

Figure 3.2: The fate and transport processes of nitrogen in the soil, by Koch Agronomic Services[3]

Nitrogen losses from the soil can be influenced by the fertilizer application method, quantity, timing, management practices, mineralization of organic N, precipitation, rotation and soil characteristics. Ju et al. (2004) illustrated potential reasons for the variability in nitrogen leaching process. An unbalanced N:P:K (Nitrogen:Phosphorous:Potassium) ratio in the fertilizer is examined as a main source for the N leaching variability. Similar findings were also concluded in Zhao et al. (2011), Sun et al. (2012) and Lawniczak et al.

[3]This graph is published online with the article title is "What is Nitrogen Loss in Plants?", by Koch Agronomic Services, Source: https://kochagronomicservices.com/knowledge-center/what-is-nitrogen-loss2217.aspx

(2016), who used surveyed or experimental data to find that different leaching rates occurred when different N:P:K ratios adopted in mixed chemical fertilizer application.

Wortmann et al. (2013) presents information on tons of nitrogen used in agricultural production from 1965 to 2005 in Heartland region states. In Iowa, the most used fertilizer is anhydrous ammonia (about 48%), urea-ammonium-nitrate solutions (UAN) (about 29%) and urea (about 10%), with percentages given for 2005. Ammonium nitrate constitutes a negligible proportion while other nitrogen sources constitute the remaining 14%. All of these forms of fertilizer are subject to loss through leaching and denitrification. However, volatilization can easily be minimized through proper application techniques (Nielsen (2006*a*) and Wortmann et al. (2013)).

In our model of farmer decision making, it will be assumed that denitrification and leaching are the only two sources of nitrogen loss. The partitioning of soil N loss between denitrification and leaching appears heavily weighted toward denitrification over leaching in the Community Land Model (Nevison et al. 2016). The partitioning of inorganic N loss varies considerably among different models, with particularly large differences in nitrate leaching. In Nevison et al. (2016), the $\frac{denitrification}{leaching}$ ratio from their crop model is $\frac{75\%}{25\%}$ and can be as high as $\frac{90\%}{10\%}$ in the other model. Nitrous oxide (N_2O) is a potent greenhouse gas that emitted from the denitrification process and contributes to climate change.

We seek an estimate of the portion of applied nitrogen (or soil nutrient content) that is lost to the environment and its relationship to the quantity of rainfall. In particular, we will summarize this relationship in terms of the average N loss per mm of rain. Lots of research has examined the N losses from nitrogen fertilizer use, but results vary widely across different papers (Horner (1975), Kanwar (1991), Patni et al. (1996), Yadav (1997*b*) Gentry et al. (1998), Ju et al. (2004), Jalali (2005), Nielsen (2006*b*), Martínez & Albiac (2006), Sawyer (2008), Bakhsh et al. (2010), Zhao et al. (2011) Sun et al. (2012), Lock-

hart et al. (2013), Basso et al. (2016), Camberato (2017), Yu et al. (2021), Paudel & Crago (2021)). For example, a statistical analysis by Paudel & Crago (2021) examined the impact of fertilizer use on the concentration of agricultural pollutants in surface water bodies (including streams, rivers, lakes and estuaries) over a period from 1951 to 2005, by regressing the log nitrate concentration on a series of explanatory variables including annual averaged precipitation, temperature, upstream precipitation, upstream nitrogen pollutant, GDP and population. Paudel & Crago (2021) found that, on average for the U.S. as a whole, a 10% increase in the use of nitrogen (kg) leads to a 1.52% increase in the concentration of nitrogen across watersheds. Current-year fertilizer application was found to have a significant impact on concentration of agricultural pollutants in the same year. In contrast, the effect of current-year fertilizer use on nitrogen pollutant in subsequent 1 to 10 years was not statistically different from zero. Paudel & Crago (2021) conclude that this provides justification for their focus on the contemporaneous impacts of nitrogen applications. In addition, the concave quadratic parameters are tested insignificant at a 5% level for the annual averaged precipitation, but tested significant for the annual averaged temperature in all of their regression specifications. Upstream precipitation is found insignificant on effecting the nitrogen concentration, while upstream pollutant is found significant on effecting the nitrogen concentration. Results in Paudel & Crago (2021) indicate that the estimated elasticities of agricultural pollutants with respect to fertilizer use have not changed drastically across several decades.

Yadav (1997*b*) estimated that about 15% of applied fertilizer leached into the groundwater in Minnesota every year. Sun et al. (2012) found that, in China, the total N fertilizer loss is about 19.1% of applied fertilizer, of which only 2% is leached. In contrast, the experiment-based total N loss rate in China by Zhao et al. (2011) is 31% of applied fertilizer, of which 25% is leached. According to Sawyer (2008), research conducted in Illinois indicated approximately 4% to 5% loss of nitrate-N by denitrification per day that soils

were saturated. An all-nitrate fertilizer was applied when corn was in the V1 to V3 growth stage (late May to early June). Sawyer (2008) estimated that excess water application can result in loss of 60 to 70 lb N/acre on silt loam and clay loam soils, due to denitrification loss. The climatic conditions in different years can significantly affect N loss and corn responsiveness to applied N in subsequent years. In a wetter year, the overall annual N loss would be in the range of perhaps twice the "normal year" loss amount. According to Sawyer (2008), at the Gilmore City, Iowa drainage research site where tile-flow nitrate has been monitored since 1990, nitrate leaching loss is greater in years with higher precipitation above normal level and hence greater tile flow. Nielsen (2006*b*) states that the two predominant N loss mechanisms that affect Indiana corn fields are leaching and denitrification of the nitrate-N form of nitrogen. Nitrogen loss due to volatilization of surface-applied urea-based products is the third source of N loss for some fields. Volatilization of the nitrogen gas can result in N losses of as much as 5% of the available nitrate-N per day, while 15% - 20% of the urea-based nitrogen may volatilize within a week after application. Rainfall, sunshine, and temperature all influence the rate of volatilization of surface-applied urea-based products. The timing and amounts of rainfall will influence the rates of leaching and denitrification losses of available nitrate-N. According to Nielsen (2006*b*), the use of a side-dress application strategy remains one of the easiest and least expensive ways to maximize nitrogen use efficiency.

On estimating the relation between N application and leaching amount, Basso et al. (2016) carried a field study in Venice Lagoon, Italy, and utilized a validated crop simulation model to simulate N leaching amounts to different N fertilization rates for three experimental zones (Zone 1, 2 and 3). The results from Basso et al. (2016) showed that the leaching amounts for Zone 3 were 14.4 and 15.8 kg/ha when N applications were 150 and 350 kg/ha, while the leaching amounts for another experimental zone (Zone 2) were 13.5 and 14.8 kg/ha when N applications were 150 and 350 kg/ha. N leaching was lower in the

zones where variable rates of N were applied when compared to uniform N fertilization. In Basso et al. (2016), precipitation was neither included as the factor that affects N leaching nor measured for the associated N leaching.

By designing a paddy field experiment in China in 2008, Yu et al. (2021) examined the nitrogen loss and its relation to rainfall under traditional flooding drainage (TID) and controlled irrigation drainage (CID) scenarios. Nitrogen loss was measured by the changes in NO_3^- and NH_4^+ concentrations in field runoff water. Surface runoff formed by rainfall was found as an important way for nitrogen loss. According to Yu et al. (2021), annual N application was 480 kg/ha, with 200, 70, 140, 70 kg/ha applied on 10 June, 20 June, 20 July and 5 August (Table 2 in Yu et al. (2021)). The growing season cumulative rainfall was 366.04 mm (Table 4 in Yu et al. (2021)). TN refers to the total nitrogen. Relations between rainfall and N discharge in Yu et al. (2021) are listed in the following Figure 3.3. From Figure 3.3, under TID scenario, one mm rain increase will cause 0.077 kg/ha total nitrogen discharge, which means an average discharge rate per mm rain can be calculated as $\frac{0.077}{480} = 0.016 \times 10^{-2}$. Similarly, the NO_3^- discharge rate per mm rain is calculated as $\frac{0.034}{480} = 0.007 \times 10^{-2}$. These results in Yu et al. (2021) are found highly sensitive to drainage methods in China.

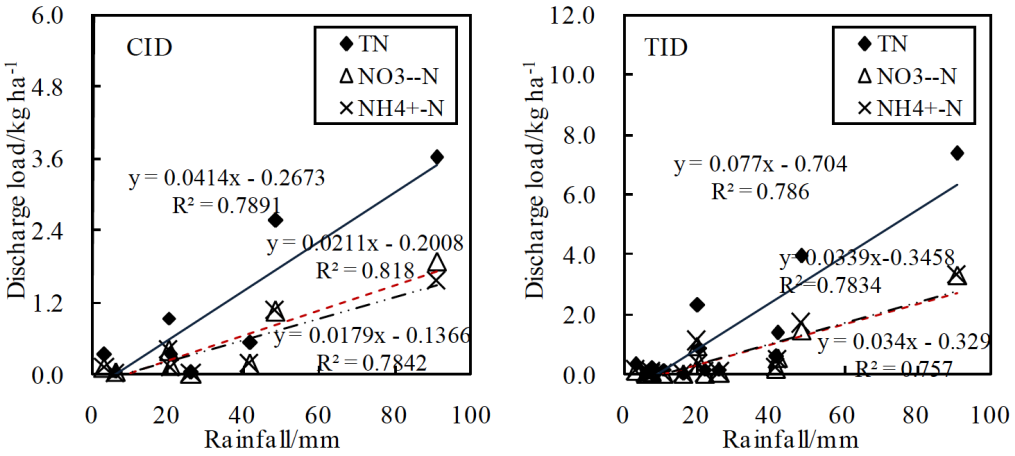

Figure 3.3: Regressions of rainfall and discharge load using daily data (Figure 8 in Yu et al. (2021))

Bakhsh et al. (2010), Kanwar (1991) and Gentry et al. (1998) used experimental studies to examine the effect of N application on N leaching losses into groundwater. For instance, the field experiments in Bakhsh et al. (2010) were conducted at the Iowa State University's northeastern research center near Nashua, Iowa from 2001 through 2005, on corn-soybean rotation plots under chisel plow system. Bakhsh et al. (2010) found that the spatial variability effects from plot to plot in some cases can result in differences of nitrate leaching losses in the range of three to four times. The uniform nitrogen fertilizer (168 kg/ha) was applied once at the beginning of growing season between the end of April and the start of May for each year of 2001 to 2005. The growing season precipitation (mm) from 2001 to 2005 was recorded by months (the growing season cumulative rainfall, March through November, from 2001 to 2005 was 674, 719, 604, 885, 839 mm in total), and the leaching loss amount was measured as 17.2, 2.2, 13.8, 18.2, 8.0 kg/ha from 2001 to 2005 on average. For instance, the N leaching loss rate per mm of rain for the year of 2001 can be calculated as $\frac{17.2}{674*168} = 0.0152 \times 10^{-2}$. Thus, we can conclude the average leaching loss rate for all years 2001-2005 as 0.0152×10^{-2}, 0.0018×10^{-2}, 0.0136×10^{-2}, 0.0122×10^{-2}, 0.0057×10^{-2}, respectively.

Sharing the same experimental site location (Iowa State University's Northeast research center at Nashua, Iowa) as Bakhsh et al. (2010), Kanwar (1991) studied the monthly average NO_3^- losses to the groundwater as a function of tillage (chisel plow, ridge tillage and no-tillage) and crop rotation (continuous corn received 200 kg/ha and corn-soybean rotation received 168 kg/ha). In the second field experiment begun in 1984 at Iowa State University's Agronomy and Agricultural Engineering Research Center near Boone, Iowa, N fertilizer application changed to two management practices (a single application of 175 kg/ha and three applications:25+50+50 kg/ha) for continuous corn using no-tillage and conventional tillage practices. They found a NO_3^- concentration of 10 mg/L threshold was exceeded by almost 100 percent of events for all tillage systems and crop rotations. N losses in Kanwar (1991) were found two to three times greater under continuous corn in comparison with the corn-soybean rotation.

Patni et al. (1996) found N loss as a range from 10 to 39 kg /ha under conventional tillage on maize fields in Ontario (around 7 to 30% of applied fertilizer), with loss primarily a function of precipitation amount during the dormant season. Patni et al. (1996) stated that the total nitrogen loss as nitrate can represent more than 20% of the amount applied as anhydrous ammonia. Annual loss can range from 10% to 30%. Using the experiment in Greenbelt Research Farm of Agricultural and Agri-food Canada, near Ottawa, Ontario, Patni et al. (1996) concluded the average nitrate-N loss rates over the 40-month study period from Jan 1991 to May 1994 were 23.7% of total N applied under no-tillage scenario and 21.1% of total N applied lost under conventional-tillage scenario. However, there is no link between these leaching rate and rainfall information.

From this survey of the literature we observe that estimates of nitrogen loss are highly variable and depend on environmental factors and farming characteristics. Most studies associate increased rainfall with higher levels of nitrogen loss. Gentry et al. (1998) is particularly relevant for our thesis since they not only evaluated the fate of applied N

fertilizer in US, but also has a direct link to rainfall amount. For our numerical example, we will base our nitrogen loss rate assumption on information from Gentry et al. (1998). The predominant cropping system in Central Illinois is a corn-soybean rotation where only corn production receives N fertilization, at an average rate in Champaign County of 196 kg/ha. All experimental fields in Gentry et al. (1998) were planted during the third week in May and harvested during the third week in September, which is close to our growing period setting.

By analyzing the soil samples collected from an agricultural watershed located 25 km south of Champaign-Urbana, over a 2-year period beginning in 1993, Gentry et al. (1998) found that 38 and 64 kg/ha nitrogen leached out of the watershed through tile drainage for the 1995 and 1996 water years. By evaluating nitrogen cycling in a corn watershed and the overall grain N accumulations for the year 1994 and 1995 growing seasons (May through August), Gentry et al. (1998) found that 33% of the total N input was corn N accumulation with leaching losses representing 29%. The balance of 38% may have remained in the soil or denitrified. Assuming 33% of the total N input represents corn N uptake, the rest 29% and 38% represent leaching and denitrification, we calculate the total N loss rate = 1 - 33% =67% of the total N input for the 1994 and 1995 growing seasons. The total growing season rainfall was recorded as 720 mm (320 mm and 400 mm for the year 1994 and 1995 growing season), the rainfall induced N loss rate per mm rain is thus calculated as $\frac{67\%}{720} = 0.093\times10^{-2}$ of the total N input over 1994-1995 growing seasons, of which 43.3% ($\frac{29\%}{67\%}$) is attributed to leaching loss and 56.7% ($\frac{38\%}{67\%}$) is attributed to denitrification.

Selected key useful conclusions regarding N leaching loss rate among above studies is presented in the following table:

Reference	Type of loss	Location	Experiment year	Crop rotation	Annual rainfall (mm) and applied nitrogen (kg/ha)	Loss amount (kg/ha)	Nitrogen loss rate, calculated by: *nitrogen lost (kg/ha) / nitrogen applied (kg/ha) / rainfall (mm)*
Bakhsh et al. (2010)	leaching	Nashua, Iowa	2001-2005	corn-soybean	5 years' rainfall and 168 kg/ha applied at the start of the season for each year	5 years' annual data (see in paper)	$0.0097\times10^{-2}$with a range of 0.0018×10^{-2}~0.0152×10^{-2} on average
Kanwar (1991)	leaching	Nashua, Iowa & Boone, Iowa	1990	continuous corn & corn-soybean & soybean-corn	1048mm 1st experiment: 200kg/ha application for continuous corn; 168 kg/ha for corn-soybean; 0 kg/ha for soybean-corn 2nd experiment is for continuous corn: no-tillage: 175 or 25+50+50 kg/ha N application conventional-tillage: 175 or 25+50+50 kg/ha	Corn-soybean: 52.36 (CP), 37.95 (CT), 36.47 (NT) Continuous corn: 99.93 (CP), 58.06 (CT), 83.41 (RT), 107.19 (NT)	Using 200, 175 or (25+50+50) kg/ha as total applied N, we derive a range of leaching loss rate: 0.051×10^{-2}~0.081×10^{-2} (for continuous corn, no-tillage) 0.028×10^{-2}~0.081×10^{-2}(for continuous corn, all tillage) 0.0297×10^{-2} (for corn-soybean, CP) 0.017×10^{-2}~0.0297×10^{-2} (for corn-soybean, all tillage)
Gentry et al. (1998)	total N loss (including leaching)	25km south of Champaign-Urbana, Central Illinois	1993-1995	corn-soybean	May through August (growing season) 1993: 650mm 1994: 320mm 1995: 400mm N applications vary by years	Vary by years and three tiles (see in paper)	For year 1994 and 1995, the total N loss rate is 0.093×10^{-2}. Leaching is 43.3% of this total N loss rate.
Patni et al. (1996)	tile effluent loss	Ottawa, Ontario	Jan 1991 to May 1994	no tillage and conventional tillage	23.7% of total applied N lost under no-tillage while 21.1% of total N lost under conventional-tillage		
Yadav (1997b)	leaching	Minnesota	About 15% of applied N enters groundwater				
Sun et al. (2012)	both	China	Total N loss is about 19.1% of applied N			5% enters surface water	2% enters groundwater by leaching
Zhao et al. (2011)	both	China	Total N loss is about 31% of applied N			7.75% enters groundwater by leaching	

The total N loss rate per *mm* rain by Gentry et al. (1998) including all sources of nitrogen loss is larger than the estimated N loss rates per *mm* rain solely by leaching reported by Kanwar (1991) and Bakhsh et al. (2010). Due to the complexity of N losses from the soil, we define the total rainfall-induced N loss as the nitrogen that moves out of the crop rooting zone and is not available for crop uptake as soil nutrient stock S. The total N loss rate is used to calculate the soil nutrient stock. In this thesis, we assume 0.093×10^{-2} of soil nutrient stock as the total N loss rate per *mm* rainfall, of which 43.3% is attributed to leaching loss and the rest 56.7% is attributed to denitrification loss.

3.5 Formulation of the farmer's fertilizer application decision model

3.5.1 State and control variables

In this section we specify a general model of the farmer's decision problem regarding the quantity of fertilizer applied to the crop. Our decision model is applicable to a number of different types of crops, however, we refer to the crop as corn since that is used in our numerical example. There are numerous mathematical notations used in this chapter and the following chapter, for reader's convenience, the meanings for notations of key variables are summarized in Appendix K.

Corn Prices It is observed in the literature that agricultural commodity prices exhibit mean-reversion to production costs[4]. Historical U.S. corn spot prices (in U.S. dollars per bushel) on a daily basis for the period between 1959 and 2019 are plotted in Figure 3.4.

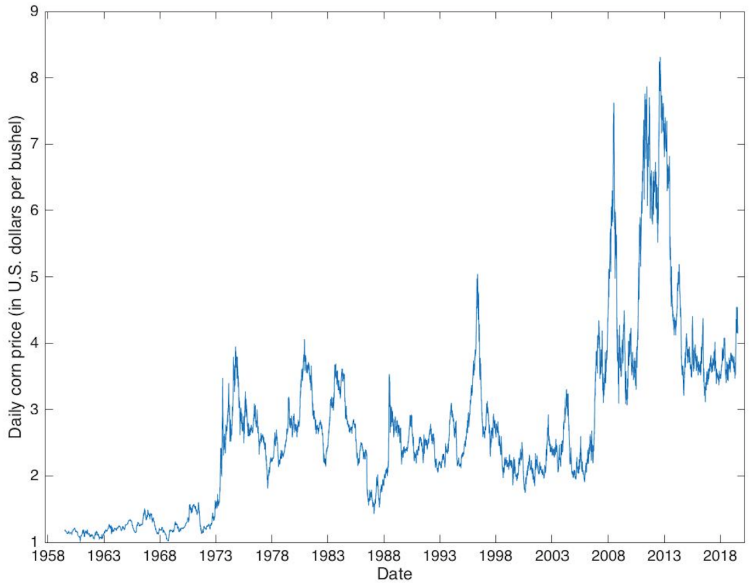

Figure 3.4: Daily corn price for the period of 1959-2019[5]

[4]For example, Bessembinder et al. (1995), Hart et al. (2016) and Jin et al. (2012).

Corn prices are observed to be highly volatile. Reversion to a mean or equilibrium price level is also in evidence and that mean or equilibrium level appears to have shifted over time. Because the analysis focuses on only one growing season, we adopt the mean reverting price process[6] with a fixed mean that was used in Section 2. The assumed corn price process in the $\mathbb{Q}$-measure is given as:

$$dP = \alpha(\kappa - P)dt + \sigma_P P dZ_t \tag{3.2}$$

where P is the corn price in U.S. dollars per bushel. The parameters α and κ are the long run mean level of price and mean-reversion rate respectively, under the $\mathbb{Q}$-measure (i.e. parameters are risk adjusted). σ is the price volatility and Z_t follows standard Brownian motion.

Corn yield, denoted by the yield response function Y, is modelled as a function of cumulative daily corn heat units in the growing-season, $\bar{H}$, growing-season cumulative rainfall, $\bar{R}$, average soil nutrient content, $\bar{S}$, and yearly time variable, t:

$$Y = Y(\bar{H}, \bar{R}, \bar{S}, t) \tag{3.3}$$

Corn heat units A corn heat unit is an index developed by OMAFRA (2017*a*) to represent the effective contribution from temperatures to the corn growth. Similar to growing degree days but designed specifically for warm-season crops (especially for corn) in Ontario, daily corn heat units are calculated as a function of daily minimum and maximum

[5]Historical U.S. daily corn spot prices are collected from MARCROTRENDS, source: //www.macrotrends.net/2532/economic-historical-daily-dollar

[6]Some researchers suggest that models of commodity prices should include jumps (including Hilliard & Reis (1999), Brigo et al. (2007), Schmitz et al. (2014), Patrick (2016) and Aiube & Levy (2019)). However, including a jump diffusion in the estimation of corn price process using $\mathbb{Q}$-measure method requires determination of the historical risk adjusted jump probability. The estimation of a jump diffusion corn price model is beyond the scope of this thesis.

temperatures. The state variable in Equation (3.3) is cumulative corn heat units, $\bar{H}$, over the growing season.

Wilks (1999*b*), Qian et al. (2002) and the weather generator WeaGETS (Chen et al. (2012*a*)) model minimum and maximum daily temperature as discrete autoregressive processes, while Mraoua (2007), Benth & Benth (2007), Wang et al. (2015) and Gyamerah et al. (2019) model daily temperature as mean reverting process with a seasonality long-run mean function. Denote the maximum and minimum daily temperatures as X_1 and X_2 respectively and let the daily temperature difference $\delta = X_1 - X_2$. For specifying the HJB equation, we define a continuous time mean reverting processes as the data generating processes for X_1 and δ:

$$dX_1 = \phi_1[\eta_1(t) - X_1]dt + \sigma_X \ dZ_{1t} \tag{3.4}$$

and

$$d\delta = \phi_\delta[\eta_\delta(t) - \delta]dt + \sigma_\delta \ \delta dZ_{\delta t} \tag{3.5}$$

where $\delta = X_1 - X_2$, $\eta_1(t)$, $\eta_\delta(t)$ are the long run means of X_1 and δ, respectively and are dependent on time which reflects seasonality. X_1 and δ may be correlated: $corr(X1, \delta) = \nu$. We choose to model δ rather than X_2 directly so that there is no probability that X_2 goes above X_1, since $d\delta \to 0$ as $X_2 \to X_1$.

In order to define daily corn heat units, we specify a set of daily dates, Ω_D:

$$\Omega_D = \{t_0 = 0 < ... < t_m < ... < t_{\hat{M}} ... < t_M = T\}, \ m = 1, ..., \hat{M}, ..., M. \tag{3.6}$$

where $t_{\hat{M}}$ is the corn maturity date and $t_M = T$ is the date when harvested corn is sold. Then daily corn heat units are given as:

$$H_{t_i} = H((X_1)_{t_i}, (X_2)_{t_i}), \ t_i \in \Omega_D \tag{3.7}$$

Note that H_{t_i} is updated only at the daily dates in Ω_D. The precise definition of the H_{t_i} function as specified by OMAFRA (2017*a*) in terms of maximum and minimum daily temperatures is given in Section 3.7.2.

Cumulative corn heat units at time $t = t_m$ denoted as $\bar{H}_{t_m}$, is given by:

$$\bar{H}_{t_m} = \bar{H}_{t_{m-1}} + H_{t_m}, \quad t_i \in \Omega_D, \ \bar{H}_{t_0} = h_0 \tag{3.8}$$

Rainfall Define a two state continuous time Markov chain, w_t, to describe switching between two rainfall regimes, $w_t \in \{0, 1\}$. $w_t = 0$ is the dry regime with no rain, while $w_t = 1$ is the wet regime when some rainfall occurs. w_t is governed by a Poisson processes $q^{w_t \to 1-w_t}$ with intensity $\lambda^{w_t \to 1-w_t}$. This implies:

$$\mathrm{d}q^{w_t \to 1-w_t} = \begin{cases} 1 & \text{with probability } (\lambda^{w_t \to 1-w_t} \mathrm{d}t), \\ 0 & \text{with probability } (1 - \lambda^{w_t \to 1-w_t} \mathrm{d}t). \end{cases} \tag{3.9}$$

Let R^{w_t} denote the instantaneous rainfall rate in regime w_t at time t. If $w_t = 0$, $R^{w_t} = 0$. If $w_t = 1$, R^{w_t} follows a known probability distribution $f(R)$. $\bar{R}_t$ denotes cumulative rainfall at time t and is described by the differential equation:

$$d\bar{R}_t = R^{w_t} dt. \tag{3.10}$$

Average Soil Nutrient Content and Fertilizer Decision S denotes the soil nutrient stock due to applied nitrogen fertilizer. It does not reflect the background level of nitrogen in the soil prior to the the addition of fertilizer. S is reduced in the event of rain, through natural processes such as denitrification, runoff and leaching. In addition, S is increased through fertilizer applications, N_t, which are permitted at fixed decision times, t_{f1} and t_{f2}

in Ω_F:

$$\Omega_F = \{t_{f1}, t_{f2}\} \quad 0 \leq t_{f1} \leq t_{f2} < T, \quad \Omega_F \subset \Omega_D. \tag{3.11}$$

Define a control set which contains all possible controls, N_t:

$$K = \{N_t | t \in \Omega_F,\ N_t \in Z_N\}, \tag{3.12}$$

where Z_N is the admissible set for fertilizer application.

For $t \in \Omega_F$,

$$S_{t^+} = S_{t^-} + N(t), \quad S_{t=0} = 0. \tag{3.13}$$

For times other than fertilizer application times, $t \notin \Omega_F$, S_t is affected only by rainfall:

$$dS_t = -l_s\ R^{w_t}\ S_t dt, \tag{3.14}$$

where l_s is an assumed constant parameter reflecting the percent loss of S per mm of rainfall. As is discussed further in Section 3.5.2, corn yield is assumed to depend on the average soil nutrient content. The average soil nutrient stock at time t_i, $\bar{S}_{t_i}$, is given as:

$$\bar{S}_{t_i} = \int_{t=0}^{t_i} \frac{S_t}{t_i}\, dt, \quad 0 < t_i \leq t_{\hat{M}}. \tag{3.15}$$

Where $t_{\hat{M}}$ refers to the maturity date of the corn, which is different than the date the harvested corn is sold, at $t_M = T$.

3.5.2 Corn yield function

The previous cropping decisions will influence the amount of available nitrogen and the variability in yields. For example, the inclusion of cover crops has been found to

improve soil health and reduce the downside risk of yields. However, in our analysis, we assume there is no previous crop planted in the corn farmland, neither continuous corn nor corn-soybean rotation.

Exponential yield-input response function is commonly used to model the crop yield in a finite time region, especially for a single growing season. Compared with linear-plateau and quadratic model, exponential model not only has fewer parameters need to be estimated, but has a strong ability in explaining the actual crop growth process where crop yield grows with the increased input at a decreasing absorbing rate and peaks when the limit of root absorbing capacity reached. In this thesis we require a parsimonious model of corn yield that includes the key factors that will affect yield and also may affect a farmers fertilizer decision. The proposed model is specified as Equation (3.16), which captures key stylized facts about corn growth and behaves appropriately at the upper and lower limits of the state variables. Details regarding to the corn yield model are discussed in later Section 3.8.

$$Y = \theta(\alpha_1 \bar{R} + \alpha_2 \bar{R}^2)(1 - e^{-\beta_1 \bar{S}})(1 - e^{-\beta_2 \bar{H}}) \tag{3.16}$$

where Y is the corn yield in bu/a at harvest time T, $\bar{R}$ is the growing season cumulative precipitation in mm, $\bar{S}$ is the growing season averaged soil nutrient stock in lb/a, $\bar{H}$ is the growing season cumulative corn heat units, $\theta, \alpha_1, \alpha_2, \beta_1, \beta_2$ are parameters.

In Equation (3.16), corn yield is the product of the effects from cumulative rainfall ($\bar{R}$), the seasonal averaged soil nutrient level ($\bar{S}$) and seasonal cumulative corn heat units ($\bar{H}$). If any of these variables is zero, corn yield is also zero. The contribution from each input variable to corn yield is dependent on the levels of all other variables. The functions relating to $\bar{S}$ and $\bar{H}$ are both concave exponential functions, implying that yield increases at a decreasing rate in $\bar{S}$ and $\bar{H}$. This reflects the reasonable assumption that beyond a certain level of $\bar{S}$ and $\bar{H}$, there will be no significant positive impact on corn yield Y.

Since $\bar{H}$ reflects the cumulative corn heat units, it does not take account of the distribution of heat over the entire growing season. For example, a season with several weeks of extremely hot weather coupled with low temperature in other weeks, compared with a season of moderate temperatures throughout, corn yield may be at the same level for a particular $\bar{H}$ at harvest time. This is a weakness of the model. A more accurate depiction of the impact of the timing of heat would require a more detailed specification of the crop growth function, and is beyond the scope of this thesis.

The average nutrient stock, $\bar{S}$, reflects the application of fertilizer by the farmer, potentially reduced by rainfall through leaching. Since soil residual N levels are usually measured in ppm (or mg N/kg soil) and hard to transformed into application unit lb/acre, we assume the initial soil nutrient stock as zero for simplicity. In the model the fertilizer application is restricted to two specific times: the starter application and the side-dressing. All things equal, the earlier application of fertilizer will have a larger impact on $\bar{S}$ and hence on crop yield than the later application. This favours the starter application in the farmer's decision. Offsetting this is the fact that the starter application has more possibility of being washed away by rainfall, since it is on field longer. These two characteristics of the starter and side dressing application, along with the cost of fertilizer application will affect the farmer's decision regarding fertilizer timing.

Using $\bar{S}$ in the corn yield function is a device to reflect the fact that the starter application and the side dressing are not perfect substitutes. From a reading of the trade literature on corn farming, it appears that farmers prefer to apply some fertilizer early in the season to ensure its presence during crucial corn development stages. While side-dressing at the appropriate time may also meet corn needs, the risk of delaying fertilizer application is that inclement weather or other unexpected issues would make it infeasible to apply side dressing, and hence the window of opportunity for fertilizer application would be missed.

Cumulative rainfall $\bar{R}$ is shown to affect yield via a quadratic function in the literature. The parameter associated with $\bar{R}^2$ will be negative, capturing the negative consequences for yield of excessive rain. In our corn yield model, we do not include moisture from irrigation, however, this is taken account of indirectly by precipitation.

3.5.3 Value function

The value of the farmer's crop at time $t = t_i$ is the expected value, under the $\mathbb{Q}$-measure, of cash flows from the crop planted at time $t_0 = 0$ and sold at time $t_M = T$, with optimal fertilizer amounts applied at time t_{f_1} and t_{f_2}, given starting values of state variables. We follow the common practice of letting lower case variables denote realizations of random variables except for δ where we use $\tilde{\delta}$ to represent a particular value:

$$V(p,\bar{h},x_1,\tilde{\delta},\bar{r},r,w,s,\bar{s},t_i) \;=\; \sup_K \mathbb{E}_K^{\mathbb{Q}}\Bigg\{ \overbrace{\sum_{t_j\in\Omega_F}\Big[-e^{-\rho(t_j-t_i)}c_{N_j}N(t_j)\Big]}^{\text{fertilizer cost}} + \overbrace{e^{-\rho(T-t_i)}P(T)Y(p,\bar{h},x_1,\tilde{\delta},\bar{r},r,w,s,\bar{s},T)}^{\text{revenue from harvest at T}} - \overbrace{e^{-\rho(T-t_i)}\Big[c_F+c_VY(p,\bar{h},x_1,\tilde{\delta},\bar{r},r,w,s,\bar{s},T)\Big]}^{\text{fixed and variable cost}} \Bigg| P(t_i)=p,\bar{H}(t_i)=\bar{h},X_1(t_i)=x_1,\delta=\tilde{\delta},\bar{R}(t_i)=\bar{r},R(t_i)=r,w_{t_i}=w,S(t_i)=s,\bar{S}(t_i)=\bar{s}\Bigg\} \tag{3.17}$$

where c_F denotes the fixed cost paid at time T, including labor cost and harvest machinery cost. c_{N_j} denotes the per unit cost associated with the application at t_j. c_V is the variable cost on corn yield, excluding fertilizer use. The expectation is with respect to control set K and ρ is the risk free discount rate.

We now derive the HJB equation which describes the evolution of crop value V between dates defined by $t_i \in \Omega_D$. Note that at dates in Ω_D, $\bar{H}$ (cumulative corn heat units) is

updated; between these dates $\bar{H}$ is fixed. At dates $\Omega_F \subset \Omega_D$ the farmer applies the chosen fertilizer amounts. In between dates specified in Ω_D, the value of the crop changes as a result of changes in price, soil nutrient levels, cumulative rainfall, and minimum and maximum temperature levels. No cash flows occur at times not in Ω_D.

Let t_m^- denote the instant before t_m and t_m^+ denote the instant after t_m. Consider a small time interval $\Delta t < (t_{m+1} - t_m)$. For small Δt, according to the dynamic programming principle,

$$
\begin{aligned}
V(p, \bar{h}, x_1, \tilde{\delta}, \bar{r}, r, w, s, \bar{s}, t_i) \;&=\; \sup_K \mathbb{E}_K e^{-\rho \Delta t} \Bigg\{ \\
V\Big(P(t_i{+}\Delta t), \bar{H}(t_i), X_1(t_i{+}\Delta t), \delta(t_i{+}\Delta t), \bar{R}(t_i{+}\Delta t), R(t_i{+}\Delta t), w(t_i{+}\Delta t), S(t_i{+}\Delta t), \bar{S}(t_i{+}\Delta t), t_i{+}\Delta t \Big) \\
\Big| P(t_i) = p, \bar{H}(t_i) = \bar{h}, X_1(t_i) = x_1, \delta = \tilde{\delta}, \bar{R}(t_i) = \bar{r}, R(t_i) = r, w_{t_i} = w, S(t_i) = s, \bar{S}(t_i) = \bar{s} \Bigg\}, \;\; t_i \notin \Omega_D
\end{aligned}
\tag{3.18}
$$

Equation (3.18) can be rewritten as follows:

$$
\begin{aligned}
V(p, \bar{h}, x_1, \tilde{\delta}, \bar{r}, r, w, s, \bar{s}, t_i) \;&=\; \sup_K \mathbb{E}_K e^{-\rho \Delta t} \Big\{ V(p, \bar{h}, x_1, \tilde{\delta}, \bar{r}, r, w_{t_i}, s, \bar{s}, t_i) + dV(\cdot) \\
\Big| P(t_i) = p, \bar{H}(t_i) = \bar{h}, X_1(t_i) = x_1, \delta = \tilde{\delta}, \bar{R}(t_i) = \bar{r}, R(t_i) = r, w_{t_i} = w, S(t_i) = s, \bar{S}(t_i) = \bar{s} \Big\}, t_i \notin \Omega_D
\end{aligned}
\tag{3.19}
$$

Rearranging and substituting $(1 - \rho \Delta t)$ for $e^{-\rho \Delta t}$ under small time interval Δt gives:

$$
(\rho \Delta t) V(p, \bar{h}, x_1, \tilde{\delta}, \bar{r}, r, w_{t_i}, s, \bar{s}, t_i) \;=\; \sup_K (1 - \rho \Delta t) \mathbb{E}_K \Big\{ dV(\cdot) \Big\} \;\; t \notin \Omega_D \tag{3.20}
$$

The term $-\rho \, \Delta t \, \mathbb{E}_K\{dV(\cdot)\}$ in Equation (3.20) can be omitted because it includes terms

that are powers of Δt which go to zero faster than Δt. Dividing Equation (3.20) by Δt and let $\Delta t \to 0$ gives:

$$\rho\, V(p, \bar{h}, x_1, \tilde{\delta}, \bar{r}, r, w_{t_i}, s, \bar{s}, t_i) \;=\; \sup_K \frac{1}{dt}\mathbb{E}_K\Big\{dV(\cdot)\Big\} \tag{3.21}$$

Then use Ito's lemma for a jump process (cumulative rainfall) and a diffusion process (crop price) to evaluate dV.

$$\begin{aligned} dV(\cdot) =& \frac{\partial V}{\partial t}dt + \left[\alpha(\kappa - p)\frac{\partial V}{\partial p} + \frac{1}{2}\sigma_p^2\, p^2\, \frac{\partial^2 V}{\partial p^2}\right]dt + \sigma_p\, p\, \frac{\partial V}{\partial p}dZ_t \\ &+ \left[\phi_1(\eta_1 - x_1)V_{x_1} + \frac{1}{2}\,\sigma_{x_1}^2\,\frac{\partial^2 V}{\partial x_1^2}\right]dt + \sigma_{x_1}dZ_t + R^{w_t}\frac{\partial V}{\partial \bar{R}} \\ &+ \left[\phi_2(\eta_2 - \bar{\delta})\frac{\partial V}{\partial \tilde{\delta}} + \frac{1}{2}\,\sigma_\delta^2\,\tilde{\delta}^2\frac{\partial^2 V}{\partial \tilde{\delta}^2}\right]dt + \sigma_\delta\,\tilde{\delta}dZ_t + \nu\,\sigma_{x_1}\sigma_\delta\frac{\partial^2 V}{\partial x_1 \partial \tilde{\delta}}dt \\ &+ \Big[V(p, \bar{h}, x_1, \tilde{\delta}, \bar{r}, r, (1 - w_{t_i}), s, \bar{s}, t_i) - V(p, \bar{h}, x_1, \tilde{\delta}, \bar{r}, r, w_{t_i}, s, \bar{s}, t_i)\Big]dq \end{aligned} \tag{3.22}$$

Take the expected value of dV and substitute into Equation (3.21) to get the following HJB partial differential equation (PDE) describing $V(\cdot)$ for $t_i \notin \Omega_D$:

$$\begin{aligned} \rho\, V(p, \bar{h}, x_1, \tilde{\delta}, \bar{r}, r, w_{t_i}, s, \bar{s}, t_i) \;=\; \sup_K \Bigg\{ & \frac{\partial V}{\partial t} + \overbrace{\alpha(\kappa - p)\frac{\partial V}{\partial p} + \frac{1}{2}\sigma_p p^2\frac{\partial^2 V}{\partial p^2}}^{\text{expected value gain from price}} \\ & + \overbrace{\left[\phi_1(\eta_1 - x_1)V_{x_1} + \frac{1}{2}\sigma_{x_1}^2\frac{\partial^2 V}{\partial x_1^2}\right] + \left[\phi_2(\eta_2 - \bar{\delta})\frac{\partial V}{\partial \tilde{\delta}} + \frac{1}{2}\sigma_\delta^2\,\tilde{\delta}^2 V_{\tilde{\delta}\tilde{\delta}}\right] + \nu\,\sigma_{x_1}\sigma_\delta\frac{\partial^2 V}{\partial x_1 \tilde{\delta}}dt}^{\text{expected value change from the change of temperature state variables}} \\ & + \overbrace{\mathbb{E}(R)\frac{\partial V}{\partial \bar{R}} + \Big[V(p, \bar{h}, x_1, \tilde{\delta}, \bar{r}, r, (1 - w_{t_i}), s, \bar{s}, t_i) - V(p, \bar{h}, x_1, \tilde{\delta}, \bar{r}, r, w_{t_i}, s, \bar{s}, t_i)\Big]\lambda^{w_t \to 1 - w_t}}^{\text{expected value change from change in rainfall state variables}} \Bigg\}, t_i \notin \Omega_D \end{aligned} \tag{3.23}$$

Now we specify what happens at fixed dates Ω_D and Ω_F. For $t \in \Omega_D$ cumulative corn

heat units, soil nutrient stock and cumulative precipitation are updated:

$$V(p, \bar{h}_t, x_1, \tilde{\delta}, \bar{r}, r, w_t, s, \bar{s}_{t^-}, t^-) = V(p, \bar{h}_t + H_t, x_1, \tilde{\delta}, \bar{r} + R^{w_t}, r, w_t, s, \bar{s}_{t^+}, t^+), \quad t \in \Omega_D \tag{3.24}$$

At decision dates defined by $\Omega_F = \{t_{f_1}, t_{f_2}\}$, the optimal control, N is chosen control which affects soil nutrient level, S.

$$V(p, \bar{h}, x_1, \tilde{\delta}, \bar{r}, r, w_t, S, \bar{S}_{t^-}, t^-) = \max_N V(p, \bar{h}, x_1, \tilde{\delta}, \bar{r}, r, w_t, S, \bar{S}_{t^-} + N_t, t+), \quad t \in \Omega_F \tag{3.25}$$

Equations (3.23), (3.24), and (3.25) do not have a closed form solution. Further, a numerical solution using a standard approach such as the finite difference method and semi-Lagrangian approach[7] is problematic given that there are five stochastic state variables, (P, X_1, δ, w_t, R) and four path dependent variables $(\bar{R}, S, \bar{S}, \bar{H})$. As an alternative to solving the decision problem directly, we instead explore the characteristics of the value function through Monte Carlo analysis. If we limit the possible controls to a few discrete choices, an optimal solution can be found through exhaustive search.

3.6 Data description

This section briefly describes the historical data sets used to calibrate the corn yield function and estimate the parameters of the stochastic differential equations describing corn heat units, rainfall and corn prices. The models of the stochastic state variables are used to generate simulated data to evaluate optimal nutrient application in the Monte Carlo analysis presented in Section 3.9.3.

We analyze the decisions of a hypothetical corn farming operation located in Iowa using

[7] See Insley (2017) and references therein.

relevant Iowa data[8]. Historical Iowa weather data are collected on daily basis over 29 years (1990-2018), annual state-level averaged nitrogen application rates and state-level averaged corn yields are collected over 19 years (1990-2003, 2005, 2010, 2014, 2016, 2018) for Iowa state in the United States. This time frame coincides with available state-level survey data for average nitrogen application in Iowa.

Historical weather data, consisting of daily precipitation (in mm), daily maximum and minimum temperature (in ^oC) over the corn development period (May 01-Oct 30, 183 days), is obtained from Iowa Average Station[9]over 29 years (1990-2018), to represent the averaged Iowa state-level weather conditions. Historical daily corn heat units (H) are then derived using daily temperature data and the definition given in Section 3.7.2. Cumulative precipitation $\bar{R}$ and cumulative corn heat units $\bar{H}$ are calculated by summing up daily precipitation and daily corn heat units H over the specified growing period. Corn spot price on a daily basis in U.S. dollars per bushel is collected from $Macrotrends$[10] over the period from Jan 01, 2010 to July 28, 2019. Cost parameters including fixed and variable costs are collected in U.S. dollars from *Ag Decision Maker*, an agricultural guidance website initiated by Iowa State University[11].

Iowa state-level annual averaged corn yield information (measured in $bu/acre$) and state-level averaged nitrogen fertilizer application (measured in $lb/acre/year$) are collected

[8]This research initially intended to model a hypothetical corn growing operation in Ontario. Based on the Ontario Corn Yield Map (www.agricorp.com/en-ca/News/2019/Pages/PI-MapShows2018CornYields.aspx), we located 5 interest areas around lake Erie in Ontario: Essex county (3 cities), Chatham-Kent county (8 cities), Elgin county (9 cities), Norfolk county (6 cities) and Haldimand county (5 cities). We investigated historical corn yield, weather and nitrogen application data on city or county level. However, this research was not pursued due to a lack of data.

[9]Data is collected from the Iowa Average station. The station ID is $IA0000$, with a latitude of $41^o75^{'}N$, a longitude of $-93^o25^{'}W$ and elevation (m) is 259. Source: https://mesonet.agron.iastate.edu/request/coop/fe.phtml

[10]Daily corn prices are collected from https://www.macrotrends.net/2532/corn-prices-historical-chart-data

[11]Details are listed on "Estimated costs of crop production in Iowa 2022", Page 2, Corn Following Corn section, source: https://www.extension.iastate.edu/agdm/crops/pdf/a1-20.pdf

from the USDA National Agricultural Statistics[12] over a period of 19 years (1990-2003, 2005, 2010, 2014, 2016 and 2018). A summary of collected data characteristics is presented in the following Table 3.1:

Table 3.1: The characteristics of collected data

Data	*min*	*mean*	*max*	*s.d.*
Daily minimum temperature (daily,1990-2018,^oC)	-7.8	12.3	24.4	5.9
Daily maximum temperature (daily,1990-2018,^oC)	1.1	24.6	37.2	5.8
Daily precipitation (daily,1990-2018,mm)	0	3.3	40.9	5.4
Annual averaged corn yield (annual,19 years,bu/a)	80	149.4	203	28.2
Annual averaged nitrogen application (annual,19 years,lb/a)	114	128	150	9.8
Corn price (daily,2010-2019,$\$/bu$)	3.1	4.6	8.3	1.4

Note: *min* refers to the minimum value; *max* refers to the maximum value; *s.d.* refers to the standard deviation.

Daily maximum and minimum temperature will be used to calibrate daily temperature models and to compute Iowa historical cumulative corn heat units H. Historical average nitrogen application data for Iowa will be used to estimate the corn yield function. Thus, the historical annual averaged soil nutrient stock (S) can be computed using historical daily precipitation, averaged nitrogen application and the rainfall-induced loss process that is discussed in Section 3.5.1 with a total N loss rate of 0.093×10^{-2} per mm rainfall. Historical daily precipitation will be used to calibrate daily precipitation model and compute the cumulative level R. Historical H, R and S will be used to estimate the corn yield model in latter Section 3.8.

[12]Both Iowa data sets are collected from U.S. Department of Agriculture (USDA) National Agricultural Statistics Service, Survey Program. Source: https://quickstats.nass.usda.gov

3.7 Parameters estimation and data simulation for price, temperature and rainfall models

This section provides the details of the parameter estimation of the stochastic models of corn prices, rainfall and temperature. The models are then used to create simulated data for these variables.

3.7.1 Corn price model: Parameter estimation and data simulation

As discussed in Sections 2.2.2 and 3.5.1, this paper adopts a mean reverting corn price process[13] which in the $\mathbb{P}$-measure is given as:

$$dP = \theta(\bar{P} - P)dt + \sigma_P P dZ_t \tag{3.26}$$

The price model will be estimated in the $\mathbb{P}$-measure and then converted to the $\mathbb{Q}$-measure using an estimated market price of risk. The discretized approximation of Equation (3.26) is given as:

$$P_t = P_{t-1} + \theta \triangle t \bar{P} - \theta \triangle t P_{t-1} + \sigma_P P_{t-1} \epsilon \sqrt{\triangle t}, \quad 1 \leq t \leq T \tag{3.27}$$

where ϵ follows standard normal distribution. A series of daily spot corn prices from Jan 01, 2010 to July 26, 2019 is obtained from MacroTrends[14] in U.S. Dollars per bushel. Using

[13]The link between this $\mathbb{P}$-measure process (3.26) and the former assumed $\mathbb{Q}$-measure process (3.2) is that, $\alpha = \theta + \lambda_P \sigma$ and $\kappa = \frac{\theta \bar{P}}{\theta + \lambda_P \sigma}$, where λ_P refers to the market price of risk.

[14]Daily corn spot prices were accessed on Aug 13, 2020 and downloaded from the source https://www.macrotrends.net/2532/corn-prices-historical-chart-data

maximum likelihood for estimating the associated parameters (in MATLAB), we present the estimated parameters of the price process (Equation (3.26)) in Table 3.2:

Table 3.2: Parameters summary for risk adjusted corn price process calibration

Input Parameter	Value
Annual market return of S&P500 index ρ_m	0.1783
One-year risk free interest rate ρ	1.76%
Estimated Parameter	**Value**
Mean reversion rate θ	0.4282
Mean level of corn price $\bar{P}$, US$/Bushel	4.6720
Volatility of price σ_P	0.2547
Initial corn price P_0, US$/Bushel	4.1450
Market price of risk for price λ_P	0.0976
P-value	0.0155

* Standard error of θ is 0.3491, 95% confidence interval is [-0.2561, 1.1125].

* Standard error of $\bar{P}$ is 0.6108, 95% confidence interval is [3.4748, 5.8692].

* Standard error of σ_P is 0.0037, 95% confidence interval is [0.2475, 0.2619].

The above estimates are in the $\mathbb{P}$-measure. We need an estimate of the market price of risk (λ_P) to convert to a risk-adjusted corn price process ($\mathbb{Q}$-measure). Our estimation uses the simplified approach suggested by Hull (2003) and employed by Insley & Lei (2007) and Insley & Wirjanto (2010). Details are provided in Appendix F. The resulting estimate of λ_P is 0.0976 (see Table 3.2).

A simulation of 110000 paths of the estimated risk-neutral corn price process with three percentile lines is shown in the following Figure 3.5.

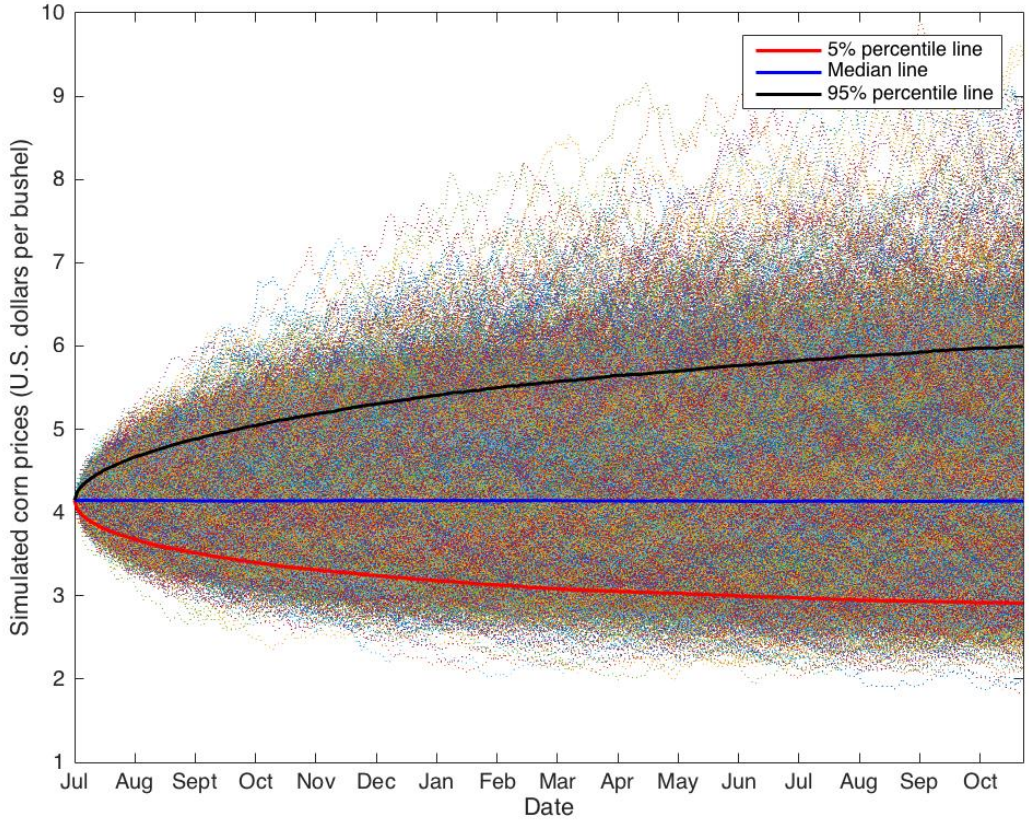

Figure 3.5: 5%, median and 95% percentile lines of simulated risk neutral corn prices

3.7.2 Corn heat units model: Parameter estimation and data simulation

Equation (3.4) describes the maximum daily temperature X_t^1 as a mean reverting stochastic process with the long run mean a function of $\eta_1(t)$. Equation (3.28) below presents a discrete version of Equation (3.4), with $\eta_1(t)$ replaced by a *sine* function: $\eta_1(t) = m + a\,sin(b\,t + c)$ to capture seasonality (Wilks & Wilby (1999) and Qian et al.

(2002)).

$$X_t^1 = [m + a\,sin(b\,t + c)]\phi_1\Delta t + (1 - \phi_1\Delta t)X_{t-1}^1 + \sigma_X\epsilon_X\sqrt{\Delta t} \tag{3.28}$$

The daily temperature difference model in Equation (3.5) can be discretized as:

$$\delta_t = (1 - \phi_\delta\Delta t)\,\delta_{t-1} + \phi_\delta\Delta t\,\eta_\delta(t) + \sigma_\delta\delta_{t-1}\epsilon_\delta\sqrt{\Delta t} \tag{3.29}$$

where the long-run mean level of the temperature difference, $\eta_\delta(t) = \eta_\delta$, is assumed as constant in estimation. $m, \phi_1, a, b, c, \sigma_X, \phi_\delta, \sigma_\delta$ are all constant parameters, t is time variable, ϵ_X and ϵ_δ follow standard normal distributions. The daily minimum temperature is $X_t^{min} = X_t^1 - \delta_t$.

The maximum likelihood technique is employed for estimating parameters (*mle* function in MATLAB). Data (as described in Section 3.6) comprises 29 years (1990-2018) of daily temperature data in Iowa, total data points are 10585. Recall that the partial differential equation describing the value of the corn field (Equation (3.23)) has a term that includes the correction coefficient between δ_t and X_t^1. The sample correlation coefficient between δ_t and X_t^1 is $\rho(\delta_t, X_t^1)$=0.1905. This was judged to be small enough that it can be ignored for simplicity. The temperature models in Equation (3.4) and (3.5) are estimated as

$$dX_1 = 89.2941\,[15.0196 + 15.4501\,sin(6.2780\,t - 1.8573) - X_1]dt + 69.3473\;dZ_{1t} \tag{3.30}$$

and

$$d\delta = 113.4981\,[11.5787 - \delta]dt + 2.8384\;\delta dZ_{\delta t} \tag{3.31}$$

with standard errors and 95% confidence intervals of estimates are summarized in Table 3.3:

Table 3.3: Estimated Parameters for Equation (3.28) and (3.29)

Parameter	Estimates	s.d.	95% Confidence interval
ϕ_1	89.2941	2.3289	[84.7293, 93.8589]
m	15.0196	0.0606	[14.9008, 15.1384]
a	15.4501	0.0768	[15.2996, 15.6006]
b	6.2780	6.12e-04	[6.2768, 6.2792]
c	-1.8573	0.0097	[-1.8763, -1.8383]
σ_X	69.3473	0.4765	[68.4134, 70.2812]
ϕ_δ	113.4981	2.7396	[108.1285, 118.8678]
η_δ	11.5787	0.5156	[10.5681, 12.5893]
σ_δ	2.8384	0.0137	[2.8115, 2.8653]
Δt	$\frac{1}{2920}$	N/A	N/A
$\rho(\delta_t, X_t^1)$	0.1905	N/A	N/A

Note: Correlation coefficient between daily maximum temperature X_t^1 and daily temperature difference δ_t is assumed to be zero for the simulation exercise.

110000 paths of daily temperature are simulated using the estimated model. Simulated daily temperatures and 29 years historical daily temperatures are plotted together in the following Figure 3.6 and 3.7, with the x-axis representing the i-th day over the 183-day length corn development period. Our simulation model can provide a reasonable representation for temperature seasonality and uncertainty.

Three percentile lines (5%, 50% and 95%) are plotted in Figure 3.6. From Figure 3.6, we can find the majority (95%) of our simulated daily temperature paths are located around the seasonality median trend line (50% percentile). This feature of simulated data can guarantee us a good representation of temperature uncertainty and accordingly a reliable

daily corn heat units calculation.

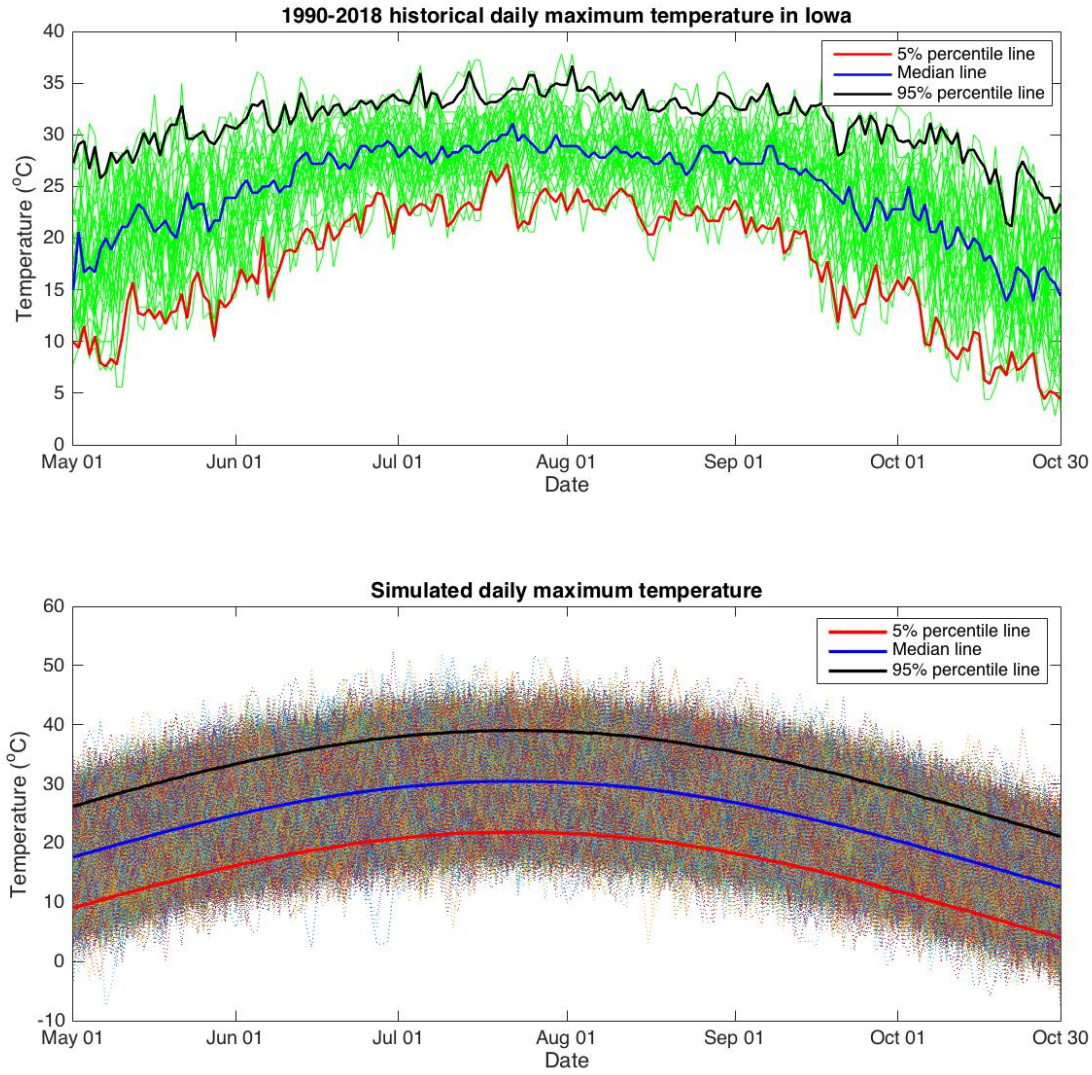

Figure 3.6: 5%, median and 95% percentile lines of historical and simulated daily maximum temperature

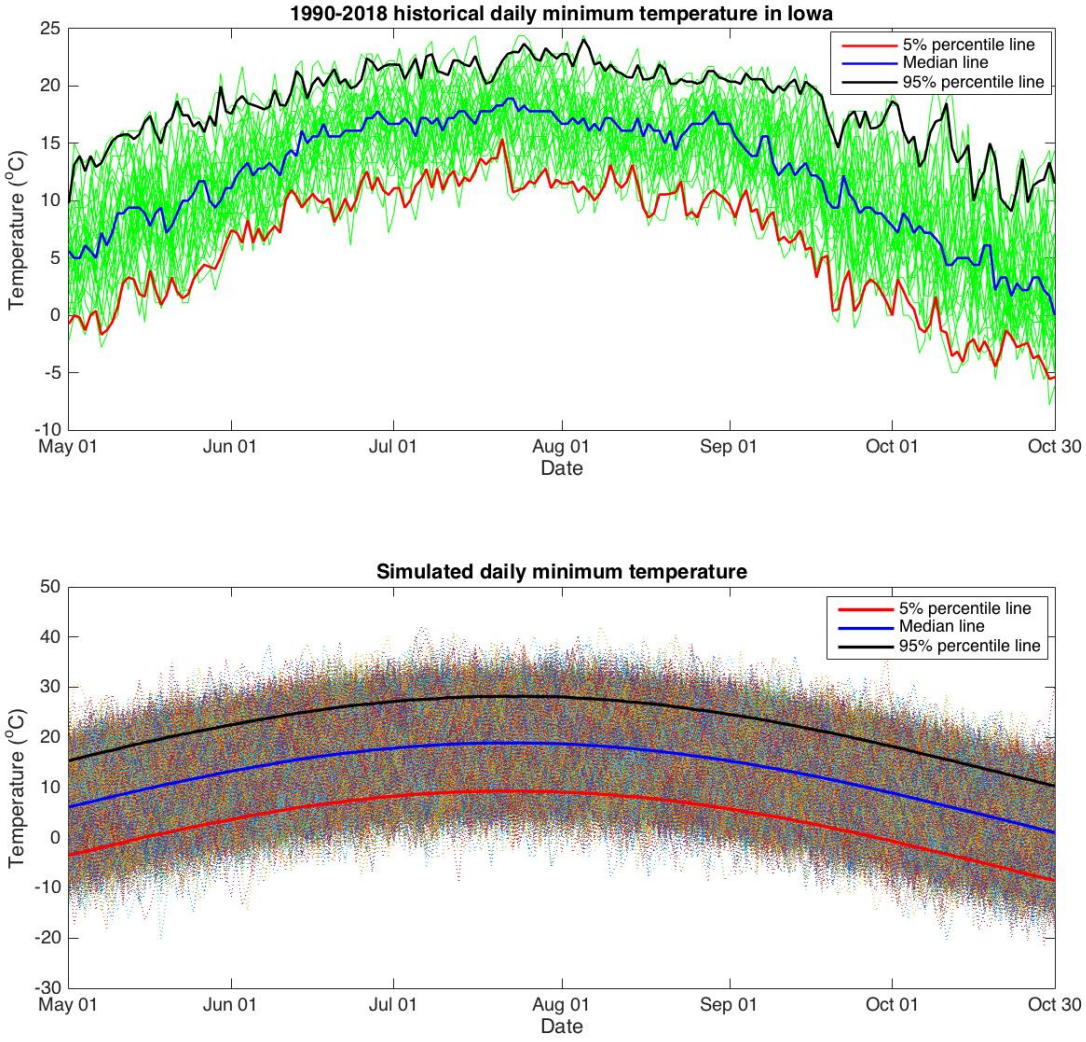

Figure 3.7: 5%, median and 95% percentile lines of historical and simulated daily minimum temperature

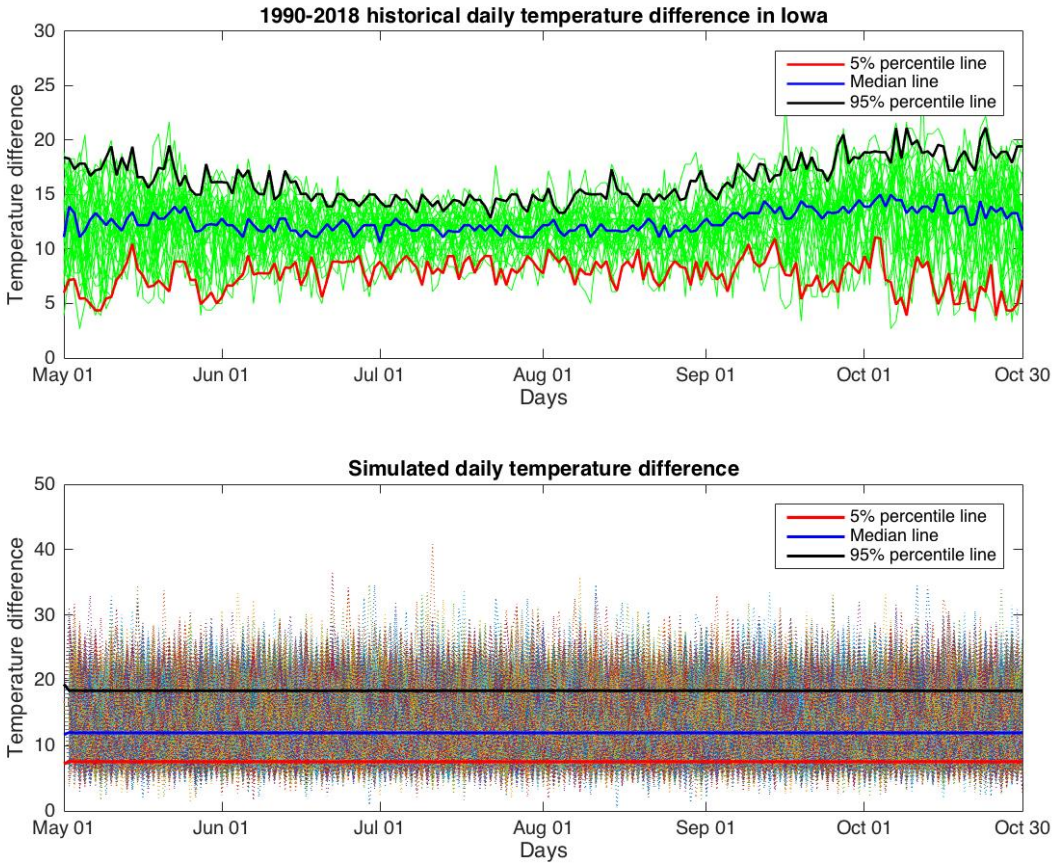

Figure 3.8: Comparison of historical and simulated daily temperature difference

Daily corn heat unit (H_{t_i}) are calculated using the simulated daily maximum and minimum temperatures and the following definition from OMAFRA (2017*a*):

Definition 3.7: Daily corn Heat Units

$$H_{t_i} = \frac{\hat{x}_{t_i}^{\max} + \hat{x}_{t_i}^{min}}{2}$$

where $\hat{x}_{t_i}^{\max} = max\Big\{3.33 * (X_{t_i}^{\max} - 10) - 0.084 * (X_{t_i}^{\max} - 10)^2, 0\Big\}$, $\hat{x}_{t_i}^{min} = max\Big\{1.8 * (X_{t_i}^{min} - 4.4), 0\Big\}$, $X_{t_i}^{\max}$ and $X_{t_i}^{min}$ are the daily maximum and minimum temperature at day t_i. Cumulative corn heat units at maturity $\bar{H}_{t_{\hat{M}}}$ are calculated by summing up daily

corn heat units H_{t_i} from the seeding date $t_i = t_0$ to the maturity date $t_i = t_{\hat{M}}$.

3.7.3 Daily precipitation

The model for rainfall was described in Equations (3.9) and (3.10). Equation (3.9) defined dry and wet days as governed by two Poisson processes. The instantaneous rainfall rate R was specified as following a known probability distribution $f(R)$. This is consistent with previous literature (including Richardson (1981) and Brissette et al. (2007)) and the weather generator WeaGETS (Chen et al. (2012*a*) and Chen et al. (2012*b*)). The Poisson process described in Equation (3.9) is represented here as a discrete time first-order Markov chain. The daily precipitation amount is modelled to follow an exponential distribution. Like daily temperature, daily precipitation has a seasonal cycle and variability, with higher probabilities and amounts of precipitation in summer and autumn (Bhandari et al. (2016), Cropper & Cropper (2016), Patil et al. (2019) and the U.S. National Weather Service (NWS)[15]). To accounting for the seasonal variability, the transition state probabilities $P_{ij}(t) = P\{w_t = j \,|w_{t-1} = i\}$, $i, j \in \{0, 1\}$ are estimated for each day of the year, where subscript 0 means *dry* state and 1 means *wet* state. For example, the probability of changing from *dry* state at day $t-1$ of the year to *dry* state at day t of the year, $P_{00}(t)$, is estimated by taking total number of days changing from *dry* at day $t-1$ to *dry* at day t across the 29-year (1990-2018) period and divide by the total number of days where state is *dry* at day $t-1$ across the 29-year (1990-2018) period. Estimates for transition probabilities P_{00}, P_{01}, P_{10} and P_{11} for all days of the year are plotted in Figure 3.9.

[15]Seasonal Variability of Climate Time Series. Source: https://training.weather.gov/pds/climate/pcu2/statistics/Stats/part1/CTS_SeaVar.htm

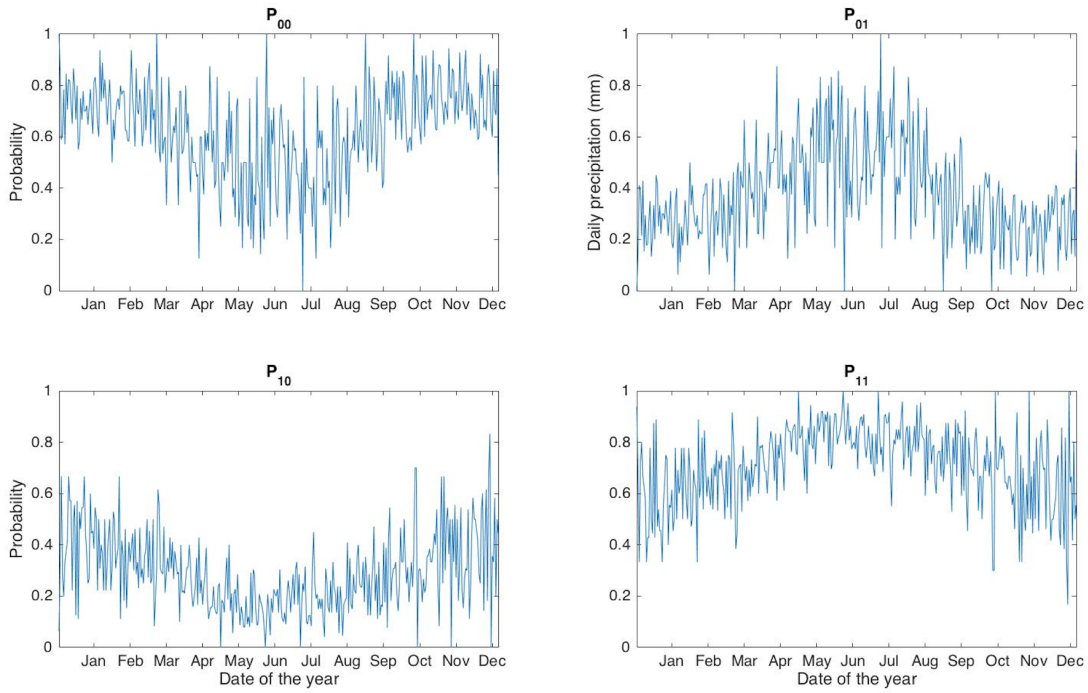

Figure 3.9: Estimates for transition probabilities P_{00}, P_{01}, P_{10} and P_{11} for all days of the year

Daily precipitation amounts on wet days, $R^{w_t=1}$, are assumed to have an exponential probability density function in Equation (3.32). To account for the seasonal variability, the parameter γ_t, is estimated for each day of the year over the 29-year (1990-2018) period. For the day t of the year, we calculate the total number of days with positive precipitation across 29 years and divided by the total precipitation amounts on day t across 29 years. Estimates and standard errors for γ_t are plotted in Figure 3.10 with the 95% confidence interval is the blue-shaded area. The density function is

$$f(R_t) = \gamma_t \cdot e^{-\gamma_t \cdot R_t} \tag{3.32}$$

Note that for an exponential distribution mean $E(R) = 1/\gamma$ and variance $Var(R) = 1/\gamma^2$. From Figure 3.10, γ has a larger variation in winter and spring and rainfall amounts are

higher in summer and fall, evidencing the seasonal variability.

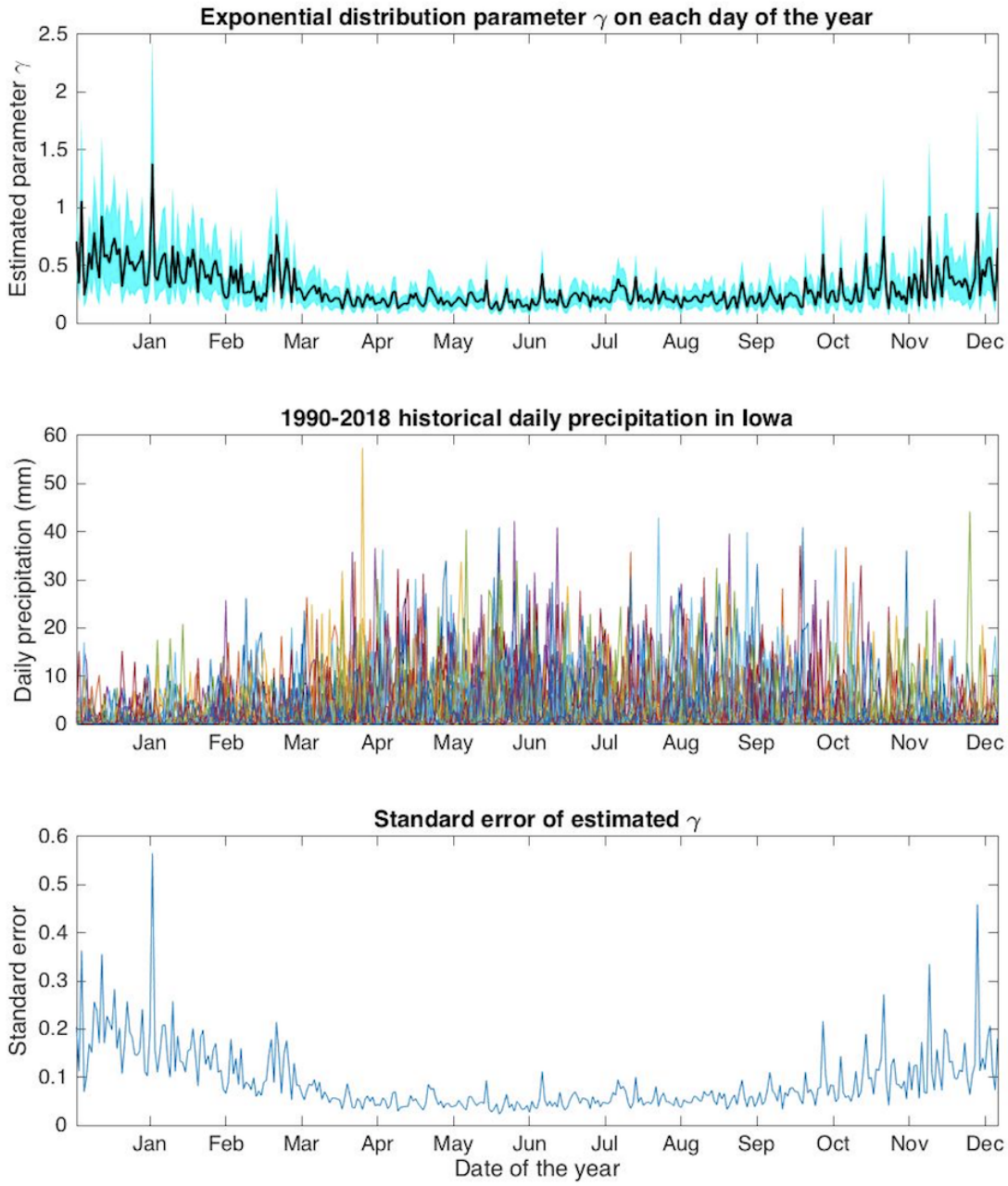

Figure 3.10: Estimates for γ_t for all days of the year

The basic algorithm to simulate a series of daily precipitation is presented as the following Algorithm 1:

Algorithm 1 Simulate daily precipitation

Input: Assume day $t = 0$ is dry state, estimated exponential distribution pdf $f(R_t)$ in Equation (3.32) and transition probabilities $P_{ij}(t)$ in Figure 3.9.

Output: daily precipitation series $R(t)$

for t= 1:365 days **do**
    if day $t-1$ is dry **then**
        $Prob = P_{00}(t)$;
    if day $t-1$ is wet **then**
        $Prob = P_{10}(t)$;
    Generate a random number $U(t)$ from the uniform distribution
    if $U(t) \leq Prob$ **then**
        day t is dry; ELSE day t is wet;
    if day t is dry **then**
        $R(t) = 0$;
    if day t is wet **then**
        generate $R(t)$ from the density function $f(R_t)$;
return daily precipitation vector of R

Apart from the exponential distribution, the gamma distribution is considered as an alternate candidate for modeling rainfall rate on a day when precipitation occurs. The gamma distribution has also been used in the literature in simulating daily precipitation (including Roldan & Woolhiser (1982), Woolhiser & Roldan (1982) and Liang et al. (2012)). A comparison of historical precipitation, simulated precipitation under exponential distribution and simulated precipitation under gamma distribution is presented in the Figure 3.11:

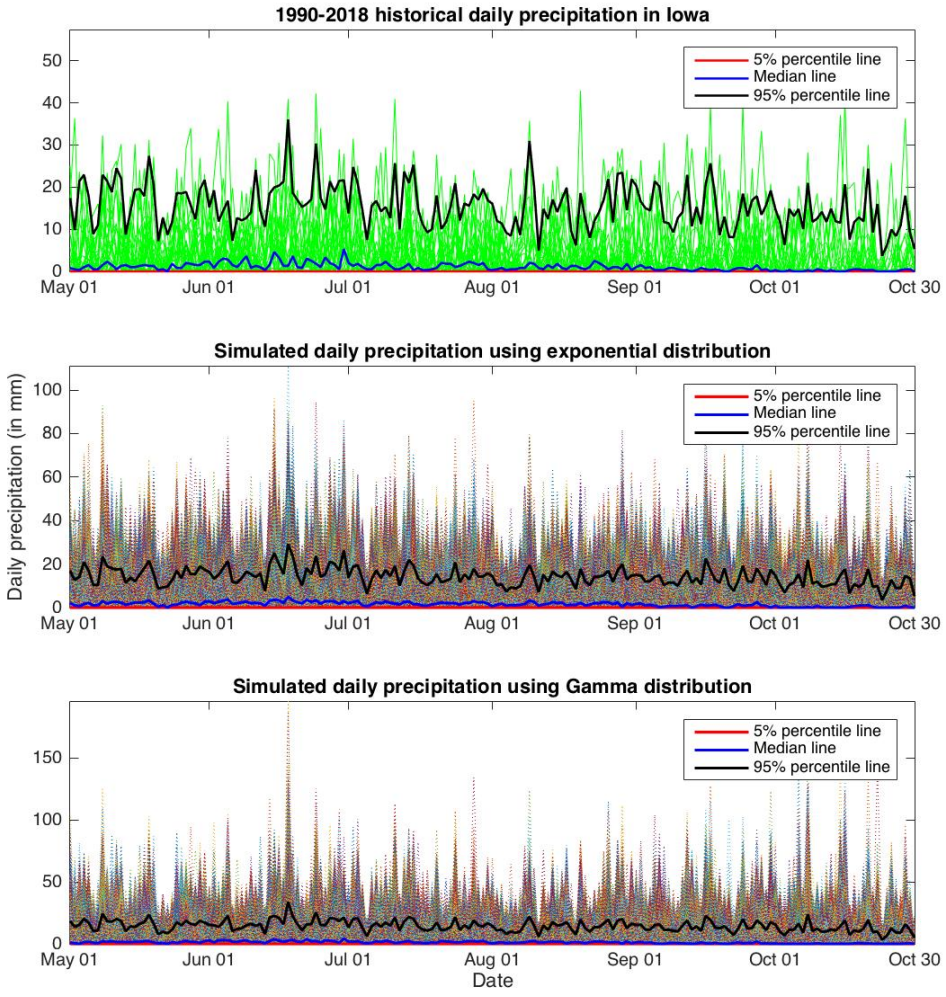

Figure 3.11: 5%, median and 95% percentile lines of Iowa historical and simulated daily precipitation

From Figure 3.11 we can see that, in contrast with the simulated precipitation from gamma distribution, the range of simulated precipitation from exponential distribution gets closer to the historical record. The exponential distribution works better in describing historical daily precipitation amounts compared to gamma distribution. In our thesis, we will use the exponential distribution for simulating daily precipitation (including Brissette et al. (2007), Chen et al. (2012*a*) and the weather generator $WeaGETS$).

From the second picture in Figure 3.11, we can see that 95% of simulated paths are located below the black line, which means even though we have large outliers beyond the black 95% percentile line as a result of volatility, the majority of our simulated paths is in the similar range with Iowa historical precipitation. That gives us an evidence that our daily precipitation simulation is a good representation for the actual precipitation uncertainty.

3.8 Calibration of the corn yield model

3.8.1 Corn growth stages

Corn planting in Iowa occurs between mid-April and mid-May depending on the particular area of Iowa and seasonal weather conditions[16]. A warm, dry period during the last week of April often allows a small amount of corn to be planted early and a few cooler events may limit planting activity until the end of the second week of May (May 14) when field work resumed on lighter textured soils. In this thesis, May 1 is chosen as the representative planting date based on information about Iowa farming practices.

In Iowa most corn harvesting is done in October, although a portion may be done in September and in cooler years harvesting may be delayed to November [17]. In this thesis, October 30 is the assumed harvest date.

Nitrogen (N) is typically the most yield-limiting nutrient for corn yield and relative to other nutrients, nitrogen is more susceptible to losses due to rainfall. We therefore use nitrogen fertilizer as the representative fertilizer. Nitrogen fertilizer application date

[16]Source: Iowa State University Extension and Outreach, Best Corn Planting Dates for Iowa, March 2012, https://crops.extension.iastate.edu/cropnews/2012/03/best-corn-planting-dates-iowa

[17]Iowa Corn FAQs, Iowa Corn Growers' Association, https://www.iowacorn.org/education/faqs.

and frequency, varies by region. According to crop experts[18], the effective time to apply phosphorus and potassium is before planting in the spring as long as the soil test levels are above the very low range. As for nitrogen fertilizer, the efficiency of pre-plant or side-dress applications depends largely on prevailing weather conditions. Thus, applying nitrogen at multiple times, usually including the time of maximum nitrogen uptake speed can lower the risk of N loss. Nitrogen uptake stages for corn in Mississippi as reported by Erick Larson Crop Situation, are shown in the following Figure 3.12:

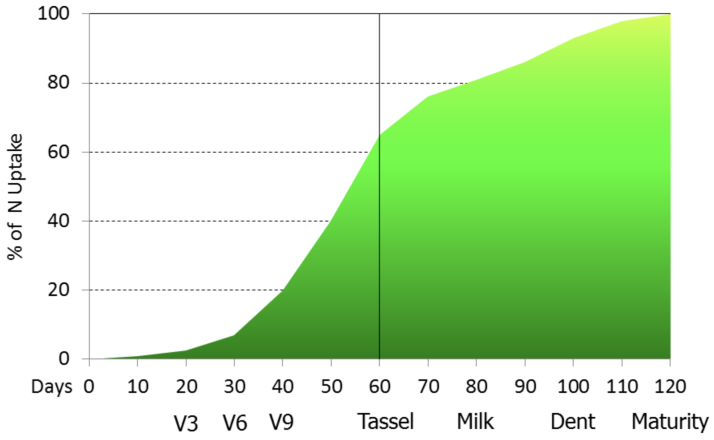

Figure 3.12: Nitrogen uptake stages for corn[19]

As the graph indicates, the most rapid N uptake stage for most crops (corn and soybean) starts from V6 stage[20], which is from the week after June, 6 to the week after July, 15, a period that roughly covers more than 30 days. According to Dupont Pioneer[21], nitrogen

[18]See for example, Mississippi Crop Situation of the Mississippi State University Extension, https://www.mississippi-crops.com and firm Dupont Pioneer, https://www.pioneer.com

[19]Source: *www.mississippi-crops.com*/2017/04/07/*importance-of-nitrogen-timing-and-methods-for-southern-corn*/

[20]V3 means plant switches from kernel reserves to photosynthesis and nodal roots begin to take over. V3 stage corn is usually about 5 to 7 inches tall. V6 stage means the growing point finally moves above the soil surface. V6 corn is normally 14 to 20 inches tall. At V9 stage, tassel is developing rapidly, but is not yet visible. New leaves appear every 2 to 3 days and ear shoots are developing. Tassel stage means the bottom-most branch of tassel completely visible. Milk stage means the kernel looks yellow outside, milky white fluid inside. Dent stage means most kernels at least partially dented.Maturity means the maximum dry weight is attained.

[21]Nitrogen Application Timing in Corn Production, by Dupont Pioneer, source: www.pioneer.com/us/agronomy/nitrogenapplicationtiming.html

may be applied by US growers at multiple times: early spring (pre-plant), at planting, and in the growing season (side-dress). However, a pre-plant application is at a high risk of loss due to a low uptake efficiency and excessive rainfall in early spring. Delaying fertilizer application until after the crop has emerged (i.e. a side dressing) is beneficial as the farmer can respond to spring weather conditions which have affected N content in the soil. However it is considered risky to rely solely on a side dressing because weather conditions may be such that the farmer misses the crucial time when corn is most in need of nutrients[22]. In our numerical exercise, it is assumed that the farmer applies fertilizer at the planting date and may apply additional fertilizer in the growing season (side-dress application). For example, if wet spring weather results in N loss, the farmer will have a second chance in growing season to avoid yield loss caused by nitrogen deficit, side-dress rate may then be increased. Thus, the farmer in this chapter is assumed to have two split-time nutrient applications (at the seeding date and in-season side-dressing). Usually side-dress application occurs near the time of maximum plant N uptake speed (mid-June). According to OMAFRA (2017*a*), June 18 can be targeted as the side-dressing date when rapid stem elongation begins and a tassel is visible upon plant dissection, without posing threat of root damage. The assumed date of maturity for our analysis is the 141^{st} day (Sept 18) from the seeding date. This is a later date than what is shown for Mississippi region in Figure 3.12 because several climate factors may delay the maturity in some areas. Sept 18 is the end of reproductive growth stage and is assumed as the latest date when corn maturity achieved. It is not uncommon for farmers to delay harvesting after corn plants are physically mature to allow corn kernels more drying time, which lengthens the time corn can be stored.[23] In Iowa, some corn farmers begin early harvesting from mid-September, though most of the harvest is takes place in October. In unfavorable weather conditions,

[22]See Steve Butzen, "Nitrogen Application Timing in Corn Production", Crop Insights, Pioneer. https://www.pioneer.com/us/agronomy/nitrogenapplicationtiming.html

[23]Iowa Corn Growers Association, Corn FAQs, https://www.iowacorn.org/education/faqs

much of Iowa's corn isn't harvested until the end of October. It is assumed in this analysis that the corn is completely harvested and sold in the market on the 183^{rd} day (October 30) from the seeding date, six weeks after corn maturity.

In summary, this chapter will adopt May 01 as the uniform seeding date and as the first nutrient application date, and June 18 as the second fertilizer application date. Physiological maturity, at the end of growing season, is targeted for September 18 when kernels have achieved maximum dry weight and weather accumulation will have no impact on corn grain filling and yield after then. After September 18, it is assumed that the crop is harvested and then sold on October 30. The corn growing season can be partitioned into multiple key growth stages, as is illustrated in the Figure 3.13:

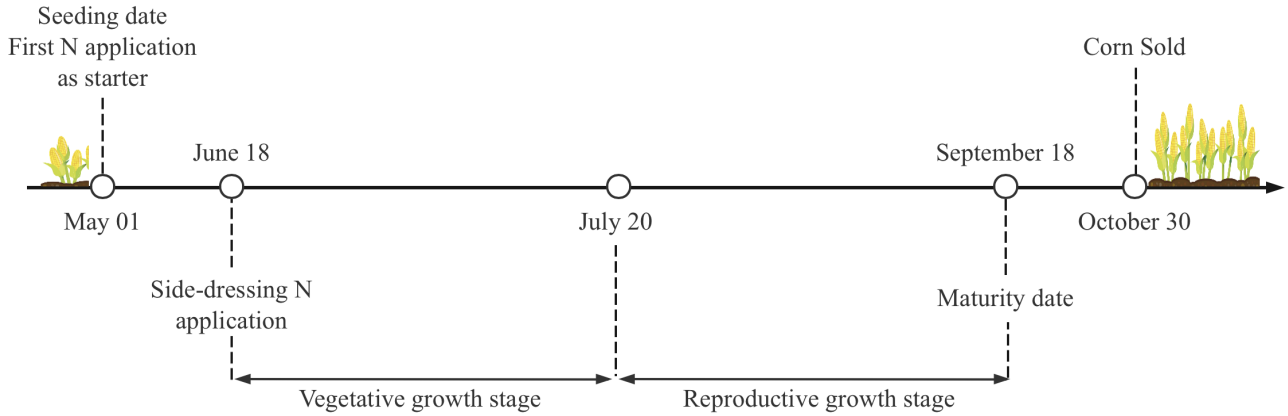

Figure 3.13: Corn growth stages in our model[24]

3.8.2 Corn yield estimation

As discussed in Section 3.3, empirical research has examined the effects of weather on crop yields, often as part of the larger question on how changing climate might affect future

[24]In actual corn growth periods, especially in the middle of growing season, corn will become increasingly sensitive to yield reduction by heat or drought events. Pollen viability may be reduced by high temperature. In our model, key stages and dates are assumed according to OMAFRA (2017*a*).

yields and fertilizer demand[25].

The unknown parameters of Equation (3.16) were calibrated using the Iowa historical data sets ($\bar{H}$, $\bar{R}$, $\bar{S}$) that are described in Section 3.6. We used the Matlab function $lsqcurvefit$ for the estimation of the non-linear function. The fitted model is given as Equation (3.33):

$$Y = 0.0153 * year * (3.5438 * \bar{R} - 0.0033 * \bar{R}^2)(1 - e^{-0.0766*\bar{S}})(1 - e^{-0.0006*\bar{H}}) \quad (3.33)$$

The calibration was done using nineteen years of historical data. The term "year" was set at 1 through 19 to capture exogenous productivity improvements over the estimation period (Recall that the corn yield data includes 1990-2003, 2005, 2010, 2014, 2016, and 2018.). For the modeling exercise the year is set to 20, which implies $\theta = 0.3060$ in Equation (3.16).

Table 3.4: Ranges of Iowa historical state variables (1990-2003, 2005, 2010, 2014, 2016, 2018)

Value	$\bar{H}$	$\bar{R}$	$\bar{S}$
[min, mean, max]	[3180.7, 3400.3, 3619.9]	[409.9, 512.0, 870.7]	[78.2, 101.4, 120.1]

$*$ All three state variables are in 19×1 dimension

Ranges of Iowa historical $\bar{H}$, $\bar{R}$ and $\bar{S}$ are displayed in the above Table 3.4. Figure 3.14 plots the estimated corn yield function versus one of $\bar{H}$, $\bar{R}$ or $\bar{S}$, with the remaining two variables set at their mean levels. For example, the first row of Figure 3.14 has a fixed $\bar{H}$ and $\bar{R}$ at their mean levels. The second row of Figure 3.14 has a fixed $\bar{S}$ and $\bar{R}$ at their mean levels. The third row of Figure 3.14 has a fixed $\bar{H}$ and $\bar{S}$ at their mean levels.

[25]For example, see Addy et al. (2020) and references therein.

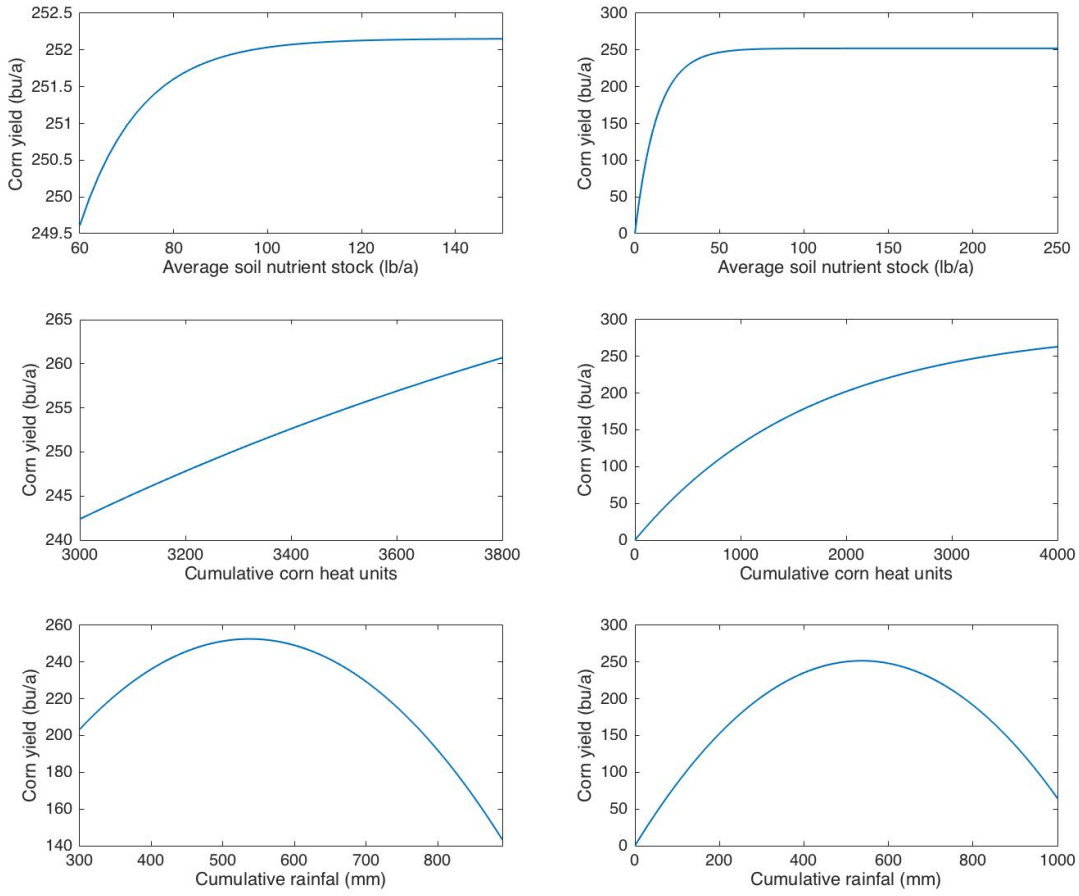

Figure 3.14: 2-dimensional plots of corn yield model. Each figure shows yield versus an independent variable with the other 2 variables at their historical mean. The first column shows the horizontal axis over the historical range; The second column shows a more extreme range for the horizontal axis.

In Figure 3.14, the left column represents the plot of corn yield model against one variable, which varies in its historical range while keeping other two variables constant at historical mean level. The right column in Figure 3.14 presents a more extreme range for the horizontal axis. We observe corn yield as a concave function of $\bar{H}$ and $\bar{S}$, with the peak yield at around 250 bu/acre. Over the historical range corn yield is a near linear function of $\bar{H}$ (left column, second row in Figure 3.14). The third row shows a significant negative

response of corn yield to cumulative rainfall amounts $\bar{R}$ beyond about 550 mm.

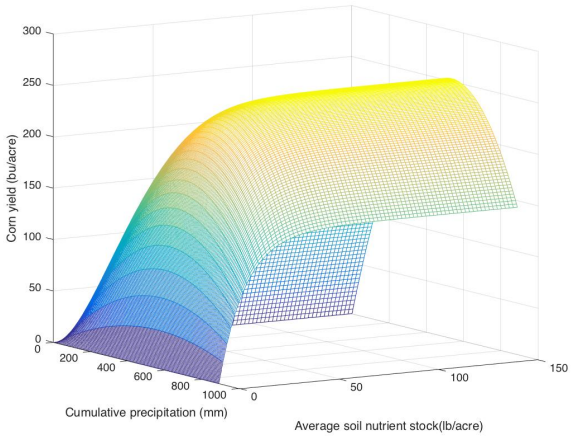

(a) $\bar{H}$ is fixed at historical mean

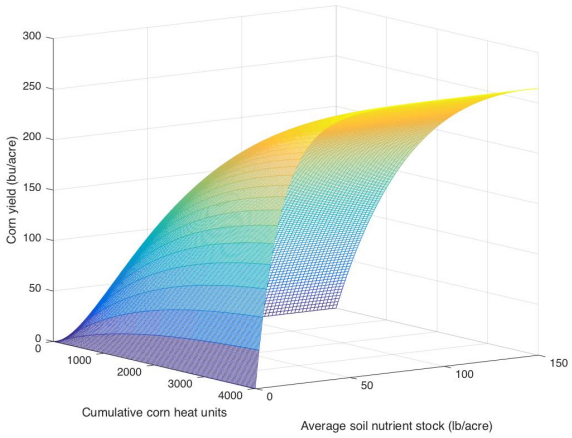

(b) $\bar{R}$ is fixed at historical mean

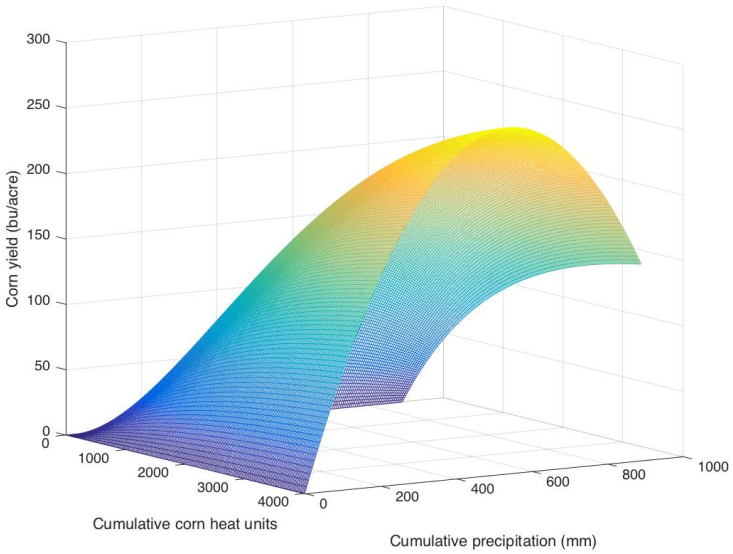

(c) $\bar{S}$ is fixed at historical mean

Figure 3.15: 3-dimensional plots of corn yield model (3.33)

We can get a more clear perspective from the 3-D plot of corn yield model from above Figure 3.15 with only one variable held fixed. For example, in Figure 3.15 (a), the change of cumulative precipitation $\bar{R}$ does not affect the shape of yield-nitrogen effect but changes

the maximum yield threshold corn can reach. A similar pattern can also be found from Figure 3.15 (b) and (c), which shows each of the inputs are limiting to the overall yield. Even if excessive soil fertility $\bar{S}$ and heat accumulation $\bar{H}$ are not harmful to the corn yield, excessive rainfall will result in the yield loss.

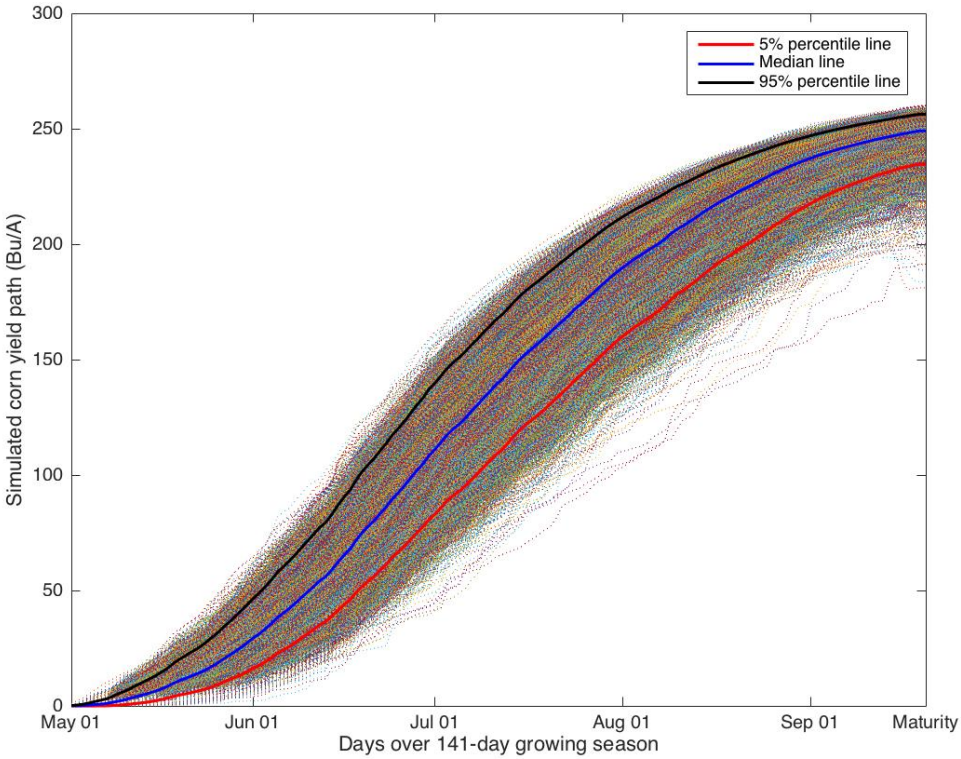

Figure 3.16: Simulated corn yield path

Monte Carlo simulations of corn yield paths over time are plotted in the above Figure 3.16. Daily corn heat unit and daily precipitation for each path are used to calculate the corresponding cumulative levels for $\bar{H}$ and $\bar{R}$ on a daily basis. Simulated daily precipitation and the mean level of historical annual nitrogen application in Iowa (128 lb/a in Table 3.1 is assumed as the uniform one-off application at the seeding date) are used to calculate the 110000 paths for the cumulative mean level of $\bar{S}$ on a daily basis. The calibrated corn

yield model Equation (3.33) is then used to compute the corresponding corn yield path over time. Three percentile lines are also plotted in the figure. The above Figure 3.16 indicates that corn will start to grow after seeding stage with a rising speed (May) and enters the rapid root development and grain filling stage with steady growth speed (June through August), after which maturity season will arrive and the yield will no longer be impacted by the input and weather accumulation.

A comparison of Figure 3.16 and Figure 3.12 in Section 3.8.1 can show us the advantage of our proposed corn yield model in describing realistic corn growth. Several green paths show a decline in yield at the end of the period in Figure 3.16, which can be attributed to our quadratic rainfall R effect term in Equation (3.33) (huge late-season rainfall amount will lower the yield).

3.9 Monte Carlo Analysis

As noted previously, with four stochastic state variables (H, R, S and P) and three path dependent variables ($\bar{S}$, $\bar{R}$, and $\bar{H}$), no closed-form solution is available for the farmer's decision problem. A numerical solution using dynamic programming is also not practical. However, if the number allowed controls is restricted, then it is possible to determine the optimal actions using Monte Carlo simulation and exhaustive search. In this section, the values of the hypothetical corn operation over the range of restricted farmer controls are computed. The optimal fertilizer strategy is determined and results are contrasted with the closed form results presented in Chapter 2.

The representative farmer is assumed to apply fertilizer twice: at the seeding date t_0 (May, 01) as a starter and at the beginning of growing season t_1 (Jun, 18) as side-dressing, with fertilizer amounts represented by of N_0 and N_1. Given a pair of application strategy

(N_0, N_1), the expected value of the crop at the seeding date $V(t_0)$ can be computed:

$$V(t_0|(N_0, N_1)) = e^{-rT}\mathbb{E}[V(T|(N_0, N_1))] \tag{3.34}$$

with

$$\begin{aligned} V(T) = & \overbrace{Y(\bar{S}^{[0,t_{\hat{M}}]}, \bar{H}^{[0,t_{\hat{M}}]}, \bar{R}^{[0,t_{\hat{M}}]})\, p(T)}^{\text{corn revenue}} - \overbrace{c_N\, N_0\, e^{r(T-t_0)} - c'_N\, N_1\, e^{r(T-t_1)}}^{\text{total fertilizer variable costs}} - \overbrace{c_F}^{\text{fixed cost}} \\ & - \overbrace{c_V\, Y(\bar{S}^{[0,t_{\hat{M}}]}, \bar{H}^{[0,t_{\hat{M}}]}, \bar{R}^{[0,t_{\hat{M}}]})}^{\text{total variable costs excluding fertilizer inputs}} \end{aligned} \tag{3.35}$$

where $t_{\hat{M}}$ refers to the maturity date of the corn, c_V is the variable cost on corn yield excluding fertilizer use (e.g., grain haul, storage), c_N is the unit variable cost of starter application while c'_N is the unit variable cost of side-dressing fertilizer application including fertilizer cost, c_F is the fixed machinery cost associated with both fertilizer applications and harvest. t_0 is the seeding time and T is the harvest date, $Y(\cdot)$ represents the estimated corn yield model Equation (3.33). $\bar{R}^{[t_0,t_{\hat{M}}]}$ is the accumulation of precipitation amount over the period from seeding date $t_0 = 0$ to the end of the growing season $t_{\hat{M}}$, $p(T)$ is the simulated risk neutral corn price at the harvesting date $T = t_M$, $\bar{H}^{[t_0,t_{\hat{M}}]}$ is the accumulation of daily corn heat units over the period from seeding date $t_0 = 0$ to the end of the growing season. $\bar{S}^{[t_0,t_{\hat{M}}]}$ is the average amount of soil nutrient stock over the same growing season period. Soil nutrient content S equals nutrient application less rainfall induced nutrient loss. Note that it is appropriate to discount using the risk free rate since corn prices are modelled in the $\mathbb{Q}$-measure for equivalent risk neutral valuation. Rain and corn heat units are modelled in the $\mathbb{P}$-measure, but it is assumed that these are diversifiable risks.

The algorithm to compute the simulated soil nutrient stock is created as the following Algorithm 2:

Algorithm 2 Compute average soil nutrient stock $\bar{S}$

Input: Simulated daily precipitation $R^{w_t}(t)$, $t \in \Omega_D$, nutrient application (N_0, N_1), l_s

Output: $\bar{S}$

Initial soil nutrient stock $\bar{s}_0 = 0$;
for i=1 : number of simulated paths **do**
    $\bar{S}(i, t_0) = N_0$;
    for j=t_0+1 : t_M **do**
        if $j \in \Omega_F$ **then**
        $S(i,j) = (1 - l_s * R^{m_{j-1}}(i, j-1)) * S(i, j-1) + N_1$
        else
        $S(i,j) = (1 - l_s * R^{m_{j-1}}(i, j-1)) * S(i, j-1)$
return $\bar{S}(i,:) = mean(S(i, t_0 : t_M))$

3.9.1 Variable and fixed costs

Due to differences in soil characteristics, the variation in the quality and quantity of inputs and other agricultural-economic factors, production costs vary from farm to farm.

Ag Decision Maker[26] provides cost estimates based on data from several sources, including Iowa State University, surveys of selected agricultural cooperatives and other input suppliers around the Iowa state. These cost estimates are intended to represent the average costs for farms in Iowa. Very large or small farms may have lower or higher fixed costs per acre. Using this information and assuming 162 bushels per acre as target yield scenario, the variable cost of fertilizer for both starter and side-dressing applications is assumed as $c_N = c'_N = \$0.72$/lb. The fixed preharvest machinery cost is assumed as

[26] Ag Decision Maker, an agricultural guidance website initiated by Iowa State University, specified the production costs. Details are listed on "Estimated costs of crop production in Iowa 2022", Page 2, Corn Following Corn section, source: https://www.extension.iastate.edu/agdm/crops/pdf/a1-20.pdf

\$24.8/*acre*. The fixed harvest machinery cost is \$39.28/*acre*. Labor cost (\$47.6/*acre*) has been treated as a fixed cost in the report since most labor on Iowa farms is supplied by the operator or permanent hired labor. The total fixed cost associated with both split applications and harvesting is assumed as $c_F = 24.8 + 39.28 + 47.6 = 111.68$ \$/acre. The variable costs in *Ag Decision Maker*, consisting of preharvest machinery, seed, herbicide, chemical fertilizer, harvest machinery variable costs, etc, is estimated as \$464.02/*acre*. The total variable cost excluding chemical fertilizer is 464.02-113.76 (Nitrogen variable cost)-37.82 (Phosphate variable cost) -27.44 (potash variable cost) =\$285/*acre*, based on per acre 162 bushels yield target scenario. The base case variable cost per bushel corn yield is calculated as $c_V = \frac{285}{162} = \$1.7593$ */bushel*. In later sensitivity analysis sections, the total variable cost that only include haul grain, dry grain and store grain is assumed as 0.2645 \$/*bu* for sensitivity examination. Since the fixed costs c_F covers harvest machinery and all labor cost, c_F is assumed to be paid at maturity date. The total variable costs per bushel on corn yield will be paid at maturity date as well.

Algorithm 3 Compute value V_0 at $t = 0$ and the optimal fertilizer strategy $(N_0^\star,\ N_1^\star)$

Input: nutrient application set $(N_{0(1\times size(N_0))},\ N_{1(1\times size(N_1))})$, c_N, c'_N, c_F, c_V, growing season $\bar{H}_{(M\times 1)}$, $\bar{R}_{(M\times 1)}$, $\bar{S}_{(M\times 1)}$, $P_{T(M\times 1)}$, ρ, $t_{f_1}, t_{f_1} \in \Omega_F$

Output: V_0, the optimal strategy $(N_0^\star,\ N_1^\star)$

for i= 1:$size(N_0)$ **do**

  $\tilde{N}_0$=$N_0(i)$

  for j= 1:$size(N_1)$ **do**

    $\tilde{N}_1 = N_1(j)$

    Compute $\bar{S}_{(M\times 1)}$ using given $(\tilde{N}_0, \tilde{N}_1)$ and Algorithm 2.

    V_T=$P_T\, Y(\bar{H}, \bar{S}, \bar{R}) - c_N \tilde{N}_0 e^{r(T-t_{f_1})} - c'_N \tilde{N}_1 e^{r(T-t_{f_2})} - c_F - c_V Y(\bar{H}, \bar{S}, \bar{R})$

    $V_0(i,j) = e^{-\rho(T-t_0)} mean(V_T)$

[a, b]=find(V_0=max(V_0));

return a, b

$(N_0^\star,\ N_1^\star) = (N_0(a),\ N_1(b))$;

3.9.2 Starting values for state variables and costs

Assumed starting values are required of all state variables for the Monte Carlo simulation, which are detailed below in Table (3.5). Assumed starting values for the state variable corn price is P_0=\$4.145/*bushel*, which is the spot price on July 26, 2019 spot price. Assumed starting values for daily maximum temperature X^1 and temperature difference δ are values on December 31, 2018. Both temperature state variables are simulated from December 31 to next year September 18 (maturity date). Simulated daily minimum temperature is computed using $X^1 - \delta$. For daily precipitation simulation, we assume the first day (January 01) of a year is dry state with no rainfall, we then use P_{01} and P_{00} to simulate 365 days rainfall series with rainfall amounts are generated from the estimated

exponential distribution. We take growing season period (May 01-Sept 18, from seeding date to maturity date) from simulated data in our computation.

Table 3.5: Starting Values for Simulating State Variables

State Variables	Starting Values	Interpretation
Daily maximum temperature	2.8^oC	Use Dec 31, 2018 data as starting value to simulate until next year maturity date Sept 18.
Daily minimum temperature	-8.3^oC	Use Dec 31, 2018 data as starting value to simulate till next year maturity date Sept 18.
Daily temperature difference	11.1^oC	Use daily maximum temperature minus daily temperature difference.
Daily precipitation	Assume the initial state (day 0) is dry	Simulate 365-day rainfall series and use May 01 to Sept 18 period for computation.
Corn price	\$4.145/*bushel*	Use Jul 26, 2019 spot price as starting value to simulate until next year Oct 30.

3.9.3 Monte Carlo Results

Nitrogen applications N_0, N_1 are in $lb/acre$, all cost and price parameters are in U.S. dollars. The admissible set of (N_0, N_1) is a set of 3721 (61×61) pairs that start from (0, 0) to (120, 120) lb/a with a uniform step size of 2 for each N_i $(i = 0, 1)$. The optimal fertilizer application strategy with the maximized corn value V_0 is chosen by exhaustive search over these pairs of possible strategies,

$$V_0^{\star} = \max_{(N_0,N_1)} \mathbb{E}\Big\{V(t_0|(N_0^{(1)}, N_1^{(1)})), V(t_0|(N_0^{(1)}, N_1^{(2)})), ..., V(t_0|(N_0^{(61)}, N_1^{(61)}))\Big\} \tag{3.36}$$

The above Algorithm 3 is thus created to describe how to compute the value of the corn field V_0 and determine the optimal nutrient application strategy.

The values per acre of corn over a range of fertilizer application decisions are depicted in the value surface in Figure 3.17. Each node on the value surface represents the expected value of corn under a given fertilizer application strategy ($N_0 = N_{t_0}$, $N_1 = N_{t_1}$) given the assumed stochastic models for corn prices, rain and corn heat units. The surface in Figure 3.17 is concave with the maximized value ($V_0 = \$453.22/acre$) at ($N_0$, N_1) = (66, 0) lb/a. This result indicates that the farmer's optimal strategy is applying all the fertilizer at the seeding date, based on our base case parameter assumptions. Based on our model setting, starter application can provide higher seasonal soil average N stock with less fertilizer amount compared to side-dressing.

The value surface in Figure 3.17 is relatively flat around the optimal application. After examining the V_0 values for each bundle of (N_0, N_1), we find that the farm value ($V_0(i, j)$) changes by very small amounts across contiguous allocations ($N_0(i-1)$, $N_1(j)$), ($N_0(i+1)$, $N_1(j)$), ($N_0(i)$, $N_1(j+1)$) and ($N_0(i)$, $N_1(j-1)$). Since we use the averaged soil N level as the state variable in our model, N_0 is more favourable and has a more significant impact

on corn yield and farmland value compared to the same amount N_1. We can see this in Figure 3.18, where both the soil nutrient stock and the value from $(N_0 > 0, N_1 = 0)$ are higher than those from $(N_0 = 0, N_1 > 0)$. However, as the application amount increases, the farmer's benefit (V_0) from "all as starter" (red line) and "all as side-dressing" (blue line) are getting closer, which can be explained by the exponential corn yield model that generate very near yield levels when the soil nutrient stock are high enough (as showed in Figure 3.14).

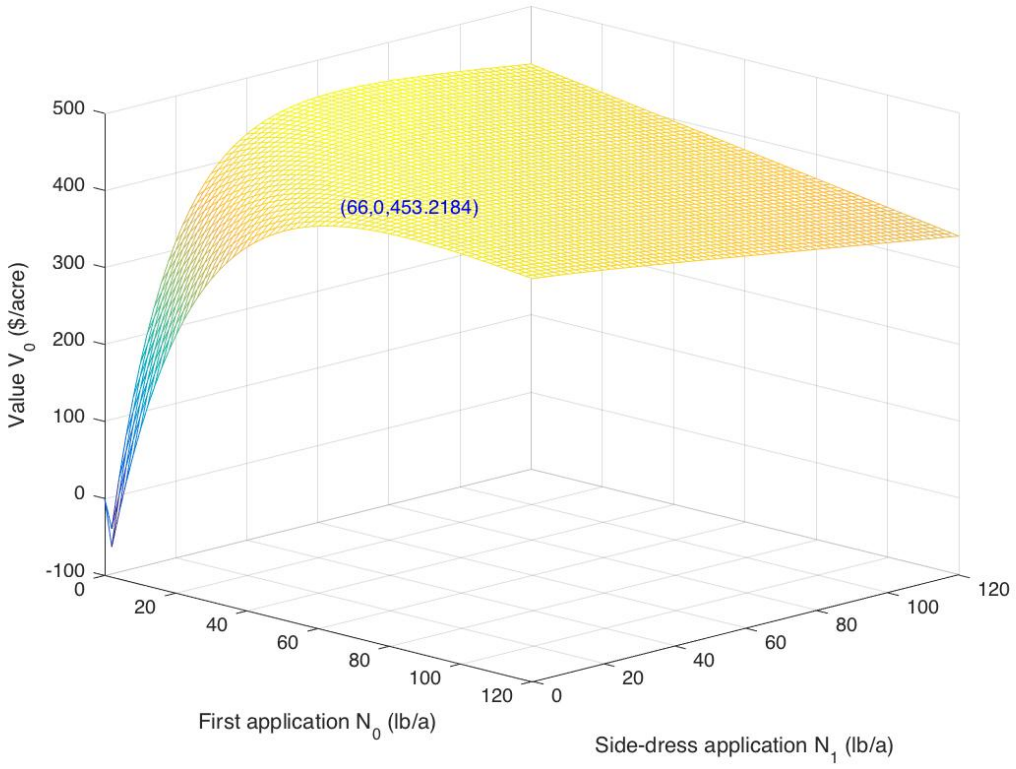

Figure 3.17: Corn Value Surface V_0, ordered triple is (First application, Second application, Value)

In Figure 3.17, V_0 rises rapidly as N_0 and N_1 are increased from zero. However, the surface declines as either N_0 or N_1 is increased after reaching certain threshold. This finding can be explained by the concave exponential corn yield assumption that excessive

fertilizer application (soil fertility accumulation) will have no further significant positive impact on corn yield level after the nutrient absorbing capacity is reached, but will decrease the net value V_0 as a result of fertilizer application costs increase.

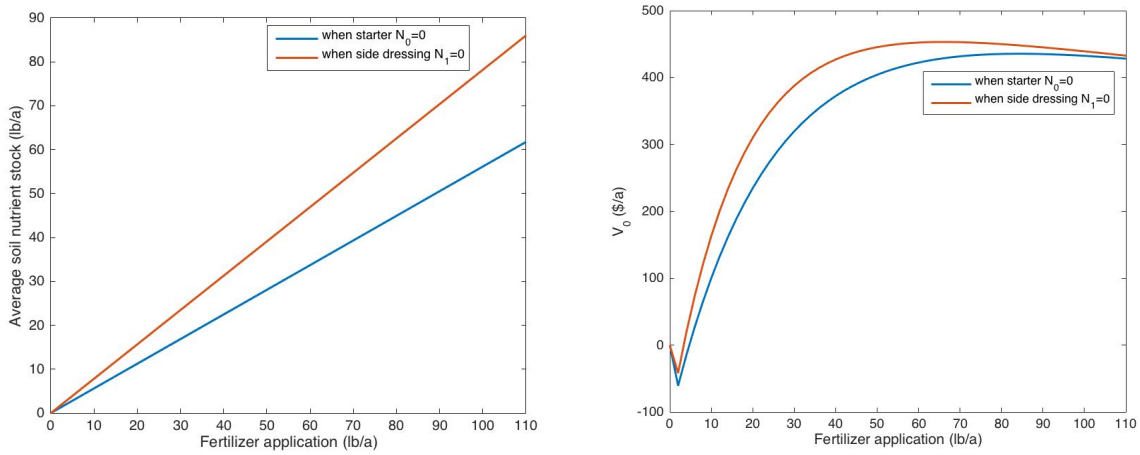

(a) The average soil nutrient stock

(b) Corn value V_0

Figure 3.18: The average soil nutrient stock and corn value when $(N_0 = 0, N_1 > 0)$ and $(N_0 > 0, N_1 = 0)$

The farmer's optimal total fertilizer application of 66 lb/acre is much less than the historical average in Iowa of 128 lb/acre over all farms surveyed in the years 1990-2003, 2005, 2010, 2014, 2016 and 2018. Over these same years the minimum average applied is 114 lb/acre and the maximum is 150 lb per acre. This is likely a reflection of the simplified modelling assumptions we have made. We may be underestimating the potential for soil fertility loss over the growing season. Another explanation is that farmers are using more fertilizer than is optimal. The factors that can affect the changes of optimal fertilizer applications are examined in the later sensitivity analysis section.

For a more detailed look at the impact of fertilizer side-dressing application N_1 on the value V_0 given various scenarios of applied N_0, a series of figures are presented in the following Figure 3.19. Figure 3.19 shows the response of V_0 to side-dressing N_1 at different

fixed starter N_0 levels. At low levels of starter amount $N_0 = 0, 10, 20$ lb/a that are far below the overall crop nutrient requirement, an increase in N_1 increases V_0 up to a maximum level after which the value curve starts to steadily decline. Even if N fertilizer is under-applied at seeding time, farmers can fully benefit from the option of the nutrient side-dressing strategy. Under-application can be compensated through exercising the option for a later side-dressing. Our model assumes there is no permanent damage to corn yield from too little N application at the early season. In Figure 3.19, beyond a certain threshold, the increased N_1 will result in a reduction in total value due to more variable costs and no further benefits in corn growth.

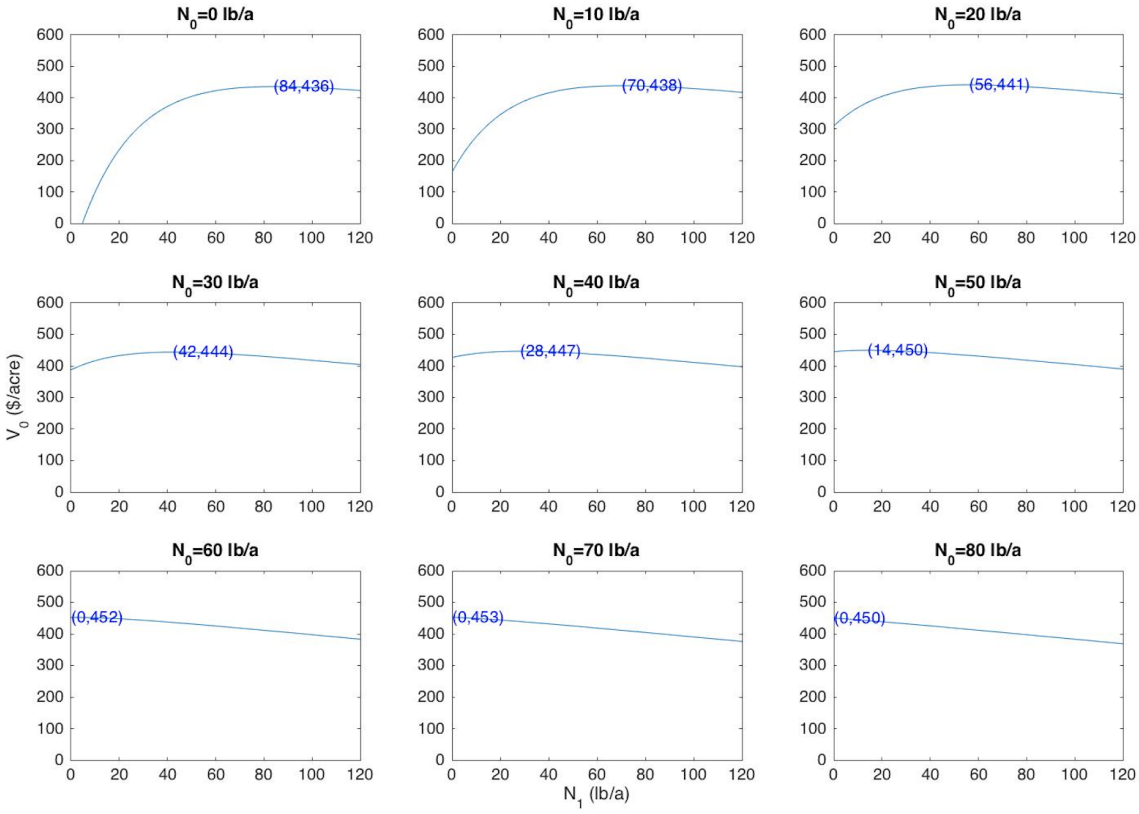

Figure 3.19: Response of V_0 to N_1 with different given N_0 (Numbers in blue show optimal N_1 amount in pounds and value in $\$/acre$ given the specified N_0 amount)

In our base case example, a positive fertilizer application followed by a zero side-dressing

application represents the optimal strategy. This result is consistent with Hyytiäinen et al. (2011), who examined the benefit of a split fertilizer decision for managing malting barley crops in Finland, using a process-based model $COUP$. They found that, without a pollution tax, the farmer's optimal decision is to apply fertilizer only once as the first application rather than through three later split applications. In their model this was due to the added fixed costs of each additional application.

The farmer's optimal strategy is determined by several factors including the relative cost of the two split fertilizer applications, the impact of application timing on soil nutrient level and hence plant growth, the expected outlook for rainfall and the expected corn price at the harvesting time. The cost of the starter and side dressing applications are assumed to be the same in this base case, so relative cost is not a factor. However, our assumption that plant growth depends on the average soil nutrient level is important, as it implies that the starter application has a larger effect on $\bar{S}$, other things equal. Uncertain corn prices and rainfall intensification may make it beneficial for the farmer to delay fertilizer application since the side-dressing application comes with the benefit of more information about the realizations of both these variables. While a large amount of starter application N_0 may increase the average soil nutrient content, it is also subject to being washed away by rainfall. Intense rainfall conditions or a crash in corn prices in the season may make the farmer regret the initial application. The private optimal N application strategy balances all of these factors and given our assumptions in this base case, the farmer prefers to use only the starter application.

To see the evolution of the daily soil nutrient stock $S(t)$, averaged soil nutrient stock $\bar{S}(t)$ and the cumulative N loss, we plot the simulated paths in the Figure 3.20, given the fertilizer application are at the optimal level $(N_0 = 66, N_1 = 0)$lb/a. Figure 3.20(a) indicates the decrease of daily soil nutrient stock as a result of rainfall and Figure 3.20(b) indicates the decrease of averaged soil nutrient stock computed on a daily basis. Figure

3.20(c) indicates the increase of the cumulative N loss caused by rainfall.

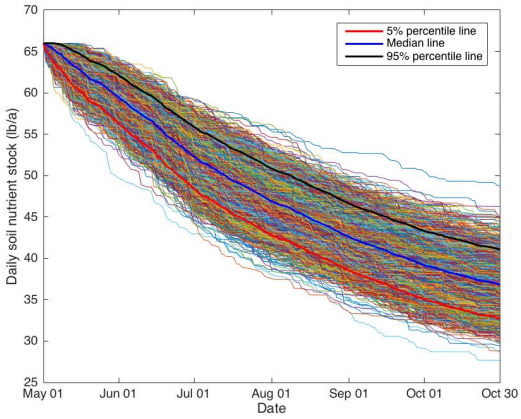

(a) Simulated daily soil nutrient stock $S(t)$

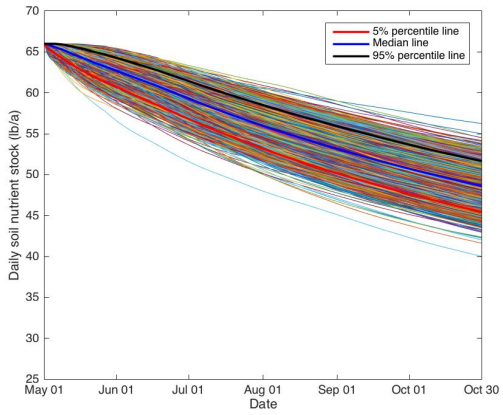

(b) Simulated averaged soil nutrient stock $\bar{S}(t)$

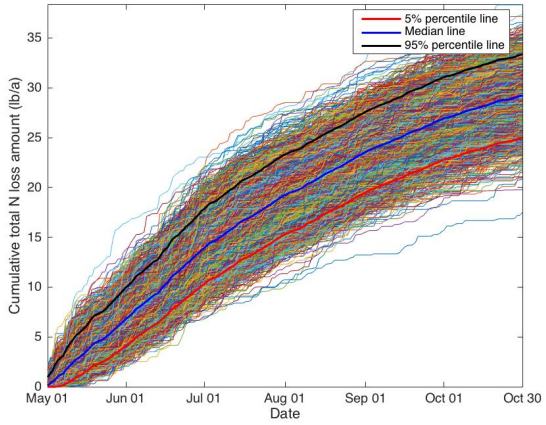

(c) Simulated cumulative N loss

Figure 3.20: Simulated paths for $S(t)$, $\bar{S}(t)$ and the total N loss, when application is at optimal level $(N_0 = 66, N_1 = 0)$lb/a

As discussed in Chapter 1, over-application of fertilizer is partially attributed to the adoption of the maximized yield target. A contrast between the farmer's optimal application and the application based on maximum yield principle is presented in Figure 3.21. Note that our corn yield model in Equation 3.33 uses soil nutrient stock as the fertility variable instead of application amount. Given a fertilizer application amount applied at

the seeding date, we compute the corn yield for each path of simulated $\bar{H}$, $\bar{R}$ and $\bar{S}$, and take average on these simulated corn yields as the yield response to the given application amount. Since the exponential yield model does not generate a unique maximized yield like the quadratic model does, we regard the red point in Figure 3.21 as the "maximum-yield" application decision, which generates a higher 247 bu/acre yield, a lower corn field value, and a higher fertilizer cost compared to the privately optimal choice. Following the "maximum-yield" fertilizer application principle will create a \$31.7/acre fertilizer cost increase and a \$19/acre field value loss. Like our conclusions in Section 2.4, Figure 3.21 shows that the farmer's optimal application is lower than the applications based on the maximum-yield principle, suggesting that fertilizer over-application relative to the economically efficient amount can be attributed to recommendations built on the yield-maximizing principle or the farmer's desire to achieve higher yield targets. The corn yield level from the blue point (242.55 bu/a) is 97% of the maximum yield 247 bu/a, showing that the privately optimal N application rate will not hinder corn productivity.

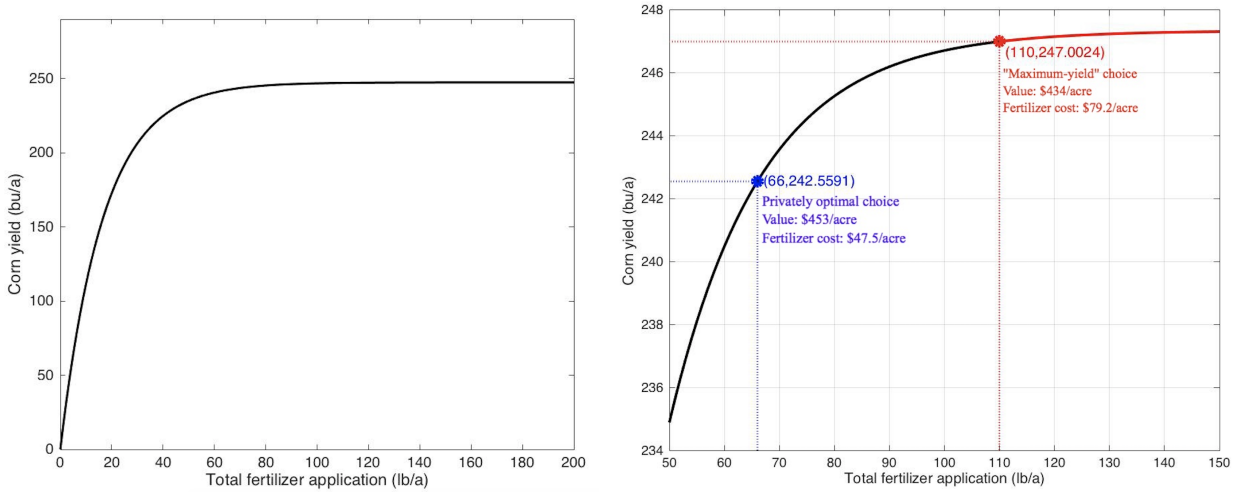

(a) Corn yield response to N application

(b) A segment in (a) with 50 to 150 lb/a application

Figure 3.21: Contrasting the farmer's optimal fertilizer application, $(N_0 = 66, N_1 = 0)$lb/a, and application based on the maximum yield principle, $(N_0 = 110, N_1 = 0)$lb/a

3.9.4 Sensitivity analysis: Variable costs

The variable cost of N application may vary depending on when, how and what nitrogen fertilizer is applied and whether specialized capital equipment, stabilizer or inhibitor is used (Sellars (2019), *farmdoc daily*[27] and *GoCorn*[28]).

Sensitivity on fertilizer application variable costs To examine the impact of variable costs regarding starter and side-dressing fertilizer application on the optimal strategy, a sensitivity analysis is performed by varying the starter unit application cost c_N and the side-dressing unit cost c'_N from their original base level. The base level of application variable cost is $c'_N = c_N = \$0.72/\text{lb}$. The optimal application (N_0, N_1) and $N_0 + N_1$ are then derived for each (c_N, c'_N) scenario, which are presented in the following Table 3.6.

Table 3.6: Sensitivity of (N_0, N_1) [V0] to different levels of variable application cost

c_N \ c'_N	$\frac{0.72}{4}$	0.72	$0.72 * 4$
$\frac{0.72}{4}$	(90, 0)[492.8815]	(90, 0)[492.8815]	(90, 0)[492.8815]
0.72	(0, 116)[486.8625]	(66, 0)[453.2912]	(66, 0)[453.2912]
$0.72 * 4$	(0, 116)[486.8625]	(0, 84)[434.7589]	(42, 0)[340.4626]

* N_0, N_1 are in lb/a. c_N refers to the unit cost of the starter application. c'_N refers to the variable cost of the side-dressing, $\$/lb$.

In Table 3.6, a reduction in c'_N or an increase in c_N relative to the base case can cause a switch in the optimal timing fertilizer application such that all fertilizer should be applied

[27] Source: "Fertilizer Prices, Rates, and Costs for 2023", https://farmdocdaily.illinois.edu/2022/09/fertilizer-prices-rates-and-costs-for-2023.html

[28] Source: Greg Stewart, OMAFRA Corn Specialist, "Side-dressing Nitrogen in Corn: Profit or Pain", 2006, http://www.gocorn.net/v2006/Nitrogen/articles/Sidedressing%20Nitrogen %20in%20Corn.html

as a side dressing. V_0 decreases going left to right along a row or down along any column in response an increase in either c_N or c'_N that changes the optimal decision.

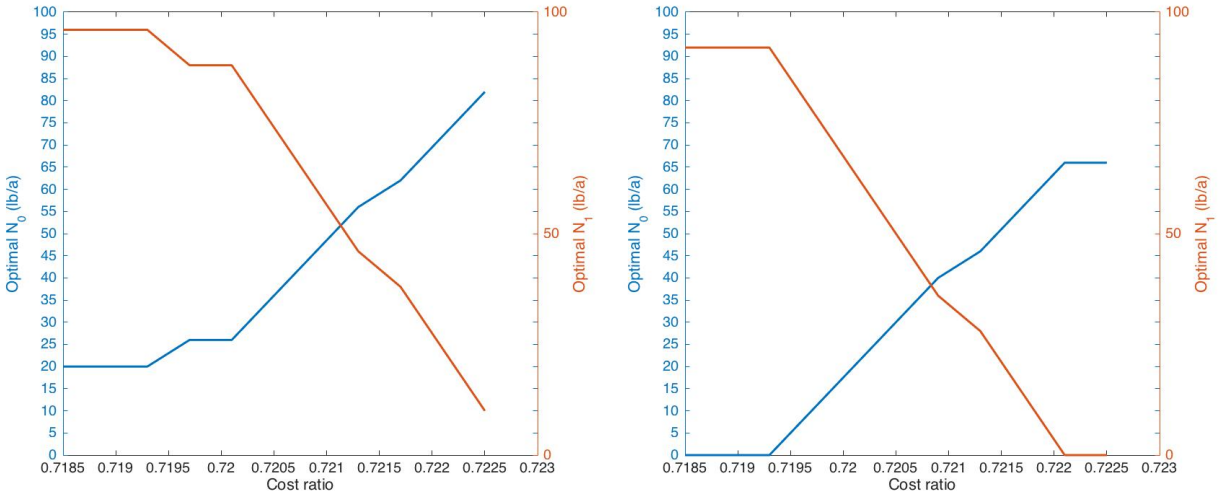

(a) when $c_N = \frac{0.72}{4}$

(b) when $c_N = 0.72$

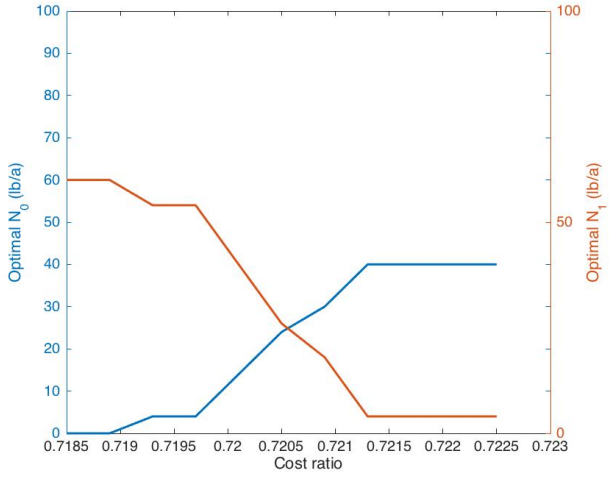

(c) when $c_N = 0.72 * 4$

Figure 3.22: Sensitivity of the optimal application (N_0, N_1) to cost ratio $\frac{c'_N}{c_N}$. Blue line is optimal N_0 application (left hand y-axis). Red line is optimal N_1 application (right hand y-axis)

Figure 3.22 depicts how changes in the the cost ratio $\frac{c'_N}{c_N}$ affect the optimal application

(N_0, N_1) (more details are listed in Appendix G).

The sensitivity of (N_0, N_1) to the cost ratio is shown at three different values of c_N: in $c_N = \frac{0.72}{4}$, $c_N = 0.72$ and $c_N = 0.72 * 4$ \$/lb. Recall that our base case is $c'_N = c_N =$ \$0.72/lb. In Figure 3.22, it will be observed that in a narrow range around a cost ratio $\frac{c'_N}{c_N}$ of 0.72, it is optimal to apply some fertilizer in both starter and side dressing applications. Outside of this narrow range, the optimal decision is to apply all fertilizer either at planting or as a side dressing, but not both. We conclude that the optimal split decision is highly dependent on the relative fertilizer application cost, $\frac{c'_N}{c_N}$, which may vary from region to region depending on technology in use and other site specific conditions.

Sensitivity on the variable cost The total variable cost, c_V, on corn yield, excluding chemical fertilizer variable cost, are examined in Table 3.7. The total variable cost is varied from $\frac{1.7593}{4}$ to $1.7593 * 4$ \$ per bushel. Unlike fertilizer variable costs, the total variable cost will not alter the optimal $N_1 = 0$ conclusion, instead, N_0 strictly decreases with the rise of total variable cost, and so does the maximized value V_0.

Table 3.7: Sensitivity of (N_0, N_1) and V_0 to different levels of total variable cost

Total variable cost	$\frac{1.7593}{4}$	$\frac{1.7593}{2}$	1.7593	1.7593×2	1.7593×4
(N_0, N_1) (lb/a)	(74, 0)	(70, 0)	(66, 0)	(46, 0)	(0, 0)
V_0 (\$/a)	770.7598	664.4021	453.2629	35.34	0

3.9.5 Sensitivity analysis: Corn price volatility and speed of mean reversion

The sensitivity of the optimal fertilizer application to corn price uncertainty is examined in this section by varying corn price volatility σ and mean reversion speed θ as shown in

the following Table 3.8. In general, a higher price volatility and/or lower speed of mean reversion imply that the farmer is faced with greater uncertainty when choosing fertilizer application levels. Three levels of price volatility and mean reversion are set to represent different levels of price uncertainty. The original σ_P and θ are estimated in Table 3.2.

Table 3.8: ^{V_0} (N_0, N_1) for different price sensitivity regimes (θ,σ_P)

parameters	$\frac{\sigma_P}{2}$	σ_P	$2\sigma_P$
$\frac{\theta}{2}$	$^{446.3}(66,\ 0)$	$^{430.2}(64,\ 0)$	$^{412.9}(60,\ 0)$
θ	$^{462.3}(70,\ 0)$	$^{453.5}(66,\ 0)$	$^{444.7}(64,\ 0)$
2θ	$^{501.1}(72,\ 0)$	$^{492.7}(68,\ 0)$	$^{477.0}(66,\ 0)$

From Table 3.8, the optimal fertilizer application (N_0, N_1) as well as the value V_0 are found sensitive not only to corn price volatility, but also to the mean reversion speed. More specifically, at a given mean reversion speed level, both starter application N_0 (which is also the total application) and the maximized value, V_0 (blue colored number on the left-top of each pair) are found to decline with the rising of price volatility level from $\frac{\sigma_P}{2}$ to $2\sigma_P$. This finding is consistent with the previous result $\frac{\partial N}{\partial \sigma} < 0$ we found in Table 2.1 (Chapter 2) in our closed form solution for a much simpler model. Increased corn price volatility has a negative impact on the fertilizer application amount.

Considering mean reversion sensitivity if we compare (N_0, N_1) and V_0 along any column in Table 3.8 it will be observed that under a given price volatility level, the optimal fertilizer application increases with an increase of the mean reversion speed from $\frac{\theta}{2}$ to 2θ. Both value V_0 and total application are sensitive to the mean reversion speed with $\frac{\partial(N_0+N_1)}{\partial\theta} > 0$ and $\frac{\partial N_0}{\partial\theta} > 0$, which is consistent[29] with the result $\frac{\partial N}{\partial\theta} > 0$ in Table 2.1 (in Section 2). As long

[29]Using the price process estimates in Table 3.2, we can calculate the value of $\bar{P}(1+F)$ in Table 2.1, which is $\bar{P}(1+F) = 15.9104 > P_0 = 4.1450$. Thus, the sensitivity of the total amount $N_0 + N_1$ on mean reversion speed θ is consistent with our previous finding $\frac{\partial N}{\partial\theta} > 0$ in Table 2.1.

as $\bar{P}$ exceeds the average variable cost of fertilizer application, as is the case under our assumptions, a higher speed of mean reversion increases the value of the crop and makes it worthwhile for the farmer to use more fertilizers.

A higher starting value for corn price simulation in Table 3.5 will shift all simulated price paths upward, resulting in higher trading prices P_T at the end of the period. To see how an increase in p_0 affects the optimal decision in our base case, we raise the starting value in Table 3.5 from \$4.145/bushel to \$6.145/bushel. The farmer's optimal application increases from (66, 0) lb/a to (76, 0), and the value V_0 per acre increases from \$453.2184 to \$935.6317. Consistent with the findings in Chapter 2, a higher corn price starting value will increase the optimal application amount. Intuitively, a good current corn market gives farmers incentive to apply more fertilizer, the marginal benefit from corn yield dominates the marginal cost from fertilizer use.

In conclusion, results indicate that price volatility and mean reversion speed will have impacts on the optimal fertilizer application as well as the optimal value. We have characterized an increase in volatility and a decrease in mean reversion speed as representing an increase in uncertainty. Both these effects will lower the optimal quantity of N applied. The benefits of increased N in terms of a higher corn yield do not outweigh the increased risk of an unfavourable corn price at harvest time when corn prices are more volatile. These two parameters are found to only affect the optimal application amount, not split decision between starter and side dressing.

3.9.6 Sensitivity analysis: Precipitation

In this section we consider the impact of a change in the probability of wet and dry days as well as a change in the expected value and variance of the quantity of rain. We vary the likelihood of rain, represented by transition probabilities between wet and dry days,

defined in Figure 3.9. For representing the *wetter* scenario (with a larger rain likelihood), we increase the transition probabilities P_{11} and P_{01} by 15% respectively, where 0 indicates the state of dry and 1 indicates the state of wet. For the *drier* scenario (with a smaller rain likelihood), we increase two transition probabilities P_{00} and P_{10} by 15% respectively. Precipitation occurrence is thus classified into three regimes according to rain likelihood as seen in Table 3.9. In addition, we examine the effect of the daily precipitation amount by varying the parameter γ_t in Equation (3.32) from the original base case (estimates in Figure 3.10) to $2\gamma_t$ (*Less* expected rainfall amount and lower variance scenario) and $\frac{1}{2}\gamma_t$ (*More* expected rainfall amount and greater variance scenario). Simulations of the nine precipitation scenarios are plotted in Figure 3.23. The increased variance of R^m is evident in the figure as γ is increased moving from left to right along a given row from "*Less*" to "*Base*" to "*More*". The optimal application results under each pair of rainfall likelihood and daily amount are presented in Table 3.9. All parameters are using our base case assumptions.

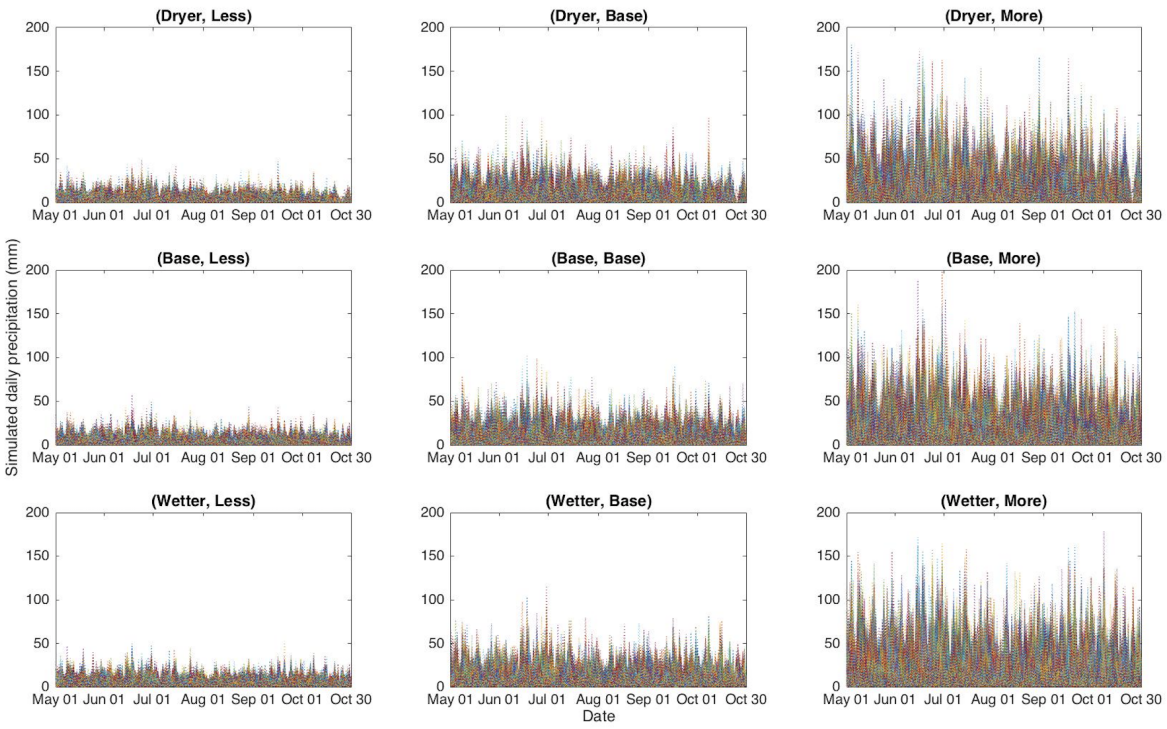

Figure 3.23: Simulated daily precipitation (mm) in 9 sensitivity scenarios. In the plot titles the first label refers to rain likelihood and the second label refers to the rain amount.

Table 3.9: Sensitivity of (N_0, N_1) [V_0] to different rainfall scenarios (The total variable cost is base case 1.7593 $\$/bu$)

Rain likelihood \ Rain amount	Less	Base Case	More
Smaller (Dryer)	(52, 0)[240]	(64, 0)[424]	(68, 0)[382]
Base Case	(56, 0)[304]	(66, 0)[453]	(64, 0)[229]
Larger (Wetter)	(58, 0)[346]	(68, 0)[437]	(50, 0)[29]

Rainfall impacts the decision maker through two avenues: (i) the impact on soil nutrient level as rain causes leaching of nitrogen, and (ii) the impact on corn growth, as too much rain causing a reduction in yield. *A priori* we cannot say how an increase in the likelihood, expected quantity or variance of rainfall will change the optimal quantity and timing of

fertilizer application. When expected rainfall likelihood is small (*Dryer* scenario), more expected daily rainfall amount will increase the fertilizer application as a way to compensate the N loss, N_0 rises from 52 to 64 to 68 lb/a. In contrast, when rainfall events become more frequent (*Wetter* scenario), an increase in the expected daily rainfall amount will initially increase N (moving along the third row), but when we reach the "*more*" entry, reflecting the largest rain amount, the optimal N amount drops significantly to 50 lb/a, and V_0 also falls precipitously. The entry in the third row, third column of the table reflects the negative impact of too much rain on corn yield. Corn farming is less profitable under these circumstances because of the lower yield and also because a significant amount of any N applied will be leached away. Similarly, at *Less* or *BaseCase* rainfall amount level, more frequent rainfall events will increase the fertilizer application N_0 (from 52 to 58 and from 64 to 68), as a fertility compensation measure to rainfall-induced N losses. However, in *more* expected rainfall amount scenario, more frequent rainfall will lower the application from 68 to 50 lb/a. These findings can be explained by the trade-off between corn yield and state variable nutrient soil stock (S) in our corn yield model, which is augmented by fertilizer application but reduced as a result of rainfall event.

Sensitivities for precipitation & the total variable cost To see the impact of a lower total variable cost on the rainfall sensitivity results, the total variable cost is assumed as 0.2645 $\$/bu$ and results are listed in the following Table 3.10.

Table 3.10: Sensitivity of (N_0, N_1) ^{V_0} when the total variable cost is 0.2645 $\$/bu$

Rain likelihood \ Rain amount	Less	Base Case	More
Smaller (Dryer)	(60, 0)[471]	(70, 0)[770]	(76, 0)[702]
Base Case	(62, 0)[573]	(74, 0)[812]	(72, 0)[457]
Larger (Wetter)	(66, 0)[641]	(76, 0)[790]	(58, 0)[131]

Comparing Table 3.23 and Table 3.10, we can find the decrease of total variable cost will neither alter the precipitation sensitivity pattern nor change the optimal application timing, but increases the fertilizer application amount under each rainfall scenario.

Sensitivities for precipitation & the fertilizer cost ratio To see how the fertilizer cost ratio $\frac{c'_N}{c_N}$ will interact with the precipitation effect in changing the optimal application, we repeat the analysis in Table 3.23 incorporating the cost ratio sensitivity (ranging from $\frac{c'_N}{c_N} = 0.5$ to $\frac{c'_N}{c_N} = 1$). Details of results are listed in Appendix H, results are visualized in the following Figure 3.24.

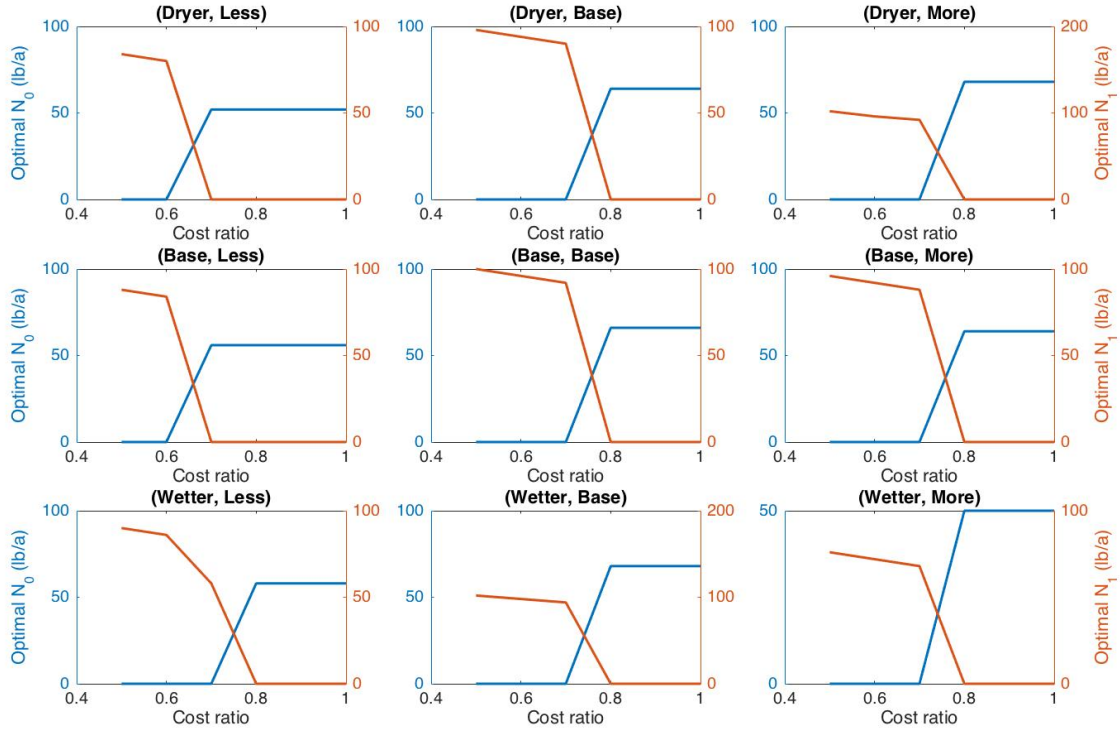

Figure 3.24: Sensitivity results regarding precipitation and cost ratio $\frac{c'_N}{c_N}$. Blue line is optimal N_0 application (left hand y-axis. Red line is optimal N_1 application (right hand y-axis)

We can see from Figure 3.24 that fertilizer cost ratio $\frac{c'_N}{c_N}$ is decisive for the optimal application timing and amount, the delayed application N_1 is sensitive to rainfall as well as to the fertilizer cost ratio. One way to look at Figure 3.24 is to consider at what cost ratio it is optimal to set $N_1 = 0$ and apply fertilizer only via N_0. Looking at the first column in Figure 3.24 (the less rain quantity scenario), moving from row 1 to row 2 (from less frequent rain to the base case), the decision maker sets $N_1 = 0$ for $\frac{c'_N}{c_N}$ at rough 0.7 and above. Moving to the third row with more frequent rain $N_1 = 0$ for $\frac{c'_N}{c_N}$ at about 0.8 and above. In other words, moving down the first column in Figure 3.24, an increasing frequency of rain means that $N_1 > 0$ will be chosen for a wider range of the cost ratio. This is as expected because wetter conditions give a benefit to N_1 since the later application

date implies less opportunity for fertilizer to be leached away.

In conclusion, rainfall likelihood and the expected daily amount will interact with each other in a complex way in affecting the evolution of the soil nutrient content, through N losses, and thus will affect the private optimal fertilizer application. Farmers' optimal fertilizer application amounts are based on the trade-off between application cost, rainfall-induced fertilizer loss and gain from yield. Depending on the $\frac{c'_N}{c_N}$ ratio, the optimal application timing is found to be sensitive to rainfall likelihood, expected quantity and variance.

3.9.7 Sensitivity analysis: Starting soil N-level

In reality, nitrogen can carryover from one growing season to the next, providing a vital fertility resource for farmer's next crop. Some amount of nitrogen, coming from the mineralization of soil organic matter or unused fertilizer, is retained in the soil as the form of nitrate. The corn yield functions estimated by ISU (2018) (Figure 1, 2 and 3) for different corn rotations indicates a potential corn yield even with zero or very little fertilizer application. To examine how involving soil N residue in our corn yield model will affect the farmer's optimal decision, we assume the initial soil fertility at the beginning of the season is $\bar{S}_{t_0} = 5$ lb/acre. The corn yield model (Equation (3.37)) is calibrated using Iowa historical data sets ($\bar{H}$, $\bar{R}$, $\bar{S}$) and Matlab function $lsqcurvefit$, which are identical to Section 3.8.

$$Y = 0.3505 * (3.0645 * \bar{R} - 0.0029 * \bar{R}^2)(1 - e^{-0.0839*\bar{S}})(1 - e^{-0.0007*\bar{H}}) \tag{3.37}$$

The following Figure 3.25 plots the corn yield model in Equation (3.37) versus one of $\bar{H}$, $\bar{R}$ or $\bar{S}$, with the remaining two variables set at their mean levels. As opposed to Figure

3.14 in Section 3.8, accounting for a 5 lb/a soil N residue at the beginning of the season does not change the overall effect of each input variable on corn yield, as showed in Figure 3.25.

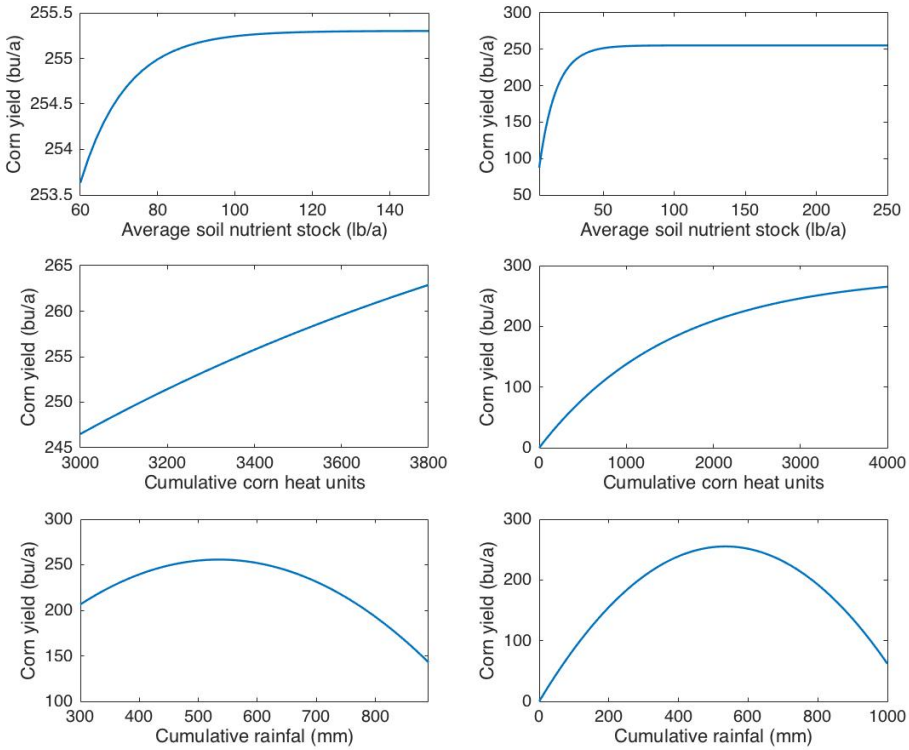

Figure 3.25: 2-dimensional plots of corn yield model with 5 lb/a initial soil N stock. Each figure shows yield versus an independent variable with the other 2 variables at their historical mean. The first column shows the horizontal axis over the historical range; The second column shows a more extreme range for the horizontal axis.

The corn yield response to N applications and the farmer's optimal application decision are examined in the following Figure 3.26. As opposed to Figure 3.21, Figure 3.26(a) has a positive intercept greater than 50 bu/a indicating a potential corn yield still can exist even when no fertilizer applied. In comparison to the farmer's optimal application ($N_0 = 66$, $N_1 = 0$) lb/a in Figure 3.17, Figure 3.26(c) shows that the incorporation of soil N residue will lower the optimal application amount to ($N_0 = 58$, $N_1 = 0$) lb/a, rather than affect

the optimal application timing. This may be attributed to the fact that soil N residue works as the same function in increasing soil nutrient stock as starter application, at the beginning of the season. The reduction in N_0 (66-58=8 lb/a) is slightly higher than the compensation from soil N residue (5 lb/a), which may be explained by the fact that soil N residue comes with no cost and our results are subject and sensitive to the corn yield model estimates. Accounting for the soil N residue gives us a higher farmer's net benefit, V_0 = \$476.5851/acre, contrasting to the base case V_0 = \$453.2184/acre in Figure 3.17. This benefit improvement may comes from the saved cost. In Figure 3.26(c), when the total N application is zero, the potential yield from the positive soil residue gives a non-negative value V_0. In addition, same as Figure 3.21, the farmer's optimal application (58, 0)lb/a (the blue point in Figure 3.26(b)) is lower than the application based on the yield maximizing principle ((110, 0)lb/a, the red point in Figure 3.26(b)). Compared to the privately optimal choice, following the "maximum-yield" fertilizer application principle will generate a \$27/acre field value loss.

Like many soil sampling-based fertilizer recommendations show, our results indicate that the adoption of pre-plant soil tests in assessing soil N availability can reduce farmers' fertilizer applications and save their costs without a scarification of net benefit, which will eventually lower the risk of fertilizer over-application and potential agricultural N loss.

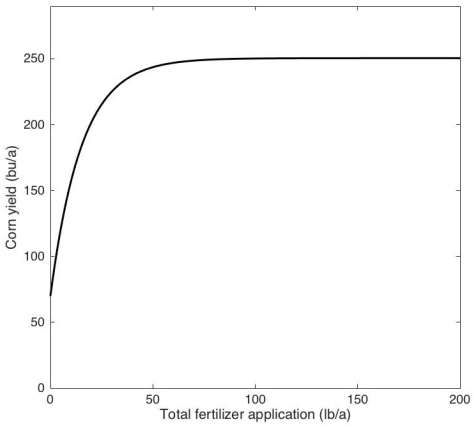

(a) corn yield response to N applications

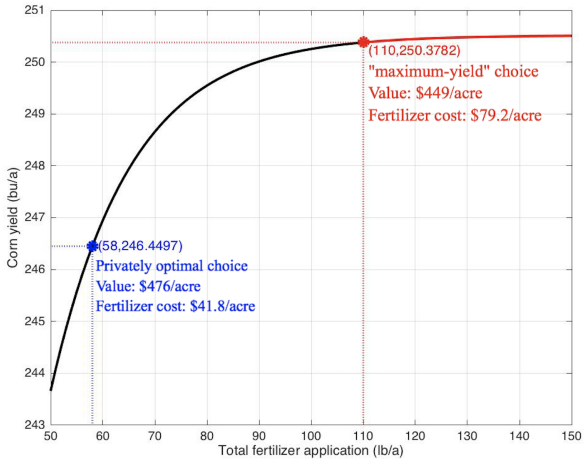

(b) corn yield response to N applications

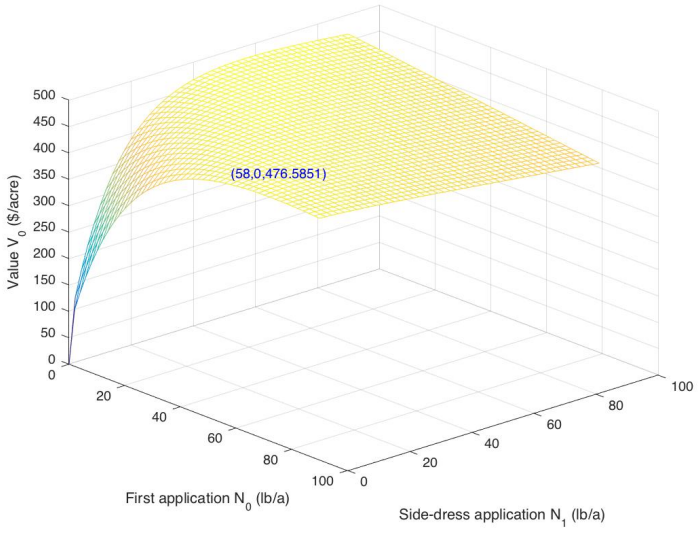

(c) The farmer's optimal decision

Figure 3.26: The farmer's optimal decision and corn yield response to N applications

3.10 Conclusions

In this chapter, we explored how farmers will change their optimal fertilizer application in the presence of growing season weather and crop price uncertainties. The farmer's deci-

sion model in Chapter 2 is extended to include crop price and weather uncertainties. Two fertilizer application dates are allowed. A corn yield function is specified and estimated, which gives corn yield as a function of average soil nutrient content and weather conditions over the growing season. Soil nutrient content is determined by fertilizer application as well as nutrient loss due to daily precipitation. The decision model is parameterized using data on weather, corn growth, and fertilizer application from Iowa, which is a main corn-growing area and is the source of serious nitrogen pollution in local water bodies and in the Mississippi River watershed. Undertaking Monte Carlo analysis, we find that, based on our base case parameter assumptions, the farmer's optimal strategy is applying all the fertilizer at the seeding date. This is partially due to our model setting stating that the starter application can bring a higher seasonal average soil N stock with a lower fertilizer application compared to the side-dressing.

Our results in sensitivity analysis provide considerable intuition about the optimal fertilizer application from the farmer's perspective. The farmer's optimal strategy is determined by several factors, including the relative cost of the two split fertilizer applications, the impact of application timing on the soil nutrient level and hence plant growth, the expected outlook for rainfall, and the expected corn price at harvest time. Like our conclusion in Section 2.4, the farmer's optimal application is lower than the application rates based on the maximum-yield principle, suggesting that fertilizer over-application relative to the economically efficient level can be attributed to the recommendations built on the yield-maximizing principle or the farmer's desire to achieve higher yield targets. The optimal application amount and timing are highly dependent on the relative fertilizer application cost, which may vary from region to region depending on site-specific conditions. Consistent with the result we found in Chapter 2, a higher level of price uncertainty, represented by a higher corn price volatility and a lower mean reverting speed, has a negative impact on the fertilizer application amount but has no impact on the split decision between

starter and side dressing. Furthermore, optimal N applications are found to change in a non-monotonic manner with increased rainfall scenarios. In some cases, increased rainfall amount or likelihood does not necessarily increase N use. Rainfall likelihood and expected daily amount will interact in a complex way to affect the evolution of soil nutrient content via N losses, and thus the optimal private fertilizer application.

Chapter 4

Socially Optimal Fertilizer Application Decisions Under Uncertainty

4.1 Introduction

Nitrogen is mobile in soils, and can leach into surface waters or percolate into groundwater. Groundwater quality is a concern in alluvial aquifers underlying agricultural areas worldwide. Surplus nitrogen can also volatilize to the atmosphere and be redeposited far downwind as acid rain or dry pollutants that may eventually reach distant aquatic ecosystems(Xepapadeas (2011)). According to the United States Environmental Protection Agency, leaching and denitrification from farmland applied nitrogen fertilizers have become significant anthropogenic sources of nitrate (NO_3^-) contamination in groundwater and greenhouse gas N_2O atmospheric pollution. Agricultural N use is also a prevalent cause of water quality deterioration in local streams and lakes. Most of such agricultural

nutrient losses is nonpoint source pollution (NPS), which refers to pollution coming from diffuse sources where it can be difficult, or impossible, to estimate the amount of pollution from each source. Nonpoint source agricultural pollution tends to be highly stochastic, as it depends on the timing, frequency, and intensity of fertilizer application and precipitation (Abler 2015).

Numerous studies have discussed the situation and the impact of agricultural N pollution, especially the adverse effects of elevated nitrate concentrations in groundwater on human health (U.S.EPA (2001), Jalali (2005), Su et al. (2013), Lockhart et al. (2013), Lawniczak et al. (2016), Keeler et al. (2016), Tang et al. (2018), Giannadaki et al. (2018), Isiuku & Enyoh (2020), Folkens et al. (2020) and Gourevitch et al. (2018)). For example, nitrate removal costs to public water supply and private well owners, lost recreational benefits and human health impacts are all considered by Tang et al. (2018) as different results from severe nitrate contamination in Iowa groundwater. According to Tang et al. (2018) and the Iowa Community Private Well Study, nitrate was detected in 57% of wells in Iowa, and violations of nitrate maximum contaminant levels (MCL) occurred in nearly one-quarter of the wells. In California, 46% of collected well water samples in Tul/Kings county exceeded the MCL for nitrate (Lockhart et al. (2013)). Nitrite formed via reduction of nitrate in the human body can react with secondary amines to form nitrosamines, which can be carcinogenic (Almasri & Kaluarachchi (2007)). In Germany, about 74% of the drinking water produced comes from groundwater and spring water reservoirs. The contaminated water will be technically treated or mixed with water from other sources, which results in increased costs for the water suppliers. Presently, the legal limit of 10 mg/L nitrate-N of fresh water is still exceeded frequently in Germany, especially in agricultural areas (Folkens et al. (2020)). Consumption of such groundwater as drinking water can cause low blood oxygen in infants, a condition known as methemoglobinemia.

In addition, agricultural denitrification and ammonia emissions strongly contribute to

N_2O greenhouse gas and fine particulate air pollution ($PM_{2.5}$) with significant impacts on respiratory health, contributing to mortality (Su et al. (2013), Giannadaki et al. (2018) and Isiuku & Enyoh (2020)).

Current research exploring the reasons for worldwide agricultural NPS pollution includes Chen et al. (2005), Wang (2006), Sun et al. (2012), Lockhart et al. (2013) and Lawniczak et al. (2016), who focused on different aspects including irrigation with untreated water, overuse of fertilizer, legislation and governmental financing, difficulty of monitoring, lack of soil type-based standards, technology restrictions, and farmers' attitude for adopting BMPs. The design and choice of measures to address agricultural NPS pollution is complicated by the typically unobservable and stochastic nature of nutrient emissions (including leaching and denitrification), as well as the site-specific nature of such NPS problems.

Many regulations have been enacted by different countries and authorities to mitigate agricultural NPS problems. For example, to alleviate groundwater nitrate pollution, the EU Nitrate Directive has been in force since 1991. It aims to improve water quality in Europe by protecting groundwater and surface water against nitrate pollution from agricultural sources. In the U.S., implementing approaches to reduce emissions from nonpoint sources are largely under the purview of states via the Total Maximum Daily Load (TMDL) program. Under this program, states are tasked with identifying the sources of urban and agricultural nonpoint source emissions that lead to waterway impairments, and also with implementing approaches to reduce those impairments. In 1996, the South Florida Agricultural Management District attempted to lower the nitrogen levels in the Everglades Agricultural Area groundwater by implementing a best management permitting program such as on-site verification and monitoring. Similarly in Ontario, the Ministry of Environment and Energy (MOEE)[1] establishes safe limits to the amount of groundwater degradation

[1]Water Management: Policies, Guidelines, Provincial Water Quality Objectives, by the Ministry of the

and provides the waste control requirements for the regulated activities (such as landfills and waste disposal) on a case by case basis. For the non-point source activities that do not require specific approval under the Ontario Water Resources Act or the Environmental protection Act but have the potential to contribute to ground water contamination, the treatment or elimination of pollution will be required where it is demonstrated that such measures are necessary to prevent further degradation or improve water quality. There are a number of mechanisms available to ensure the safety of groundwater, which include the use of ministerial orders, outside consultants and voluntary programs. For example, in 1993, Ontario began a voluntary educational program: Environmental Farm Plan (EFP), to help farmers address site-specific environmental risks and to increase farmers' awareness and motivation to implement BMPs.

This chapter contributes to the literature on socially optimal N fertilization decisions by formulating a stochastic optimal control model for a social planner and parameterizing it for the cultivation of corn in Iowa. Both corn price and weather uncertainties are included in our social welfare model. The social damage from N fertilizer use is modelled using two different approaches: a linear damage function and a threshold damage function. Our modelling exercise seeks to illuminate how key factors affect the optimal fertilizer choice from the social planner's point of view.

The literature on agricultural NPS pollution control largely focuses on evaluating the efficiency of various policy tools, such as voluntary programs, command and control programs and economic instruments (input taxes, ambient taxes, tradable permits, and liability rules) (Horan et al. (1998), Shortle & Horan (2001), Horan et al. (2002), Ju et al. (2004), Wang (2006), Semaan et al. (2007), Dowd et al. (2008), O'Shea & Wade (2009), Xepapadeas (2011), Sun et al. (2012), Rabotyagov et al. (2014*a*), Abler (2015), Drevno

Environment and Energy. Source: https://www.ontario.ca/page/water-management-policies-guidelines-provincial-water-quality-objectives#section-5

(2016*a*), Tang et al. (2016) and Horan & Shortle (2017)). For example, Shortle & Horan (2001), Horan et al. (2002) and Xepapadeas (2011) discuss the paucity of information as a tangible limitation when implementing NPS pollution abatement tools. The advantage of an input-based tax is that observed inputs can be used as proxies of the unobserved individual emissions. However, a first-best solution can be achieved only when a polluter's impact on ambient conditions, nonpoint emissions, fate and transport functions, and other essential information can be quantified. In addition, a tax on the use of one input may increase the demand for a non-targeted input that could also be harmful to the environment. Likewise, liability rules may be inefficient when a polluter may not be held liable due to difficulties in identifying the source and proving responsibility. Ambient taxes have the advantage of directly addressing the moral hazard problem when asymmetric information presents, and they have fewer informational requirements for the regulator, as only ambient pollution needs to be measured. Yet, since an ambient tax penalizes polluters according to their collective emissions and environmental performance, a polluter's response to an ambient tax will depend on its own expectations about the impact of its choices, the choices of others, and natural events on ambient conditions. In other words, the efficiency of ambient based instruments may be restricted by polluters' expectations (or conjectural variations) about other polluters' behavior, and the regulator's knowledge of these expectations (Shortle & Horan (2001) and Xepapadeas (2011)). In addition, Horan et al. (2002) demonstrate that ambient taxes cannot achieve first-best outcomes when polluters are risk averse, but an approach mixing input taxes with an ambient tax can. In conclusion, either input tax or ambient tax require perfect information to attain efficiency. The use of one single policy tool, without site-specific integrated or mixed policy instruments, will lead to a loss of efficiency.[2] It is beyond the scope of our thesis to evaluate different policy options

[2]An early paper by Shortle & Dunn (1986) described a nonlinear input tax scheme that can obtain the first-best solution under asymmetric information about profit types in the limiting case of a single nonpoint polluter and zero transactions costs. Horan et al. (1998) showed that the linear ambient tax is

to achieve the efficient social NPS abatement outcome. This is left for future research.

4.2 Social costs of agricultural nitrogen pollution: a literature overview

In the literature, the measurement of externalities or social costs of agricultural nitrogen pollution has been addressed by a large volume of studies (Horner (1975), U.S.EPA (2001), Martínez & Albiac (2006), Murdock (2006), Almasri & Kaluarachchi (2007), Egan et al. (2009), Abidoye et al. (2012), Su et al. (2013), Van Houtven et al. (2014), Rabotyagov et al. (2014*a*), Tang et al. (2018), Long et al. (2019), Schmid et al. (2019) Folkens et al. (2020), Isiuku & Enyoh (2020) and Sihvonen et al. (2021)). One early research paper by Horner (1975) first proposed the concept that charging farmers the costs on the basis of nitrate concentration in the drainage water from their lands can represent the internalization of externalities. The cost function Horner (1975) used for removal of nitrate from the drainage water was developed through testing by a U.S. government study group as detailed in a U.S EPA report cited in the paper:

$$C = \$282144 + \$21.52W + \$0.12Z$$

where C is cost in dollars at a particular treatment centre in California, W is the amount of drainage water in acre-feet and Z is the pounds of nitrate in acre-feet. The paper calculates and compares the county-based farmland revenue reductions and abatement costs using

efficient in providing the correct incentives to attain the desired ambient pollution only under restricted conditions where the choice set of polluters is sufficiently small or the marginal damages and the marginal effects of polluters' choices on the distribution of the ambient pollutants are independent. In contrast to the linear ambient taxes, a nonlinear tax of the expected ambient damage can also achieve efficiency, where each polluter pays an amount equals to the total damages. Shortle & Horan (2001), Xepapadeas (2011) and Drevno (2016*a*) concluded that an integrated approach mixing input taxes with ambient taxes can obtain the first-best outcomes.

this cost function under different policy scenarios.

A common approach to measure the social cost of nitrate is to focus on how to measure and internalize the treatment costs of groundwater resources (Lewandowski et al. (2008), Vedachalam et al. (2018*b*) and Folkens et al. (2020)). For instance, since the nitrate-contaminated groundwater (NO_3^- concentration > MCL) in some areas in Europe needs to be technically treated or mixed with water from other sources for drinking, associated water treatment costs are incurred. Both Lewandowski et al. (2008) and Folkens et al. (2020) investigated the associated cost from alleviating the groundwater nitrate contamination, including the cost of NO_3^- removal system construction. Especially, the latest nitrate pollution case study in Germany by Folkens et al. (2020) quantified external pollution costs by estimating the fixed cost for installing the system of substitutable drinking water supply and the variable cost from external water supply for mixing with local contaminated well water, with the use of municipality data of Hauneck, Germany. The findings from Folkens et al. (2020) indicated that around 54% of the current drinking water price is directly linked to the internalization of externality costs. Similarly, a report published by Vedachalam et al. (2018*b*) investigated the costs of nitrate treatment for three counties (Des Moines, Decatur and Vermilion county) in the Mississippi river basin. Daily nitrate-as-nitrogen concentration data in Vedachalam et al. (2018*b*) were obtained from each of the study sites for a 10-year period beginning on January 1, 2008 and ending on December 31, 2017. In their study, Des Moines and Vermilion county operate their nitrate treatment units when the nitrate concentration in the intake waters exceeds 9.5 mg/L, while Decatur county uses 8.5 mg/L as a threshold for operating the nitrate removal unit. Thus, the estimated average annual nitrate treatment cost per unit volume (in $\$/kilogallons$) are different for Des Moines, Decatur and Vermilion county, which are 0.04, 0.06 and 0.12 respectively. However, in other nearby locations such as Hastings, Minnesota, this average nitrate treatment cost per unit volume is as high as \$0.22 per kilo gallons, which shows

that the variation of groundwater nitrate treatment cost is dependent on safe concentration levels, technologies and different sites.

An alternative approach to measure social cost of nitrate is to look at the health consequences of elevated nitrate levels in groundwater. In this context, van Grinsven et al. (2010), Su et al. (2013) and Isiuku & Enyoh (2020) all tried to determine the relation between nitrate concentration and health risks by employing various indicators of health impacts. For example, Su et al. (2013) based their health risk assessment of groundwater in Northeast China on the non-carcinogens health risk model (recommended by U.S. EPA). Similarly, Isiuku & Enyoh (2020) adopted different indices (Hazard Quotient, Nutrient Pollution Index and Chronic Daily Intake) to measure waterbody quality and health risks. Attempts to quantify the social cost of such health impacts are less common. An exception is van Grinsven et al. (2010) who use data on colon cancer incidence, nitrogen leaching, drinking water supply in the EU and one epidemiological study in Iowa to estimate the monetary value of the increased incidence of colon cancer attributed to the nitrate contamination of groundwater-based drinking water in EU. The estimated unit health damage cost from nitrate leaching by van Grinsven et al. (2010) for the 11 EU countries ranges between 0.1 and 2.4 €per kg leached N, with an average of 0.7 €per kg leached N.

A recent study of socially optimal fertilizer management was performed by Sihvonen et al. (2021) in a situation where both water and atmosphere externalities were considered. In Sihvonen et al. (2021), the social net present value (NPV) equals the discounted profit from crop production minus the discounted monetary value of the environmental damage, and thus the social planner's problem is the maximization of NPV where the monetary value of environmental damage in year t was presented as

$$\mu^N e_t^N + \mu^c e_t^c + \mu^{GHG} e_t^{GHG}$$

μ^N and μ^c are the constant external marginal damage cost of the N loss (€/kg) and carbon loss (€/kg), e_t^N and e_t^c are the annual N loss (kg/ha) and annual carbon loss (kg/ha) for year t. e_t^{GHG} is annual net GHG emissions (kg/ha). The annual GHG emissions are valued with the constant social cost of carbon μ^{GHG} (€/kg, measured as CO_2 or CO). The marginal damage cost of N loss, μ^N, used in Sihvonen et al. (2021) is derived from Gren & Folmer (2003), which gave us the unit social cost of N: $\mu^N = 6.6$ €/kg. A comparison can be made between Sihvonen et al. (2021) and an earlier paper by Martínez & Albiac (2006), using constant social cost parameter per kg of N pollutant, both of them linearly modeled social damages of N, however, Martínez & Albiac (2006) only considered leaching whereas Sihvonen et al. (2021) include leaching and greenhouse gas emission. In Martínez & Albiac (2006), the cost of nitrogen leaching was represented by λle_t, where le_t is nitrogen leaching in kg/ha and λ is the marginal pollution damage $\lambda = 1.23$ €/kg. In Sihvonen et al. (2021), the mean social damage from N leaching in coarse soils is 374.06 €/ha. In contrast, the base scenario social damage from N leaching in Planteros soil is 187.58 €/ha in Martínez & Albiac (2006), which is almost the half of social damage in Sihvonen et al. (2021).

Rather than directly linking the cost to the nitrate leaching amount (in kg), an empirical study by Rabotyagov et al. (2014*a*) used a hydrological model and simulation-optimization algorithm to examine the relation between the watershed-level cost and the percentage of nitrate concentration reductions (as in Figure 4.1). Boone River Watershed in Iowa was used for empirical demonstration and the data for populating the watershed-based hydrological model (Soil Water Assessment Tool, SWAT) was collected at the scale of a "Common Land Unit" level.

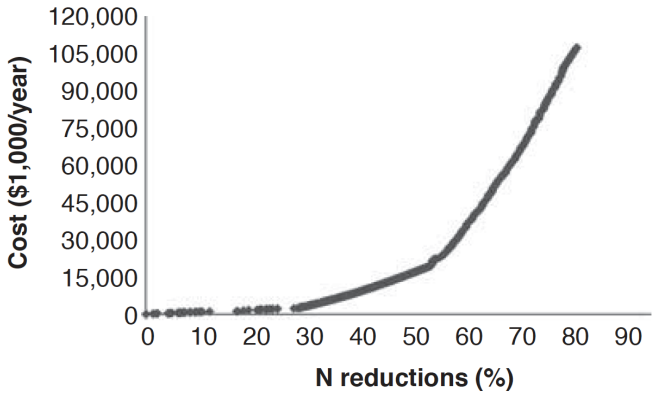

Figure 4.1: Total nitrate abatement cost curve in Boone river watershed, Iowa (Rabotyagov et al. (2014*a*))

In dealing with the unobservable and nonlinear characteristics of the transport and fate of agricultural non-point source pollutants, Rabotyagov et al. (2014*a*) proposed and evaluated a range of policy approaches for regulating emissions that are focused on abatement actions at the farm scale. In particular, Rabotyagov et al. (2014*a*) addressed three types of second-best policies and explored cost estimates for each proposed abatement action. Costs for conservation practices were expressed as opportunity costs in dollars per acre, for example, the mean cost of reducing fertilization rate by 20% is \$7.4 per acre. However, this sort of cost estimate was based on the abatement action (target-based, or action-based) instead of a measure from socially optimal perspective.

Non-market valuation studies estimating household's willingness-to-pay (WTP) for reduced nitrate pollution (or improved water quality) represent another approach to measuring the social cost of pollution from agricultural sources (Murdock (2006), Egan et al. (2009),Abidoye et al. (2012) and Van Houtven et al. (2014)). The U.S.EPA (2001) surveyed the valuations of recreational welfare loss, which is national in scope, characterizing households' annual willingness to pay for improving water quality from baseline conditions to fishable or swimmable quality. Since random utility model (RUM) can avoid the bias in welfare estimation caused by unobserved site characteristics, both Murdock (2006)

and Abidoye et al. (2012) adopted the random utility model (RUM) and travel cost approach to predict the welfare change from lake quality improvement through estimating lake visitors' demand for lake recreational services and their utility. In contrast, integrating environmental modeling and expert elicitation, Van Houtven et al. (2014) utilized a stated preference survey to predict the welfare change from a given lake quality improvement, and estimated households' WTP. Distinct from Van Houtven et al. (2014), Egan et al. (2009) estimated compensating variation per household as the WTP for achieving certain water quality improvements by developing a repeated mixed logit model of recreational lake usage. Like Murdock (2006), Abidoye et al. (2012) and Van Houtven et al. (2014), the non-market valuation of water quality improvement in Egan et al. (2009) are based on the lake quality improvement scenarios and relies on a wide combination of attributes (e.g., total nitrogen, total phosphorus, chlorophyll). However, the separate social valuation of agricultural nitrogen loss and the linkage between the social damage of N and agricultural N use are not explored in this research.

Estimating the social cost of nitrogen (SCN) in a monetary value is challenging since N is lost to aquatic, regional atmospheric, and global atmospheric pools in a variety of forms. These loss pathways are associated with damages to water quality, air quality, and climate change, respectively, which can occur over heterogeneous spatial and temporal scales. Even though Martínez & Albiac (2006) and Sihvonen et al. (2021) have proposed a monetary measurement of pollution from N, neither of these cost parameters can be used directly as the social cost of N in this thesis. For example, in Martínez & Albiac (2006), the cost of removing per kilogram of leached nitrogen from groundwater in Spain is estimated as €1.23, based on a 2.8 cents/m^3 engineering estimate to remove nitrogen from water, which may not be applicable to the US. Sihvonen et al. (2021) gave the marginal damage of N loss from barley production in Finland as €6.6 per kg N. However, this estimate may not apply in a U.S. context, and this cost refers to the annual N loss with separate costs for

leaching or denitrification is not given.

Several studies have explicitly examined the social cost of N (SCN) for three main channels of agricultural nitrogen loss in the U.S. (Keeler et al. (2016), Gourevitch et al. (2018) and Giannadaki et al. (2018)). Both Keeler et al. (2016) and Gourevitch et al. (2018) focused on the three end points of interest making up the greatest fraction of the total N-related social damage in Minnesota: greenhouse gas emissions (N_2O) from N denitrification, air pollutants ($PM_{2.5}$ formed from NO_x and NH_3^+) from N volatilization, and groundwater nitrate contamination (NO_3^-) from N leaching. The social damages of N in both papers are measured at the county level in Minnesota. Specifically, the costs due to global climate change from N_2O emissions in both papers are estimated by applying the non-CO_2 gas social cost valuation method with N_2O converted into CO_2 equivalents. They first estimated the long-term N_2O-specific damages using integrated assessment models (IAMs). Using this approach, the authors developed the social cost ratios for N_2O relative to CO_2, and got the unit social cost of N_2O by scaling the social cost of carbon (a standard value of $\$0.038/kg$, as defined by the U.S. Goverment Interagency Working Group). In Keeler et al. (2016), social damages from nitrate pollution in both private and public water sources were represented by the costs incurred in Minnesota due to water treatments needed to comply with federal drinking water standards. The costs of private well contamination were estimated on the basis of surveyed costs, including the weighted average annualized costs of well owners that opted to construct a new well, purchase bottled water, or invest in a nitrate removal system. For public water suppliers in Minnesota, the authors assembled costs for treatment, monitoring, and wellhead protection from survey data.

Applying the same approach as Keeler et al. (2016) for estimating the climate-related damage caused by denitrification, Gourevitch et al. (2018) estimated the social cost of N_2O by scaling the social cost of carbon relative to the ratio of damages for N_2O relative to CO_2, which can be understood as the avoided damages from reducing N_2O emissions.

Nevertheless, distinct with Keeler et al. (2016) in measuring costs from leaching, Gourevitch et al. (2018) adopted and contrasted six different approaches (reported in their Table 1, labelled as model W1 through W6) in estimating the costs of exposure to nitrate in groundwater. Two approaches (models W1 and W2) are based on a suite of stated and revealed preference non-market valuation methods. The economic value of groundwater is estimated as the household's stated annual willingness to pay (WTP) for nitrate-free and nitrate-safe drinking water. For example, in their model W1, they surveyed the household's annual WTP ($\$/year$) for nitrate-free drinking water by asking the respondent a series of questions such as "Suppose the local water agency could install and maintain a filter in your home that can completely eliminate nitrates in your drinking water. Would you pay for it if it costs $\$**$ per month?" Then, the county-level total damages from elevated nitrate in groundwater water are derived by multiplying the household's annual WTP ($) by the number of affected households in each county. They estimated the per-unit social cost ($\$/kg$) of nitrate from N fertilizer application in each county by dividing the county-level total damage ($) by the county-level annual on-farm N fertilizer application quantity (kg). The social cost estimates in model W3, similar to Keeler et al. (2016), are based on the treatment costs of adopting the least-cost water treatment option, assuming all households with drinking water exceeds the MCL choose the least-cost treatment option (install a reverse-osmosis system). Model W4 through W6 are based on the weighted-average cost of observed household's responses to nitrate contaminated drinking water, which include install a reverse osmosis system, drill a deeper well, install a distillation system, buy bottled water and do nothing. As opposed to model W4 that assumes no health impacts from "do nothing", model W5 and W6 incorporate the costly health impacts borne by households with exposure to contaminated drinking water from "do nothing", which are premature mortality and lost quality-adjusted life years, respectively.

Distinguished in objective from Keeler et al. (2016) that focused on valuing social cost

of N, Gourevitch et al. (2018) estimated socially optimal N fertilizer application rates for corn in Minnesota (0-161 kg/ha) and compared with the private optimum (165 kg/ha), with the social cost of N was internalized. Lowering application rates from what is privately optimal results in marginal benefits to society that outweigh the costs to farmers. As another contribution, Gourevitch et al. (2018) explicitly examined how different non-market valuation techniques affected the cost estimates by varying the modeling assumptions. Domestic well data from the County Well Index and concentration data from community and non-community public water supplies currently treating or monitoring for NO_3^- in Minnesota were used in both Keeler et al. (2016) and Gourevitch et al. (2018) to estimate the exposure to nitrate concentrations in groundwater for Minnesota households that rely on drinking water wells. The Intervention Model for Air Pollution (InMAP) was also used in both papers to examine the climate effects from N_2O emissions.

Results in Keeler et al. (2016) confirm that there is no uniform SCN, instead, changes in N management will result in different N-related costs depending on where N moves and the location, vulnerability, and preferences of populations affected by N. The authors found that the SCN per kilogram of N fertilizer applied in Minnesota ranges over several orders of magnitude, from less than \$0.001/kg N to greater than \$10/kg N, illustrating the importance of considering the site, the form of N, and end points of interest. In Keeler et al. (2016), the social cost of nitrogen per kilogram of N fertilizer applied in Minnesota associated with leaching (NO_3^-) and denitrification (N_2O) were \$0.01 per kg applied N (with a range of 0-0.23, from their Table S1) and \$0.22 per kg applied N, respectively. Nevertheless, for groundwater nitrate contamination in Gourevitch et al. (2018), model W1 (the willingness to pay for nitrate-free drinking water) and W2 (the willingness to pay for nitrate-safe drinking water) generated a median social cost of \$0.66 per kg N and \$0.005 per kg N, respectively. Model W3, based on the costs of adopting the least-cost water treatment option, gave a median of \$0.023 per kg N, whereas model W4, W5 and W6

were based on the cost of households observed response to contaminated drinking water assuming no health impacts, premature mortality and lost quality-adjusted life years, which gave a median of \$0.039, \$0.044 and \$0.077 per kg N, respectively. The median cost of N_2O emissions (model C1) is estimated as roughly \$0.07 per kg N (Fig.1 in Gourevitch et al. (2018)). In addition, the location of N application was found to cause significant variation in the estimates of the SCN, for instance, the SCN of NO_3^- based on W_1 model (the willingness to pay for nitrate-free drinking water) can reach as high as around \$100 per kg N (Fig.1 in Gourevitch et al. (2018)). The social cost estimates for different counties in MN can vary in a range of \$0-\$50 per kg applied N (Keeler et al. (2016)).

Groundwater quality deterioration and adverse climate change effects from agricultural production are serious issues in Iowa. According to the Iowa Department of natural Resources[3], about 26% of global greenhouse gas emissions are caused by food production and over 75% of Iowans rely on groundwater as their primary source of drinking water. Around 230000 people in Iowa rely on private well water. The Iowa Community Private Well Study, conducted in 2003 by Iowa State University and USGS, detected nitrate in 57% of wells and 8-25% of wells in different regions exceeded the maximum contaminant level limit (10 mg/L by USEPA). In the recent 16 years (2001-2016) the proportion of private wells with nitrate concentrations exceeding MCL was found increased. Thus, valuing the social cost of N in terms of groundwater nitrate NO_3^- contamination and greenhouse gas N_2O effect is very important in Iowa.

Since both Keeler et al. (2016) and Gourevitch et al. (2018) estimated the social cost of N from both leaching and denitrification for Minnesota state in the U.S., their results are judged to be the most relevant papers for our research in Iowa, and will be used for our social decision-making problem. Our objective is to link the rainfall-induced N loss

[3]Iowa Department of natural Resources. Source: www.iowadnr.gov/Environmental-Protection/Water-Quality/Water-Monitoring/Groundwater

amounts to the social damages, by choosing the estimates from these papers as proxies for the cost of elevated nitrogen in groundwater and atmosphere. The social cost estimates in these papers are per kilogram of applied nitrogen, and these are not explicitly tied to the portion of nitrogen that is lost through leaching or denitrification. In contrast in our model, social damages from nitrogen relate only to the portion subject to leaching and denitrification. The social cost estimates from these papers are thus not directly applicable given our modeling assumptions and should be grossed up by a factor that accounts for the portion of N applied that actually causes damages. However, given the wide range of social cost estimates reported, it was decided to account for this issue via sensitivity analysis.

As a result, we use the values of social costs from Keeler et al. (2016) and Gourevitch et al. (2018) as the base case in our model and allow for additional cost values to be examined in a later sensitivity analysis sections. The social cost estimates in both papers are conservative because other damages associated with N fertilizer application are omitted due to our limited understanding of adverse impacts, and the subsequent transformation of N is not included (Gourevitch et al. (2018)). Because the social cost per kilogram of denitrified or leached N will be greater than what the authors estimated in terms of per kilogram of applied N, the highest median value of \$0.66 (from model W1 in Gourevitch et al. (2018)) is preferred as the base case for the cost from N leaching (per kilogram of leached N), which reflects the economic value of removing every unit of nitrate pollutant in groundwater. Similarly, \$0.22 (from Table S1 in Keeler et al. (2016)) is assumed as the base case for the cost from N denitrification (per kilogram of denitrified N). Gourevitch et al. (2018) discovered that the social cost per kg of applied N in Minnesota ranges over several orders of magnitude from less than \$0.001 to greater than \$10. In the sensitivity analysis sections, the social cost of N for leaching, d_L, is assumed as \$0.01, \$0.66 (Base Case), \$10, \$20, \$30, \$40 and \$50 per kilogram leached N, and the social cost of N_2O denitrification, d_D, is assumed as \$0.01, \$0.22 (Base Case), \$10, \$20, \$30, \$40 and \$50

per kilogram denitrified N. These assumed cost levels are all within the range of marginal social costs of N for all Minnesota counties, as estimated by Keeler et al. (2016) and shown in Fig.1.

4.3 Literature on modelling nitrogen emissions for policy analysis

There is a significant literature studying the negative externalities caused by nitrogen fertilizer and optimal policies to address these issues. Of particular interest for this thesis is the modelling of nitrogen fate and transport and the factors that affect harmful emissions into waterways and the atmosphere. This section reviews a selection of that literature.

A number of economics papers develop optimal control models of nitrogen usage given an objective function to maximize a social welfare function from agricultural activities over infinite time, or a very long time horizon. Typically, there is no uncertainty involved. They include a leaching function for nitrogen and a state variable that keeps track of nitrogen concentration in water. Some papers include an empirical component whereby the model is parameterized using data for a particular region or watershed. Kim et al. (1993), Kim et al. (1996) and Lee & Kim (2002) develop a stylized model to evaluate the efficiency of different policies for regulating nitrogen emissions. The papers assume a fixed proportion of nitrogen fertilizer is leached into groundwater. The former two papers also assume a delay between the time that nitrogen is added to the field and then leaches to the groundwater. The time delayed equation of motion for nitrogen in the soil is given as:

$$\dot{N}_t = \alpha n_{t-\tau} + \beta k N_{t-\tau} - \rho N_t$$

where N is the stock of nitrates in groundwater, α and β are exogenous proportionate leaching coefficients, n is applied fertilizer quantity, ρ is the rate of N discharge from the aquifer, τ represents a constant time lag between fertilizer application and its arrival to the groundwater.

Yadav (1997*b*) and Yadav (1997*a*) present optimal control models to study optimal nitrogen use. Both authors used a nitrate concentration function, based on the work by Kim et al. (1993), keeping track of the stock of nitrogen. They calibrated an equation of motion for nitrate concentration that includes additions from fertilizer as well as natural attenuation, which was

$$C_{t+1} = (1-\gamma)\eta N_{t-\tau} - (1-\delta)C_t$$

where C_t is contamination concentration at aquifer at time t, $N_{t-\tau}$ is nitrogen-related activity (N application) at time $t-\tau$, δ is the degradation rate of nitrogen in the groundwater aquifer, γ is the degradation rate of nitrogen at the surface level including volatilization and runoff, η is a scaling parameter describing conversion of applied nitrogen into nitrate pollutant, τ is residence time of nitrogen in the vadose zone (area between root zone and water table). They derived an expression showing total nitrate contamination of groundwater in year t as a function of C at time 0 and all subsequent N applications. A simplified equation of motion for nitrogen was used by Yadav (1997*a*) for an empirical analysis of the socially optimal nitrogen use using 1987-1990 experimental data based on three sites in Minnesota. Since the literature did not report an aggregate nitrate social damage function that includes costs to human health as well as to the environment, in their social net benefit model, the aggregated social cost of nitrate contamination was assumed as a general quadratic function of the concentration: θC_t^2. Solving the social planner's problem resulted in an optimal application rule (a closed form solution) that depends on C_t. They also analyzed the dynamics and steady state equilibrium of N application N^* and nitrate

concentration C^*. Because of the assumed form of their objective function, Yadav (1997*b*) and Yadav (1997*a*) are able to derive an optimal policy rule for nitrogen use.

Hart (2003) uses a dynamic optimal control model to evaluate the groundwater contamination and optimal restoration of marine ecosystems. The model is parameterized using data for Sweden. His model consists of two control measures, one upstream (agricultural abatement) and one downstream (mussel cultivation at the coast). Hart (2003) first derived a simple optimal control model where all pollution is assumed to come from a single basin. The equation of motion for the pollution stock is similar to those of the two previous articles Yadav (1997*b*) and Yadav (1997*a*): $G_{t+1} = (1-\delta)(L_t + (1-k)G_t)$, where G_t is pollution amount in a groundwater reservoir at period t, L_t is the nitrogen leachates enter the reservoir, a proportion δ is attenuated through processes such as denitrification or decay, kG_t is the pollution mass flow out from the reservoir. In his second model, Hart (2003) divides land area into three zones with different properties, and includes a model of simulating river and groundwater flows. The three zones have different soil and climate characteristics that affect the cost of reducing N use to the farm. Hart (2003) finally modelled N abatement cost as a quadratic function of the degree of abatement, and a quadratic social damage function for N pollution (a quadratic function of N quantity removed by mussel farming and a decreasing function of the stock of N pollution) is assumed in his paper.

Fishman et al. (2012) examined a cost efficient input tax policy to address drinking water contamination by nitrogen fertilizer under varying conditions of water scarcity. They study the use of revenue from tax payments to cover groundwater contamination treatment costs. Their equation of motion for groundwater nitrogen concentration, includes the contribution of nitrogen in rain, the contribution of nitrogen in irrigation water and the contribution of nitrogen fertilizer application.

Another class of papers incorporates process-based or structural models (water quality models) to simulate on-ground nitrogen loading, soil dynamics, and finally determine the fate and transport of nitrate in groundwater in response to different regulatory policies and under different agricultural practices. Various hydrological and hydro-chemical simulation models are mentioned in the literature. These models were calibrated using experimental data. For example, the Soil and Water Assessment Tool (SWAT) is a water quality, watershed-based hydrological model developed by the US Department of Agriculture to simulate the impact of point and non-point source emissions, was adopted by Rabotyagov et al. (2014*a*). The soil-plant-atmosphere model CoupModel was employed by Sihvonen et al. (2021) for running long-term simulations, where inorganic and organic N fertilizers are given in different amounts as inputs. The modular design of such process-based model allows plugging in any choice of process descriptions for various parts of different natural ecosystems. One important feature of such process-based model is its capability to handle more than one site.

Other relevant papers include Almasri & Kaluarachchi (2007), Puckett et al. (2008), Welch et al. (2011), Huang et al. (2013). These papers mainly employed a large set of metadata, structural tools, bio-physical simulation models, process-based models, such as the Soil and Water Assessment Tool (SWAT), to model complex relationships between land activities and water quality. The advantage of these mechanistic water quality models is the ability to reflect the key nonlinearities and interactions between different bio-physical factors in predicting contaminant transport and fate, however, such process-based models may be too complex to statistically simplifies the description of the hydro-geologic systems and the nitrogen cycle.

4.4 Model Specification

In this section we consider the optimal actions of a social planner or regulator concerned with maximizing the total net benefits from corn harvest. The regulator's objective function includes two negative externalities from nitrogen fertilizer: damages from the leaching of nitrogen into groundwater and damages from greenhouse gas emissions due to denitrification. N leaching and denitrification are assumed as fixed proportions of the total N loss. There are two social damage models proposed in this thesis: linear damage model and threshold damage model.

Recall that for times other than fertilizer application dates, $t \notin \Omega_F$, soil nutrient content S_t (as defined in Equation (3.14)) is affected only by the instantaneous rate rainfall R^{w_t}, where $w_t \in \{0, 1\}$ refers to the two rainfall regimes defined in Equation (3.9).

$$dS = -l_s R^{w_t} S(t) dt \,, \tag{4.1}$$

where l_s is an assumed constant parameter reflecting the total N loss rate of S per mm of rainfall. In this chapter, $L(t)$ is defined as the **cumulative** amount of nitrogen that has travelled to groundwater by time t as a result of leaching. The change in the cumulative leaching dL is assumed to be a constant proportion l_e of the change in soil nutrient level S.

$$dL = -l_e dS = l_e l_s R^{w_t} S(t) dt \,,$$

where l_e is an assumed constant parameter reflecting the proportion of leached nitrogen in the total N loss amount. The other portion of lost nitrogen is due to denitrification, where Υ refers to cumulative denitrification losses.:

$$d\Upsilon = -(1 - l_e) dS = (1 - l_e) l_s R^{w_t} S(t) dt \tag{4.2}$$

The social damage from nitrogen is defined as the present value of all damages, over an infinite future time frame, caused by an increase in a unit of nitrogen today at a particular site. We define d_L to be the social cost of nitrogen related to groundwater nitrate contamination from leaching and d_D as the social cost of nitrogen related to the release of greenhouse gas emissions due to denitrification. For simplicity, we calculate the social damages of nitrogen only at the end of the season at time T, ignoring the timing of when that nitrogen was deposited over the growing season. Then for the linear social damage function, the monetary value (in dollars per acre) of damages at time T from leaching and denitrification is specified as:

$$D(T) = d_L L(T) + d_D \Upsilon(T) \tag{4.3}$$

Note that since $L(T)$ and $\Upsilon(T)$ are measures of cumulative nitrogen emissions from leaching and denitrification, respectively, $D(T)$ represents the present value of all future damages that arise from cumulative nitrogen emissions up to time T.

For the threshold social damage function, damages from leaching occur only when the cumulative nitrogen in the groundwater exceeds a specific concentration threshold. If the simulated N concentration is above that threshold, the social damage of N leaching will be calculated according to the linear damage model, which is the product of leaching amount and unit nitrate social cost plus the denitrification amount times the per unit cost from N_2O emissions. If the nitrogen concentration in groundwater is less than the threshold, then the social damage of N leaching vanishes in the regulator's model and only social damage of denitrification remains. The N concentration in groundwater is a state variable denoted as Θ (mg/L). The relationship between leaching amount and Θ is assumed as:

$$d\Theta = \varpi dL, \quad \text{given } \Theta(t=0) = \Theta_0 \tag{4.4}$$

where ϖ is the constant parameter. Social damages now depend on nitrate concentration at the end of the season, $\Theta(T)$. Denote the N concentration threshold for leaching damages as $\hat{\Theta}$.

$$D(T) = \begin{cases} d_D \Upsilon(T) & \text{if } \Theta(T) < \hat{\Theta} \\ d_L L(T) + d_D \Upsilon(T) & \text{if } \Theta(T) \geq \hat{\Theta} \end{cases} \tag{4.5}$$

The regulator's objective function is specified below.

$$V(p, \bar{h}, x_1, \tilde{\delta}, r, w_{t_i}, \bar{r}, s, \bar{s}, \tilde{\Upsilon}, l, t_i) = \sup_K \mathbb{E}_K^{\mathbb{Q}} \Bigg\{ \overbrace{e^{-\rho(T-t_i)} P(T) Y(\bar{h}, x_1, \tilde{\delta}, r, w_{t_i}, \bar{r}, s, \bar{s}, T)}^{\text{Discounted revenue from corn harvest at T}}$$
$$- \overbrace{\sum_{t_j \in \Omega_F} \left[e^{-\rho(t_j - t_i)} c_N N(t_j) \right]}^{\text{Total fertilizer cost}} - \overbrace{e^{-\rho(T-t_i)} D(T)}^{\text{Social damages}} - \overbrace{\left[e^{-\rho(T-t_i)} (c_F + c_V Y(\bar{h}, x_1, \tilde{\delta}, r, w_{t_i}, \bar{r}, s, \bar{s}, T)) \right]}^{\text{Discounted total variable and fixed cost}}$$
$$\Big| P(t_i) = p, \bar{H}(t_i) = \bar{h}, X_1(t_i) = x_1, \delta(t_i) = \tilde{\delta}, \bar{R}(t_i) = \bar{r}, R(t_i) = r, w_{t_i} = w, S(t_i) = s,$$
$$\bar{S}(t_i) = \bar{s}, \Upsilon(t_i) = \tilde{\Upsilon}, L(t_i) = l \Bigg\} \tag{4.6}$$

where c_V is the total variable cost for corn yield excluding fertilizer, and c_F is the total fixed cost associated with both fertilizer applications and harvest machinery use. The expectation is with respect to control set K and other notation is consistent with the previous farmer's decision model (3.17). We explore the characteristics of the social planner's problem through Monte Carlo analysis.

4.5 Detailed specification of Monte Carlo analysis

This section describes the choice of parameters for the leaching and denitrification equations as well as the associated social costs.

4.5.1 Parameter specification

Agronomists usually define leaching loss as N moving out of the crop rooting zone (not available for crop uptake) while environmentalists consider its entering the water bodies. Given the complexity of the agricultural N cycle in the soil, this thesis adopts the simplifying assumption that N leaching and denitrification are fixed proportions of the total N loss. This allows us to employ two unit social costs of N representing the average damages from nitrogen leaching and denitrification. Specifically, this chapter assumes in the base case that leaching losses represent 43.3% of the total N loss and denitrification represents the rest 56.7%, which is consistent with Gentry et al. (1998). As noted in Section 3.4, in a modelling exercise using the Community Land Model, Nevison et al. (2016) found high variation in the proportion of N-loss due to leaching versus denitrification[4]. Sensitivity analyses regarding N loss partition are performed in later sections where the $\frac{denitrification}{leaching}$ ratio is assumed as $\frac{90\%}{10\%}$ and $\frac{10\%}{90\%}$.

Assumptions for the social cost of leaching are based on the estimates of Keeler et al. (2016) who provided a range of estimates for the social cost of nitrogen due to agriculture in Minnesota. We assume the costs in Iowa will be similar. The social cost of nitrogen is intended to reflect the present value of damages resulting from an incremental increase in nitrogen at a particular site, such as groundwater or the atmosphere. The social cost from N leaching causing groundwater contamination by NO_3^- is assumed to be d_L =0.66 $\$/kg$ and from denitrification due to the contribution of N_2O emissions to climate change is assumed to be d_D =0.22 $\$/kg$, as the base case. In later sensitivity sections, the social cost of nitrate leaching (d_L) is varied as 0.01, 10, 20, 30, 40, 50 $\$/kg$N, and the social cost of N_2O denitrification (d_D) is varied as 0.01, 10, 20, 30, 40, 50 $\$/kg$N. All social cost parameters are transformed into $\$/lb$ and examined in the later sensitivity analysis section.

[4]The Community Land Model is maintained by the Climate and Global Dynamics Laboratory at the National Center for Atmospheric Research in the United States.

For the threshold damage model, the initial N concentration is assumed as zero, $\Theta_0 = 0$. According to U.S. Environmental Protection Agency[5], a nitrate concentration in groundwater greater than 3 mg/L generally indicates contamination from human activity, thus, we assume $\hat{\Theta} = 3$ mg/L.

An estimate is needed for the parameter ϖ in Equation (4.4), which reflects the change in N concentration as a result of nitrogen leaching. The units of ϖ will be (mg/litre in N concentration) $\div$ (mg/acre in quantity of N leached). The concentration measure would reflect a value at a particular location, or an average over several locations where N concentration is monitored. An estimate of ϖ is derived using historical averages from Iowa:

- (i) **Quantity of N leached**. We utilize the base case assumptions for the total N loss rate (percent of N applied that is lost to the environment $\div$ mm of rainfall), base case leaching proportion of the total N loss, historical Iowa fertilizer application for 1993-2003, 2005, 2010, 2014, 2016 and 2018 (averaged county-level, in $lb/acre$) and historical Iowa daily precipitation to compute the total N leaching amount for each year in Iowa. We assume the N fertilizer is all applied as starter without soil N legacy.

- (ii) **Nitrate concentration**. Iowa groundwater nitrate concentration data is obtained from the AQuIA database[6], which comes from different wells or springs in Iowa. The raw concentration data (in mg/L) includes 5672 observations, for the

[5]Nitrate concentrations greater than 3 mg/L generally indicate contamination, according to "Estimated Nitrate Concentrations in Groundwater Used for Drinking", by U.S. Environmental Protection Agency. Source:www.epa.gov/nutrient-policy-data/estimated-nitrate-concentrations-groundwater-used-drinking

[6]AQuIA database, Water Quality Monitoring System, Department of natural Resources, Iowa, accessed on March 01, 2021 (Source: https://programs.iowadnr.gov/aquia/search). Since the separate nitrate concentration data on the website is discontinuous in years, we choose inorganic nitrogen (nitrate and nitrite) concentrations to use. Indeed, in the environment, nitrite generally converts to nitrate, which means nitrite occurs very rarely in groundwater (Source: waterquality.montana.edu/well-ed/interpretingresults/fsnitratenitrite.html)

period of 1993-2003, 2005, 2010, 2014, 2016 and 2018, from different days of the year and from different sites across Iowa state. To represent the annual Iowa state-level nitrate concentration in groundwater, we take the average of observations for the same year. A summary of the data is presented in the following Table 4.1.

- (iii) The estimated ϖ (concentration per unit of leached nitrogen) in Iowa for the period of 1993-2003, 2005, 2010, 2014, 2016 and 2018 is derived from

$$\varpi = mean\left\{\frac{\text{Annual nitrate concentration (red font in Table 4.1, mg/l)}}{\text{Annual N leaching amount (from step (i), mg/a)}}\right\} = \frac{1}{1647200}$$

This is clearly a rough approximation of the value of ϖ, based on averages, and is used for illustrative purposes. Ideally we would like to know how an increase in N leaching affects concentration levels at the margin.

Table 4.1: Summary of groundwater nitrate concentration data in Iowa (in mg/L)

Year	# of observations	[min, mean, max]
1993	296	[0.1, 9.23, 35]
1994	392	[0.1, 9.0, 34.5]
1995	379	[0.1, 6.5, 24]
1996	351	[0.1, 6.03, 38]
1997	212	[0.1, 6.89, 20.1]
1998	245	[0.1, 7.31, 40]
1999	142	[0.1, 9.51, 46]
2000	140	[0.1, 9.18, 44]
2001	98	[0.1, 11.34, 94]
2002	255	[0.1, 3.16, 35]
2003	258	[0.1, 4.65, 250]
2005	274	[0.1, 3.83, 118]
2010	87	[0.1, 8.8, 20]
2014	45	[0.1, 6.23, 17]
2016	114	[0.1, 3.53, 40]
2018	91	[0.1, 4.57, 29.98]

4.5.2 Monte Carlo algorithms

In this section the algorithms are presented for calculating the linear and threshold based damages. Both Algorithm 4 and Algorithm 5 share the same way in calculating social damages from denitrification $d_D\Upsilon$. However, for damages from leaching, in Algorithm 5, if the simulated nitrate concentration crosses the contamination threshold 3 mg/L, the

associated path will be regarded as "leaching damage ocurred", we then use the product of total N leaching amount and unit social cost of NO_3^- $(d_L L)$as the leaching damage in the social damages D as the Algorithm 4 does. Otherwise, the social damage for the associated path will be set to zero as a result of insignificant detrimental social leaching impacts by low nitrate concentration, and the social damage will be identical to the denitrification damage, $D = d_D \Upsilon$.

Algorithm 4 Compute linear social damage

Input: Simulated daily precipitation $R^{w_t}(t_m)$, $t_m \in \Omega_D$, given nutrient application (N_0, N_1), l_e, l_s, unit social cost of leaching and denitrification: d_L and d_D;

Output: L, Υ, D

for i=1 : number of simulated paths **do**
  $S(i, t_0) = N_0$;
  $L(i, t_0) = l_e * l_s * R^{w_{t_0}}(i, t_0) * S(i, t_0)$;
  $\Upsilon(i, t_0) = (1 - l_e) * l_s * R^{w_{t_0}}(i, t_0) * S(i, t_0)$;
  for j=t_0+1 : t_M **do**
    if $j \in \Omega_F$ **then**
    $S(i, j) = (1 - l_s * R^{w_{j-1}}(i, j-1)) * S(i, j-1) + N_1$
    $L(i, j) = l_e * l_s * R^{w_j}(i, j) * S(i, j) + e^{r\Delta t} * L(i, j-1)$
    $\Upsilon(i, j) = (1 - l_e) * l_s * R^{w_j}(i, j) * S(i, j) + e^{r\Delta t} * \Upsilon(i, j-1)$
    else
    $S(i, j) = (1 - l_s * R^{w_{j-1}}(i, j-1)) * S(i, j-1)$
    $L(i, j) = l_e * l_s * R^{w_j}(i, j) * S(i, j) + e^{r\Delta t} * L(i, j-1)$
    $\Upsilon(i, j) = (1 - l_e) * l_s * R^{w_j}(i, j) * S(i, j) + e^{r\Delta t} * \Upsilon(i, j-1)$
  end
  $D(i, t_M = T) = d_L L(i, t_M = T) + d_D \Upsilon(i, t_M = T)$

16: **end**

17: The discounted cumulative damages over the entire season, at time t_0 is $\hat{D}(t_0) = e^{-r(t_M - t_0)} * mean(D(t_M))$.

Algorithm 5 Compute threshold social damage

Input: $R^{w_t}(t_m)$, $t_m \in \Omega_D$, (N_0, N_1), l_e, l_s, d_L, d_D, ϖ;

Output: L, Υ, Θ, D;

1: **for** i=1 : number of simulated paths **do**

2: $S(i, t_0) = N_0$;

3: $L(i, t_0) = l_e * l_s * R^{w_{t_0}}(i, t_0) * S(i, t_0)$; $\Theta(i, t_0) = \varpi L(i, t_0)$;

4: $\Upsilon(i, t_0) = (1 - l_e) * l_s * R^{w_{t_0}}(i, t_0) * S(i, t_0)$;

5: **for** j=t_0+1 : t_M **do**

6: **if** $j \in \Omega_F$ **then**

7: $S(i, j) = (1 - l_s * R^{w_{j-1}}(i, j-1)) * S(i, j-1) + N_1$

8: $L(i, j) = l_e * l_s * R^{w_j}(i, j) * S(i, j) + e^{r\Delta t} * L(i, j-1)$

9: $\Theta(i, j) = \Theta(i, j-1) + \varpi(L(i, j) - L(i, j-1))$

10: $\Upsilon(i, j) = (1 - l_e) * l_s * R^{w_j}(i, j) * S(i, j) + e^{r\Delta t} * \Upsilon(i, j-1)$

11: **else**

12: $S(i, j) = (1 - l_s * R^{w_{j-1}}(i, j-1)) * S(i, j-1)$

13: $L(i, j) = l_e * l_s * R^{w_j}(i, j) * S(i, j) + e^{r\Delta t} * L(i, j-1)$

14: $\Theta(i, j) = \Theta(i, j-1) + \varpi(l_e * l_s * R^{w_j}(i, j) * S(i, j))$

15: $\Upsilon(i, j) = (1 - l_e) * l_s * R^{w_j}(i, j) * S(i, j) + e^{r\Delta t} * \Upsilon(i, j-1)$

16: **end**

17: **if** $\Theta(i, t_M = T) < 3$ **then** $D(i, t_M = T) = d_D \Upsilon(i, t_M = T)$

18: **else** $D(i, t_M = T) = d_L L(i, t_M = T) + d_D \Upsilon(i, t_M = T)$

19: **end**

20: $\hat{D}(t_0) = e^{-r(t_M - t_0)} * mean(D(t_M))$.

4.5.3 Monte Carlo results

The value surfaces of social net welfare are computed respectively from incorporating the linear social damage and the threshold social damage functions into the social planners objective function. Results are presented in the following Figure 4.2. The impact of fertilizer side-dressing application N_1 on the value V_0 given various starter applications N_0, is presented in the following Figure 4.3 and 4.4.

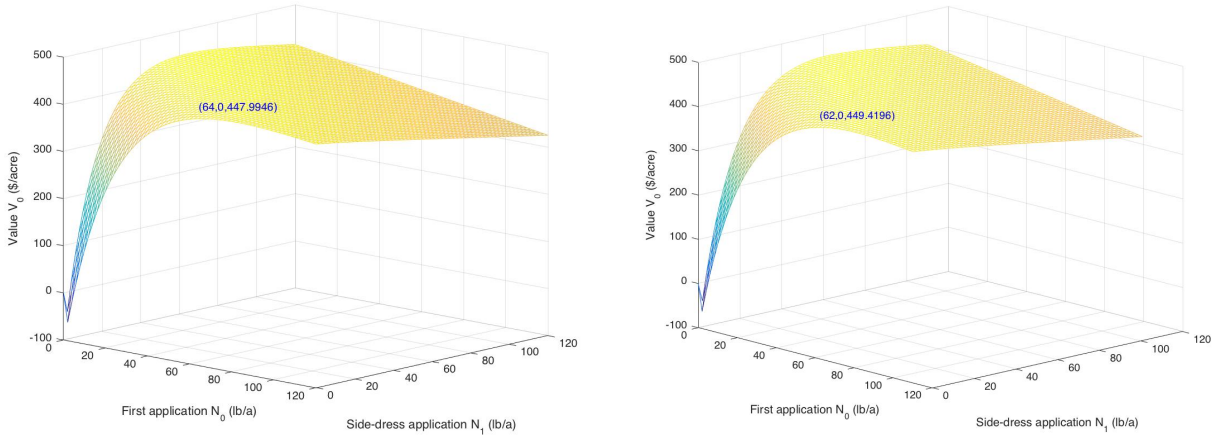

(a) Linear damage model

(b) Threshold damage model

Figure 4.2: Social welfare surface, the ordered triplet shows (N_0, N_1, and Value at time 0)

From Figure 4.2, the socially optimal fertilizer application strategy is ($N_0 = 64$, $N_1 = 0$) lb/acre when using the linear damage model and ($N_0 = 62$, $N_1 = 0$) lb/acre when using the threshold damage model. Compared with the private optimal application ($N_0 = 66$, $N_1 = 0$) in Figure 3.17, Figure 4.2 indicates that the optimal fertilizer application amount is reduced by 2 lb/a and 4 lb/a with the presence of social cost of N, whereas the optimal application timing remains the same. It might be anticipated that including a social damage function would cause the optimal fertilizer split to shift to the side dressing, since this leaves a shorter length of time for rainfall induced N-losses. However this effect is not

evident under our base case assumptions.

When comparing Figure 4.2 (a) and (b), we can note that, in our base case, using the threshold social cost function gives us a slightly lower fertilizer application amount. In our base case, the mean nitrate concentration for $(N_0 = 64, N_1 = 0)$lb/a is 3.0527 mg/L, whereas the mean concentration for $(N_0 = 62,\ N_1 = 0)$lb/a is 2.9926 mg/L which is lower than the threshold implying there is no leaching damage. This gives the social planner incentive to choose a lower application plan. Comparing the social monetary net benefit in Figure 4.2(a) and (b), we can find the threshold social damage framework implies a very slightly higher value of $V_0 = \$449.42/acre$ compared to $V_0 = \$447.99/acre$ for the linear damage function. In summary, under our base case assumptions, the incorporation of social costs of N will not alter the optimal application timing, but will decrease the application amount compared with private optimal results.

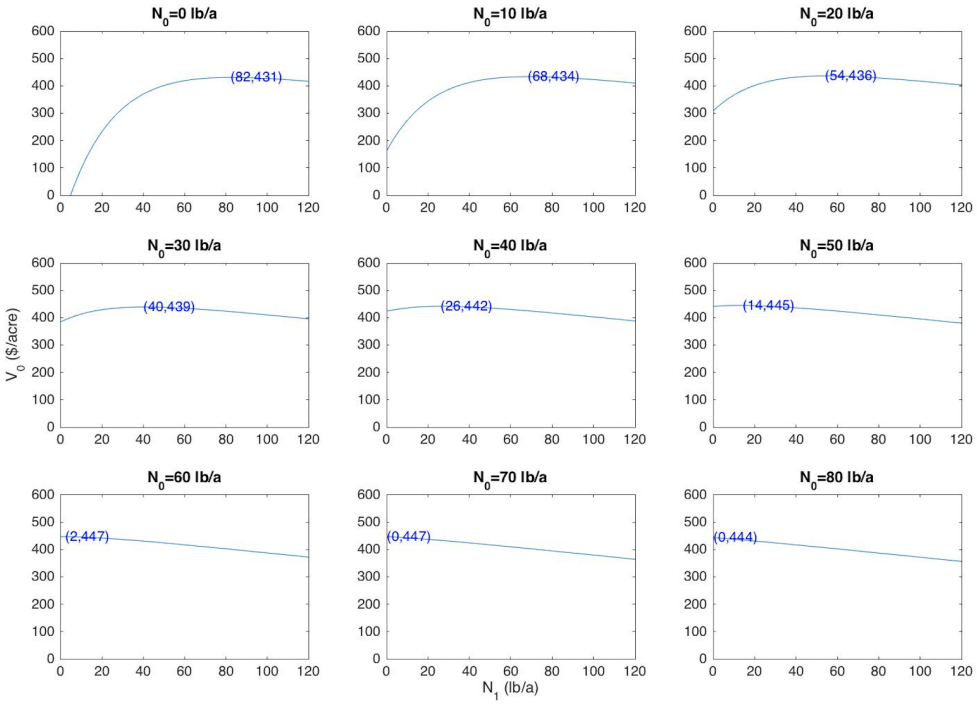

Figure 4.3: Response of V_0 to N_1 with different given N_0 (linear damage model), the ordered pair shows (N_1, V_0)

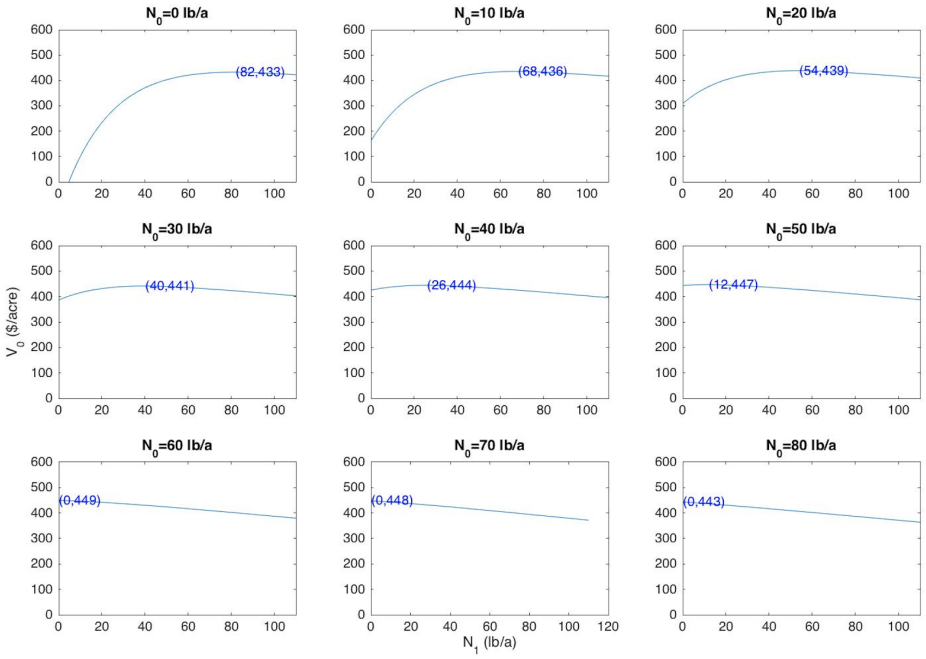

Figure 4.4: Response of V_0 to N_1 with different given N_0 (threshold damage model), the ordered pair shows (N_1, V_0)

To compare the results from sole split application, we assume $N_0 = 0$ or $N_1 = 0$ and increase the other fertilizer application from 0 to 110 lb/a to see how the average soil nutrient stock, corn value, total leaching amount and the estimated corn yield from linear damage model will be changed, which are plotted in Figure 4.5. The blue line represents the results from ($N_0 = 0$, $N_1 > 0$) and the red line represents the results from ($N_0 > 0$, $N_1 = 0$). Figure 4.5(a) tells us the fact that starter application will always bring a higher soil nutrient level compared with the same amount of side-dressing application. This finding explains our results that for a social optimum all fertilizers should be applied as starter despite a higher amount of leaching compared to side-dressing (as in Figure 4.5(c)). ($N_0 > 0$, $N_1 = 0$) generates a higher corn value compared to ($N_0 = 0$, $N_1 > 0$) in Figure 4.5(b). As showed in Figure 4.5(d), a higher averaged soil nutrient level gives a higher corn yield when other weather variables are the same.

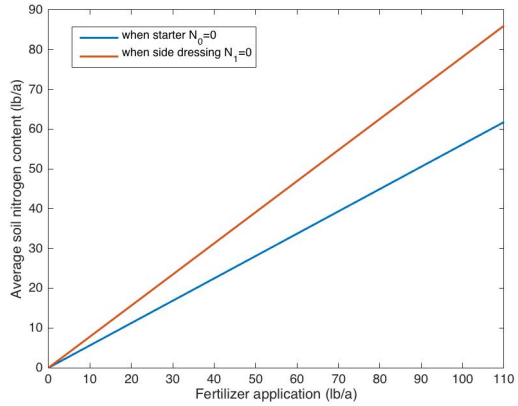

(a) The average soil nutrient stock

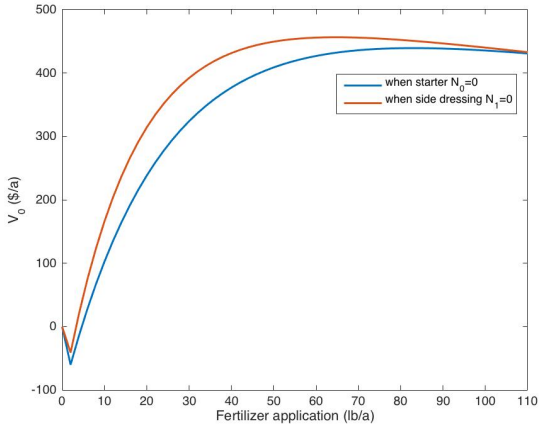

(b) Corn value V_0

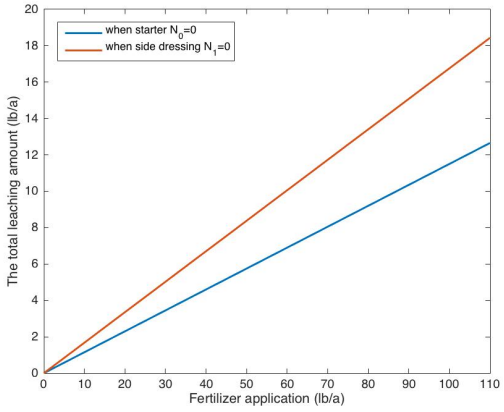

(c) The total leaching amount

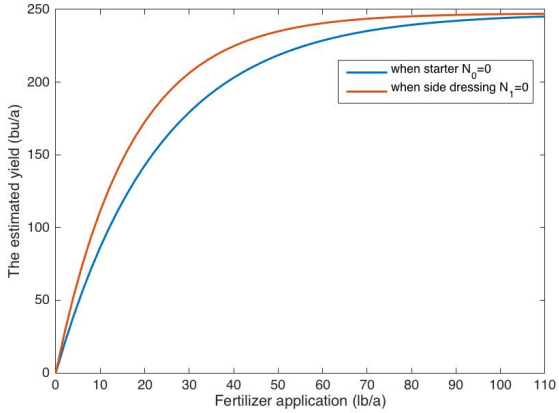

(d) The estimated corn yield

Figure 4.5: The average soil nutrient stock, corn value, total leaching amount and the estimated corn yield from linear damage model under ($N_0 = 0$, $N_1 > 0$) and ($N_0 > 0$, $N_1 = 0$)

A more detailed look into the evolution of the average soil nutrient stock $\bar{S}$ is presented in the following Figure 4.6, where green colored paths are from $(N_0 = 64, N_1 = 0)$ and cyan color represents the simulated paths given $(N_0 = 0, N_1 = 64)$. In Figure 4.6, even if later side-dressing application has a shorter loss period and a smaller amount of N waste, the averaged soil nutrient levels from side dressing-only plan (cyan colored) are lower than

those from starter-only plan (green colored). As a result, at maturity date September 18, the average growing season soil nutrient stock from $(N_0 = 64, N_1 = 0)$ is higher than that from $(N_0 = 0, N_1 = 64)$, and so does the corn yield.

The simplifying assumption that corn yield depends on average soil N levels has a significant effect on the results. As discussed previously, this assumption captures the fact that these two fertilizer application times are not perfect substitutes. More detailed modelling of the effect of the N application date versus corn growth is beyond the scope of this thesis. The quantitative results derived must be considered illustrative.

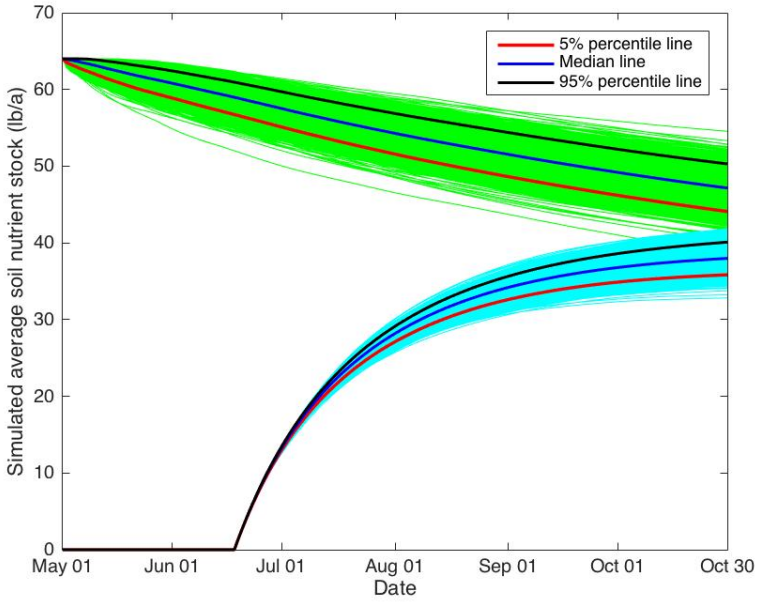

Figure 4.6: The simulated average soil nutrient stock for $(N_0 = 64, N_1 = 0)$ shown in green and $(N_0 = 0, N_1 = 64)$ shown in cyan

The social damage of N from the linear and threshold damage models under $(N_0 = 0,$ $N_1 > 0)$ and $(N_0 > 0,\ N_1 = 0)$ are examined in Figure 4.7. Since both leaching and denitrification damages are included in the linear damage model, Figure 4.7(a) shows the total damages increase almost linearly with the rising of fertilizer application, and starter application brings a higher social damage compared to side dressing. In contrast, as the

social damage of N depends on whether the nitrate concentration threshold is triggered or not, the non-linearity feature of the social damage curve (both lines in Figure 4.7(c), as marked with a rectangle) is therefore found. Scatter plots of N concentration and social damages are presented in Figures 4.7(b) and 4.7(d), respectively.

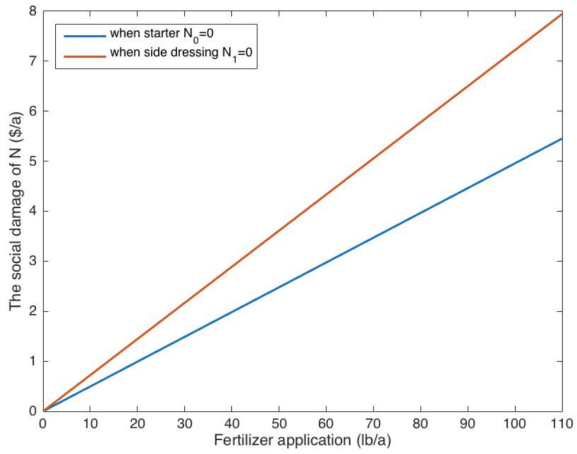

(a) Linear damage model

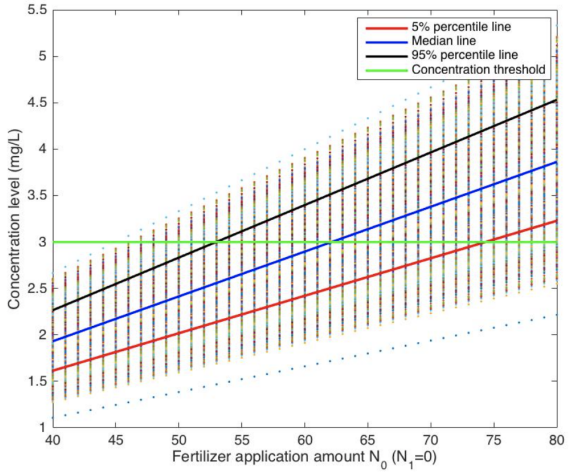

(b) Concentration levels when $N_1 = 0$ in (c)

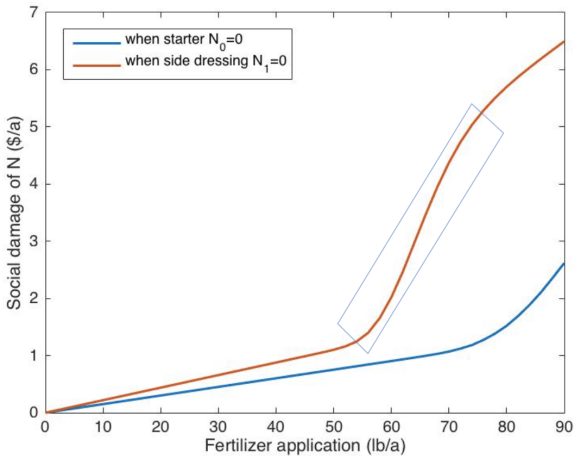

(c) Threshold damage model

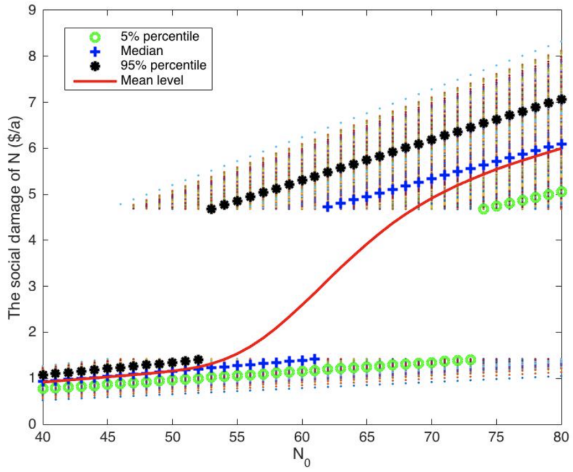

(d) Social damages when $N_1 = 0$ in (c)

Figure 4.7: The social damage of N from linear and threshold damage model under ($N_0 = 0$, $N_1 > 0$) and ($N_0 > 0$, $N_1 = 0$)

In addition, we plot the simulated paths for daily leaching amount, cumulative leaching

amount $L(t)$ and N concentration $\Theta(t)$ in groundwater in the following Figure 4.8.

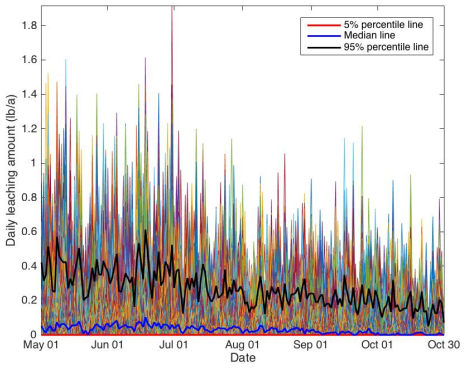

(a) Simulated daily leaching amount when ($N_0 =$ 62, $N_1 = 0$)

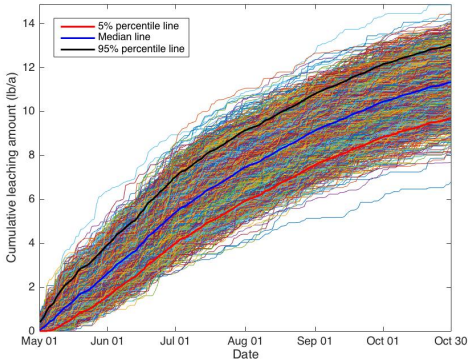

(b) Simulated $L(t)$ when ($N_0 = 62$, $N_1 = 0$)

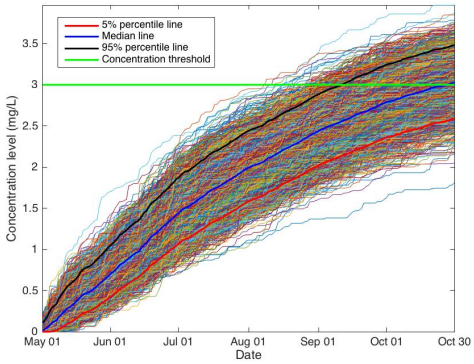

(c) Simulated $\Theta(t)$ when ($N_0 = 62$, $N_1 = 0$)

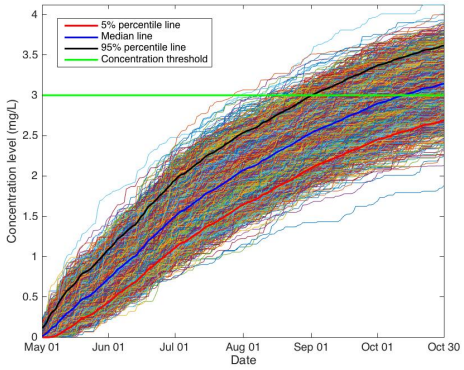

(d) Simulated $\Theta(t)$ when ($N_0 = 64$, $N_1 = 0$)

Figure 4.8: Simulated paths for daily leaching amount, cumulative leaching amount $L(t)$ and groundwater N concentration $\Theta(t)$

Given the socially optimal application $(N_0 = 62, N_1 = 0)$lb/a from the threshold damage model, Figure 4.8(a) presents the daily leaching amount caused by daily rainfall, Figure 4.8(b) presents the simulated paths for cumulative leaching amount at day t. To compare the simulated nitrate concentration paths given the two socially optimal results, Figure 4.8(c) and (d) are presented for $(N_0 = 62, N_1 = 0)$lb/a and $(N_0 = 64, N_1 = 0)$lb/a, respectively. The mean nitrate concentration level at time T in Figure 4.8(d), 3.0527 mg/L, is

slightly higher than that in Figure 4.8(c), 2.9926 mg/L.

We compare the total net returns and marginal returns from our model (using base case assumptions) to results in Gourevitch et al. (2018) as both studies examined the private and socially optimal N fertilizer application in a midwest state. The Gourevitch et al. (2018) paper studies N application in Minnesota. Distinct from our approach, both private and socially optimal decisions in Gourevitch et al. (2018) are derived from the static net benefit models without incorporating any uncertainty of corn price or weather, as well as the total amount of N applications are not split. We calculate total net returns V_0 with and without social damages from the linear damage model at each level of N application, assuming all N fertilizers are applied at planting rather in season. Marginal return is calculated as the change in net return resulting from an additional N application. Returns to N fertilizer as the rate of application increases are presented in Figure 4.9 where the total net returns to N (lb/a) are shown on top and marginal returns are shown on the bottom. Figure 4.10 shows the same information for the Gourevitch et al. (2018) study (as presented in their Figure 3). Note that the units are not the same in Figures 4.9 and 4.10. The social cost parameter used in the demonstrative example in Gourevitch et al. (2018) is $SCN = \$0.50/kg$, which is close to our base case values $d_L = \$0.66/kg$ and $d_D = \$0.22/kg$. As in Gourevitch et al. (2018), in Figure 4.9, we find that there are diminishing marginal returns to N as the rate of N application increases. Private returns are higher than social returns, which implies a lower socially optimal N application rate. Gourevitch et al. (2018) shows a higher value for a cornfield, with value peaking at around \$1700/ha (around \$688/acre) for the social planner compared to our value of \$448/acre, and around \$1800/ha (around \$728/acre) for the private decision maker compared to our value of \$453/acre. Their optimal N application rates for the private and socially optimal cases are 165 kg/ha and 137 kg/ha (147 lb/a and 122 lb/a), which are significantly higher than our value of 66 lb/a and 64 lb/a.

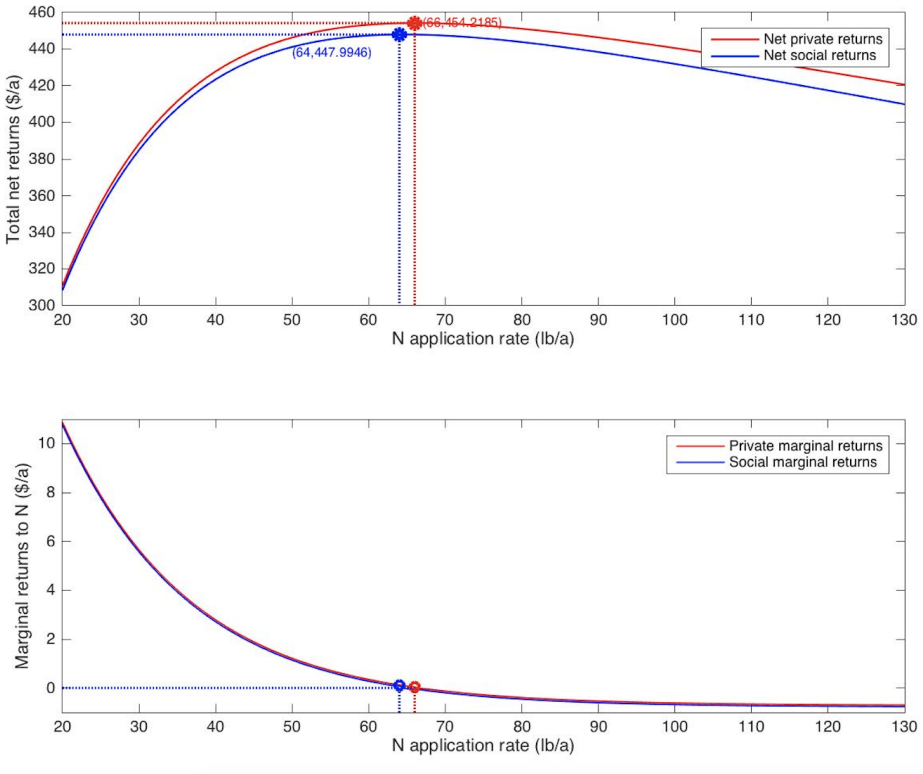

Figure 4.9: Returns to N fertilizer as the application rate increases

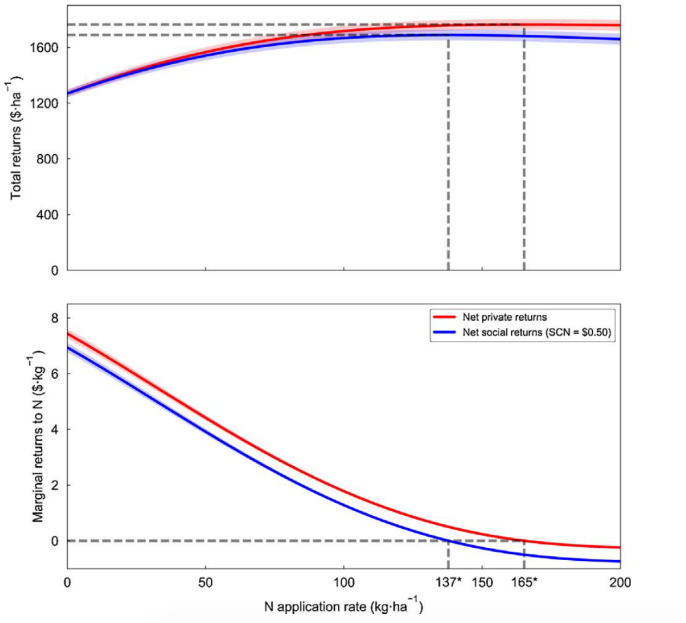

Figure 4.10: Returns to N fertilizer as the rate of application increases, Fig. 3 in Gourevitch et al. (2018)

Our results depend not only on the features of state variables in the model, but on parameter assumptions which we know are highly site-dependent. Optimal decisions for N_0 and N_1 will change for different assumptions about variable cost of fertilizer, social cost of leaching and denitrification, and rainfall intensification. To get a complete picture of how the optimal decision formed in our model, a wide range of sensitivity analysis is performed in the next section to examine the factors that could affect optimal application amount and timing. Key parameters tested in the sensitivity are listed in the following Table 4.2, where the sensitivity level represents the values varied from the baseline case.

Table 4.2: Parameter levels in sensitivity analysis

Parameter	Base case	Sensitivity level
Fertilizer application cost ratio, $\frac{c'_N}{c_N}$	1	as specified in tables or figures
Starter application variable cost, c_N	0.72 \$/lb	[$\frac{0.72}{4}$, $\frac{0.72}{2}$, 0.72, 0.72*2, 0.72*4]
Side-dressing application variable cost, c'_N	0.72 \$/lb	[$\frac{0.72}{4}$, $\frac{0.72}{2}$, 0.72, 0.72*2, 0.72*4]
social cost of N from leaching, d_L	0.66 \$/kg	[0.01, 10, 20, 30, 40, 50]
social cost of N from denitrification, d_D	0.22 \$/kg	[0.01, 10, 20, 30, 40, 50]
$\frac{leaching}{denitrification} = \frac{l_e}{1-l_e}$ in the total N loss	$\frac{43.3\%}{56.7\%}$	$\frac{90\%}{10\%}$ and $\frac{10\%}{90\%}$
Variable cost, c_V	1.7593 \$/bu	0.2645

4.5.4 Sensitivity analysis: Variable costs

Sensitivity on fertilizer application variable costs Fertilizer application variable costs c_N and c'_N are examined in the same way as Section 3.9.4, other parameters used in Table 4.3 are set at the base case. N_0, N_1 are in lb/a. c_N refers to the unit cost of the starter application. c'_N refers to the variable cost of the side-dressing, \$/lb. Sensitivity results are displayed in the following Tables 4.3 and 4.4. Similar to Table 3.6 in Section

3.9.4, fertilizer costs are found to determine both the optimal application amount and optimal timing. Both threshold and linear damage models give us very similar results.

Comparing with the private optimal cases in Table 3.6, we can observe that the optimal fertilizer application for the social planner is less than or equal to that of the private decision maker who ignores social costs from nitrogen. The optimum value V_0 in social planner's model is lower than the private model. However, the variations in V_0 are relatively small. Sensitivity analysis regarding the social costs of N will be performed in the next sections.

Table 4.3: Sensitivity of $(N_0, N_1)^{V_0}$ to variable application costs (linear damage method)

c_N \ c'_N	$\frac{0.72}{4}$	0.72	$0.72 * 4$
$\frac{0.72}{4}$	$(84, 0)^{486.65}$	$(84, 0)^{486.65}$	$(84, 0)^{486.65}$
0.72	$(0, 100)^{481.27}$	$(64, 0)^{447.99}$	$(64, 0)^{447.99}$
$0.72 * 4$	$(0, 100)^{481.59}$	$(0, 82)^{431.68}$	$(42, 0)^{337.17}$

Table 4.4: Sensitivity of $(N_0, N_1)^{V_0}$ to variable application costs (threshold damage method)

c_N \ c'_N	$\frac{0.72}{4}$	0.72	$0.72 * 4$
$\frac{0.72}{4}$	$(84, 0)^{486.68}$	$(84, 0)^{486.68}$	$(84, 0)^{486.68}$
0.72	$(0, 100)^{481.54}$	$(62, 0)^{449.46}$	$(62, 0)^{449.46}$
$0.72 * 4$	$(0, 100)^{481.54}$	$(0, 82)^{432.96}$	$(42, 0)^{339.54}$

Further comparison between private and socially optimal results $(N_0, N_1)_{V_0}$ when $\frac{c'_N}{c_N}$ varies is presented in the following Table 4.5. Within a small range of cost ratio, the socially optimal application timing, as well as the amount in each split application are

highly depend on the damage model choice. In the threshold damage model, we observe that there is a wider range of cost ratios for which the social planner chooses $N_1 > 0$. Increased side dressing reduces the likelihood of leaching. However, there is a cost to delaying to the side planting in terms of corn growth, since average soil fertility is reduced. The social planner must balance these offsetting effects. Furthermore, we observe that for particular cost ratios where the social planner chooses $N_1 > 0$, the total fertilizer used is actually greater than that by the private decision maker, however, when the social planner's optimal choice at particular cost ratios is $N_1 = 0$, the total amount used is less than that by the private decision maker. Notice that for the range of cost ratios shown, all $N_1 > 0$ in the threshold damage model which contrasts with the linear damages model. There is a potential leaching damage saving in the threshold damage model, which gives the social planner more incentive to delay N application and reduce the concentration level.

Table 4.5: A comparison between private and socially optimal results $(N_0, N_1)_{V_0}^{N_0+N_1}$ when $\frac{c'_N}{c_N}$ changes

$\frac{c'_N}{c_N}$	Socially optimal		Private optimal
	Linear damage	Threshold damage	
0.721	$(0,\ 90)_{447.86}^{90}$	$(2,\ 84)_{449.82}^{86}$	$(40,\ 36)_{452.39}^{76}$
0.723	$(14,\ 70)_{447.73}^{84}$	$(12,\ 70)_{449.71}^{82}$	$(66,\ 0)_{452.38}^{66}$
0.725	$(50,\ 20)_{447.67}^{70}$	$(22,\ 56)_{449.62}^{78}$	$(66,\ 0)_{452.38}^{66}$
0.727	$(64,\ 0)_{447.66}^{64}$	$(42,\ 28)_{449.55}^{70}$	$(66,\ 0)_{452.38}^{66}$
0.729	$(64,\ 0)_{447.66}^{64}$	$(46,\ 22)_{449.51}^{68}$	$(66,\ 0)_{452.38}^{66}$
0.731	$(64,\ 0)_{447.66}^{64}$	$(54,\ 10)_{449.49}^{64}$	$(66,\ 0)_{452.38}^{66}$
0.733	$(64,\ 0)_{447.66}^{64}$	$(60,\ 2)_{449.48}^{62}$	$(66,\ 0)_{452.38}^{66}$
0.735	$(64,\ 0)_{447.66}^{64}$	$(60,\ 2)_{449.47}^{62}$	$(66,\ 0)_{452.38}^{66}$
0.737	$(64,\ 0)_{447.66}^{64}$	$(60,\ 2)_{449.47}^{62}$	$(66,\ 0)_{452.38}^{66}$

Sensitivity on the variable cost The variable cost (c_V, excluding fertilizer application cost) is examined in the following Table 4.6. Recall that the total variable cost is defined to exclude the cost of fertilizer. Like Table 3.7 from the private decision maker's model, increasing variable cost decreases the optimal fertilizer use since farming is less profitable. Application amounts in Table 4.6 are generally lower than those in Table 3.7, and as are the optimal values V_0.

Table 4.6: Sensitivity of $(N_0, N_1)^{V_0}$ to different levels of total variable cost

Total variable cost	$\frac{1.7593}{4}$	$\frac{1.7593}{2}$	1.7593	1.7593×2	1.7593×4
linear damage model	$(72, 0)^{765.5}$	$(70, 0)^{659.3}$	$(64, 0)^{447.7}$	$(44, 0)^{32.4}$	$(0, 0)^{0}$
threshold damage model	$(68, 0)^{766.4}$	$(66, 0)^{660.6}$	$(62, 0)^{449.4}$	$(46, 0)^{34.9}$	$(0, 0)^{0}$

4.5.5 Sensitivity analysis: Social costs of nitrogen

The sensitivity of the socially optimal fertilizer application strategy (N_0, N_1) to different social cost parameters of N, computed respectively from linear damage and threshold damage model, is examined in the following tables: Tables 4.7 and 4.8 (Leaching is assumed as the base case 43.3% of total N losses, the total variable cost is the base case \$1.7593/bu), Tables 4.9 and 4.10 (leaching is assumed as 10% of total N losses, the total variable cost is the base case \$1.7593/bu), Tables 4.11 and 4.12 (leaching is assumed as 90% of total N losses, the total variable cost is the base case \$1.7593/bu). d_L indicates the social cost in terms of NO_3^- leaching and d_D indicates the cost in terms of N_2O denitrification. All social cost parameters (the social cost of leaching, d_L and the social cost of denitrification, d_D) displayed in the following tables are in $\$/kg$.

From Tables 4.7 and 4.8, increasing either denitrification or leaching social costs will reduce the total application amount regardless of which damage model we adopt. Since all

social damages caused by N use have to be paid in the linear damage model, the optimal fertilizer application amount in Table 4.7 strictly decreases with the increase of either social cost parameter. In contrast, since the damages from leaching are paid only when the nitrate contamination threshold is triggered in the threshold damage model, application amounts in Table 4.8 are less sensitive to leaching cost d_L but more sensitive to the increase in denitrification cost d_D. Results from the base case parameter assumptions are bold in font in the subsequent tables.

Table 4.7: Sensitivity of (N_0, N_1) to social cost parameters: Linear damage model (all other parameters are set at **base case**)

Linear damage (N_0, N_1)		d_D, in \$/kg						
		0.01	0.22	10	20	30	40	50
d_L, in \$/kg	0.01	(66, 0)	(66, 0)	(52, 0)	(44, 0)	(38, 0)	(34, 0)	(30, 2)
	0.66	(64, 0)	**(64, 0)**	(50, 0)	(44, 0)	(38, 0)	(34, 0)	(30, 2)
	10	(54, 0)	(54, 0)	(46, 0)	(40, 0)	(36, 0)	(32, 0)	(28, 2)
	20	(46, 0)	(46, 0)	(40, 0)	(36, 0)	(32, 0)	(30, 0)	(0, 38)
	30	(42, 0)	(42, 0)	(38, 0)	(34, 0)	(30, 0)	(2, 36)	(0, 36)
	40	(38, 0)	(38, 0)	(34, 0)	(30, 2)	(24, 6)	(0, 36)	(0, 34)
	50	(36, 0)	(36, 0)	(32, 0)	(28, 2)	(0, 38)	(0, 34)	(0, 32)

Table 4.8: Sensitivity of (N_0, N_1) to social cost parameters: Threshold damage model (all other parameters are set at **base case**)

Threshold damage		d_D, in \$/kg						
		0.01	0.22	10	20	30	40	50
d_L, in \$/kg	0.01	(66, 0)	(66, 0)	(52, 0)	(44, 0)	(38, 0)	(34, 0)	(30, 2)
	0.66	(62, 0)	**(62, 0)**	(52, 0)	(44, 0)	(38, 0)	(34, 0)	(30, 2)
	10	(54, 0)	(54, 0)	(50, 0)	(44, 0)	(38, 0)	(34, 0)	(30, 2)
	20	(54, 0)	(54, 0)	(50, 0)	(44, 0)	(38, 0)	(34, 0)	(30, 2)
	30	(52, 0)	(52, 0)	(50, 0)	(44, 0)	(38, 0)	(34, 0)	(30, 2)
	40	(52, 0)	(52, 0)	(50, 0)	(44, 0)	(38, 0)	(34, 0)	(30, 2)
	50	(52, 0)	(52, 0)	(50, 0)	(44, 0)	(38, 0)	(34, 0)	(30, 2)

When looking at the optimal application timing in Table 4.7 and 4.8, we can find that it is optimal to delay some application to the side dressing for very high social cost parameters. Even though application as starter has more impact on increasing the average soil N level, side-dressing is favoured when social costs of N are at a high level (\$20-50 per kg). These effects are more prominent in Table 4.7, in such cases, the demerits from delaying application, the loss of decreased averaged soil N level, can be compensated by the benefit from the shorter period for N losses and reduced social N damages. In Table 4.8, since a low application amount will not trigger the harmful nitrate concentration threshold and only denitrification damages occur, the optimal application timing and amounts are found more sensitive to d_D. Thus, the delaying effect of application is not as prominent as Table 4.7. This result follows from our assumption that the initial nitrogen concentration level is very low. At a high initial concentration level, the linear and threshold models would coincide.

Sensitivities for SCN & leaching proportion To examine if the change of assumed leaching proportion will affect the optimal application amount and timing, we consider two further sensitivities in which we assume leaching constitutes 10% and 90% of the total N loss. Table 4.9 and 4.10 shows that denitrification cost parameter d_D has a more prominent impact on the optimal fertilizer application decision when denitrification constitutes by far the largest proportion of total N loss. In contrast, when leaching constitutes the most in the N loss, Table 4.11 and 4.12 indicate that both optimal application amounts and timing are less sensitive to d_D, but more sensitive to d_L.

Thus, we can conclude that, when the social cost parameters go above certain level, fertilizer application will be shifted from starter to side-dressing with the total fertilizer amounts falling significantly. In the linear damage model, either of social cost parameters (d_L and d_D) increasing can cause the drop of fertilizer application amount as well as affect the application timing. In the threshold damage model, the optimal application amount and timing are more sensitive to the denitrification cost d_D when the denitrification proportion is not very low, and more sensitive to the leaching cost d_L when the leaching proportion is very high. The constitution ratio of total N loss, $\frac{leaching}{denitrification}$, can change the optimal fertilizer decisions through varying the sensitivity of social welfare to two social costs of N (d_L and d_D).

Table 4.9: Sensitivity of (N_0, N_1) to social cost parameters: Linear damage model ($\frac{leaching}{denitrification} = \frac{10\%}{90\%}$, all other parameters are set at **base case**)

Linear damage (N_0, N_1)		d_D, in \$/kg				
		0.01	0.22	10	30	50
d_L, in \$/kg	0.01	(66, 0)	(66, 0)	(46, 0)	(32, 0)	(0, 34)
	0.66	(66, 0)	**(64, 0)**	(46, 0)	(32, 0)	(0, 34)
	10	(62, 0)	(62, 0)	(46, 0)	(32, 0)	(0, 34)
	30	(56, 0)	(56, 0)	(44, 0)	(30, 0)	(0, 32)
	50	(52, 0)	(52, 0)	(42, 0)	(28, 2)	(0, 32)

Table 4.10: Sensitivity of (N_0, N_1) to social cost parameters: Threshold damage model ($\frac{leaching}{denitrification} = \frac{10\%}{90\%}$, all other parameters are set at **base case**)

Threshold damage (N_0, N_1)		d_D, in \$/kg				
		0.01	0.22	10	30	50
d_L, in \$/kg	0.01	(66, 0)	(66, 0)	(46, 0)	(32, 0)	(0, 34)
	0.66	(66, 0)	**(66, 0)**	(46, 0)	(32, 0)	(0, 34)
	10	(66, 0)	(66, 0)	(46, 0)	(32, 0)	(0, 34)
	30	(66, 0)	(66, 0)	(46, 0)	(32, 0)	(0, 34)
	50	(66, 0)	(66, 0)	(46, 0)	(32, 0)	(0, 34)

Table 4.11: Sensitivity of (N_0, N_1) to social cost parameters: Linear damage model ($\frac{leaching}{denitrification} = \frac{90\%}{10\%}$, all other parameters are set at base case)

Linear damage (N_0, N_1)		d_D, in \$/kg				
		0.01	0.22	10	30	50
d_L, in \$/kg	0.01	(66, 0)	(66, 0)	(62, 0)	(56, 0)	(52, 0)
	0.66	(64, 0)	**(64, 0)**	(60, 0)	(56, 0)	(52, 0)
	10	(46, 0)	(46, 0)	(46, 0)	(44, 0)	(42, 0)
	30	(32, 0)	(32, 0)	(32, 0)	(30, 0)	(28, 2)
	50	(0, 34)	(0, 34)	(0, 34)	(0, 32)	(0, 32)

Table 4.12: Sensitivity of (N_0, N_1) to social cost parameters: Threshold damage model ($\frac{leaching}{denitrification} = \frac{90\%}{10\%}$, all other parameters are set at base case)

Threshold damage (N_0, N_1)		d_D, in \$/kg				
		0.01	0.22	10	30	50
d_L, in \$/kg	0.01	(66, 0)	(66, 0)	(62, 0)	(56, 0)	(52, 0)
	0.66	(64, 0)	**(64, 0)**	(60, 0)	(56, 0)	(52, 0)
	10	(26, 4)	(26, 4)	(26, 4)	(26, 4)	(28, 0)
	30	(24, 4)	(24, 4)	(24, 4)	(24, 4)	(26, 0)
	50	(26, 0)	(26, 0)	(26, 0)	(26, 0)	(26, 0)

The sensitivity of leaching proportion assumption and application timing on the N concentration level is illustrated by the following Figure 4.11, where the application is assumed as $(N_0 = 64, N_1 = 0)$ and $(N_0 = 0, N_1 = 64)$, and $\frac{leaching}{denitrification}$ is assumed as $\frac{43.3\%}{56.7\%}$ and $\frac{90\%}{10\%}$. In Figure 4.11, side-dressing application can reduce the N concentration compared to the same amount starter application. Changing either the assumption of leaching proportion or the level of concentration threshold can change the risk of concentration threshold being

crossed and therefore will affect the socially optimal decision.

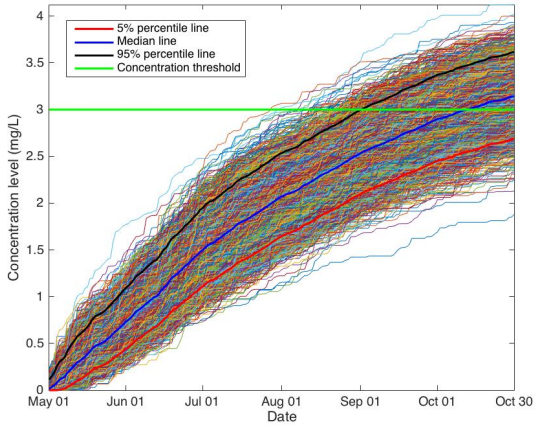

(a) $(N_0 = 64,\ N_1 = 0),\ \frac{leaching}{denitrification} = \frac{43.3\%}{56.7\%}$

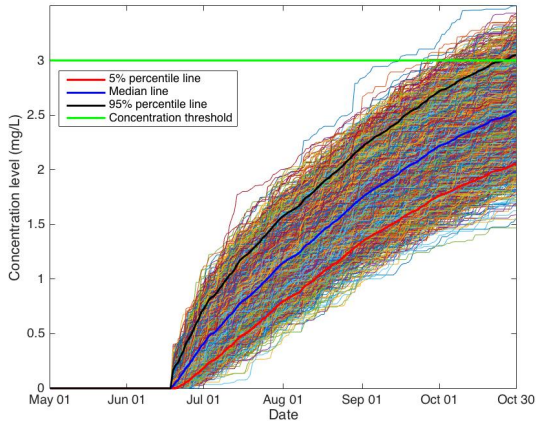

(b) $(N_0 = 0,\ N_1 = 64),\ \frac{leaching}{denitrification} = \frac{43.3\%}{56.7\%}$

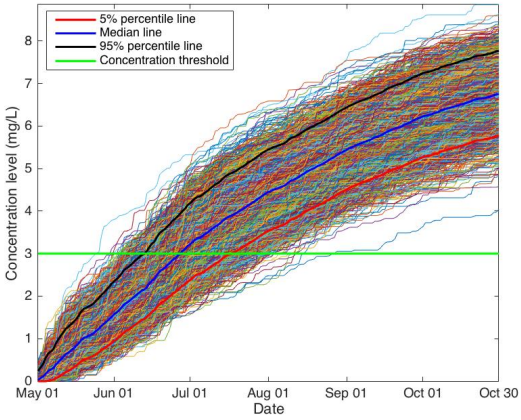

(c) $(N_0 = 64,\ N_1 = 0),\ \frac{leaching}{denitrification} = \frac{90\%}{10\%}$

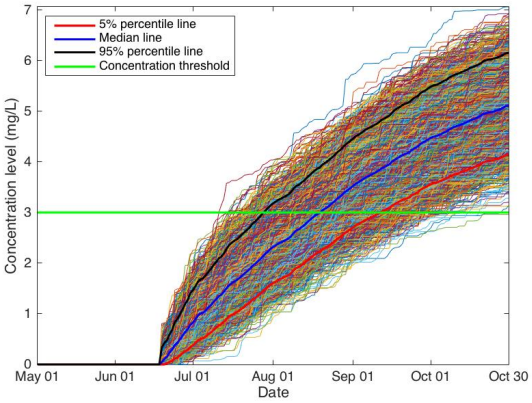

(d) $(N_0 = 0,\ N_1 = 64),\ \frac{leaching}{denitrification} = \frac{90\%}{10\%}$

Figure 4.11: Simulated paths for N concentration $\Theta(t)$ when different fertilizer applications and leaching proportions assumed

Sensitivities for the SCN & the total variable cost To see how social cost of N interacts with the total variable cost, we perform sensitivity analysis in the following Table 4.13, 4.14 and 4.15 with black font representing the results from linear damage method and blue font representing the results from threshold damage method. Leaching proportion is

varied from 10% to 90% in three tables, where the base case is 43.3%. A conclusion can be derived from Table 4.13, 4.14 and 4.15 that a lower total variable cost will not change the way social costs affect optimal fertilizer decisions, but only increase the total application amount.

Table 4.13: Sensitivity of $(N_0, N_1)_{V_0}$ to social cost parameters ($\frac{leaching}{denitrification} = \frac{10\%}{90\%}$, the total variable cost is \$0.2645/bu, all other parameters are set at base case)

d_L \ d_D	Model choice	0.01\$/kg	0.22\$/kg	50\$/kg
0.01 \$/kg	linear damage	(74, 0) 813	(72, 0) 810	(0, 44) 458
	threshold damage	(74, 0) 813	(72, 0) 810	(0, 44) 458
0.66 \$/kg	linear damage	(74, 0) 812	**(72, 0)** 809	(0, 44) 458
	threshold damage	(74, 0) 812	**(72, 0)** 809	(0, 44) 458
50 \$/kg	linear damage	(60, 0) 754	(60, 0) 752	(0, 42) 432
	threshold damage	(74, 0) 811	(72, 0) 808	(0, 44) 458

Table 4.14: Sensitivity of $(N_0, N_1)_{V_0}$ to social cost parameters ($\frac{leaching}{denitrification} = \frac{43.3\%}{56.7\%}$, the total variable cost is \$0.2645/bu, all other parameters are set at base case)

d_L \ d_D	Model choice	0.01\$/kg	0.22\$/kg	50\$/kg
0.01 \$/kg	linear damage	(74, 0) 813	(74, 0) 812	(38, 2) 559
	threshold damage	(74, 0) 813	(74, 0) 812	(38, 2) 559
0.66 \$/kg	linear damage	(72, 0) 809	**(72, 0)** 808	(38, 2) 559
	threshold damage	(70, 0) 810	**(70, 0)** 808	(38, 2) 559
50 \$/kg	linear damage	(42, 0) 608	(42, 0) 606	(0, 42) 432
	threshold damage	(52, 2) 795	(52, 2) 794	(38, 2) 559

Table 4.15: Sensitivity of $(N_0, N_1)_{V_0}$ to social cost parameters ($\frac{leaching}{denitrification} = \frac{90\%}{10\%}$, the total variable cost is \$0.2645/bu, all other parameters are set at base case)

d_L \ d_D	Damage model	0.01\$/kg	0.22\$/kg	50\$/kg
0.01 \$/kg	linear damage	(74, 0) 813	(74, 0) 812	(60, 0) 755
	threshold damage	(74, 0) 813	(74, 0) 812	(60, 0) 755
0.66 \$/kg	linear damage	(72, 0) 806	**(72, 0)** 805	(60, 0) 749
	threshold damage	(72, 0) 806	**(72, 0)** 805	(60, 0) 749
50 \$/kg	linear damage	(0, 44) 459	(0, 44) 458	(0, 42) 432
	threshold damage	(24, 4) 647	(24, 4) 646	(24, 4) 623

Sensitivities for the SCN & fertilizer cost ratio We examine the joint sensitivity of value and optimal decisions to the fertilizer cost ratio and social costs in the following Figure 4.12 and 4.13. More details on these results are displayed in Appendix I. The x-axis in both figures is the SCN, assuming $d_L = d_D$ from \$5/kg to \$50/kg with a step size of 5. The cost ratio of the two application variable costs, $\frac{c'_N}{c_N}$, is assumed as 0.8, 0.9 and 1. The blue line represents the optimal N_0 on the left y-axis, the red line represents the optimal N_1 on the right y-axis.

We can conclude from Figure 4.12 and 4.13 that, the choice of social damage model (linear damage or threshold damage) has a strong effect on the socially optimal application amounts and timing. For both damage models, the rising of social cost of N (SCN) decreases the optimal starter amount N_0 and increases the side-dressing N_1. However, in the threshold damage model it takes a higher SCN, compared to the linear damage model, to trigger the switch to a positive side dressing application. This is because nitrogen is less damaging under the threshold model as long as the N application is such low that con-

centration level of nitrogen is below the threshold. In addition, we find that the relative cost of two split fertilizer applications, $\frac{c'_N}{c_N}$, can determine the level of SCN at which each split application is zero or positive. For example, the cost ratio $\frac{c'_N}{c_N}$ increasing from 0.8 to 1 will make the SCN "threshold" for triggering a positive side-dressing application ($N_1 > 0$) larger. While all the values of the corn harvest (V_0) fall sharply as the SCN is increased, the cost ratio $\frac{c'_N}{c_N}$ has only a very limited effect on the optimal value V_0 variation.

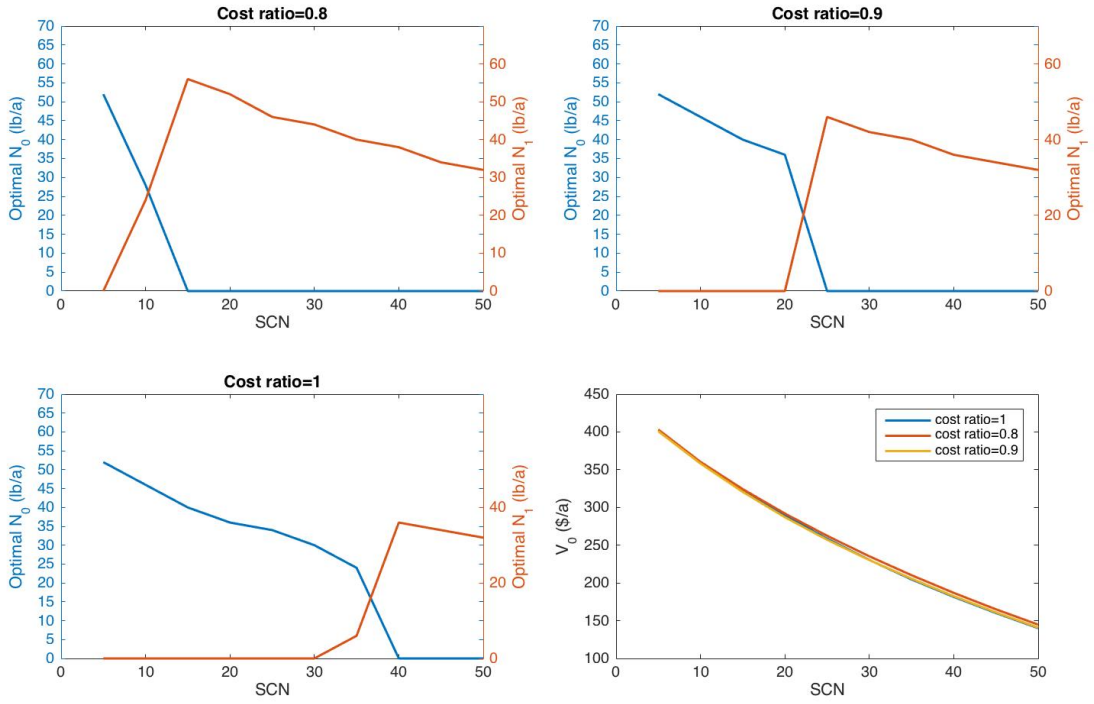

Figure 4.12: Sensitivity on social costs and fertilizer application cost ratio $\frac{c'_N}{c_N}$ (Linear damage model results), the blue line represents the optimal N_0 on the left y-axis, the red line represents the optimal N_1 on the right y-axis

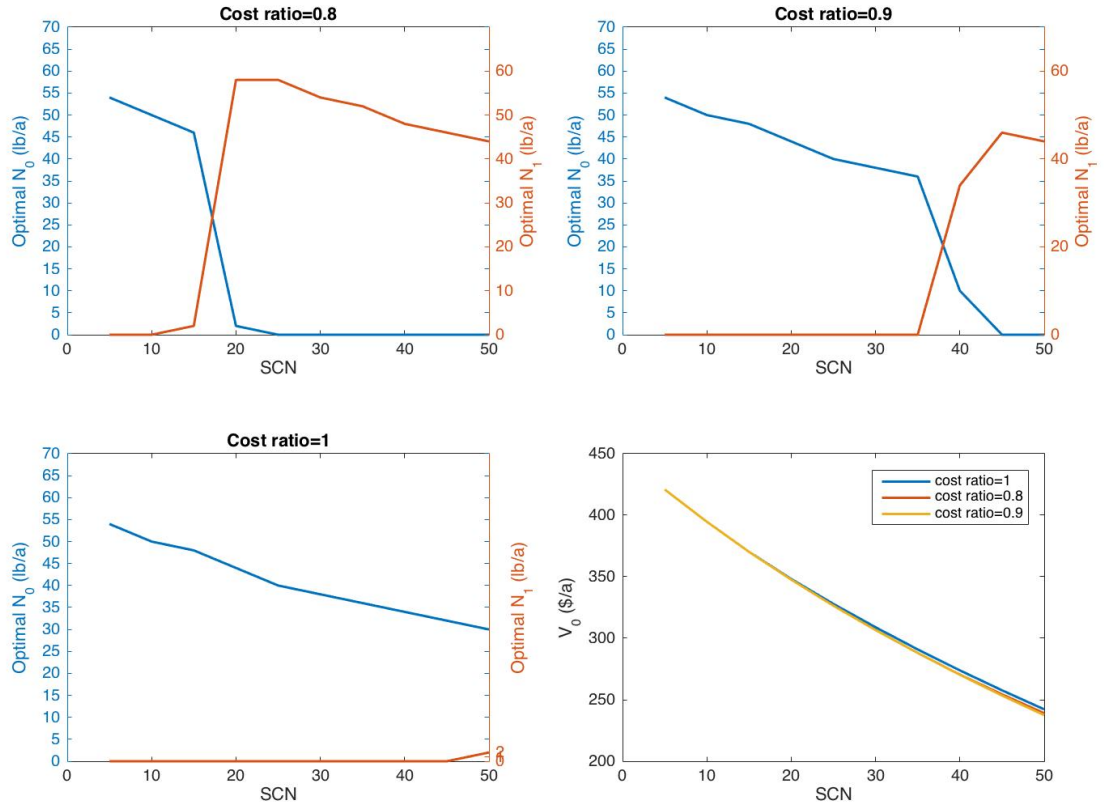

Figure 4.13: Sensitivity on social costs and fertilizer application cost ratio $\frac{c'_N}{c_N}$ (Threshold damage model results), the blue line represents the optimal N_0 on the left y-axis, the red line represents the optimal N_1 on the right y-axis

In summary, the socially optimal N_0 and N_1 amounts are found to be sensitive to the leaching proportion assumption, social cost parameters, the relative cost of two split fertilizer applications, and the model for measuring social damage. In most scenarios where leaching proportion and social costs are in moderate range, results from the linear damage model and results from the threshold damage model are close. However, in some extreme cases of leaching proportion and/or social costs, socially optimal application decisions from two damage models are significantly divergent. The social damage from leaching has to be counted regardless of N concentration is high or low in the linear damage model,

which offsets to some extent the benefit to corn of earlier fertilizer application. However, in the threshold damage model, choosing N to maximize profits from the corn harvest, and minimize denitrification costs is the objective as long as the harmful N concentration threshold is not triggered. Early season fertilizer application N_0 at t_0 always means a longer period for N loss than N_1 applied at t_1. Yet, the relationship between corn yield and fertilizer use is driven by our model assumption that the seasonal averaged soil nutrient content S is what matters. Thus, the optimal N_0 applications from the threshold damage model are generally higher than those from the linear damage model in all of Table 4.7, 4.8, 4.9, 4.10, 4.11, 4.12, 4.13, 4.14 and 4.15.

4.5.6 Sensitivity analysis: Precipitation

In our model, social damages from nitrogen application are highly dependent on the quantity and frequency of rainfall. Given changing expected rainfall patterns associated with climate change, it is instructive to consider how optimal nitrogen fertilizer decisions are affected by the frequency of rainfall as well as the expected quantity and variance. Optimal application amounts under different rainfall scenarios are presented in the following Table 4.16. The parameters describing the probability of rainfall, $P_{ij}, i, j = \{0, 1\}$, as well as the γ parameter in the exponential distribution for the quantity of rainfall, are varied in the same way as in Section 3.9.6. All other parameters are set as the base case level.

Similar to the conclusions drawn in Section 3.9.6 regarding Table 3.9, Table 4.16 shows that whether an increasing likelihood of rainfall (rainfall frequency) will increase or decrease the optimal application amount depends on the expected daily rainfall quantity. Similarly, the effect of expected rainfall amount on the optimal application depends on the level of rainfall frequency. In both damage models, more frequent rainfall reduces the optimal application amount only when the expected daily precipitation amount is high (moving

down the third column of numbers). As well, an increase in the expected daily rainfall amount will reduce the optimal application amount only when the rain likelihood is high (along the fifth and sixth rows). When comparing results from both damage models, socially optimal application amounts from the threshold damage model are less than or equal to those from the linear damage model, especially in those cases where intensified rainfall happens (*More* and/or *Wetter* scenario). This is because the risk for concentration exceeding the threshold is higher with more leaching as a result of increased rainfall.

Table 4.16: Sensitivity of (N_0, N_1) to rainfall scenarios (Base case)

Rain likelihood \ Rain amount		Less	Base Case	More
Smaller (*Dryer*)	linear damage	(52, 0)	(62, 0)	(66, 0)
	threshold damage	(52, 0)	(62, 0)	(64, 0)
Base Case	linear damage	(56, 0)	(64, 0)	(62, 0)
	threshold damage	(56, 0)	(62, 0)	(62, 0)
Larger (*Wetter*)	linear damage	(58, 0)	(66, 0)	(46, 0)
	threshold damage	(58, 0)	(62, 0)	(40, 0)

Comparing both first columns in Table 4.16 and Table 3.9, the social planner's optimal results are identical to results from the private decision maker's model. This may be attributed to the insufficiently large base case social cost parameters and daily rainfall amounts, which underpin a social N damage that is insufficiently significant to change the optimal decision.

Sensitivities for precipitation & SCN To see the joint impact of precipitation and increased social cost on the socially optimal application, we increase the parameter from

the base case $d_L = 0.66\$/kg$, $d_D = 0.22\$/kg$ to the higher level $d_L = d_D = 30\$/kg$. Results are displayed in the following Table 4.17. We can see in Table 4.17 that N applications are generally higher under the threshold damage function compared to the linear damage function, which is as expected since those N applications under the threshold damage function cause no leaching damage. With the increase in the expected quantity of rainfall, the groundwater nitrate concentration due to leaching is more likely to touch the threshold, and thus the application amount is reduced and some fertilizer is applied as side-dressing. With higher social costs, the rainfall-induced social damage becomes more prominent and thus can change the socially optimal application decision. For example, under the *More* expected daily rain amount scenario, delayed application (side-dressing $N_1 > 0$) is favoured by the social planner as a result of the higher social damages of N caused by higher N losses.

Table 4.17: Sensitivity of (N_0, N_1) to rainfall scenarios (when $d_L = d_D = 30$ \$/kg)

Rain likelihood \ Rain amount		Less	Base Case	More
Smaller (*Dryer*)	linear damage	(32, 0)	(32, 0)	(0, 36)
	threshold damage	(38, 0)	(40, 0)	(34, 2)
Base Case	linear damage	(32, 0)	(30, 0)	(0, 30)
	threshold damage	(38, 0)	(38, 0)	(28, 2)
Larger (*Wetter*)	linear damage	(32, 0)	(26, 4)	(0, 26)
	threshold damage	(38, 0)	(36, 2)	(24, 4)

Sensitivities for precipitation , SCN & the total variable cost To see how total variable cost (excluding the fertilizer use) will affect the socially optimal applications, we examine the sensitivity of (N_0, N_1) by repeating the above analysis in Table 4.16 and 4.17 assuming the total variable cost c_V is decreased from 1.7593 to 0.2645 \$/bu. Results are

displayed in the following Table 4.18. Two social cost scenarios are presented: the base case $d_L = 0.66, d_D = 0.22$ and $d_L = d_D = 30$ $\$/kg$. From the table, several conclusions can be made: First, a lower variable cost on corn yield will increase the socially optimal application amount. Intuitively, a lower variable costs increases the benefits from the corn harvest. The marginal profit obtained from a unit of fertilizer application is thereby increased, thereby increasing the optimal quantity.

Second, the increase in social cost parameters will significantly reduce the optimal fertilizer application amounts in all precipitation scenarios, regardless of which of the social damage models is chosen.

Table 4.18: Sensitivity of (N_0, N_1) rainfall, when the total variable cost is $c_V = \$0.2645/bu$

			$d_L = 0.66, d_D = 0.22$			$d_L = d_D = 30$		
			Rain amount					
			Less	Base	More	Less	Base	More
Rain likelihood	Smaller	linear damage	(58, 0)	(70, 0)	(74, 0)	(38, 0)	(38, 2)	(0, 48)
		threshold damage	(60, 0)	(68, 0)	(74, 0)	(44, 0)	(46, 0)	(38, 4)
	Base	linear damage	(62, 0)	(72, 0)	(70, 0)	(38, 0)	(36, 2)	(0, 36)
		threshold damage	(62, 0)	(70, 0)	(70, 0)	(46, 0)	(44, 0)	(36, 0)
	Larger	linear damage	(64, 0)	(74, 0)	(56, 0)	(38, 0)	(34, 4)	(0, 20)
		threshold damage	(64, 0)	(74, 0)	(56, 0)	(46, 0)	(44, 0)	(30, 0)

Third, the effect of a change in the frequency and expected value (and variance) of rainfall is much more apparent when the social cost of damages is high. Higher social costs can make the damage large enough that optimal application decisions can be altered significantly, not only in amounts but in timing. For example, (N_0, N_1) in the left half of Table 4.18 are not significantly varied with all $N_1 = 0$. However, with higher social

nitrogen loss costs (right half of Table 4.18), intensified rainfall with higher likelihood and daily amounts will both lower application amounts and change the optimal application timing (delay the application for a shorter period of loss, marked in red color).

Sensitivities for precipitation & the fertilizer application cost ratio Since the cost ratio of variable costs for two split applications, $\frac{c'_N}{c_N}$, is found to be decisive for optimal timing in private decision maker's model in Section 3.9.4, we examine both $\frac{c'_N}{c_N}$ and rainfall as part of our joint sensitivity analysis. The main findings are depicted in the following Figure 4.14 and 4.15, details regarding results are listed in Appendix J. The cost ratio $\frac{c'_N}{c_N}$ in Figure 4.14 and 4.15 is varied from 0.5 to 1, with a step size of 0.1.

Among our tested values of $\frac{c'_N}{c_N}$, the effect of cost ratio on socially optimal application timing is found to be immune to the social damage model choice (linear damage or threshold damage). For example, in the $(Dryer, Base)$ rainfall case, both damage models give $N_0 = 0$ when $\frac{c'_N}{c_N} = 0.7$ and $N_1 = 0$ when $\frac{c'_N}{c_N} = 0.8$. However, this finding does not contradict the findings from Table 4.5, which used a much smaller cost ratio range (from 0.721 to 0.737). For both damage functions in Figure 4.14 and 4.15, we see the range of cost ratios at which $N_0 > 0$ and $N_1 = 0$ varies with changes in the expected quantity of rainfall. As the expected rainfall quantity increases, the cost ratio $\frac{c'_N}{c_N}$ at which N_1 falls to zero rises, implying a wider range of cost ratios at for which side-dressing $N_1 > 0$.

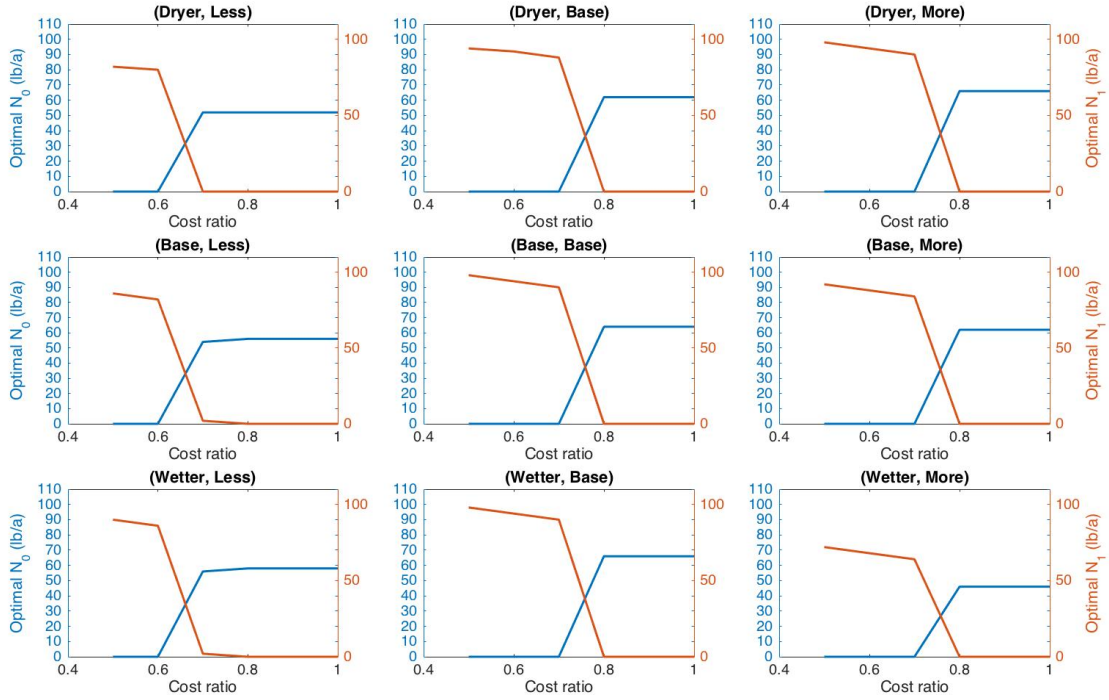

Figure 4.14: Sensitivities for precipitation and the cost ratio $\frac{c'_N}{c_N}$ (Linear damage results)

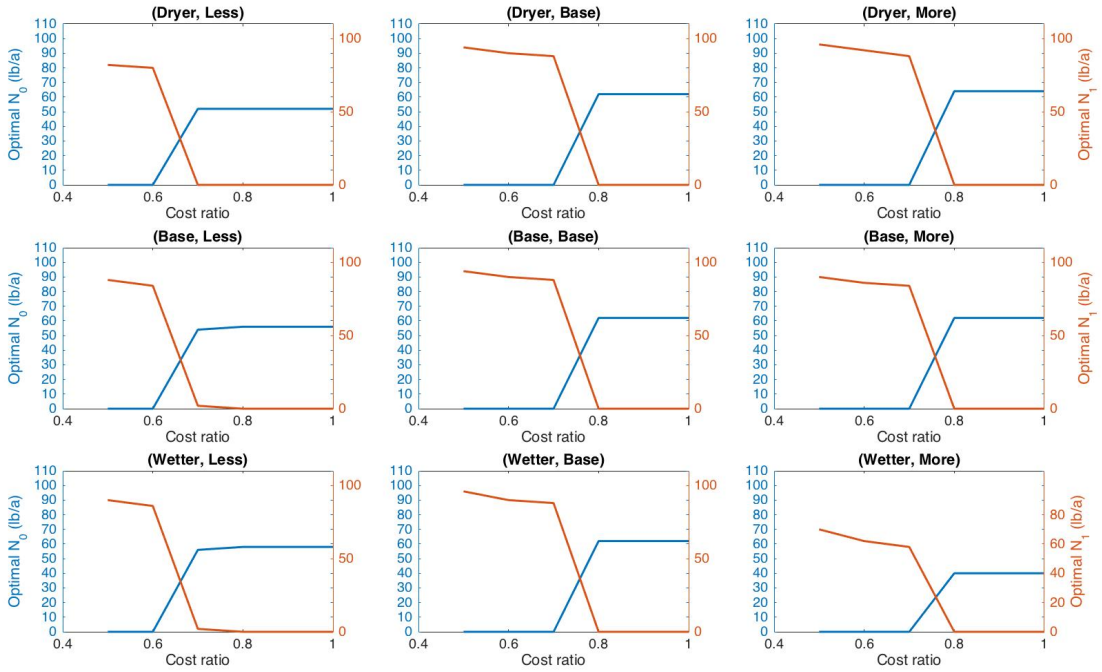

Figure 4.15: Sensitivities for precipitation and the cost ratio $\frac{c'_N}{c_N}$ (Threshold damage results)

In conclusion, our assumptions about the frequency and quantity of rainfall have a strong effect on the optimal quantity of fertilizer application, and also interact with other parameters such as the fertilizer variable costs, social costs of N and the total variable cost. There is a trade-off between early and delayed fertilizer application. Starter N_0 has the advantage of being on the field longer and contributes more to average soil nutrient content, but it is also more likely to get washed away and cause a higher social damage. Side-dressing N_1 has a shorter N loss period and thus can lower the social damage of N, however, average soil nutrient content is lower unless using more N_1. Conclusions about the optimal application decision will depend critically on empirical estimates of the farmer's costs and damages from nitrogen applications, as well as on modelling assumptions about corn growth, leaching, denitrification, rainfall, etc.

We are left with the puzzle as to why the optimal fertilizer quantities calculated in this

thesis are all lower than the historical average application amounts in Iowa. For example, the highest amount of optimal fertilizer application in Appendix H is 102 lb/a, still lower than the 1990-2018 historical averaged N application in Iowa (a minimum of 114 lb/a, a mean of 128 lb/a and a maximum of 150 lb/a). Further discussion of this puzzle is left to Chapter 5.

4.5.7 Sensitivity analysis: Corn price volatility and speed of mean reversion

The sensitivity of the socially optimal fertilizer application to corn price parameters is examined by varying volatility σ_P and mean reversion speed θ as shown in the following Table 4.19. Three levels of price volatility and mean reversion are set to represent different levels of price uncertainty. The original σ_P and θ are estimated in Table 3.2.

Table 4.19: $(N_0, N_1)_{V_0}$ for different price sensitivity regimes (θ,σ_P) (All other parameters are at base level)

Parameter	Model choice	$\frac{\sigma_P}{2}$	σ_P	$2\sigma_P$
$\frac{\theta}{2}$	linear damage	(64, 0) $_{440}$	(62, 0) $_{429}$	(60, 0) $_{400}$
	threshold damage	(62, 0) $_{441}$	(60, 0) $_{427}$	(60, 0) $_{414}$
θ	linear damage	(66, 0) $_{471}$	(64, 0) $_{447}$	(62, 0) $_{436}$
	threshold damage	(64, 0) $_{473}$	(62, 0) $_{449}$	(60, 0) $_{433}$
2θ	linear damage	(68, 0) $_{503}$	(66, 0) $_{495}$	(62, 0) $_{475}$
	threshold damage	(66, 0) $_{506}$	(64, 0) $_{494}$	(62, 0) $_{480}$

In Table 4.19, both linear damage and threshold damage models give us similar findings. First, at a given mean reversion speed level in Table 4.19, both starter application N_0 (which is also the total application) and the maximized value, V_0 (on the right-bottom of each pair)

are found to decline with the rising of price volatility level from $\frac{\sigma_P}{2}$ to $2\sigma_P$. Increased corn price volatility has a negative impact on the fertilizer application. Second, it is observed that under a given price volatility level, the optimal fertilizer application increases with an increase of the mean reversion speed from $\frac{\theta}{2}$ to 2θ. For both linear damage and threshold damage models, as long as $\bar{P}$ exceeds the average variable cost of fertilizer application, as is the case under our assumptions, a higher speed of mean reversion increases the value of the crop and makes it worthwhile for the farmer to use more fertilizers.

To see how an increase in p_0 affects the socially optimal decision in our base case, we raise the starting value in Table 3.5 from \$4.145/bushel to \$6.145/bushel. The social planner's optimal application increases from (64, 0) lb/a to (74, 0), and the value V_0 per acre increases from \$447.9946 to \$930.2216. A higher corn price starting value is examined to increase the socially optimal application amount.

Similar to the results in Section 3.9.5, price volatility and mean reversion speed will have impacts on the socially optimal fertilizer application as well as the optimal value. Both an increase in volatility and a decrease in mean reversion speed will lower the optimal quantity of N applied. However, when other parameters set at base case levels, the optimal split decisions between starter and side dressing are found not sensitive to these two price parameters.

Sensitivities for SCN & corn price parameters To see how SCN interacts with corn price in affecting the socially optimal application, we increase the social cost of N from the base case, d_L = \$0.66/kg and d_L = \$0.66/kg, to $d_L = d_D$ = \$30/kg. Results from both damage models are presented in the Table 4.20.

Table 4.20: (N_0, N_1) for different price sensitivity regimes (θ,σ_P) ($d_L = d_D =$ \$30/kg, all other parameters are at the base level)

Parameter	Model choice	$\frac{\sigma_P}{2}$	σ_P	$2\sigma_P$
$\frac{\theta}{2}$	linear damage	(30, 0)	(28, 0)	(26, 0)
	threshold damage	(38, 0)	(36, 0)	(32, 0)
θ	linear damage	(34, 0)	(30, 0)	(28, 0)
	threshold damage	(40, 0)	(38, 0)	(36, 0)
2θ	linear damage	(36, 0)	(32, 0)	(32, 0)
	threshold damage	(42, 0)	(40, 0)	(40, 0)

From Table 4.20, both an increase in volatility and a decrease in mean reversion speed will lower the optimal quantity of N applied, same as the conclusion we found from Table 4.19. The optimal split decisions between starter and side dressing are also found not sensitive to price parameters. The socially optimal application amount from threshold damage model are larger than those from linear damage model, and the amount differences between two damage results are larger than those in Table 4.19. We can conclude that the rising of social cost separately will not change the way corn price uncertainty affects the socially optimal fertilizer application, but lower the application amount and amplify the amount gap between results from linear and threshold damage models.

Sensitivities for precipitation & corn price parameters To see if the corn price uncertainty effect will be changed by the increased frequency of rainfall as well as the increased expected quantity and variance, we vary the rainfall scenario from the base case to $(Wetter, Base)$, $(Base, More)$ and $(Wetter, More)$, where changed rainfall parameters are described in Section 3.9.6. Results from both damage models are presented in the Table 4.21, 4.22 and 4.23.

Table 4.21: (N_0, N_1) for different price sensitivity regimes (θ,σ_P) ($(Wetter, Base)$ rainfall scenario, other parameters are at the base level)

Parameter	Model choice	$\frac{\sigma_P}{2}$	σ_P	$2\sigma_P$
$\frac{\theta}{2}$	linear damage	(66, 0)	(64, 0)	(62, 0)
	threshold damage	(62, 0)	(60, 0)	(60, 0)
θ	linear damage	(68, 0)	(66, 0)	(64, 0)
	threshold damage	(64, 0)	(62, 0)	(60, 0)
2θ	linear damage	(70, 0)	(68, 0)	(64, 0)
	threshold damage	(64, 0)	(64, 0)	(62, 0)

Table 4.22: (N_0, N_1) for different price sensitivity regimes (θ,σ_P) ($(Base, More)$ rainfall scenario, other parameters are at the base level)

Parameter	Model choice	$\frac{\sigma_P}{2}$	σ_P	$2\sigma_P$
$\frac{\theta}{2}$	linear damage	(62, 0)	(60, 0)	(58, 0)
	threshold damage	(62, 0)	(62, 0)	(60, 0)
θ	linear damage	(64, 0)	(62, 0)	(60, 0)
	threshold damage	(66, 0)	(62, 0)	(62, 0)
2θ	linear damage	(66, 0)	(64, 0)	(60, 0)
	threshold damage	(66, 0)	(64, 0)	(64, 0)

Table 4.23: (N_0, N_1) for different price sensitivity regimes (θ,σ_P) ($(Wetter, More)$ rainfall scenario, other parameters are at the base level)

Parameter	Model choice	$\frac{\sigma_P}{2}$	σ_P	$2\sigma_P$
$\frac{\theta}{2}$	linear damage	(46, 0)	(44, 0)	(42, 0)
	threshold damage	(40, 0)	(40, 0)	(36, 0)
θ	linear damage	(48, 0)	(46, 0)	(42, 0)
	threshold damage	(44, 0)	(40, 0)	(38, 0)
2θ	linear damage	(50, 0)	(48, 0)	(46, 0)
	threshold damage	(44, 0)	(42, 0)	(40, 0)

From Table 4.21, 4.22 and 4.23, either an increase in volatility or a decrease in mean reversion speed will lower the optimal quantity of N application, as prior discussion. The optimal split decisions between starter and side dressing are also found not sensitive to price parameters. We can conclude that, like the SCN, the rising of rainfall amount and/or frequency will not change the way corn price uncertainty affects the socially optimal fertilizer application.

In addition, we find that results from both damage models are close in Table 4.22, with the amount differences are 0, 2, or 4 lb/a. The amount gap between results from both damage models in Table 4.21 and 4.23 are larger, with the largest gap is 6 lb/a. In Table 4.21 and 4.23, the socially optimal application amount from threshold damage model are smaller than those from linear damage model, and the amount differences between two damage results are larger than those in base case, Table 4.19.

Sensitivities for SCN, precipitation & corn price parameters Since the effect of corn price uncertainty on the socially optimal fertilizer applications are not altered in the presence of the increased frequency and the expected quantity of rainfall, or the increased

SCN, we need to see if both increased precipitation and SCN can jointly affect the optimal decisions, especially the optimal split decisions between starter and side dressing. To do so, we increase the social cost of N from the base case, d_L = \$0.66/kg and d_D = \$0.22/kg, to $d_L = d_D$ = \$30/kg, as well as vary the rainfall scenario from the base case to $(Wetter, Base)$, $(Base, More)$ and $(Wetter, More)$. Results from both damage models are presented in the Table 4.24, 4.25 and 4.26.

Table 4.24: (N_0, N_1) for different price sensitivity regimes (θ,σ_P) ($(Wetter, Base)$ rainfall scenario, $d_L = d_D$ = \$30/kg)

Parameter	Model choice	$\frac{\sigma_P}{2}$	σ_P	$2\sigma_P$
$\frac{\theta}{2}$	linear damage	(28, 2)	(26, 2)	(24, 2)
	threshold damage	(36, 2)	(36, 0)	(34, 0)
θ	linear damage	(30, 2)	(26, 4)	(24, 4)
	threshold damage	(38, 2)	(36, 2)	(34, 2)
2θ	linear damage	(30, 4)	(28, 4)	(28, 4)
	threshold damage	(38, 4)	(38, 2)	(38, 2)

Table 4.25: (N_0, N_1) for different price sensitivity regimes (θ,σ_P) ($(Base, More)$ rainfall scenario, $d_L = d_D$ = \$30/kg)

Parameter	Model choice	$\frac{\sigma_P}{2}$	σ_P	$2\sigma_P$
$\frac{\theta}{2}$	linear damage	(0, 30)	(0, 28)	(0, 28)
	threshold damage	(30, 2)	(28, 2)	(28, 0)
θ	linear damage	(0, 32)	(0, 30)	(0, 28)
	threshold damage	(30, 2)	(28, 2)	(28, 2)
2θ	linear damage	(0, 34)	(0, 32)	(0, 30)
	threshold damage	(34, 2)	(32, 2)	(30, 2)

Table 4.26: (N_0, N_1) for different price sensitivity regimes (θ,σ_P) ($(Wetter, More)$ rainfall scenario, $d_L = d_D = \$30/\text{kg}$)

Parameter	Model choice	$\frac{\sigma_P}{2}$	σ_P	$2\sigma_P$
$\frac{\theta}{2}$	linear damage	(0, 28)	(0, 26)	(0, 24)
	threshold damage	(26, 4)	(24, 2)	(24, 2)
θ	linear damage	(0, 28)	(0, 26)	(0, 24)
	threshold damage	(26, 4)	(24, 4)	(24, 4)
2θ	linear damage	(0, 30)	(0, 28)	(0, 26)
	threshold damage	(30, 4)	(28, 4)	(26, 4)

It is observed that, from Table 4.24, 4.25 and 4.26, an increase in price volatility or a decrease in mean reversion speed reduces the socially optimal total fertilizer application. We can conclude that the socially optimal application quantity and timing from each level of price parameters are sensitive to the level of precipitation and social cost of N. For example, increasing from σ_P to $2\sigma_P$ will reduce N_1 from 2 to 0 in the threshold model in Table 4.25, whereas will not change their counterparts in Table 4.26. In addition, the impact of price uncertainty on socially optimal split application decisions, starter N_0 and side-dressing N_1, are found sensitive to the social damage model choice. For example, for N_0 and $N_0 + N_1$ in Table 4.24, 4.25, 4.26 and N_1 in Table 4.25 and 4.26, the rising of price volatility will decrease or not change them for both damage models in all cases. However, in Table 4.24, with the rising of volatility, N_1 increases or is unchanged for the linear damage model while N_1 decreases or unchanged for the threshold damage model. Like previously found, in Table 4.24, 4.25 and 4.26, the decreasing mean reversion speed will lower or not change both split applications and the total application amount for both damage models.

Therefore, we can make the conclusions that, the total application amount, as well as both split application amounts increase or remain the same with the increase of mean reversion speed regardless of how we vary SCN, rainfall or the choice of social damage model. The optimal split decisions are determined jointly by a series of multiple factors including SCN, rainfall and price parameters. Rising price volatility will decrease or not change the starter application N_0, the total application N_0+N_1, and almost all side-dressing N_1 regardless of what SCN, rainfall and damage model assumptions are.

4.5.8 Sensitivity analysis: Starting soil N-level

As what we did in Section 3.9.7, we examine the effect of corn yield model (Equation (3.37)) on the socially optimal decision. The following Figure 4.16 plots the socially optimal fertilizer applications and the social welfare surface from both damage models, using the new estimated corn yield function in Equation (3.37).

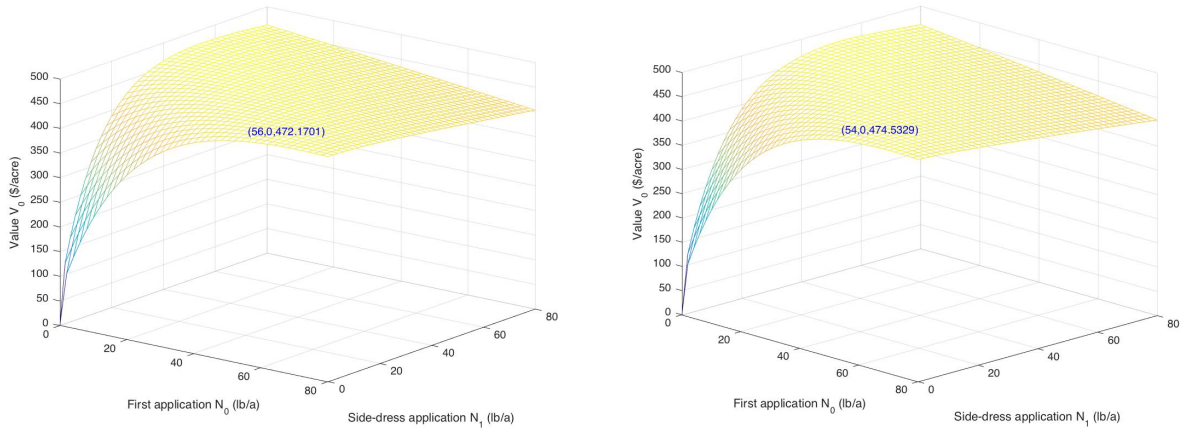

(a) Using the linear damage model

(b) Using the threshold damage model

Figure 4.16: The socially optimal fertilizer applications and the social welfare surface, the ordered triplet shows (N_0, N_1, and Value at time 0)

As the finding in Section 3.9.7, assuming a 5 lb/a soil N residue at the beginning of

the season decreases the socially optimal application amount from ($N_0 = 64$, $N_1 = 0$) and ($N_0 = 62$, $N_1 = 0$) lb/a in Figure 4.2 to ($N_0 = 56$, $N_1 = 0$) and ($N_0 = 54$, $N_1 = 0$) lb/a in Figure 4.16, with the optimal application timing left unchanged. The socially optimal application amount from using the linear damage model is 2 lb/a higher than that from using the threshold damage model, which is identical to what is found in Figure 4.2. The social welfare, V_0, increase from \$447.9946 and \$449.4196 per acre in Figure 4.2 to \$472.1701 and \$474.5329 per acre in Figure 4.16, suggesting pre-plant soil tests are beneficial from the social planner's perspective.

A higher potential of agricultural N loss and over-application may present when farmers didn't use soil test prior to starter application. They may base their fertilizer applications on their yield-maximizing rule or improper expectations on weather and yield targets. Our results show that the adoption of pre-plant soil test in assessing soil N availability prior to starter application will reduce both the farmer's and social planner's optimal total fertilizer application amounts, which will not only lower the risk of fertilizer over-application, save their costs without a scarification of net benefit, but also increase the social welfare.

Chapter 5

Discussion and Conclusions

Intensive fertilizer application is causing extensive nutrient pollution. Nutrient losses from agricultural uses of fertilizer, especially in forms of leaching and denitrification, has become the most pressing non-point source pollution problem in Iowa. Most of the nutrients that are applied to agricultural lands serve their intended purpose of increasing crop yields, but also cause groundwater quality deterioration and contribute to climate change, which are detrimental to human health and the environment. As outlined in the Introduction, nutrient pollution is a problem worldwide. This thesis focuses its analysis on Iowa, largely because of data availability. The modelling approach and conclusions derived are more generally applicable.

Despite the Iowa Nutrient Reduction Strategy and other best management practices, Iowa has relied mostly on farmers' voluntary efforts in avoiding excess fertilizer application. Many farmers in Iowa are not adhering to the recommendations based on maximum economic return to N, and excess fertilizer application is frequently observed. As a consequence, more than two hundred of Iowa's community water systems struggle with high nitrate levels, periodically issuing "Do Not Drink" orders. The application of nitrogen

fertilizer on Iowa farms has increased about 15 percent on average across counties over the past 40 years. Iowa has become the second-largest contributor of nitrates to the Mississippi River Basin.[1] According to a study by the Union of Concerned Scientists (UCS)[2], Iowans will be on the hook for up to 333 million dollars over the next five years to remove nitrates polluting the state's drinking water supplies and threatening public health. Algal blooms also makes surface water unfit for recreational use.

The purpose of this thesis is to analyze the impact of corn price uncertainty and weather factors (precipitation and heat) on the farmer's and social planner's optimal fertilizer applications, and the divergence between them, by constructing a model of the stochastic optimal control problem for each decision maker. This thesis first investigates the farmer's optimal fertilizer application under crop price uncertainty in Chapter 2 by constructing an inter-temporal farmer's decision model under two alternative stochastic price processes for corn: geometric Brownian motion and mean reversion. Corn yield is assumed to be a simple quadratic function of applied fertilizer. Employing a real options approach, a Hamilton-Jacobi-Bellman equation is developed describing the value of the corn field. We derive closed form results for the farmer's optimal fertilizer application decision. Numerous factors that could impact the optimal fertilization decision are examined as well.

The farmer's decision model is then enhanced in Chapter 3 by allowing for two possible fertilizer application times in the growing season and the inclusion of additional stochastic state variables or path-dependent variables such as average soil nutrient stock, rainfall and temperature, in the corn yield model. Significant care is taken in developing reasonable models for all these state variables. Key modelling assumptions are summarized below.

- Corn prices and daily temperatures are modelled as mean reverting stochastic pro-

[1]Source: https://www.nationalgeographic.com/science/article/iowa-agriculture-runoff-water-pollution-environment

[2]Source: https://www.ucsusa.org/about/news/rural-iowans-bear-brunt-water-treatment-costs-nitrate-pollution-farms-and-cafos

cesses.

- The probability of rainfall follows a continuous time Markov chain, while the rainfall quantity follows an exponential distribution.
- Corn yield depends on cumulative rainfall, cumulative corn heat units, and average soil nutrient level.

A Hamiltonian-Jacobi-Bellman equation describing the value of the corn field is derived for this much more complex decision model. With nine state variables, a closed form solution is not available. Numerical solution using a standard semi-Lagrangian approach is also not practical. Instead, the choice set of optimal controls is restricted, and a Monte Carlo approach is employed to explore model solutions. The model is parameterized for average conditions in Iowa corn growing regions. Numerical results conclude that for a wide range of parameter assumptions the farmer's optimal strategy is to apply fertilizer at planting rather than later as a side dressing.

In Chapter 4, the thesis analyzes the optimal decisions of a social planner whose objective function includes an estimate of the damages caused by nitrogen leakage and denitrification. Socially optimal fertilizer applications are compared with the privately optimal results in Chapter 2 and 3. In addition, as parameters are highly site-dependent, sensitivity analysis is performed to analyze the impacts of price uncertainty, precipitation, fertilizer cost and other economic parameters on the farmer's and socially optimal fertilizer applications. The findings concluded in Chapter 3 and 4 not only broaden our understanding of the degree of market failure from agricultural fertilizer use which is dictated by the extent to which the farmer's optimal choice differs from the social planner's decision, but also reveal the most significant factors that drive the divergence between the two. A comprehensive literature survey is also performed in our thesis, which investigates and summarizes

the soil nitrogen cycle, the social cost of N, the modeling of rainfall and temperature, the impact of weather and nitrogen use on corn yield.

The findings of the analysis in this thesis provide answers to the main questions raised at the beginning of our thesis and also point to further questions requiring more research. In summarizing the results we focus on the difference between the farmer's and social planner's optimal decisions as well as on factors that change the optimal total N application and the split between the two application times. Under our base case assumptions, the farmer's optimal fertilizer application (66 lb/a) is slightly higher than the socially optimal ones (64 and 62 lb/a for the linear and the threshold damage functions, respectively), whereas both farmer and social planner are found to prefer to apply all fertilizer at planting rather than in season. This is, in part, because of our specific corn yield model assumption that starter has the advantage of being on the field longer and contributes more to the averaged soil N level compared to side-dressing. The fertilizer applied at planting has more opportunity to contribute to N-pollution than does mid-season application, but the relatively low social cost of N assumed in the base case ensures this outcome. In average weather conditions, we find the socially optimal strategy deviating from the private optimal strategy, indicating a market failure from agricultural fertilizer use, similar to the finding in Kabir et al. (2021). These results depend on a host of factors including the average soil nutrient level which is subject to losses by uncertain rainfall, the relative cost of two split fertilizer applications, the expected outlook for corn price and rainfall, the total variable cost on yield and corn yield model choice. Apart from these factors, the socially optimal fertilizer application is further impacted by social cost parameters from leaching and denitrification, and social damage model choice.

Both the farmer's corn value surface and social welfare surface are concave in the N-application as we use the concave exponential corn yield function in Chapters 3 and 4. After a certain point further fertilizer application will have no significant additional

positive impact on corn yield, but will decrease the net revenues as a result of increased costs. As an important finding, we show that the farmer's optimal application is lower than the applications based on higher yield targets, suggesting that fertilizer over-application relative to the economically efficient amount may be attributed to recommendations built on the yield-maximizing principle or the farmer's desire to achieve higher yield targets.

For the effect from corn price uncertainty, results in Chapter 2 indicate that an increase in price volatility implies a reduction in the farmer's fertilizer application amount while an increase in the speed of mean reversion for corn prices implies an increase in the nitrogen application. The benefits of increased N in terms of a higher corn yield do not outweigh the increased risk of an unfavorable corn price at harvest time when prices are more volatile. This finding is also confirmed in Chapter 3 where private optimal decisions are examined under weather uncertainty and with two different fertilizer application times. In Chapter 4, in accordance with the other two chapters, the increase of price volatility will decrease or not change the socially optimal starter application, total application and almost all side-dressing applications. However, in some scenarios in Chapter 4, the socially optimal side-dressing amount can shift between zero and positive without changing the starter amount, showing that the corn price effects are subject to other factors such as rainfall, social cost parameters and damage model choice, and are more complex especially when elevated rainfall and the social damages from nitrogen are present.

We find that, in both Chapter 3 and Chapter 4, the relative cost of the two split fertilizer applications, which may vary from region to region, is a key determinant of the optimal application amount and timing. A variation in the relative cost over a rather small range can cause a drastic switch between the allocation of fertilizer over the two possible application times. As expected, an increase in total variable costs reduces the optimal N-application but does not alter the optimal application timing.

Rainfall affects the decision maker through two avenues: (i) the impact on soil nutrient levels as rain causes losses of nitrogen, and (ii) the impact on corn growth as excessive rain causes a reduction in yield. Unlike conventional arguments that precipitation has a one-way effect (increases or decreases) on N application (Bora (2022)), we have found that, rainfall has a complex impact on N application through two dimensions: rainfall likelihood (rainfall frequency) and expected daily rainfall amount. Whether an increase in one of them will decrease or increase the private and socially optimal fertilizer application depends on the level of the other one. For example, from the perspectives of farmers and social planners, when rainfall events are less frequent, a higher expected daily rainfall amount will increase the fertilizer application as a way to compensate the fertility loss. However, when rainfall events become more frequent, an increase in the daily rainfall amount above certain level will decrease N use as a response to save the cost of wasting N and social damage. This reduction effect is more prominent in social planner's model as social damages are more significant in the intensified rainfall scenarios. Similarly, given a low expected daily rain amount, more frequent rain will bring a higher N use while given a high expected rain amount more frequent rain will bring a lower N use. Corn farming becomes less profitable under the most intensive rainfall circumstances as a result of the negative impact of too much rain on corn yield and a significant amount of N waste. It is worth noting that under the low expected daily rainfall amount scenario in our base case, the social planner's optimal choices are identical to the farmer's, which is because low social damages in our base case have only a small effect on the socially N application behavior. In addition, since the social damages are determined by rainfall-induced N losses and social cost parameters, the rainfall effects are much more apparent when the social cost levels are very high, at which point social damages become more prominent, and the increase in the expected quantity of rainfall will reduce the total application amount, shifting from the starter to the side dressing application. The choice of damage model also matters, the socially optimal

choice in the threshold damage model prefers starter application whereas side-dressing is favorable in the linear damage model especially when social cost parameters are very high. The effect of fertilizer relative cost on side-dressing is also examined subject to rainfall. More frequency or expected quantity of rainfall implies a wider range of the cost ratios for which a positive side-dressing will be chosen by the farmer or social planner.

For the social planner, increasing either denitrification or leaching social costs can reduce the total fertilizer application and more N is shifted to side-dressing regardless of which damage model we adopt. However, in the threshold damage model, as the damages from leaching are paid only when the nitrate contamination threshold is triggered, optimal amounts are less sensitive to leaching cost but more sensitive to the denitrification cost. Even though starter has more impact on increasing the average soil N level, side-dressing is favored when social costs of N (SCN) are above certain level as the loss of yield benefits from decreased averaged soil N level caused by delayed application can be compensated by the saving from the reduced social N damages. The assumption regarding leaching and denitrification proportion in the total N loss also matters as is discussed in Chapters 3 and 4. For both damage models, the increase of both SCN decreases the starter application and increases the side-dressing amount, as side-dressing has a shorter period for N loss. However, in the threshold damage model it takes a higher SCN, compared to the linear damage model, to trigger the switch to side-dressing application. This is because nitrogen is less damaging under the threshold model as long as the N concentration level is below the threshold.

Therefore, conclusions on private and socially optimal fertilizer applications depend critically on the separate or joint effect from: (i) The cost estimates of both split fertilizer applications; (ii) The empirical estimates of social damages from nutrient pollution which is highly location-specific; (iii) Assumptions about volatility and mean reversion rates in the corn price model; and (iv) The models describing and integrating the impact of fertilizer

use quantity, timing, N losses, soil nutrient dynamics and weather factors on corn yield. For reader's convenience, a brief summary of main sensitivity conclusions are presented in Table 5.1 where whether there is a switch between $(N_0 > 0, N_1 = 0)$ and $(N_0 \geq 0, N_1 > 0)$ also showed in the table as "Affects timing?".

Table 5.1: A brief summary of main conclusions in this thesis

<table>
<tr><th>When parameter changes</th><th>N_0 amount</th><th>N_1 amount</th><th>N_0+N_1</th><th>Affects timing?</th></tr>
<tr><td colspan="5">Both farmer and social planner:</td></tr>
<tr><td>Starter variable cost ↑</td><td>↓, shifts to N_1</td><td>↑ from 0 or unchanged</td><td>Depends on cost levels, may ↑ or ↓</td><td rowspan="3">YES</td></tr>
<tr><td>Side-dressing variable cost ↑</td><td>↑</td><td>↓ from 0 or unchanged</td><td>↓ or unchanged</td></tr>
<tr><td>The relative fertilizer application cost ↑</td><td>↑</td><td>↓</td><td>↓</td></tr>
<tr><td>Price mean reversion rate ↑</td><td>↑</td><td rowspan="2">unchanged</td><td>↑</td><td rowspan="2">No</td></tr>
<tr><td>Price volatility ↑</td><td>↓</td><td>↓</td></tr>
<tr><td colspan="5">For the farmer:</td></tr>
<tr><td>Rainfall likelihood and amount ↑</td><td>↑ or ↓ depends on the level of rainfall likelihood and expected daily amount</td><td>0</td><td>Same as N_0</td><td>Yes, at certain fertilizer relative cost levels</td></tr>
<tr><td colspan="5">For the social planner:</td></tr>
<tr><td>Rainfall likelihood and amount ↑</td><td>base case : ↑ or ↓
higher SCN:↓ or unchanged</td><td>base case : 0
higher SCN: most ↑</td><td>↑ or ↓ depends on the total damages</td><td>Yes, with high SCN or at certain fertilizer relative cost levels</td></tr>
<tr><td>Social cost from leaching ↑</td><td rowspan="2">↓</td><td rowspan="2">↑</td><td rowspan="2">↓</td><td rowspan="3">Yes</td></tr>
<tr><td>Social cost from denitrification ↑</td></tr>
<tr><td>Leaching / denitrification ↑</td><td colspan="3">When leaching dominates, N_0 and N_1 are more sensitive to the social cost from leaching</td></tr>
</table>

One of our contributions is in developing a theoretical model of the farmer's and social planner's fertilizer application decision that incorporates economic and environmental uncertainty, which provide richer details than any other models in the economics literature. It is also simpler and more transparent than approaches that rely on process-based models which specify detailed fate and transport relationships in the subsurface. Our results are complementary to the existing agricultural economics literature starting with Babcock

(1992) who examined the effects of uncertainty on optimal N applications. The findings concluded in our thesis have broadened our understanding of the factors that drive the variability of agricultural fertilizer application decision, and the degree of market failure which is dictated by the extent to which the farmer's optimal choice deviates from the social planner's decision. As the most vital conclusion to private and public decision-maker, the influence from one factor on the optimal decision is found neither monotonic nor uniform but depends on the levels of the other factors. Although the model is parameterized for corn and for weather conditions in Iowa that allow only one corn harvest per year, the approach is more generally applicable.

As another contribution to the literature, our findings can provide numerous insights for policy-maker seeking to design effective regulations and best management practices to mitigate nitrogen pollution. To begin with, conclusions on rainfall effects are important for public policy as climate change affects weather patterns over the next decade and beyond. At certain fertilizer relative costs, an increase in frequency, expected quantity and variance of rainfall leads to a larger divergence between the farmer's and social planner's decisions, indicating the greater is the market failure. This implies that if we expect climate to become rainier or more volatile rain events present in the future, there is an increased need for strict regulation of N emissions by government. Technical measures to improve N use efficiency and minimize N losses should be the key of policy work.

Our numerical results are sensitive to modeling assumptions and should be viewed as illustrative only. Important limitations that should be mentioned are summarized below.

- Our corn yield model excludes the effect of some yield-limiting factors such as extreme heat or frost in the growing season. In addition, delayed fertilizer applications present yield risks, especially close to R1 (vegetative-stage). Further, corn growth depends on average soil nutrient stock, which oversimplifies the impact of fertilizer timing.

- The corn yield model is calibrated using Iowa state-level average data and may be less accurate for a particular field or an individual decision-maker.

- The modeling of leaching and denitrification may not be a good representation of reality and ignores the time delay effects between nitrogen application and subsequent leaching and denitrification. There is a developing agronomy and soil science literature on this topic.

- The social damages of nitrogen are based on estimates from the literature, which is not well developed. Current social damage estimates tend to focus on the treatment costs incurred in dealing with groundwater for drinking purposes, ignoring the damages to ecosystem services, climate change, and human health caused by excess N pollutants.

References

Abdallah, S. B. & Lasserre, P. (2012), 'A Real Option Approach to The Protection of a Habitat Dependent Endangered Species', *Resource and Energy Economics* **34**(3), 295–318.

Abid, S., Nasir, J., Anwar, M. Z. & Zahid, S. (2018), 'Exponential Growth Model for Forecasting of Area and Production of Potato Crop in Pakistan', *Pakistan Journal of Agricultural Research* **31**(1).

Abidoye, B. O., Herriges, J. A. & Tobias, J. L. (2012), 'Controlling for Observed and Unobserved Site Characteristics in RUM Models of Recreation Demand', *American Journal of Agricultural Eco-nomics* **94**(5), 1070–1093.

Abler, D. (2015), 'Economic Evaluation of Agricultural Pollution Control Options for China', *Journal of Integrative Agriculture* **14**(6), 1045–1056.

Addy, J. W., Ellis, R. H., Macdonald, A. J., Semenov, M. A. & Mead, A. (2020), 'Investigating the Effects of Inter-annual Weather Variation (1968–2016) on the Functional Response of Cereal Grain Yield to Applied Nitrogen, Using Data from the Rothamsted Long-Term Experiments', *Agricultural and Forest Meteorology* **284**, 107898.

Aggarwal, P. (1995), 'Uncertainties in Crop, Soil and Weather Inputs Used in Growth Mod-

els: Implications for Simulated Outputs and Their Applications', *Agricultural Systems* **48**(3), 361–384.

Agriculture, M. & Development, R. (n.d.), 'Volatilization Losses from Surface Applied Nitrogen'.
URL: *https://www.gov.mb.ca/agriculture/crops/soil-fertility/volatilization-losses-from-surface-applied-nitrogen.html*

Ailliot, P., Allard, D., Monbet, V. & Naveau, P. (2015), 'Stochastic Weather Generators: An Overview of Weather Type Models', *Journal de la Société Française de Statistique* **156**(1), 101–113.

Aiube, F. A. L. & Levy, A. (2019), 'Recent Movement of Oil Prices and Future Scenarios', *Nova Economia* **29**(1), 223–248.

Alaton, P., Djehiche, B. & Stillberger, D. (2002), 'On Modelling and Pricing Weather Derivatives', *Applied Mathematical Finance* **9**(1), 1–20.

Ali, D. (2017), Towards Site-Specific Nitrogen Management in Hard Red Winter Wheat, Master's thesis, The University of Guelph, Guelph, Ontario, Canada.

Almasri, M. N. & Kaluarachchi, J. J. (2007), 'Modeling Nitrate Contamination of Groundwater in Agricultural Watersheds', *Journal of Hydrology* **343**(3-4), 211–229.

Arbuckle, J. G. & Rosman, H. (2014), 'Iowa Farmers' Nitrogen Management Practices and Perspectives', *Extension Report PM3066. Ames, IA: Iowa State University Extension* .

Babcock, B. A. (1992), 'The Effects of Uncertainty on Optimal Nitrogen Applications', *Review of Agricultural Economics* **14**(2), 271–280.

Baethgen, W. E., Christianson, C. B. & Lamothe, A. G. (1995), 'Nitrogen Fertilizer Effects on Growth, Grain Yield, and Yield Components of Malting Barley', *Field Crops Research* **43**(2), 87–99.

Bakhsh, A., Kanwar, R. S. & Baker, J. (2010), 'N-application Methods and Precipitation Pattern Effects on Subsurface Drainage Nitrate Losses and Crop Yields', *Water, Air, and Soil Pollution* **212**(1), 65–76.

Barbieri, P. A., Rozas, H. S. & Echeverría, H. (2008), 'Time of Nitrogen Application Affects Nitrogen Use Efficiency of Wheat in The Humid Pampas of Argentina', *Canadian Journal of Plant Science* **88**(5), 849–857.

Basso, B., Dumont, B., Cammarano, D., Pezzuolo, A., Marinello, F. & Sartori, L. (2016), 'Environmental and Economic Benefits of Variable Rate Nitrogen Fertilization in a Nitrate Vulnerable Zone', *Science of the total environment* **545**, 227–235.

Bélanger, G., Walsh, J. R., Richards, J. E., Milburn, P. H. & Ziadi, N. (2000), 'Comparison of Three Statistical Models Describing Potato Yield Response to Nitrogen Fertilizer', *Agronomy Journal* **92**(5), 902–908.

Benth, F. E. & Benth, J. š. (2007), 'The Volatility of Temperature and Pricing of Weather Derivatives', *Quantitative Finance* **7**(5), 553–561.

Bessembinder, H., Coughenour, J. F., Seguin, P. J. & Smoller, M. M. (1995), 'Mean Reversion in Equilibrium Asset Prices: Evidence From The Futures Term Structure', *The Journal of Finance* **50**(1), 361–375.

Bhandari, S., Srivastava, R. & Mehta, V. (2016), 'Long-Term Changes in the Within-Season Temporal Profile of Southwest Monsoon over Western India', *Journal of Earth System Science* **125**(7), 1313–1319.

Biswanath Dari, C. W. R. & Walsh, O. S. (2019), Understanding Factors Controlling Ammonia Volatilization from Fertilizer Nitrogen Applications, Technical report, University of Idaho Extension.

Bora, K. (2022), 'Rainfall Shocks and Fertilizer Use: A District Level Study of India', *Environment and Development Economics* pp. 1–22.

Boyer, C. N., Larson, J. A., Roberts, R. K., McClure, A. T., Tyler, D. D. & Zhou, V. (2013), 'Stochastic Corn Yield Response Functions to Nitrogen for Corn-after-corn, Corn-after-cotton, and Corn-after-soybeans', *Journal of Agricultural and Applied Economics* **45**(1379-2016-113848), 669–681.

Bréchet, T. & Jouvet, P.-A. (2008), 'Environmental Innovation and the Cost of Pollution Abatement Revisited', *Ecological Economics* **65**(2), 262–265.

Brigo, D., Dalessandro, A., Neugebauer, M. & Triki, F. (2007), 'A Stochastic Processes Toolkit for Risk Management', *Available at SSRN 1109160* .

Brissette, F., Khalili, M. & Leconte, R. (2007), 'Efficient Stochastic Generation of Multi-site Synthetic Precipitation Data', *Journal of Hydrology* **345**(3-4), 121–133.

Browner, C. M., Fox, J. C., Frace, S. E., Goodwin, J. & John-son, R. S. (2001), 'Economic Analysis for the Proposed Revisions to the National Pollutant Discharge Elimination System Regulation and the Effluent Guidelines for Concentrated Animal Feeding Operations', *Environmental Protection* **20460**.

Budantsev, A. Y., Uversky, V. N. & Kutyshenko, V. P. (2010), 'Analysis of the Metabolites in Apical Area of Allium Cepa Roots by High Resolution NMR Spectroscopy Method', *Protein and Peptide Letters* **17**(1), 86–91.

Cabas, J., Weersink, A. & Olale, E. (2010), 'Crop Yield Response to Economic, Site and Climatic Variables', *Climatic Change* **101**(3-4), 599–616.

Cabrera, F., Fernández Boy, E., Aparicio, M., Murillo Carpio, J. M. & Moreno Lucas, F. (1995), 'Leaching of Nitrate from a Sandy Loam Soil under Corn and Two N fertilizations'.

Camberato, J. (2017), Soil Sampling to Assess Current Soil Nitrogen Availability, Technical report, Purdue Extension Agriculture Agronomy, Purdue University.

Camberato, J. & Nielsen, R. (2017), 'Soil Sampling to Assess Current Soil N Availability', *Purdue University. url: https://www. agry. purdue. edu/ext/corn/news/timeless/assessavailablen. html* .

Carson, R. T. & LaRiviere, J. (2018), 'Structural Uncertainty and Pollution Control: Optimal Stringency with Unknown Pollution Sources', *Environmental and resource economics* **71**(2), 337–355.

Castellano, M. J., Helmers, M. J., Sawyer, J. E., Barker, D. W. & Christianson, L. (2012), 'Nitrogen, Carbon, and Phosphorus Balances in Iowa Cropping Systems: Sustaining the Soil Resource'.

Cerrato, M. & Blackmer, A. (1990), 'Comparison of Models for Describing Corn Yield Response to Nitrogen Fertilizer', *Agronomy Journal* **82**(1), 138–143.

Challinor, A. J., Müller, C., Asseng, S., Deva, C., Nicklin, K. J., Wallach, D., Vanuytrecht, E., Whitfield, S., Ramirez-Villegas, J. & Koehler, A.-K. (2018), 'Improving The Use of Crop Models for Risk Assessment and Climate Change Adaptation', *Agricultural Systems* **159**, 296–306.

Chen, B. (2007), 'Climate Change and Pesticide Loss in Watershed Systems: A Simulation Modeling Study', *Journal of Environmental Informatics* **10**(2).

Chen, C.-C. & Chang, C.-C. (2005), 'The Impact of Weather on Crop Yield Distribution in Taiwan: Some New Evidence from Panel Data Models and Implications for Crop Insurance', *Agricultural Economics* **33**, 503–511.

Chen, C.-C., McCarl, B. A. & Schimmelpfennig, D. E. (2004), 'Yield Variability as Influenced by Climate: A Statistical Investigation', *Climatic Change* **66**(1-2), 239–261.

Chen, J., Brissette, F. & Leconte, R. (2012*a*), 'Weagets-A Matlab-Based Daily Scale Weather Generator for Generating Precipitation and Temperature', *Procedia Environmental Sciences* **13**, 2222–2235.

Chen, J. & Brissette, F. P. (2014), 'Comparison of Five Stochastic Weather Generators in Simulating Daily Precipitation and Temperature for the Loess Plateau of China', *International Journal of Climatology* **34**(10), 3089–3105.

Chen, J., Brissette, F. P. & Leconte, R. (2012*b*), 'Downscaling of Weather Generator Parameters to Quantify Hydrological Impacts of Climate Change', *Climate Research* **51**(3), 185–200.

Chen, J., Tang, C., Sakura, Y., Yu, J. & Fukushima, Y. (2005), 'Nitrate Pollution from Agriculture in Different Hydrogeological Zones of the Regional Groundwater Flow System in the North China Plain', *Hydrogeology Journal* **13**(3), 481–492.

Chen, S., Chen, X. & Xu, J. (2016), 'Impacts of Climate Change on Agriculture: Evidence from China', *Journal of Environmental Economics and Management* **76**, 105–124.

Chen, S. & Insley, M. (2012), 'Regime Switching in Stochastic Models of Commodity

Prices: An Application to an Optimal Tree Harvesting Problem', *Journal of Economic Dynamics and Control* **36**(2), 201–219.

Chen, Y.-h., Wen, X.-w., Wang, B. & Nie, P.-y. (2017), 'Agricultural Pollution and Regulation: How to Subsidize Agriculture?', *Journal of cleaner production* **164**, 258–264.

Cropper, T. E. & Cropper, P. E. (2016), 'A 133-Year Record of Climate Change and Variability from Sheffield, England', *Climate* **4**(3), 46.

Cui, Z., Zhang, F., Chen, X., Dou, Z. & Li, J. (2010), 'In-season Nitrogen Management Strategy for Winter Wheat: Maximizing Yields, Minimizing Environmental Impact in an Over-fertilization Context', *Field Crops Research* **116**(1), 140–146.

Culman, S., Fulford, A., Camberato, J. & Steinke, K. S. (2020), Tri-State Fertilizer Recommendations for Corn, Soybean, Wheat, and Alfalfa, Technical report, College of Food, Agricultural, and Environmental Sciences, The Ohio State University. https://agcrops.osu.edu/FertilityResources/tri-stateinfo.

Dahnke, W., Olson, R. et al. (1990), 'Soil Test Correlation, Calibration and Recommendation', *Soil Test Correlation, Calibration and Recommendation.* pp. 45–71.

Dasgupta, R. (2018), Tuber Crop Growth Model, Performance Rate, and Some Characterization Theorems, *in* 'Advances in Growth Curve and Structural Equation Modeling', Springer, pp. 95–103.

Davis, J. (2007), Nitrogen Efficiency and Management, Technical report, United States Department of Agricultural. https://directives.sc.egov.usda.gov/OpenNonWebContent.aspx?content=18563.wba.

Derby, N. E., Steele, D. D., Terpstra, J., Knighton, R. E. & Casey, F. X. (2005), 'Inter-

actions of Nitrogen, Weather, Soil, and Irrigation on Corn Yield', *Agronomy Journal* **97**(5), 1342–1351.

Dixit, A. K., Dixit, R. K. & Pindyck, R. S. (1994), *Investment under Uncertainty*, Princeton university press.

Dixon, B. L., Hollinger, S. E., Garcia, P. & Tirupattur, V. (1994), 'Estimating Corn Yield Response Models to Predict Impacts of Climate Change', *Journal of Agricultural and Resource Economics* pp. 58–68.

Dowd, B. M., Press, D. & Los Huertos, M. (2008), 'Agricultural Nonpoint Source Water Pollution Policy: The Case of California's Central Coast', *Agriculture, ecosystems and environment* **128**(3), 151–161.

Drevno, A. (2016*a*), 'Policy Tools for Agricultural Nonpoint Source Water Pollution control in the US and EU', *Management of Environmental Quality: An International Journal* .

Drevno, A. (2016*b*), 'Policy Tools for Agricultural Nonpoint Source Water Pollution Control in the US and EU', *Management of Environmental Quality: An International Journal* .

Eagle, A. J., Locklier, K., Heffernan, J., Bernhardt, E., Vegh, T. & Olander, L. P. (2015), Nitrogen Losses: A Meta Analysis of 4R Nutrient Management in US Corn Based Systems, Technical report, 4R Research Fund Project, Duke University.

Egan, K. J., Herriges, J. A., Kling, C. L. & Downing, J. A. (2009), 'Valuing Water Quality As a Function of Water Quality Measures', *American Journal of Agricultural Eco-nomics* **91**(1), 106–123.

Färe, R., Grosskopf, S. & Weber, W. L. (2006), 'Shadow Prices and Pollution Costs in US Agriculture', *Ecological economics* **56**(1), 89–103.

Fishman, Y., Becker, N. & Shechter, M. (2012), 'An Input Tax on Nitrogen Fertilizer Pollution in The Presence of Transaction Costs', *Journal of Environmental Planning and Management* **55**(9), 1206–1227.

Folkens, L., Wiedemer, V. & Schneider, P. (2020), 'Monetary Valuation and Internalization of Externalities in German Agriculture Using the Example of Nitrate Pollution: A Case-Study', *Sustainability* **12**(16), 6681.

Furtan, W. H., Gray, R. S. & Holzman, J. (2003), 'The Optimal Time to License a Biotech "Lemon"', *Contemporary Economic Policy* **21**(4), 433–444.

Gabriel, A. O. & Kreutzwiser, R. D. (1993), 'Drought Hazard in Ontario: A Review of Impacts, 1960–1989, and Management Implications', *Canadian Water Resources Journal* **18**(2), 117–132.

Gandorfer, M. & Rajsic, P. (2008), 'Modeling Economic Optimum Nitrogen Rates for Winter Wheat when Inputs Affect Yield and Output Price', *Agricultural Economics Review* **9**(389-2016-23335).

Gentry, L. E., David, M. B., Smith, K. M. & Kovacic, D. A. (1998), 'Nitrogen Cycling and Tile Drainage Nitrate Loss in a Corn-Soybean Watershed', *Agriculture, ecosystems and Environment* **68**(1-2), 85–97.

Giannadaki, D., Giannakis, E., Pozzer, A. & Lelieveld, J. (2018), 'Estimating Health and Economic Benefits of Reductions in Air Pollution From Agriculture', *Science of the total environment* **622**, 1304–1316.

Golder, B., Misra, S. & Mukherji, B. (2001), 'Water Pollution Abatement Cost function: Methodological Issues and Application to Small-Scale Factories in an Industrial Estate in India', *Environment and Development Economics* **6**(2001), 103–122.

Gourevitch, J. D., Keeler, B. L. & Ricketts, T. H. (2018), 'Determining Socially Optimal Rates of Nitrogen Fertilizer Application', *Agriculture, Ecosystems and Environment* **254**, 292–299.

Gren, M. & Folmer, H. (2003), 'Cooperation with Respect to Cleaning of an International Water Body with Stochastic Environmental Damage: the Case of the Baltic Sea', *Ecological Economics* **47**(1), 33–42.

Gyamerah, S. A., Ngare, P. & Ikpe, D. (2019), 'Hedging Crop Yields against Weather Uncertainties–A Weather Derivative Perspective', *ArXiv Preprint ArXiv:1905.07546* .

Halvorson, A. D. & Bartolo, M. E. (2014), 'Nitrogen Source and Rate Effects on Irrigated Corn Yields and Nitrogen Use Efficiency', *Agronomy Journal* **106**(2), 681–693.

Hansen, L. T. (1991), 'Farmer Response to Changes in Climate: The Case of Corn Production', *Journal of Agricultural Economics Research* **43**(1491-2016-130103).

Hargrave, A. & Shaykewich, C. (1997), 'Rainfall Induced Nitrogen and Phosphorus Losses from Manitoba Soils', *Canadian Journal of Soil Science* **77**(1), 59–65.

Hart, C. E., Lence, S. H., Hayes, D. J. & Jin, N. (2016), 'Price Mean Reversion, Seasonality, and Options Markets', *American Journal of Agricultural Economics* **98**(3), 707–725.

Hart, R. (2003), 'Dynamic Pollution Control—Time Lags and Optimal Restoration of Marine Ecosystems', *Ecological Economics* **47**(1), 79–93.

Hatfield, J. L. & Prueger, J. H. (2015), 'Temperature Extremes: Effect on Plant Growth and Development', *Weather and Climate Extremes* **10**, 4–10.

Henke, J., Breustedt, G., Sieling, K. & Kage, H. (2007), 'Impact of Uncertainty on the Optimum Nitrogen Fertilization Rate and Agronomic, Ecological and Economic Fac-

tors in an Oilseed Rape Based Crop Rotation', *The Journal of Agricultural Science* **145**(5), 455–468.

Hennessy, D. A. (1998), 'The Production Effects of Agricultural Income Support Policies under Uncertainty', *American Journal of Agricultural Economics* **80**(1), 46–57.

Hersvik, K. & Endrerud, O. V. (2017), A High-fidelity Weather Time Series Generator Using the Markov Chain Process on A Piecewise Level, *in* 'IOP Conference Series: Materials Science and Engineering', Vol. 276, IOP Publishing, p. 012003.

Hess, L. J., Hinckley, E. S., Robertson, G. P. & Matson, P. A. (2020), 'Rainfall Intensification Increases Nitrate Leaching from Tilled but not No-till Cropping Systems in the US Midwest', *Agriculture, Ecosystems and Environment* **290**, 106747.

Hilbert, G., Soyer, J., Molot, C., Giraudon, J., Milin, M. & Gaudillere, J. (2015), 'Effects of Nitrogen Supply on Must Quality and Anthocyanin Accumulation in Berries of Merlot', *VITIS-Journal of Grapevine Research* **42**(2), 69.

Hilliard, J. E. & Reis, J. A. (1999), 'Jump Processes in Commodity Futures Prices and Options Pricing', *American Journal of Agricultural Economics* **81**(2), 273–286.

Ho, J. C. & Michalak, A. M. (2015), 'Challenges in Tracking Harmful Algal Blooms: A Synthesis of Evidence from Lake Erie', *Journal of Great Lakes Research* **41**, 317–325.

Horan, R. D. & Shortle, J. S. (2017), 'Endogenous Risk and Point-nonpoint Uncertainty Trading Ratios', *American Journal of Agricultural Economics* **99**(2), 427–446.

Horan, R. D., Shortle, J. S. & Abler, D. G. (1998), 'Ambient Taxes when Polluters Have Multiple Choices', *Journal of Environmental Economics and Management* **36**(2), 186–199.

Horan, R. D., Shortle, J. S. & Abler, D. G. (2002), 'Ambient Taxes under m-Dimensional Choice Sets, Heterogeneous Expectations, and Risk-aversion', *Environmental and Resource Economics* **21**(2), 189–202.

Horner, G. L. (1975), 'Internalizing Agricultural Nitrogen Pollution Externalities: A Case Study', *American Journal of Agricultural Economics* **57**(1), 33–39.

Huang, T., Pang, Z. & Yuan, L. (2013), 'Nitrate in Groundwater and the Unsaturated Zone in (Semi) Arid Northern China: Baseline and Factors Controlling its Transport and Fate', *Environmental earth sciences* **70**(1), 145–156.

Hull, J. C. (2003), *Options Futures and Other Derivatives*, Pearson Education India.

Hyytiäinen, K., Niemi, J. K., Koikkalainen, K., Palosuo, T. & Salo, T. (2011), 'Adaptive Optimization of Crop Production and Nitrogen Leaching Abatement under Yield Uncertainty', *Agricultural Systems* **104**(8), 634–644.

Insley, M. (2017), 'Resource Extraction with a Carbon Tax and Regime Switching Prices: Exercising Your Options', *Energy Economics* **67**, 1–16.

Insley, M. C. & Wirjanto, T. S. (2010), 'Contrasting Two Approaches in Real Options Valuation: Contingent Claims versus Dynamic Programming', *Journal of Forest Economics* **16**(2), 157–176.

Insley, M. & Lei, M. (2007), 'Hedges and Trees: Incorporating Fire Risk into Optimal Decisions in Forestry Using a No-arbitrage Approach', *Journal of Agricultural and Resource Economics* pp. 492–514.

Isik, M. (2002), 'Resource Management under Production and Output Price Uncertainty: Implications for Environmental Policy', *American Journal of Agricultural Economics* **84**(3), 557–571.

Isik, M. (2004), 'Incentives for Technology Adoption under Environmental Policy Uncertainty: Implications for Green Payment Programs', *Environmental and Resource Economics* **27**(3), 247–263.

Isiuku, B. O. & Enyoh, C. E. (2020), 'Pollution and Health Risks Assessment of Nitrate and Phosphate Concentrations in Water Bodies in South Eastern, Nigeria', *Environmental Advances* **2**, 100018.

ISU, E. (2018), Nitrogen Use in Iowa Corn Production, Technical report, Iowa State University Extension and Outreach. https://store.extension.iastate.edu/product/Nitrogen-Use-in-Iowa-Corn-Production.

Ivana, S., Kristina, P. & Tomislav, B. (2016), 'Effectiveness of Weather Derivatives as a Hedge Against the Weather Risk in Agriculture', *Agricultural Economics* **62**(8), 356–362.

Jalali, M. (2005), 'Nitrates Leaching from Agricultural Land in Hamadan, Western Iran', *Agriculture, ecosystems and environment* **110**(3-4), 210–218.

Janjua, P. Z., Samad, G. & Khan, N. (2014), 'Climate Change and Wheat Production in Pakistan: An Autoregressive Distributed Lag Approach', *NJAS-Wageningen Journal of Life Sciences* **68**, 13–19.

Jin, N., Lence, S., Hart, C. & Hayes, D. (2012), 'The Long-term Structure of Commodity Futures', *American Journal of Agricultural Economics* **94**(3), 718–735.

Jones, C. J. (n.d.), 'Management to Minimize Nitrogen Fertilizer Volatilization'.
URL: *https://landresources.montana.edu/soilfertility/documents/PDF/pub/UvolBMPEB0209.pdf*

Ju, X., Liu, X., Zhang, F. & Roelcke, M. (2004), 'Nitrogen Fertilization, Soil Nitrate Accumulation, and Policy Recommendations in Several Agricultural Regions of China', *AMBIO: a Journal of the Human Environment* **33**(6), 300–305.

Juntakut, P., Haacker, E. M., Snow, D. D. & Ray, C. (2020), 'Risk and Cost Assessment of Nitrate Contamination in Domestic Wells', *Water* **12**(2), 428.

Just, R. E. & Pope, R. D. (1979), 'Production Function Estimation and Related Risk Considerations', *American Journal of Agricultural Economics* **61**(2), 276–284.

Kabir, T., De Laporte, A., Nasielski, J. & Weersink, A. (2021), 'Adjusting Nitrogen Rates with Split Applications: Modelled Effects on N Losses and Profits Across Weather Scenarios', *European Journal of Agronomy* **129**, 126328.

Kablan, L. A., Chabot, V., Mailloux, A., Bouchard, M.-È., Fontaine, D. & Bruulsema, T. (2017), 'Variability in Corn Yield Response to Nitrogen Fertilizer in Eastern Canada', *Agronomy Journal* **109**(5), 2231–2242.

Kannan, S. K. & Farook, J. A. (2015), 'Stochastic Simulation of Precipitation Using Markov Chain-mixed Exponential Model', *Applied Mathematical Sciences* **65**(9), 3205–3212.

Kanwar, R. S. (1991), 'Impact of Tillage, Crop Rotation, and Chemical Management Practices on Groundwater Quality'.

Kaufmann, R. K. & Snell, S. E. (1997), 'A Biophysical Model of Corn Yield: Integrating Climatic and Social Determinants', *American Journal of Agricultural Economics* **79**(1), 178–190.

Keeler, B. L., Gourevitch, J. D., Polasky, S., Isbell, F., Tessum, C. W., Hill, J. D. & Marshall, J. D. (2016), 'The Social Costs of Nitrogen', *Science advances* **2**(10), e1600219.

Khanna, M., Isik, M. & Winter-Nelson, A. (2000), 'Investment in Site-specific Crop management under uncertainty: implications for nitrogen pollution control and environmental policy', *Agricultural Economics* **24**(1), 9–12.

Kim, C., Hostetler, J. & Amacher, G. (1993), 'The Regulation of Groundwater Quality with Delayed Responses', *Water Resources Research* **29**(5), 1369–1377.

Kim, C., Sandretto, C. & Hostetler, J. (1996), 'Effects of Farmer Response to Nitrogen Fertilizer Management Practices on Groundwater Quality', *Water Resources Research* **32**(5), 1411–1415.

Kim, M.-K. & Pang, A. (2009), 'Climate Change Impact on Rice Yield and Production Risk', *Journal of Rural Development/Nongchon-Gyeongje* **32**(1071-2016-86914), 17.

Kling, C. L. (2011), 'Economic Incentives to Improve Water Quality in Agricultural Landscapes: Some New Variations on Old Ideas', *American Journal of Agricultural Economics* **93**(2), 297–309.

Kong, L., Xie, Y., Hu, L., Si, J. & Wang, Z. (2017), 'Excessive Nitrogen Application Dampens Antioxidant Capacity and Grain Filling in Wheat as Revealed by Metabolic and Physiological Analyses', *Scientific Reports* **7**.

Lassaletta, L., Billen, G., Grizzetti, B., Anglade, J. & Garnier, J. (2014), '50 Year Trends in Nitrogen Use Efficiency of World Cropping Systems: The Relationship Between Yield and Nitrogen Input to Cropland', *Environmental Research Letters* **9**(10), 105011.

Lauer, J. (2006), 'Concerns about Drought as Corn Pollination Begins', *Field Crops* .

Lawniczak, A. E., Zbierska, J., Nowak, B., Achtenberg, K., Grześkowiak, A. & Kanas, K. (2016), 'Impact of Agriculture and Land Use on Nitrate Contamination in Groundwater and Running Waters in Central-West Poland', *Environmental monitoring and assessment* **188**(3), 172.

Lee, D. J. & Kim, C. (2002), 'Nonpoint Source Groundwater Pollution and Endogenous Regulatory Policies', *Water resources research* **38**(12), 11–1.

Leslie, J. E., Weersink, A., Yang, W. & Fox, G. (2017), 'Actual versus Environmentally Recommended Fertilizer Application Rates: Implications for Water Quality and Policy', *Agriculture, Ecosystems and Environment* **240**, 109–120.

Lewandowski, A. M., Montgomery, B., Rosen, C. J. & Moncrief, J. (2008), 'Groundwater Nitrate Contamination Costs: A Survey of Private Well Owners', *Journal of soil and water conservation* **63**(3), 153–161.

Li, Z., Brissette, F. & Chen, J. (2014), 'Assessing the Applicability of Six Precipitation Probability Distribution Models on the Loess Plateau of China', *International Journal of Climatology* **34**(2), 462–471.

Liang, L., Zhao, L., Gong, Y., Tian, F. & Wang, Z. (2012), 'Probability Distribution of Summer Daily Precipitation in the Huaihe Basin of China Based on Gamma Distribution', *Acta Meteorologica Sinica* **26**(1), 72–84.

Libra, R. D., Wolter, C. F. & Langel, R. J. (2004), 'Nitrogen and Phosphorus Budgets for Iowa and Iowa Watersheds'.

Lobell, D. B., Bänziger, M., Magorokosho, C. & Vivek, B. (2011), 'Nonlinear Heat Effects on African Maize as Evidenced by Historical Yield Trials', *Nature Climate Change* **1**(1), 42.

Lobell, D. B. & Burke, M. B. (2010), 'On the Use of Statistical Models to Predict Crop Yield Responses to Climate Change', *Agricultural and Forest Meteorology* **150**(11), 1443–1452.

Lobell, D. B., Cahill, K. N. & Field, C. B. (2007), 'Historical Effects of Temperature and Precipitation on California Crop Yields', *Climatic Change* **81**(2), 187–203.

Lobell, D. B., Field, C. B., Cahill, K. N. & Bonfils, C. (2006), 'Impacts of Future Climate

Change on California Perennial Crop Yields: Model Projections with Climate and Crop Uncertainties', *Agricultural and Forest Meteorology* **141**(2-4), 208–218.

Lockhart, K., King, A. & Harter, T. (2013), 'Identifying Sources of Groundwater Nitrate Contamination in a Large Alluvial Groundwater Basin with Highly Diversified Intensive Agricultural Production', *Journal of contaminant hydrology* **151**, 140–154.

Long, S., Zhao, L., Liu, H., Li, J., Zhou, X., Liu, Y., Qiao, Z., Zhao, Y. & Yang, Y. (2019), 'A Monte Carlo-based Integrated Model to Optimize the Cost and Pollution Reduction in Wastewater Treatment Processes in a Typical Comprehensive Industrial Park in China', *Science of the total environment* **647**, 1–10.

Mahvi, A., Nouri, J., Babaei, A. & Nabizadeh, R. (2005), 'Agricultural Activities Impact on Groundwater Nitrate Pollution', *International Journal of Environmental Science and Technology* **2**(1), 41–47.

Martin-Vide, J. (2004), 'Spatial Distribution of a Daily Precipitation Concentration Index in Peninsular Spain', *International Journal of Climatology: A Journal of the Royal Meteorological Society* **24**(8), 959–971.

Martínez, Y. & Albiac, J. (2006), 'Nitrate Pollution Control under Soil Heterogeneity', *Land Use Policy* **23**(4), 521–532.

Mavromatis, T. & Hansen, J. W. (2001), 'Interannual Variability Characteristics and Simulated Crop Response of Four Stochastic Weather Generators', *Agricultural and Forest Meteorology* **109**(4), 283–296.

Mearns, L. O., Katz, R. W. & Schneider, S. H. (1984), 'Extreme High-temperature Events: Changes in Their Probabilities with Changes in Mean Temperature', *Journal of Climate and Applied Meteorology* **23**(12), 1601–1613.

Mendelsohn, R. (2014), 'The Impact of Climate Change on Agriculture in Asia', *Journal of Integrative Agriculture* **13**(4), 660–665.

Mengel, D. B. (n.d.), 'Types and Uses of Nitrogen Fertilizers for Crop Production'. **URL:** *https://www.extension.purdue.edu/extmedia/ay/ay-204.html*

Meyer-Aurich, A., Weersink, A., Gandorfer, M. & Wagner, P. (2010), 'Optimal Site-specific Fertilization and Harvesting Strategies with Respect to Crop Yield and Quality Response to Nitrogen', *Agricultural Systems* **103**(7), 478–485.

Mraoua, M. (2007), 'Temperature Stochastic Modeling and Weather Derivatives Pricing: Empirical Study with Moroccan Data', *Afrika Statistika* **2**(1).

Mullen, R., Johnson, G., Raun, W. & Howell, B. (2000), 'Simulating Volatilization Losses from Anhydrous Ammonia Applications: A Simple Laboratory Exercise', *Journal of Natural Resources and Life Sciences Education* **29**(1), 107–110.

Murdock, J. (2006), 'Handling Unobserved Site Characteristics in Random Utility Models of Recreation Demand', *Journal of environmental economics and management* **51**(1), 1–25.

Nevison, C., Hess, P., Riddick, S. & Ward, D. (2016), 'Denitrification, Leaching, and River Nitrogen Export in The Community Earth System Model', *Journal of Advances in Modeling Earth Systems* **8**(1), 272–291.

Nicks, A. & Gander, G. (1994), CLIGEN: A Weather Generator for Climate Inputs to Water Resource and Other Models, *in* 'Proc. Fifth Int. Conf. on Computers in Agriculture', pp. 903–909.

Nicks, A., Lane, L. & Gander, G. (1995), 'Weather Generator', *USDA-Water Erosion Prediction Project. NSERL Report* (10), 2–1.

Nielsen, R. (2006*a*), N Loss Mechanisms and Nitrogen Use Efficiency, *in* 'Purdue nitrogen management workshops', Purdue University West Lafayette, Indiana, US, pp. 1–5.

Nielsen, R. B. (2006*b*), N Loss Mechanisms and Nitrogen Use Efficiency, Technical report, Purdue Nitrogen Management Workshops, Purdue University. URL= https://www.agry.purdue.edu/ext/pubs/2006NLossMechanisms.pdf.

OMAFRA (2017*a*), Agronomy Guide for Field Crops, Publication 811, Technical report, Ontario Ministry of Agriculture, Food, and Rural Affairs, Government of Ontario, Canada. URL=http://www.omafra.gov.on.ca/english/crops/pub811/pub811.pdf.

OMAFRA (2017*b*), Soil Fertility Handbook, Publication 611, Technical report, Ontario Ministry of Agriculture, Food, and Rural Affairs, Government of Ontario, Canada. URL=http://www.omafra.gov.on.ca/english/crops/pub611/pub611.pdf.

OMAFRA (2020), 2020 field crop budgets, publication 60, Technical report, Ontario Ministry of Agriculture, Food, and Rural Affairs, Government of Ontario, Canada. URL=http://www.omafra.gov.on.ca/english/busdev/facts/pub60.pdf.

Ortiz-Bobea, A. (2013), 'Is Weather Really Additive in Agricultural Production? Implications for Climate Change Impacts', *Implications for Climate Change Impacts (December 20, 2013). Resources for the Future Discussion Paper* (13-41).

Oury, B. (1965), 'Allowing for Weather in Crop Production Model Building', *Journal of Farm Economics* **47**(2), 270–283.

O'Shea, L. & Wade, A. (2009), 'Controlling Nitrate Pollution: An Integrated Approach', *Land use policy* **26**(3), 799–808.

Paltasingh, K. R., Goyari, P. & Mishra, R. (2012), 'Measuring Weather Impact on Crop

Yield Using Aridity Index: Evidence from Odisha', *Agricultural Economics Research Review* **25**(2).

Pannell, D. J. (2003), Uncertainty and Adoption of Sustainable Farming Systems, *in* 'Risk Management and the Environment: Agriculture in Perspective', Springer, pp. 67–81.

Patil, N., Venkataraman, C., Muduchuru, K., Ghosh, S. & Mondal, A. (2019), 'Disentangling Sea-Surface Temperature and Anthropogenic Aerosol Influences on Recent Trends in South Asian Monsoon Rainfall', *Climate Dynamics* **52**(3), 2287–2302.

Patni, N., Masse, L. & Jui, P. (1996), 'Tile Effluent Quality and Chemical Losses under Conventional and No Tillage—part 1: Flow and Nitrate', *Transactions of the ASAE* **39**(5), 1665–1672.

Patrick, M. (2016), 'A Comparison of Prices Generated by The Derivative Commodity Model (Ornstein-Uhlenbeck Process) With Those Obtained by The Conventional Arbitrage-Free Method of Pricing Forward Derivatives with Respect to Tea in Nduti Tea Factory Kenya', *Journal of Statistics and Actuarial Research* **1**(1), 12–23.

Paudel, J. & Crago, C. L. (2021), 'Environmental Externalities from Agriculture: Evidence from Water Quality in the United States', *American Journal of Agricultural Economics* **103**(1), 185–210.

Paul, J. & Zebarth, B. (1997), 'Denitrification and Nitrate Leaching during the Fall and Winter Following Dairy Cattle Slurry Application', *Canadian Journal of Soil Science* **77**(2), 231–240.

Pires, M. V., da Cunha, D. A., de Matos Carlos, S. & Costa, M. H. (2015), 'Nitrogen Use Efficiency, Nitrous Oxide Emissions, and Cereal Production in Brazil: Current Trends and Forecasts', *PloS one* **10**(8), e0135234.

Powell, J. & Reinhard, S. (2016), 'Measuring the Effects of Extreme Weather Events on Yields', *Weather and Climate Extremes* **12**, 69–79.

Prager, D., Burns, C., Tulman, S. & MacDonald, J. (2020), Farm Use of Futures, Options, and Marketing Contracts, Technical report, United States Department of Agriculture. https://ageconsearch.umn.edu/record/305690/.

Price, T. J. & Wetzstein, M. E. (1999), 'Irreversible Investment Decisions in Perennial Crops with Yield and Price Uncertainty', *Journal of Agricultural and Resource Economics* pp. 173–185.

Puckett, L. J., Zamora, C., Essaid, H., Wilson, J. T., Johnson, H. M., Brayton, M. J. & Vogel, J. R. (2008), 'Transport and Fate of Nitrate at the Ground Water/Surface Water Interface', *Journal of environmental quality* **37**(3), 1034–1050.

Qian, B., Corte-Real, J. & Xu, H. (2002), 'Multisite Stochastic Weather Models for Impact Studies', *International Journal of Climatology* **22**(11), 1377–1397.

Rabotyagov, S. S., Valcu, A. M. & Kling, C. L. (2014*a*), 'Reversing Property Rights: Practice-based Approaches for Controlling Agricultural Nonpoint-source Water Pollution when Emissions Aggregate Nonlinearly', *American Journal of Agricultural Economics* **96**(2), 397–419.

Rabotyagov, S. S., Valcu, A. M. & Kling, C. L. (2014*b*), 'Reversing Property Rights: Practice-based Approaches for Controlling Agricultural Nonpoint-source Water Pollution when Emissions Aggregate Nonlinearly', *American Journal of Agricultural Eco-nomics* **96**(2), 397–419.

Racsko, P., Szeidl, L. & Semenov, M. (1991), 'A Serial Approach to Local Stochastic Weather Models', *Ecological Modelling* **57**(1-2), 27–41.

Radersma, S. & Smit, A. (2011), 'Assessing Denitrification and N Leaching in A Field with Organic Amendments', *NJAS-Wageningen Journal of Life Sciences* **58**(1-2), 21–29.

Rajsic, P. & Weersink, A. (2008), 'Do Farmers Waste Fertilizer? A Comparison of Ex-post Optimal Nitrogen Rates and Ex-ante Recommendations by Model, Site and Year', *Agricultural Systems* **97**(1), 56–67.

Rajsic, P., Weersink, A. & Gandorfer, M. (2009), 'Risk and Nitrogen Application Levels', *Canadian Journal of Agricultural Economics* **57**(2), 223–239.

Ramaswami, B. (1992), 'Production Risk and Optimal Input Decisions', *American Journal of Agricultural Economics* **74**(4), 860–869.

Richardson, C. W. (1981), 'Stochastic Simulation of Daily Precipitation, Temperature, and Solar Radiation', *Water Resources Research* **17**(1), 182–190.

Richardson, C. W. & Wright, D. A. (1984), 'WGEN: A Model for Generating Daily Weather Variables'.

Ritchie, H. (2021), Can We Reduce Fertilizer Use Without Sacrificing Food Production?, Technical report, Our World in Data. https://ourworldindata.org/reducing-fertilizer-use.

Roberts, M. J., Braun, N. O., Sinclair, T. R., Lobell, D. B. & Schlenker, W. (2017), 'Comparing and Combining Process-based Crop Models and Statistical Models with Some Implications for Climate Change', *Environmental Research Letters* **12**(9), 095010.

Roberts, M. J., Schlenker, W. & Eyer, J. (2012), 'Agronomic Weather Measures in Econometric Models of Crop Yield with Implications for Climate Change', *American Journal of Agricultural Economics* **95**(2), 236–243.

Roldan, J. & Woolhiser, D. A. (1982), 'Stochastic Daily Precipitation Models: 1. a Comparison of Occurrence Processes', *Water Resources Research* **18**(5), 1451–1459.

Ross, S. M. (2014), *Introduction to Probability Models*, Academic press.

Roth, R. T., Ruffatti, M. D., O'Rourke, P. D. & Armstrong, S. D. (2018), 'A Cost Analysis Approach to Valuing Cover Crop Environmental and Nitrogen Cycling Benefits: A Central Illinois On-farm Case Study', *Agricultural Systems* **159**, 69–77.

Roy, A. K., Wagner-Riddle, C., Deen, B., Lauzon, J. & Bruulsema, T. (2014), 'Nitrogen Application Rate, Timing and History Effects on Nitrous Oxide Emissions from Corn (Zea mays L.)', *Canadian Journal of Soil Science* **94**(4), 563–573.

Sanusi, W., Jemain, A. A., Zin, W. Z. W. & Zahari, M. (2015), 'The Drought Characteristics Using the First-order Homogeneous Markov Chain of Monthly Rainfall Data in Peninsular Malaysia', *Water Resources Management* **29**(5), 1523–1539.

Sawyer, J. (2003), Pay Attention to Management Needs of Fertilizer Products, Technical report, Wiley Online Library.

Sawyer, J. (2008), Estimating Nitrogen Losses, Technical report, Iowa State University Extension and Outreach. URL=https://crops.extension.iastate.edu/search/content.

Schlegel, A. J. & Havlin, J. L. (2017), 'Corn Yield and Grain Nutrient Uptake from 50 years of Nitrogen and Phosphorus Fertilization', *Agronomy Journal* **109**(1), 335–342.

Schlenker, W. & Roberts, M. J. (2006), 'Nonlinear Effects of Weather on Corn Yields', *Review of Agricultural Economics* **28**(3), 391–398.

Schmid, D., Korkmaz, P., Blesl, M., Fahl, U. & Friedrich, R. (2019), 'Analyzing Transformation Pathways to a Sustainable European Energy System—Internalization of Health Damage Costs Caused by Air Pollution', *Energy Strategy Reviews* **26**, 100417.

Schmitz, A., Wang, Z. & Kimn, J.-H. (2014), 'A Jump Diffusion Model for Agricultural Commodities with Bayesian Analysis', *Journal of Futures Markets* **34**(3), 235–260.

Schoof, J. & Pryor, S. (2008), 'On the Proper Order of Markov Chain Model for Daily Precipitation Occurrence in the Contiguous United States', *Journal of Applied Meteorology and Climatology* **47**(9), 2477–2486.

Schwartz, E. S. (1997), 'The Stochastic Behavior of Commodity Prices: Implications for Valuation and Hedging', *The Journal of Finance* **52**(3), 923–973.

Sellars, S. (2019), Cost and Returns from Different Nitrogen Application Timing in Illinois, Technical report, Department of Agricultural and Consumer Economics, University of Illinois. https://farmdocdaily.illinois.edu/2019/11/cost-and-returns-from-different-nitrogen-application-timing-in-illinois.html.

Semaan, J., Flichman, G., Scardigno, A. & Steduto, P. (2007), 'Analysis of Nitrate Pollution Control Policies in the Irrigated Agriculture of Apulia Region (Southern Italy): A Bio-economic Modelling Approach', *Agricultural Systems* **94**(2), 357–367.

Semenov, M. A., Brooks, R. J., Barrow, E. M. & Richardson, C. W. (1998), 'Comparison of the WGEN and LARS-WG Stochastic Weather Generators for Diverse Climates', *Climate Research* **10**(2), 95–107.

Semenov, M. & Barrow, E. (2002), 'LARS-WG: A Stochastic Weather Generator for Use in Climate Impact Studies, Version 3, User Manual'.

Shaik, S., Helmers, G. A. & Langemeier, M. R. (2002), 'Direct and Indirect Shadow Price and Cost Estimates of Nitrogen Pollution Abatement', *Journal of Agricultural and Resource Economics* pp. 420–432.

Sheriff, G. (2005), 'Efficient Waste? Why Farmers Over-apply Nutrients and the Implications for Policy Design', *Review of Agricultural Economics* **27**(4), 542–557.

Shi, C.-l., GUO, Y. & ZHU, J.-f. (2016), 'Evaluation of Over Fertilization in China and Its Influencing Factors', *Research of Agricultural Modernization* **4**, 009.

Shi, W., Tao, F. & Zhang, Z. (2013), 'A Review on Statistical Models for Identifying Climate Contributions to Crop Yields', *Journal of Geographical Sciences* **23**(3), 567–576.

Shortle, J. S. & Dunn, J. W. (1986), 'The Relative Efficiency of Agricultural Source Water Pollution Control Policies', *American Journal of Agricultural Economics* **68**(3), 668–677.

Shortle, J. S. & Horan, R. D. (2001), 'The Economics of Nonpoint Pollution Control', *Journal of economic surveys* **15**(3), 255–289.

Sihvonen, M., Pihlainen, S., Lai, T.-Y., Salo, T. & Hyytiäinen, K. (2021), 'Crop Production, Water Pollution, or Climate Change Mitigation—Which Drives Socially Optimal Fertilization Management Most?', *Agricultural Systems* **186**, 102985.

Sitthaphanit, S., Limpinuntana, V., Toomsan, B., Panchaban, S. & Bell, R. (2009), 'Fertilizer Strategies for Improved Nutrient Use Efficiency on Sandy Soils in High Rainfall Regimes', *Nutrient Cycling in Agroecosystems* **85**(2), 123–139.

Skiba, U. (2008), 'Denitrification'.

Smil, V. (1997), 'China's Environment and Security: Simple Myths and Complex Realities', *SAIS Review* **17**(1), 107–126.

Smith, E. G., Card, G. & Young, D. L. (2006), 'Effects of Market and Regulatory Changes on Livestock Manure Management in Southern Alberta', *Canadian Journal of Agricultural Economics* **54**(2), 199–213.

Song, F., Zhao, J. & Swinton, S. M. (2011), 'Switching to Perennial Energy Crops under Uncertainty and Costly Reversibility', *American Journal of Agricultural Economics* **93**(3), 768–783.

SriRamaratnam, S., Bessler, D. A., Rister, M. E., Matocha, J. E. & Novak, J. (1987), 'Fertilization under Uncertainty: An Analysis Based on Producer Yield Expectations', *American Journal of Agricultural Economics* **69**(2), 349–357.

Stöckle, C., Campbell, G. S. & Nelson, R. (1999), 'ClimGen Manual', *Biological Systems Engineering Department, Washington State University, Pullman, WA* p. 28.

Su, X., Wang, H. & Zhang, Y. (2013), 'Health Risk Assessment of Nitrate Contamination in Groundwater: a Case Study of an Agricultural Area in Northeast China', *Water resources management* **27**(8), 3025–3034.

Sun, B. & van Kooten, G. C. (2015), 'Financial Weather Derivatives for Corn Production in Northern China: A Comparison of Pricing Methods', *Journal of Empirical Finance* **32**, 201–209.

Sun, B., Zhang, L., Yang, L., Zhang, F., Norse, D. & Zhu, Z. (2012), 'Agricultural Non-point Source Pollution in China: Causes and Mitigation Measures', *Ambio* **41**(4), 370–379.

Sunantara, B. J. D. & Ramírez, J. A. (1997), 'Optimal Stochastic Multi-crop seasonal and Intra-seasonal Irrigation Control', *Journal of Water Resources Planning and Management* **123**(1), 39–48.

Tadesse, A. & Kim, H. K. (2014), 'Yield Related Traits and Yield of Quality Protein Maize (Zea mays L.) Affected by Nitrogen Levels to Achieve Maximum Yield in the Central Rift Valley of Ethiopia', *Journal of Biology, Agriculture and Healthcare* **5**(15), 139–148.

Tanaka, K. & Wu, J. (2004), 'Evaluating the Effect of Conservation Policies on Agricultural Land Use: A Site-specific Modeling Approach', *Canadian Journal of Agricultural Economics* **52**(3), 217–235.

Tang, C., Lade, G. E., Keiser, D., Kling, C., Ji, Y. & Shr, Y.-H. (2018), 'Economic Benefits of Nitrogen Reductions in Iowa'.

Tang, K., Gong, C. & Wang, D. (2016), 'Reduction Potential, Shadow Prices, and Pollution Costs of Agricultural Pollutants in China', *Science of the Total Environment* **541**, 42–50.

Tao, F., Xiao, D., Zhang, S., Zhang, Z. & Rötter, R. P. (2017), 'Wheat Yield Benefited from Increases in Minimum Temperature in The Huang-Huai-Hai Plain of China in The Past Three Decades', *Agricultural and Forest Meteorology* **239**, 1–14.

Tao, Y., Wei, M., Ongley, E., Li, Z. & Jingsheng, C. (2010), 'Long-term Variations and Causal Factors in Nitrogen and Phosphorus Transport in the Yellow River, China', *Estuarine, Coastal and Shelf Science* **86**(3), 345–351.

Todorovic, P. & Woolhiser, D. A. (1975), 'A Stochastic Model of n-day Precipitation', *Journal of Applied Meteorology* **14**(1), 17–24.

Torbert, H. A., Potter, K. N., Hoffman, D. W., Gerik, T. J. & Richardson, C. (1999), 'Surface Residue and Soil Moisture Affect Fertilizer Loss in Simulated Runoff on a Heavy Clay Soil', *Agronomy Journal* **91**(4), 606–612.

Turvey, C. G. (2001), 'Weather Derivatives for Specific Event Risks in Agriculture', *Review of Agricultural Economics* **23**(2), 333–351.

Turvey, C. G. (2005), 'The Pricing of Degree-day Weather Options', *Agricultural Finance Review* **65**(1), 59–85.

U.S.EPA (2001), 'Environmental and Economic Benefit Analysis of Proposed Revisions to the National Pollutant Discharge Elimination System Regulation and the Effluent Guidelines for Concentrated Animal Feeding Operations', *U.S. Environmental Protection Agency* **20460**.

Van der Paauw, F. (1962), 'Effect of Winter Rainfall on the Amount of Nitrogen Available to Crops', *Plant and Soil* **16**(3), 361–380.

Van der Vlist, A. J., Withagen, C. & Folmer, H. (2007), 'Technical Efficiency under Alternative Environmental Regulatory Regimes: the Case of Dutch Horticulture', *Ecological Economics* **63**(1), 165–173.

van Grinsven, H. J., Rabl, A. & de Kok, T. M. (2010), 'Estimation of Incidence and Social Cost of Colon Cancer Due to Nitrate in Drinking Water in the EU: A Tentative Cost-benefit Assessment', *Environmental health* **9**(1), 1–12.

Van Houtven, G., Mansfield, C., Phaneuf, D. J., von Haefen, R., Milstead, B., Kenney, M. A. & Reckhow, K. H. (2014), 'Combining Expert Elicitation and Stated Preference Methods to Value Ecosystem Services from Improved Lake Water Quality', *Ecological Economics* **99**, 40–52.

Vanotti, M. & Bundy, L. (1994), 'An Alternative Rationale for Corn Nitrogen Fertilizer Recommendations', *Journal of Production Agriculture* **7**(2), 243–249.

Vedachalam, S., Mandelia, A. & Heath, E. (2018*a*), 'Source Water Quality and the Cost of Nitrate Treatment in the Mississippi River Basin, Northeast-Midwest Institute Report'.

Vedachalam, S., Mandelia, A. & Heath, E. (2018*b*), 'Source Water Quality and the Cost of Nitrate Treatment in the Mississippi River Basin, Northeast-Midwest Institute Report, 44 pp'.

Vercammen, J. (2011), 'Agri-Environmental Regulations, Policies, and Programs', *Canadian Journal of Agricultural Economics* **59**(1), 1–18.

Wang, X. (2006), 'Management of Agricultural Nonpoint Source Pollution in China: Current Status and Challenges', *Water Science and Technology* **53**(2), 1–9.

Wang, Z., Li, P., Li, L., Huang, C. & Liu, M. (2015), 'Modeling and Forecasting Average Temperature for Weather Derivative Pricing', *Advances in Meteorology* **2015**.

Welch, H. L., Green, C. T. & Coupe, R. H. (2011), 'The Fate and Transport of Nitrate in Shallow Groundwater in Northwestern Mississippi, USA', *Hydrogeology Journal* **19**(6), 1239–1252.

Wheeler, T. R., Craufurd, P. Q., Ellis, R. H., Porter, J. R. & Prasad, P. V. (2000), 'Temperature Variability and The Yield of Annual Crops', *Agriculture, Ecosystems and Environment* **82**(1-3), 159–167.

Whitman, C. et al. (2002), The Benefits of Reducing Nitrate Contamination in Private Domestic Wells under CAFO Regulatory Options, Technical report, EPA-821-R-03-008.

Wilks, D. S. (1999*a*), 'Interannual Variability and Extreme-value Characteristics of Several Stochastic Daily Precipitation Models', *Agricultural and Forest Meteorology* **93**(3), 153–169.

Wilks, D. S. (1999*b*), 'Multisite Downscaling of Daily Precipitation with a Stochastic Weather Generator', *Climate Research* **11**(2), 125–136.

Wilks, D. S. & Wilby, R. L. (1999), 'The Weather Generation Game: A Review of Stochastic Weather Models', *Progress in Physical Geography* **23**(3), 329–357.

Willcutts, J. F., Overman, A. R., Hochmuth, G. J., Cantliffe, D. J. & Soundy, P. (1998), 'A Comparison of Three Mathematical Models of Response to Applied Nitrogen: A Case Study Using Lettuce', *HortScience* **33**(5), 833–836.

Woolhiser, D. A. & Roldan, J. (1982), 'Stochastic Daily Precipitation Models: A Comparison of Distributions of Amounts', *Water Resources Research* **18**(5), 1461–1468.

Wortmann, C., Al-Kaisi, M., Helmers, M., Sawyer, J., Devlin, D., Barden, C., Scharf, P., Ferguson, R., Kranz, W., Shapiro, C. et al. (2013), 'Agricultural Nitrogen Management for Water Quality Protection in the Midwest', *Heartland Regional Water Coordination Initiative Report* **189**.

Xepapadeas, A. (2011), 'The Economics of Nonpoint-source Pollution', *Annu. Rev. Resour. Econ.* **3**(1), 355–373.

Xue, J., Zhao, S., Zhao, L., Zhu, D. & Mao, S. (2020), 'Cooperative Governance of Interprovincial air pollution based on a Black-Scholes Options Pricing Model', *Journal of Cleaner Production* **277**, 124031.

Yadav, S. N. (1997*a*), 'Dynamic Optimization of Nitrogen Use when Groundwater Contamination is Internalized at The Standard in The Long Run', *American Journal of Agricultural Economics* **79**(3), 931–945.

Yadav, S. N. (1997*b*), Formulation and Estimation of Nitrate-Nitrogen Leaching from Corn Cultivation, Technical report, Wiley Online Library.

Yu, Y., Xu, J., Zhang, P., Meng, Y. & Xiong, Y. (2021), 'Controlled Irrigation and Drainage Re-duce Rainfall Runoff and Nitrogen Loss in Paddy Fields', *International Journal of Environmental Research and Public Health* **18**(7), 3348.

Yuan, X. (2000), 'Primary Appraisal of Pollution for Lakes of China', *Volcanology and Mineral Resources* **21**(2), 128–136.

Yusuf, A. U., Adamu, L. & Abdullahi, M. (2014), 'Markov Chain Model and Its Application to Annual Rainfall Distribution for Crop Production', *American Journal of Theoretical and Applied Statistics* **3**(2), 39–43.

Zhao, B., Li, X., Liu, H., Wang, B., Zhu, P., Huang, S., Bao, D., Li, Y. & So, H. (2011), 'Results from Long-term Fertilizer Experiments in China: The Risk of Groundwater Pollution by Nitrate', *NJAS-Wageningen Journal of Life Sciences* **58**(3-4), 177–183.

APPENDICES

Appendix A

Nutrient management practices and policies in Iowa and Ontario

In this appendix, an overview of main nutrient management practices and policies in Iowa and Ontario is presented. A wide range of BMPs have been developed by US Environmental Protection Agency to reduce water pollution from agricultural, which includes conservation tillage, crop nutrient management, pest management, irrigation management, erosion control and conservation buffers. In Iowa for example, to reduce the loading of nitrogen and phosphorus in water bodies, nutrient management programs are implemented at the county level, which include Iowa 4R and 4R Plus nutrient stewardship practices[1] and Iowa Nutrient Reduction Strategy (INRS)[2].

[1] 4R: the right source applied at the right rate and the right time, in the right place. Launched by a grant from chemical fertilizer industries in Iowa, 4R Plus is being guided by a coalition of agricultural and conservation organizations as a part of the Iowa 4R program to support farmers' efforts to implement precise nutrient management and conservation practices that boost soil health, crop productivity, and profitability.

[2] In 2013, the state of Iowa released the Iowa Nutrient Reduction Strategy, including the science and technology assessments for both non-point and point source pollution. The strategy document highlights numerous pathways through which farmers and agricultural stakeholders can take action toward attainment of those objectives, including prioritization of watersheds, determine watershed goals and ensure effectiveness of nutrient permits.

The Iowa Nutrient Reduction Strategy (INRS) is a science and technology-based framework to assess and reduce nutrients to Iowa waters and the Gulf of Mexico. It made efforts to reduce nutrients in surface water from both point and nonpoint sources in a scientific, reasonable, and cost-effective manner. According to Iowa State University Extension and Outreach[3], INRS established a number of conservation options that reduce N and P loss ranging from in-field fertilizer and soil management practices to strategic conversion of row crop acres to perennial systems. The INRS identifies practices as follows.

- **In-field management practices** are annual management practices including cover crops, reduced and no-tillage, and fertilizer management.
- **Edge-of-field and erosion control practices** are structural practices or vegetation that prevent nitrate and/or eroded soil from leaving the field and entering nearby surface water or subsurface drainage. These practices include bioreactors, saturated buffers, terraces, and nutrient removal wetlands.
- **Land use change** is the practice that incorporate additional crops or convert row crops to perennial vegetation, which include extended rotations, conversion to pasture or prairie, and perennial bio-energy crops.

According to Iowa Nutrient Reduction Strategy 2018-19 Annual Progress Report[4], several changes in statewide efforts toward meeting the INRS goals including acres of various conservation practices such as cover crops, tillage, are made. For instance, cover crops planted in Iowa increased from 379000 acres in fall 2011 to 973000 in fall 2016. No-tillage acreage increased from 6.9 million acres in 2012 to 8.2 million in 2017. Iowa has 86 nitrate-removal wetlands that treat 107000 acres, an additional 30 wetlands are currently under

[3]See details in "Measuring Conservation and Nutrient Reduction in Iowa Agriculture". https://crops.extension.iastate.edu/cropnews/2020/07/measuring-conservation-and-nutrient-reduction-iowa-agriculture

[4]Report was published by Iowa State University, Iowa Department of Agriculture and Land Stewardship and Iowa Department of Natural Resources. Source: *https* : *//store.extension.iastate.edu/product*/15915

development for completion in the coming years. Since 2011, approximately 22.5 million feet of terraces have been constructed using state cost-share funds. These terraces treated 174000 acres of land and reduced phosphorus losses by 40 tons in 2018.

In addition, Iowa, Illinois, Minnesota, Wisconsin, Indiana, Michigan, and Ohio have adopted updated corn N fertilizer rate recommendations that are based on extensive N response trials conducted over several years in each state. These trials have determined the N rate at which the last pound of added nitrogen fertilizer returns a yield increase large enough to pay for the cost of the additional fertilizer. This approach, called the maximum return to nitrogen (MRTN) which considers the region where the fields are located and soil characteristics, the price of corn, and the price of fertilizer.

Across Canada, programs are implemented at and across multiple levels. In Ontario for example, these include: farm-level nutrient management plans; Municipal nutrient management by-laws; Watershed strategies such as Domestic Action Plans under development for the Lake Erie basin; Provincial legislation and International agreements such as the Great Lakes Agreement between Canada and U.S. In particular, OMAFRA has created a series of publications describing Best Management Practices and Nutrient Management Practice for agriculture[5]. These BMP guide books can help growers determine what nutrients they need and how to apply them for maximum efficiency and minimal risk to the environment. For example, OMAFRA has made up an agronomy guide for field crops including soil managing, nutrient use and soil fertility tests (Table 1-18 and 1-19, OMAFRA (2017*a*)). In this guide, OMAFRA has a detailed suggestion on the soil sampling time, how to deal with soil tests, and give a nitrogen guidelines based on soil test results. Actual nitrogen suggestions are decreasing with the increased nitrate-nitrogen concentration level from tested soil. Even more specific, OMAFRA has made nitrogen guidelines based on

[5]The complete series of Best Management Practices (BMP library) by OMAFRA can be obtained from http://www.omafra.gov.on.ca/english/environment/bmp/series.htm

pre-side-dress nitrate-nitrogen levels from soil. However, such nitrogen recommendations do not rely on the type of crop, but on the soil test results.

The Nutrient Management Act in Ontario (O.Reg 267/03 and O.Reg 338/09[6]) has defined the legally maximum application rules for different types of fertilizer and soil types. The act specifies detailed reporting requirements referred to as Nutrient Management Strategies (NMS) and Nutrient Management Plans (NMP). A Nutrient Management Strategy is applicable to manure management for farming operations with five or more nutrient units. As a rough guide, this would represent about 15 head of cattle being raised for beef. An NMP outlines "nutrient applications in farm fields, crop rotation, tillage, projected yields and other management approaches to optimize the utilization of nutrients by the crops." (OMAFRA, 2018)[7]. A farm is required to have an NMP when it has livestock greater than or equal to 300 nutrient units (about 900 head of beef cattle) or it is a phased-in farm (i.e. required to have a NMS) and is located within 100 metres of a municipal well. As an example of limitations of nutrient application, the maximum land nitrogen application is regulated by O.Reg 267/03 and O.Reg 338/09 as:

(1) The maximum application rate to land with reference to plant available nitrogen is a rate such that the plant available nitrogen that is applied to the land per hectare, for any 12-month period, does not exceed the lesser of,

(a) the quantity determined under subsection (2); and

(b) 200 kilograms per hectare.

(2) The quantity for the purposes of clause (1) (a) is the greater of,

(a) the crop production requirements for nitrogen, minus plant available nitrogen sup-

[6]Nutrient Management Act, 2002. Source: https://www.ontario.ca/laws/regulation/030267#BK4

[7]"Ontario Nutrient Management Act, 2002, Understanding when farms require and NMS, NMP or NASM Plan", Fact Sheet Agdex720/538, Publication Date: March 2018. http://www.omafra.gov.on.ca/english/engineer/facts/18-009.htm#NMS)

plied by other nutrient sources; and

(b) the quantity of nitrogen removed from the field in the harvested portion of the crop, minus plant available nitrogen supplied by other nutrient sources.

(3) the plant available nitrogen shall be calculated in accordance with the formula for plant available nitrogen in Nutrient Management Protocol.

Correspondingly, agricultural planning tools (NMAN and MDS[8]) were developed by the Ministry of Agriculture, Food and Rural Affairs (OMAFRA) to deliver farmers nutrient management strategies and plans, demonstrating compliance with the Nutrient Management Act and its protocols. For example, crop growers can use these tools to create agricultural or field management plans by calculating the estimated on-farm nutrient generation, the required nutrient storage they need and nutrient application rates that will maximize crop production. All nutrient management plans must be filed with OMAFRA and renewed every five years[9]. For all prescribed materials (such as manure and fertilizers) destined to be land applied on farm units, the nutrient management plan requires detailed information, including the type and quantity of prescribed material, the date farm units received those materials, etc. Further, all prescribed materials intended for land application must meet the quality standards by providing laboratory nutrient analysis. Farm-level field properties must also be reported in the nutrient management plan for each farm unit. Besides, the nutrient management plan needs a specified report on farm-level soil sampling, tillage practices and nutrient application. Specifically, the nutrient application method, timing and frequency must be reported in the nutrient management plan (NMP). A rate of application for each prescribed material intended to be applied to land must be determined

[8] AgriSuite is a web application that hosts OMAFRA's nutrient management planning software, called NMAN, and the Minimum Distance Separation (MDS) Formulae software. http://www.omafra.gov.on.ca/english/nm/nman/agrisuite.htm

[9] "Nutrient Management Protocol for Ontario Regulation 267/03 Made under the Nutrient Management Act", OMAFRA, 2002. http://www.omafra.gov.on.ca/english/nm/regs/nmpro/nmpro07-jun03.htm#1

for each part of the land managed in the farm unit (for example, each field). Application rates are based on many factors including: the characteristics of the land, and cropping and nutrient information set out in the nutrient management plan.

In summary, Ontario legislation specifies maximum allowed fertilizer application on fields. In addition, farms meeting certain criteria regarding livestock production and nearness to municipal wells must complete Nutrient Management Strategies and Nutrient Management Plans, which are subject to approval by OMAFRA. Fertilizer recommendations tend to be based on yield goals, and in some documents soil fertility is not considered. In other documents, recommendations are based on soil fertility as indicated by soil test results. Current recommendations do not appear to account for weather uncertainty and do not consider the economically optimal fertilizer application.

Appendix B

Deriving the expectation of the GBM process

In this appendix, we formally derive the expectation of the GBM process. Assuming the GBM process is

$$dP_t = \mu P_t dt + \sigma_1 P_t dZ_t$$

In order to solve for $P(t)$, we apply Ito's lemma to $dlnP(t)$

$$dlnP(t) = \mu dt + \sigma_1 dZ_t - \frac{1}{2}\sigma_1^2 dt$$

Then we integrate between $[0, t]$ to get:

$$lnP(t) - lnP(0) = (\mu - \frac{1}{2}\sigma_1^2)t + \sigma_1[Z(t) - Z(0)]$$

$$P(t) = P(0)e^{(\mu - \frac{1}{2}\sigma_1^2)t + \sigma_1[Z(t) - Z(0)]}$$

We now take the expectation of the above expression, with $Z(0) = 0$:

$$E[P(t)] = E[P(0)e^{(\mu - \frac{1}{2}\sigma_1^2)t + \sigma_1 Z_t}]$$

$$= P(0)e^{(\mu - \frac{1}{2}\sigma_1^2)t} E[e^{\sigma_1 Z_t}]$$

$$= P(0)e^{(\mu - \frac{1}{2}\sigma_1^2)t} e^{\frac{1}{2}\sigma_1^2 t}$$

$$E[P(t)] = P(0)e^{\mu t}$$

Appendix C

Contrasting $\mathbb{P}$-measure and $\mathbb{Q}$-measure valuation framework

In this appendix, we review the two approaches to asset valuation commonly used in the literature. This section is based on Dixit et al. (1994) and Insley & Wirjanto (2010). One approach uses $\mathbb{Q}$-measure Contingent Claims (CC) arguments which is based on the risk-neutral valuation framework. The other approach is the $\mathbb{P}$-measure Dynamic Programming (DP) with a risk-adjust discount rate instead of risk-free interest. To contrast both approaches, we first define the value of farming one growth cycle as $V(P,t)$. Crop price follows the general unadjusted Ito's process:

$$dP = a(P,t)dt + b(P,t)dZ = adt + bdZ \tag{C.1}$$

For the GBM process:

$$dP = adt + bdZ = \alpha Pdt + \sigma PdZ$$

For the MR process:

$$dP = adt + bdZ = \theta\left(\bar{P} - P\right)dt + \sigma P dZ$$

Under dynamic programming, we form the HJB equation and solve the value of a project by backward induction using a risk adjusted discount rate. CC allows us to construct a risk free portfolio consisting of underlying risky project and another asset or contract which tracks the underlying's uncertainty. This paper use CC more than DP for the reason that CC is preferred when market data is accessible which allows us to estimate the market price of risk. Another advantage of using CC is we could avoid estimating the risk adjusted discount rate by using constant risk free rate.

C.1 Dynamic programming $\mathbb{P}$-measure approach

The value of farming V depends on the crop price P. Employing the dynamic programming method, we need to use the risk-adjusted discount rate ζ and $\mathbb{P}$-measure price process Equation (2.4). By Ito's lemma,

$$dV = \left(V_t + aV_P + \frac{1}{2}b^2 V_{PP}\right)dt + bV_P dZ$$

where $V_t = \frac{\partial V}{\partial t}$, $V_P = \frac{\partial V}{\partial P}$, $V_{PP} = \frac{\partial^2 V}{\partial P^2}$, $a = a(P,t)$, $b = b(P,t)$. Using risk-adjusted discount rate (or return rate) ζ, we could write the partial differential equation (PDE) that derived from the equilibrium condition that $E(dV) = \zeta V dt$

$$\zeta V = V_t + aV_P + \frac{1}{2}b^2 V_{PP} \tag{C.2}$$

The difficulty with using dynamic programming approach is in determining the appropriate value for ζ. Once using dynamic programming, we would not expect ζ to be a constant as it will depend on the ratio $\frac{V_P}{V}$.

C.2 Contingent claims $\mathbb{Q}$-measure approach

Contingent Claims approach assumes we have access to asset markets that are sufficiently complete so that price risk can be eliminated through hedging with another risky asset or contract. We also assume no arbitrage principle when using this approach. We denote the value of farming by V_1, the value of another hedging asset or contract that depends on crop price (e.g. share of ownership of the underlying farmland) by V_2. The value of our hedging portfolio with n_1 of V_1, n_2 of V_2 is $\pi = n_1 V_1 + n_2 V_2$. Then $d\pi = n_1 dV_1 + n_2 dV_2$. By Ito's lemma, for $i = 1, 2$:

$$dV_i = \left((V_i)_t + a(V_i)_P + \frac{1}{2} b^2 (V_i)_{PP} \right) dt + b(V_i)_P dZ$$

Rewriting above process into

$$\frac{dV_i}{V_i} = \left((V_i)_t + a(V_i)_P + \frac{1}{2} b^2 (V_i)_{PP} \right) \frac{1}{V_i} dt + \frac{b}{V_i} (V_i)_P dZ = \mu_i dt + s_i dz$$

where

$$\mu_i = \left((V_i)_t + a(V_i)_P + \frac{1}{2} b^2 (V_i)_{PP} \right) \frac{1}{V_i} \tag{C.3}$$

$$s_i = \frac{b}{V_i} (V_i)_P \tag{C.4}$$

Now, to eliminate price risk in this portfolio, we choose n_1, n_2 such that the following

is satisfied:

$$n_1 s_1 V_1 + n_2 s_2 V_2 = n_1 b(V_1)_P + n_2 b(V_2)_P = 0 \tag{C.5}$$

which means the risk term dZ is eliminated in our hedging strategy. Without price risk, the portfolio π must earn a constant risk-free return r, which implies $d\pi = r\pi dt$.

Combining dV_1, dV_2, π and Equation (C.5), we form a 2-by-2 linear system equations:

$$\begin{cases} n_1(\mu_1 V_1 - rV_1) + n_2(\mu_2 V_2 - rV_2) = 0 \\ n_1 b(V_1)_P + n_2 b(V_2)_P = 0 \end{cases}$$

Solving the homogeneous system equations, we can define a constant

$$\lambda_P = \frac{(\mu_1 - r)V_1}{b(V_1)_P} = \frac{\mu_1 - r}{s_1} = \frac{\mu_2 - r}{s_2} \tag{C.6}$$

λ_P is called market price of risk of P and represents the excess return over the risk free rate per unit of variability. Then $\lambda_P \sigma$ is the total value obtained from uncertainty. Dropping the subscript $i = 1, 2$, we obtain the following PDE using the above result (C.6):

$$\lambda_P \frac{b}{V} V_P = \frac{1}{V}(V_t + aV_P + \frac{1}{2}b^2 V_{PP}) - r$$

which evolves to the PDE:

$$rV = V_t + (a - \lambda_P b)V_P + \frac{1}{2}b^2 V_{PP} \tag{C.7}$$

The term $a - \lambda_P b = a(P,t) - \lambda_P b(P,t)$ is the risk adjusted drift rate that reflects the extra return required to compensate for price risk. The PDE must be satisfied by the value of farming and assuming that price uncertainty could be hedged. This could be compared with the PDE which can be derived assuming no risk hedging and earn a risk-adjusted

return ζ.

Specifically, to make results from two approaches are equivalent, we set the correct risk adjusted discount rate $\zeta = r + \lambda_P s$ where $s = \frac{b(P,t)}{V} V_P$. This rate should change with the value of project. Under certain simplifying assumptions the risk adjusted discount rate will be constant: $\zeta = r + \lambda_P \sigma$.

Appendix D

Proofs of sensitivity analysis in Section 2.4

In this appendix, we provide proofs of associated sensitivity analysis in Chapter 2. First, to provide a proof of the negative price uncertainty effect ($\frac{\partial N_{\mathbb{Q}}^{\star mr}}{\partial(\lambda_P\sigma)} < 0$) in Chapter 2, we take the first order derivative on Equation (2.21) and get:

$$\frac{\partial N_{\mathbb{Q}}^{\star mr}}{\partial(\lambda_P\sigma)} = -\frac{c}{2a_1}\frac{P_0e^{-(\theta+r+\lambda_P\sigma)T}(-T) + \left(e^{-rT} - e^{-(\theta+r+\lambda_P\sigma)T}\right)\frac{-\bar{P}\theta}{(\theta+\lambda_P\sigma)^2} + \frac{\bar{P}\theta}{\theta+\lambda_P\sigma}\left(Te^{-(\theta+r+\lambda_P\sigma)T}\right)}{\left[P_0e^{-(\theta+r+\lambda_P\sigma)T} + \frac{\bar{P}\theta}{\theta+\lambda_P\sigma}\left(e^{-rT} - e^{-(\theta+r+\lambda_P\sigma)T}\right)\right]^2}$$

After rearranging the above equation, the sign of above equation is the same with the sign of the following part

$$-P_0T - \left(e^{(\theta+\lambda_P\sigma)T} - 1\right)\frac{\bar{P}\theta}{(\theta+\lambda_P\sigma)^2} + \frac{\bar{P}\theta}{\theta+\lambda_P\sigma}T \tag{D.1}$$

which is

$$-P_0T + \frac{\bar{P}\theta}{(\theta+\lambda_P\sigma)}\left[\frac{-\left(e^{(\theta+\lambda_P\sigma)T} - 1\right)}{(\theta+\lambda_P\sigma)} + T\right] \tag{D.2}$$

Now, we can use Taylor expansion $e^x - 1 = x + R_n$, for the term $\frac{-\left(e^{(\theta+\lambda_P\sigma)T}-1\right)}{(\theta+\lambda_P\sigma)}$ in Equation (D.2), where $x = (\theta+\lambda_P\sigma)T$ and R_n is the remainder term. Given that the mean reverting speed $\theta > 0$ and market price of risk $\lambda_P > 0$, we have the remainder $R_n > 0$. Substituting $e^x - 1 = x + R_n$ and $x = (\theta + \lambda_P\sigma)T$ into Equation (D.2),

$$-P_0T - \frac{T\bar{P}\theta}{x}\left[\frac{(x+R_n)T}{x} - T\right] = -P_0T - \frac{T\bar{P}\theta}{x}\frac{R_nT}{x}$$

With $R_n > 0$, $\theta > 0$, $x > 0$, $\bar{P} > 0$, $P_0 > 0$ and $T > 0$, we have Equation (D.2) is negative, which equivalents to $\frac{\partial N_{\mathbb{Q}}^{\star mr}}{\partial(\lambda_P\sigma)} < 0$. Therefore, by assuming $\lambda_P > 0$, we can conclude that

$$\frac{\partial N_{\mathbb{Q}}^{\star mr}}{\partial\sigma} < 0$$

To measure the effect of the mean reverting speed θ on $N_{\mathbb{Q}}^{\star mr}$, we take the first order derivative for $N_{\mathbb{Q}}^{\star mr}$ with respect to θ:

$$\frac{\partial N_{\mathbb{Q}}^{\star mr}}{\partial\theta} = \underbrace{\frac{c}{2a_1}\left[-\frac{1}{\left(e^{-(\theta+r+\lambda_P\sigma)T}(p_0 - \frac{\bar{P}\theta}{\theta+\lambda_P\sigma}) + \frac{\bar{P}\theta}{\theta+\lambda_P\sigma}e^{-rT}\right)^2}\right]}_{>0} \underbrace{\left[e^{-rT}\left(\frac{\bar{P}}{\theta+\lambda_P\sigma} - \frac{\bar{P}\theta}{(\theta+\lambda_P\sigma)^2}\right)\right.}_{\text{A}}$$

$$\underbrace{\left. + \left(p_0 - \frac{\bar{P}\theta}{\theta+\lambda_P\sigma}\right)e^{-(\theta+r+\lambda_P\sigma)T}(-T) + e^{-(\theta+r+\lambda_P\sigma)T}\left(-\frac{\bar{P}}{\theta+\lambda_P\sigma} + \frac{\bar{P}\theta}{(\theta+\lambda_P\sigma)^2}\right)\right]}_{\text{A}}$$

Since $a_1 < 0$,$c > 0$, the sign of A is identical to the sign of $\frac{\partial N_{\mathbb{Q}}^{\star mr}}{\partial\theta}$. After rearrangement of A, we can have

$$A = e^{-rT}\frac{1}{(\theta+\lambda_P\sigma)^2}\underbrace{\left[\bar{P}\lambda_P\sigma + e^{-(\theta+\lambda_P\sigma)T}\left(-\bar{P}\lambda_P\sigma - T((\theta+\lambda_P\sigma)^2p_0 - \bar{P}\theta(\theta+\lambda_P\sigma))\right)\right]}_{\text{B}}$$

Since $e^{-rT}\frac{1}{(\theta+\lambda_P\sigma)^2} > 0$, the sign of A is identical to the sign of B, which can be evolved into

$$B = \underbrace{e^{-(\theta+\lambda_P\sigma)T}}_{>0}\left[e^{(\theta+\lambda_P\sigma)T}\bar{P}\lambda_P\sigma - \bar{P}\lambda_P\sigma - T((\theta+\lambda_P\sigma)^2 p_0 + T\bar{P}\theta(\theta+\lambda_P\sigma)\right]$$

Thus, we have

$$B\begin{cases} > 0 & \text{iff } p_0 < \frac{\bar{P}\lambda_P\sigma}{T(\theta+\lambda_P\sigma)^2}(e^{(\theta+\lambda_P\sigma)T}-1) + \frac{\bar{P}\theta}{\theta+\lambda_P\sigma} \\ < 0 & \text{iff } p_0 > \frac{\bar{P}\lambda_P\sigma}{T(\theta+\lambda_P\sigma)^2}(e^{(\theta+\lambda_P\sigma)T}-1) + \frac{\bar{P}\theta}{\theta+\lambda_P\sigma} \end{cases}$$

which means,

$$\frac{\partial N_{\mathbb{Q}}^{\star mr}}{\partial\theta} = \begin{cases} > 0 & \text{iff } p_0 < \bar{P}F(\theta,\lambda_P\sigma,T) \\ < 0 & \text{iff } p_0 > \bar{P}F(\theta,\lambda_P\sigma,T) \end{cases}$$

where $F(\theta,\lambda_P\sigma,T) = \frac{\lambda_P\sigma}{T(\theta+\lambda_P\sigma)^2}(e^{(\theta+\lambda_P\sigma)T}-1) + \frac{\theta}{\theta+\lambda_P\sigma}$.

Under the mean-reverting process and From Equation (2.21), to show the fertilizer over-application can result from mistakenly adopting the yield-maximizing principle, we use the fact that $e^{(\theta+\lambda_P\sigma)T} > 1$, Thus, we can show that

$$P_0 + \frac{\bar{P}\theta}{\theta+\lambda_P\sigma}\left(e^{(\theta+\lambda_P\sigma)T}-1\right) > 0 \Longleftrightarrow P_0 e^{-(\theta+r+\lambda_P\sigma)T} + \frac{\bar{P}\theta}{\theta+\lambda_P\sigma}\left(e^{-rT} - e^{-(\theta+r+\lambda_P\sigma)T}\right) > 0$$

which indicates the denominator part inside Equation (2.21), is positive, thus $N_{\mathbb{Q}}^{\star mr} < N^{\star maxyield} = -\frac{a_2}{2a_1}$

Appendix E

Deriving closed forms of $N^\star$ in Chapter 2 using the exponential corn yield model

In this appendix, closed form results for the optimal fertilizer application in Section 2.3 are re-derived using the exponential corn yield function in Chapter 3 instead of the quadratic form in Chapter 2. Using the exponential corn yield model in Equation (3.16) with the soil nutrient stock $\bar{S}$ replaced by fertilizer application variable N, We can rewrite the objective function in Equation (2.6) as:

$$V(P, N, t = 0) = \max_{N} \left\{ e^{-rT} p_0 e^{\mu T} \left[\theta(\alpha_1 \bar{R} + \alpha_2 \bar{R}^2)(1 - e^{-\beta_1 N})(1 - e^{-\beta_2 \bar{H}}) \right] - cN \right\} \quad \text{(E.1)}$$

Then, we can find the optimal solution through the first order condition:

$$\frac{\partial V}{\partial N} = e^{-rT} p_0 e^{\mu T} \left[\theta(\alpha_1 \bar{R} + \alpha_2 \bar{R}^2)(1 - e^{-\beta_2 \bar{H}}) \beta_1 e^{-\beta_1 N} \right] - c = 0$$

After necessary rearrangement, the closed form expression for the optimal amount of fertilization under the assumption that price follows a GBM process is

$$N^{\star gbm} = -\frac{1}{\beta_1}\left\{ln\left[\frac{c}{p_0\theta(\alpha_1\bar{R}+\alpha_2\bar{R}^2)(1-e^{-\beta_2\bar{H}})\beta_1}\right]+(r-\alpha+\lambda_p\sigma_1)T\right\} \tag{E.2}$$

With the restriction of $N^{\star gbm} > 0$, and given $\beta_1 > 0$, it follows that $\frac{c}{p_0\theta(\alpha_1\bar{R}+\alpha_2\bar{R}^2)(1-e^{-\beta_2\bar{H}})\beta_1} < e^{(\alpha-\lambda_p\sigma_1-r)T}$ as a constraint.

When crop price is assumed to follow MR process, Equation 2.20 in Section 2.3 can be rewrote as

$$V(N,P,t=0) = Y\left[Pe^{-(\theta+r+\lambda_P\sigma)T}+\frac{\bar{P}\theta}{\theta+\lambda_P\sigma}\left(e^{-rT}-e^{-(\theta+r+\lambda_P\sigma)T}\right)\right]-cN \tag{E.3}$$

where $Y = \theta_Y(\alpha_1\bar{R}+\alpha_2\bar{R}^2)(1-e^{-\beta_1 N})(1-e^{-\beta_2\bar{H}})$. To determine the optimal fertilizer application amount $N^\star$, we simply take the first order derivative for $V(N,P,t=0)$ with respect to N and set it to 0, which eventually gives the optimal fertilizer application amount N under the $\mathbb{Q}$-measure:

$$N_{\mathbb{Q}}^{\star mr} = -\frac{1}{\beta_1}ln\left\{\frac{c}{\left[e^{-(\theta+r+\lambda_P\sigma)T}\left(p_0-\frac{\bar{P}\theta}{\theta+\lambda_P\sigma}\right)+\frac{\bar{P}\theta}{\theta+\lambda_P\sigma}e^{-rT}\right]\theta_Y(\alpha_1\bar{R}+\alpha_2\bar{R}^2)(1-e^{-\beta_2\bar{H}})\beta_1}\right\} \tag{E.4}$$

With the restriction of $N_{\mathbb{Q}}^{\star mr} > 0$, and given $\beta_1 > 0$, it follows that

$$\left[e^{-(\theta+r+\lambda_P\sigma)T}\left(p_0-\frac{\bar{P}\theta}{\theta+\lambda_P\sigma}\right)+\frac{\bar{P}\theta}{\theta+\lambda_P\sigma}e^{-rT}\right]\theta_Y(\alpha_1\bar{R}+\alpha_2\bar{R}^2)(1-e^{-\beta_2\bar{H}})\beta_1 > c$$

as a constraint. Since there is a common factor in the denominator in both optimal decisions (Equation (E.4) and (2.21)), we take advantage of the proofs in Appendix D and find that the parameter sensitivity conclusions are identical to results in Table 2.1 in Section 2.4. Therefore, as presented in the following Table E.1, the farmer's optimal

fertilizer applications (Equation (E.2) and (E.4)) based on the exponential corn yield model will give us the same conclusions as Section 2.4.

Table E.1: A summary of parameter sensitivity results

Parameter Sensitivity	Under GBM assumption	Under MR assumption
$\frac{\partial N}{\partial c}$	< 0	< 0
$\frac{\partial N}{\partial P_0}$	> 0	> 0
$\frac{\partial N}{\partial \alpha}$ or $\frac{\partial N}{\partial \theta}$	> 0	> 0 iff $\bar{P}(1+F) > P_0$
$\frac{\partial N}{\partial \sigma}$	< 0	< 0

Note that λ_P is assumed to be positive.

where $\psi_{\mathbb{Q}} = \left[1 - \frac{re^{(\theta+\lambda_P\sigma)T}}{\theta+\lambda_P\sigma+r}\right] \frac{\theta}{\theta+\lambda_P\sigma}$ and $F = \frac{2\theta}{\theta+\lambda\sigma} + \frac{2\theta+\lambda\sigma}{T(\theta+\lambda\sigma)^2}\left[e^{(\theta+\lambda\sigma)T} - 1 - (\theta+\lambda\sigma)T\right]$.

Appendix F

Corn market price of risk calculation

In this appendix, we provide the calculation of the corn market price of risk λ_P in Section 3.7.1. Using the classic CAPM (Capital Asset Pricing Model, Insley & Lei (2007)), we assume the expected return of corn price is described as:

$$\mu^\star = \rho + [E(\rho_m) - \rho]\beta$$

where ρ_m is the return on the S&P 500 index, β is parameter, which is positive in our estimation. Under no-arbitrage principle, we know

$$\mu^\star = \rho + \lambda_P \sigma_P$$

which means

$$\lambda_P = \frac{[E(\rho_m) - \rho]\beta}{\sigma_P} \tag{F.1}$$

The risk-free interest rate used in price process estimation is ρ=1.76%, which is averaged from Q1, 2018 to Q2, 2019[1]. Annual market return of S&P500 index ρ_m is computed using

[1]Quarterly reported Government of Canada benchmark bond yields for 1-year term are collected as risk free interest rates from http://assurage.com/en/blog. The risk free interest rate used in this paper is

the daily data from Jan 01, 2010 to Jul 26, 2019. $\sigma_P = 0.2547$ in Table 3.2, the estimated standard deviation of corn price. The estimated value β is determined by OLS regression of $\mu^\star - \rho$ on $\rho_m - \rho$. Historical values for $\mu^\star$ and ρ_m are the series of percentage change in corn price and S&P 500 index, thus the estimated β is 0.1547. Annual expected return on S&P 500 index is $E(\rho_m) = 0.1783$. Thus, the market price of risk is

$$\lambda_P = \frac{[E(\rho_m) - \rho]\beta}{\sigma_P} = \frac{[0.1783 - 0.0176] \times 0.1547}{0.2547} = 0.0976$$

ρ=1.76%, which is quarterly averaged from Q1, 2018 to Q2, 2019.

Appendix G

Fertilizer variable cost sensitivity results in the farmer's optimal decisions

This appendix provides the detailed results presented graphically in Figure 3.22. The optimal split fertilizer applications and farm value under each cost ratio are listed as below:

$\frac{c'_N}{c_N}$	$c_N = \frac{0.72}{4}$ \$/lb			$c_N = 0.72$ \$/lb			$c_N = 0.72 * 4$ \$/lb		
	N_0	N_1	V_0	N_0 (lb/a)	N_1 (lb/a)	V_0 (\$/a)	N_0	N_1	V_0
0.5000	18	100	496.8552	0	100	467.5603	0	68	380.7548
0.6000	18	100	495.0594	0	96	460.5113	0	64	361.8330
0.7000	18	100	493.2637	0	92	453.7393	0	60	344.0326
0.7185	20	96	492.9326	0	92	452.5168	0	60	340.8433
0.7189	20	96	492.9257	0	92	452.4904	0	60	340.7744
0.7193	20	96	492.9188	0	92	452.4639	4	54	340.7093
0.7197	26	88	492.9120	10	78	452.4411	4	54	340.6473
0.7201	26	88	492.9057	20	64	452.4217	14	40	340.5938
0.7205	36	74	492.9001	30	50	452.4055	24	26	340.5534
0.7209	46	60	492.8953	40	36	452.3926	30	18	340.5265
0.7213	56	46	492.8914	46	28	452.3831	40	4	340.5162
0.7217	62	38	492.8884	56	14	452.3777	40	4	340.5116
0.7221	72	24	492.8863	66	0	452.3753	40	4	340.5070
0.7225	82	10	492.8849	66	0	452.3753	40	4	340.5024
0.8000	90	0	492.8815	66	0	452.3753	42	0	340.4626
0.9000	90	0	492.8815	66	0	452.3753	42	0	340.4626
1.0000	90	0	492.8815	66	0	452.3753	42	0	340.4626
1.1000	90	0	492.8815	66	0	452.3753	42	0	340.4626
1.2000	90	0	492.8815	66	0	452.3753	42	0	340.4626

Appendix H

Precipitation sensitivity results in the farmer's optimal decisions

This appendix provides the detailed results presented graphically in Figure 3.24. The optimal fertilizer application (N_0, N_1) under each rainfall scenario, for each fertilizer cost ratio $\frac{c'_N}{c_N}$ are listed as below. Parameters used here are base case, the total variable cost is \$1.7593/bu.

Rain likelihood	$\frac{c'_N}{c_N}$	Rain amount		
		Less	Base Case	More
Smaller (Dryer)	0.5	(0, 84)	(0, 98)	(0, 102)
	0.6	(0, 80)	(0, 94)	(0, 96)
	0.7	(52, 0)	(0, 90)	(0, 92)
	0.8	(52, 0)	(64, 0)	(68, 0)
	0.9	(52, 0)	(64, 0)	(68, 0)
	1	(52, 0)	(64, 0)	(68, 0)
Base Case	0.5	(0, 88)	(0, 100)	(0, 96)
	0.6	(0, 84)	(0, 96)	(0, 92)
	0.7	(56, 0)	(0, 92)	(0, 88)
	0.8	(56, 0)	(66, 0)	(64, 0)
	0.9	(56, 0)	(66, 0)	(64, 0)
	1	(56, 0)	(66, 0)	(64, 0)
Larger (Wetter)	0.5	(0, 90)	(0, 102)	(0, 76)
	0.6	(0, 86)	(0, 98)	(0, 72)
	0.7	(58, 0)	(0, 94)	(0, 68)
	0.8	(58, 0)	(68, 0)	(50, 0)
	0.9	(58, 0)	(68, 0)	(50, 0)
	1	(58, 0)	(68, 0)	(50, 0)

Appendix I

Sensitivity results for fertilizer cost ratio and SCN in the socially optimal model

This appendix provides the detailed results presented graphically in Figure 4.12 and 4.13. The socially optimal N_0, N_1 and V_0 for both damage models are listed as below. Social cost parameter are set as $d_L = d_D = SCN$, all other parameters are set at base case.

SCN	Linear damage									Threshold damage								
	$\frac{c'_N}{c_N} = 0.8$			$\frac{c'_N}{c_N} = 0.9$			$\frac{c'_N}{c_N} = 1$			$\frac{c'_N}{c_N} = 0.8$			$\frac{c'_N}{c_N} = 0.9$			$\frac{c'_N}{c_N} = 1$		
	N_0	N_1	V_0	N_0	N_1	V_0	N_0	N_1	V_0	N_0	N_1	V_0	N_0	N_1	V_0	N_0	N_1	V_0
5	52	0	403.1	52	0	400.9	52	0	403.1	54	0	420.9	54	0	420.9	54	0	420.9
10	28	24	360.3	46	0	358.1	46	0	360.3	50	0	394.6	50	0	394.6	50	0	394.6
15	0	56	324.3	40	0	320.6	40	0	322.7	46	2	370.2	48	0	370.2	48	0	370.2
20	0	52	291.9	36	0	287.0	36	0	289.1	2	58	348.1	44	0	347.6	44	0	347.6
25	0	46	262.4	0	46	257.2	34	0	258.4	0	58	327.9	40	0	326.4	40	0	326.4
30	0	44	235.3	0	42	230.3	30	0	230.4	0	54	308.9	38	0	306.6	38	0	306.6
35	0	40	210.2	0	40	205.5	24	6	204.6	0	52	290.9	36	0	288.0	36	0	288.0
40	0	38	186.8	0	36	182.4	0	36	181.5	0	48	273.8	10	34	270.4	34	0	270.3
45	0	34	165.0	0	34	160.9	0	34	160.1	0	46	257.6	0	46	254.3	32	0	253.4
50	0	32	144.7	0	32	140.8	0	32	140.1	0	44	242.1	0	44	239.0	30	2	237.4

Appendix J

Precipitation sensitivity results in the socially optimal model

This appendix provides the detailed results presented graphically in Figure 4.14 and 4.15. The socially optimal fertilizer application (N_0, N_1) under each rainfall scenario, for each fertilizer cost ratio $\frac{c'_N}{c_N}$ are examined as below. Parameters used here are base case, with the total variable cost is \$1.7593/bu, nitrate social cost is \$0.66/kg, denitrification social cost is \$0.22/kg.

Table J.1: Rainfall sensitivity with fertilizer cost ratio (linear damage model)

Rain likelihood	$\frac{c'_N}{c_N}$	Rain amount		
		Less	Base Case	More
Smaller (Dryer)	0.5	(0, 82)	(0, 94)	(0, 98)
	0.6	(0, 80)	(0, 92)	(0, 94)
	0.7	(52, 0)	(0, 88)	(0, 90)
	0.8	(52, 0)	(62, 0)	(66, 0)
	0.9	(52, 0)	(62, 0)	(66, 0)
	1	(52, 0)	(62, 0)	(66, 0)
Base Case	0.5	(0, 86)	(0, 98)	(0, 92)
	0.6	(0, 82)	(0, 94)	(0, 88)
	0.7	(54, 2)	(0, 90)	(0, 84)
	0.8	(56, 0)	(64, 0)	(62, 0)
	0.9	(56, 0)	(64, 0)	(62, 0)
	1	(56, 0)	(64, 0)	(62, 0)
Larger (Wetter)	0.5	(0, 90)	(0, 98)	(0, 72)
	0.6	(0, 86)	(0, 94)	(0, 68)
	0.7	(56, 2)	(0, 90)	(0, 64)
	0.8	(58, 0)	(66, 0)	(46, 0)
	0.9	(58, 0)	(66, 0)	(46, 0)
	1	(58, 0)	(66, 0)	(46, 0)

Table J.2: Rainfall sensitivity with fertilizer cost ratio (threshold damage model)

Rain likelihood	$\frac{c'_N}{c_N}$	Rain amount		
		Less	Base Case	More
Smaller (Dryer)	0.5	(0, 82)	(0, 94)	(0, 96)
	0.6	(0, 80)	(0, 90)	(0, 92)
	0.7	(52, 0)	(0, 88)	(0, 88)
	0.8	(52, 0)	(62, 0)	(64, 0)
	0.9	(52, 0)	(62, 0)	(64, 0)
	1	(52, 0)	(62, 0)	(64, 0)
Base Case	0.5	(0, 88)	(0, 94)	(0, 90)
	0.6	(0, 84)	(0, 90)	(0, 86)
	0.7	(56, 0)	(0, 88)	(0, 84)
	0.8	(56, 0)	(62, 0)	(62, 0)
	0.9	(56, 0)	(62, 0)	(62, 0)
	1	(56, 0)	(62, 0)	(62, 0)
Larger (Wetter)	0.5	(0, 90)	(0, 96)	(0, 70)
	0.6	(0, 86)	(0, 90)	(0, 62)
	0.7	(58, 0)	(0, 88)	(0, 58)
	0.8	(58, 0)	(62, 0)	(40, 0)
	0.9	(58, 0)	(62, 0)	(40, 0)
	1	(58, 0)	(62, 0)	(40, 0)

Appendix K

A summary of notations for key variables in this thesis

Since there are numerous mathematical notations used in Chapter 3 and 4, for reader's convenience, the meanings for notations of key variables are summarized in this appendix. This appendix also provides the equation numbers where these variables are modeled.

Table K.1: A summary of notations for key variables

Notation	Variable name
P	Corn price, in Equation (3.2) and (3.26)
Y	Corn yield, in Equation (3.16) and (3.33)
H	Daily corn heat units, in Equation (3.7) and Definition 3.7
$\bar{H}$	Cumulative corn heat units, in Equation (3.3)
X_1	Daily maximum temperature, in Equation (3.4) and (3.28)
δ	Daily temperature difference, in Equation (3.5) and (3.29)
w_t	Daily rainfall regime, in Equation (3.9)
R^{w_t}	Daily rainfall amount, in Equations (3.10) and (3.32)
$\bar{R}$	Cumulative rainfall amount, in Equation (3.10)
S	Daily soil nutrient stock, in Equation (3.14)
$\bar{S}$	Seasonal averaged soil nutrient stock, in Equation (3.15)
L	Cumulative amount of nitrogen from leaching, in Equation (4.4)
Υ	Cumulative amount of nitrogen from denitrification, in Equation (4.2)
$D(T)$	Total damages at time T, in Equation (4.3)
Θ	N concentration in groundwater, in Equation (4.4)